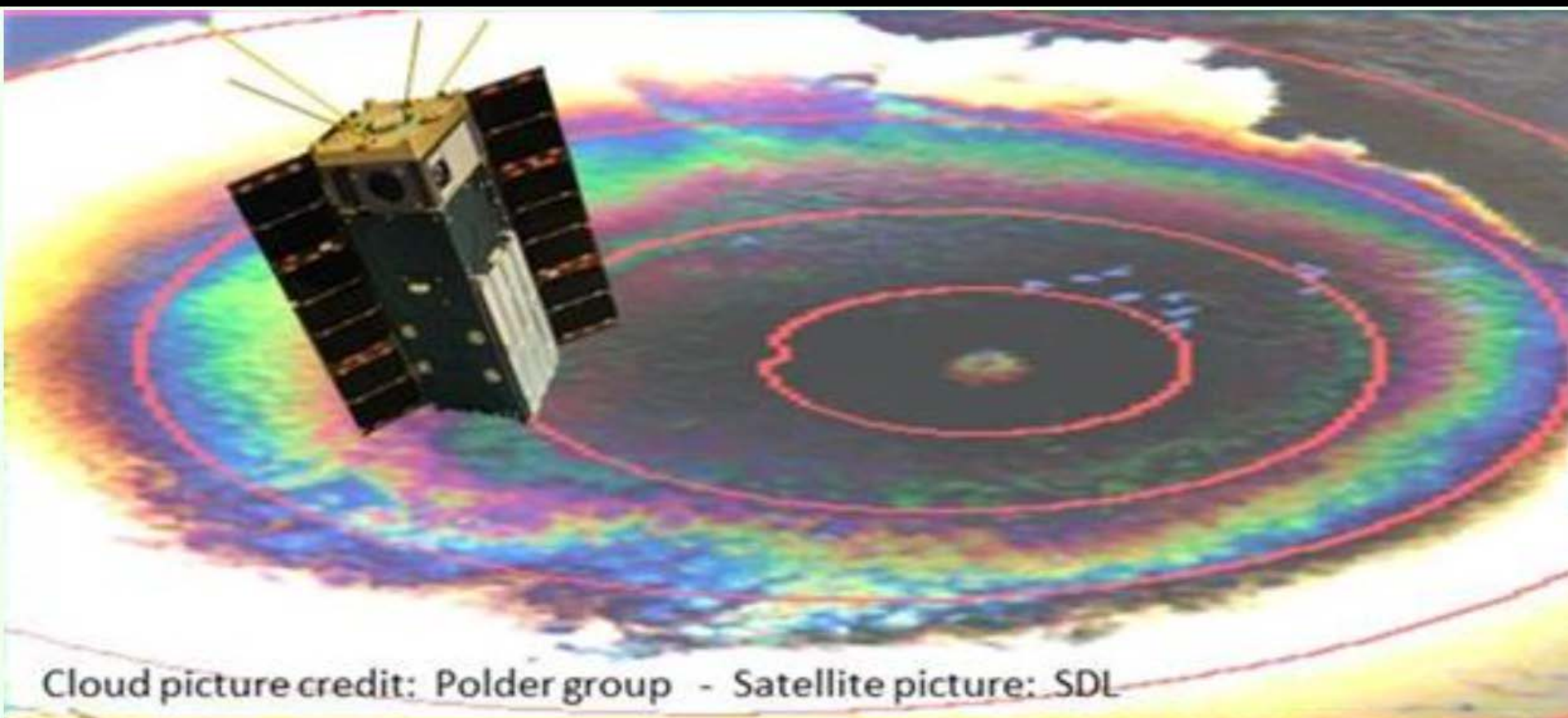


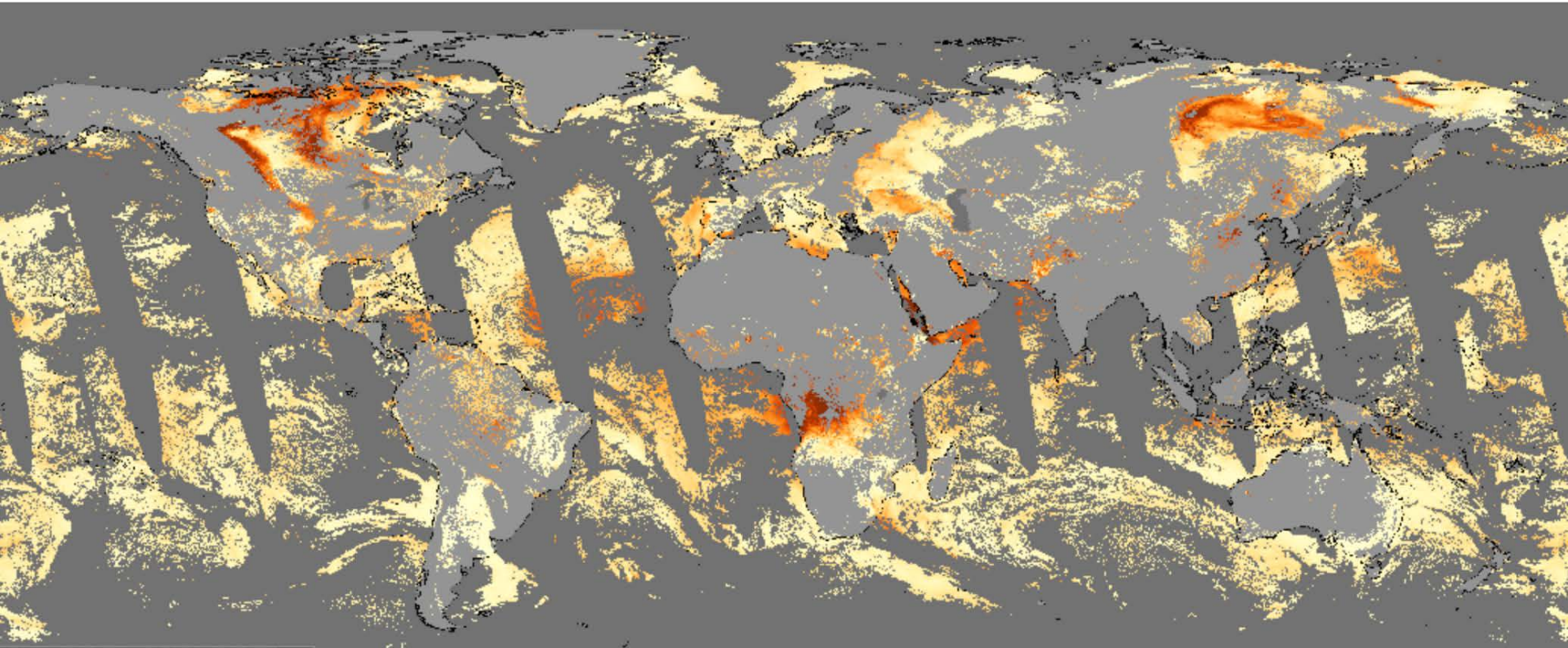
Aerosol Remote Sensing and Atmospheric Correction Beyond VIIRS: What will Expanded Wavelengths, Hyperspectral, Multi-angle, and Polarization Bring to the Table

Lorraine A. Remer
JCET-UMBC



Global Aerosol Optical Depth at 550 nm from VIIRS (IDPS)

13 August 2017



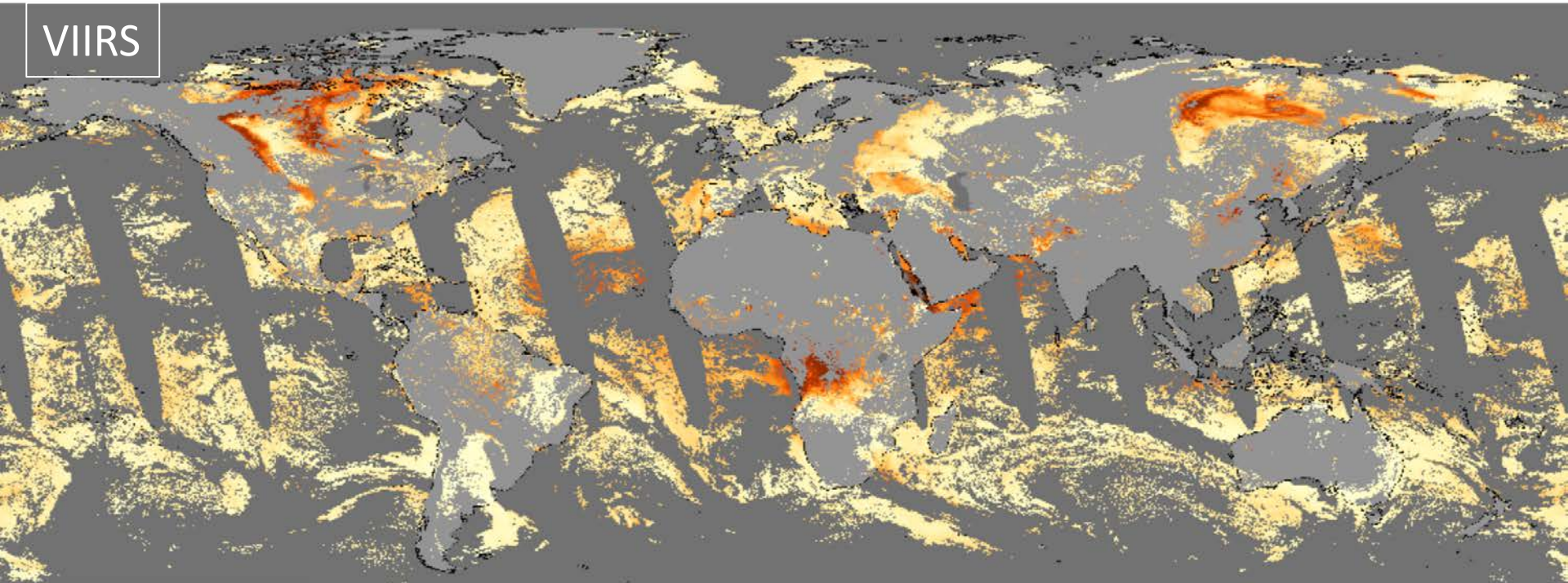
Global Aerosol Optical Depth at 550 nm from Aqua MODIS (DT)

13 August 2017

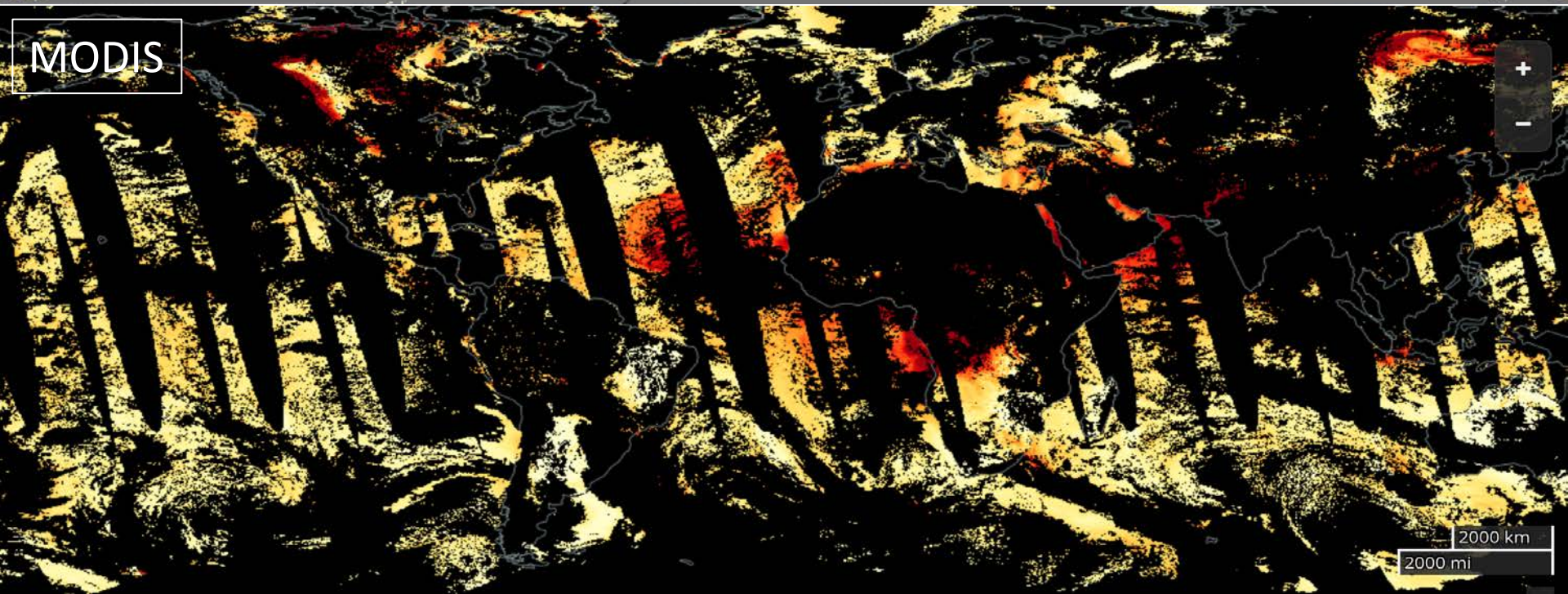


NASA World View

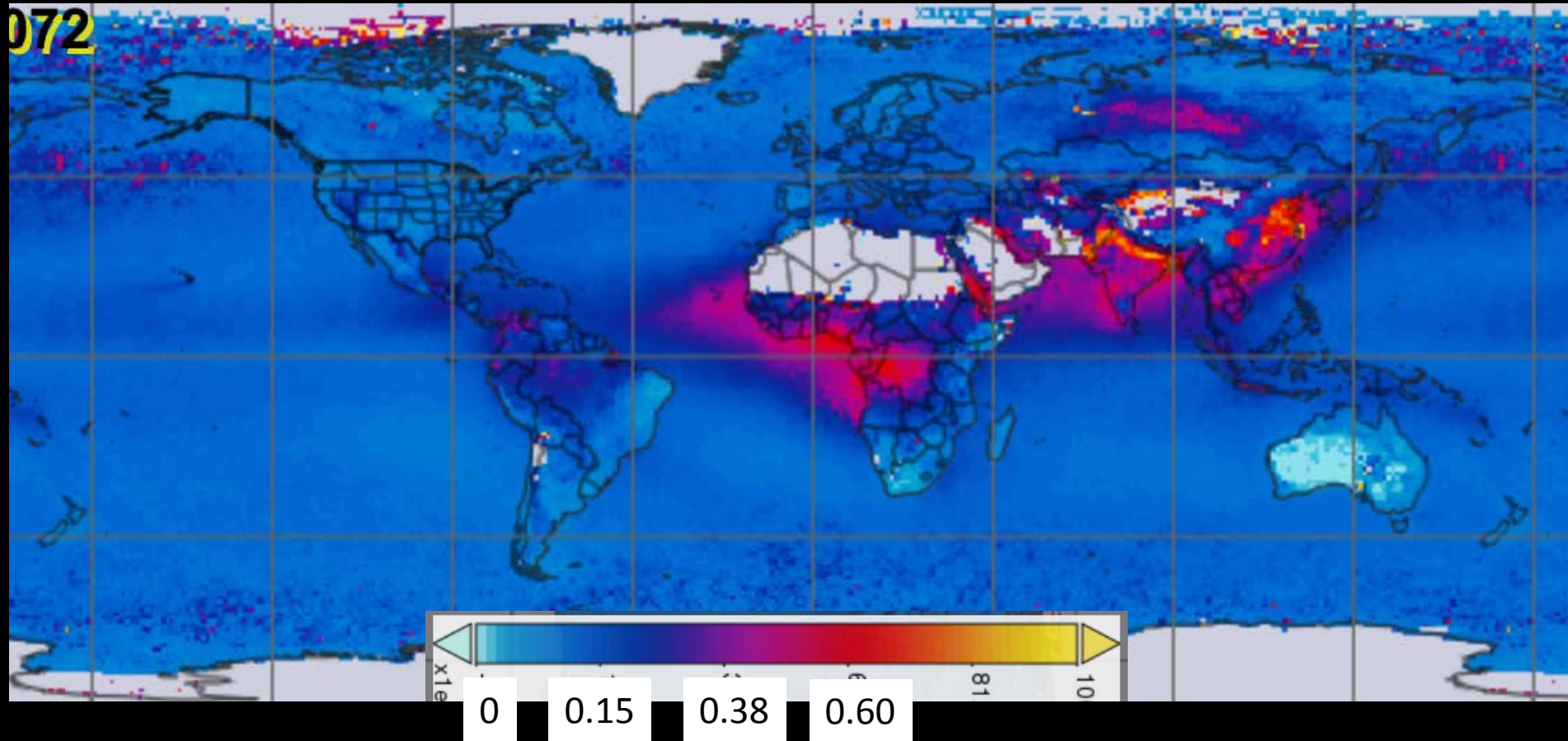
VIIRS



MODIS



Global Aerosol Optical Depth at 550 nm from Aqua MODIS (DT) 2016 Annual Mean



$$L(\tau^*, \mu_o, \mu, \varphi) = L_o(\tau^*, \mu_o, \mu, \varphi) + \frac{RE_o T_t(\tau^*, \mu)}{1 - RS}$$

Diagram illustrating the components of the radiance equation:

- $L(\tau^*, \mu_o, \mu, \varphi)$: Radiance measured at satellite
- $L_o(\tau^*, \mu_o, \mu, \varphi)$: Radiance from atmosphere
- $\frac{RE_o T_t(\tau^*, \mu)}{1 - RS}$: Radiance from surface

$\mu_o = \cos(\text{solar zenith angle})$

$\mu = \cos(\text{sensor zenith angle})$

$\varphi = \text{relative azimuth}$

$\tau^* = \text{aerosol optical thickness}$

$R = \text{surface reflectance}$

$E_o = \text{extraterrestrial irradiance}$

$T_t = \text{total transmission}$

$S = \text{spherical albedo}$

$$L(\tau^*, \mu_o, \mu, \varphi) = L_o(\tau^*, \mu_o, \mu, \varphi) + \frac{RE_o T_t(\tau^*, \mu)}{1 - RS}$$

Diagram illustrating the components of the radiance equation:

- $L(\tau^*, \mu_o, \mu, \varphi)$: Radiance measured at satellite
- $L_o(\tau^*, \mu_o, \mu, \varphi)$: Radiance from atmosphere
- $\frac{RE_o T_t(\tau^*, \mu)}{1 - RS}$: Radiance from surface

$\mu_o = \cos(\text{solar zenith angle})$

$\mu = \cos(\text{sensor zenith angle})$

$\varphi = \text{relative azimuth}$

$\tau^* = \text{aerosol optical thickness}$

$R = \text{surface reflectance}$

$E_o = \text{extraterrestrial irradiance}$

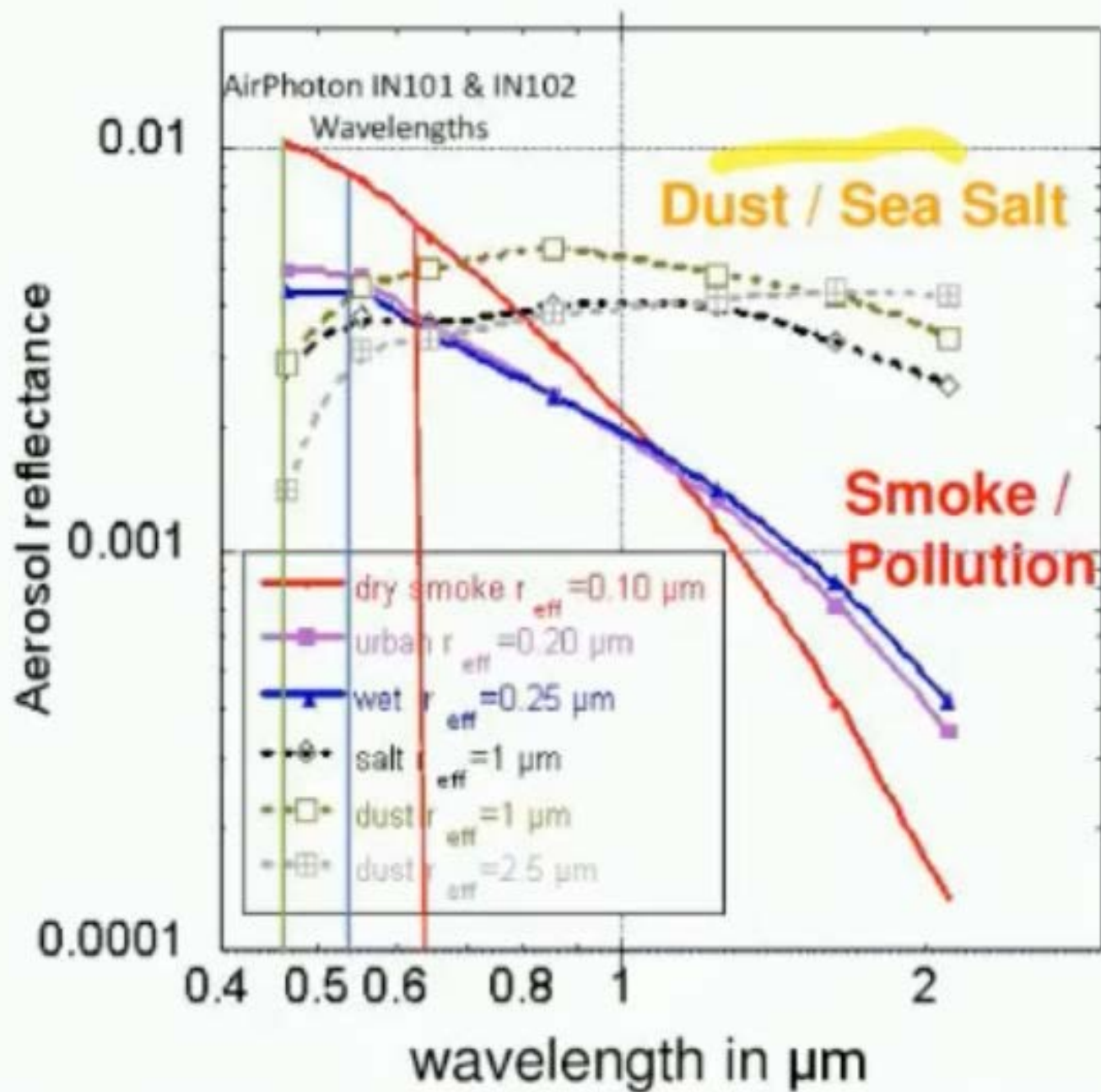
$T_t = \text{total transmission}$

$S = \text{spherical albedo}$

This is a single channel Dark Target retrieval.
(one wavelength at a time)

Requires assumptions of particle size and refractive index, as well as surface reflectance

Returns 1 piece of information: τ^*



Aerosol_Optical_Depth_Small_Ocean_Mean_Mean

01Jul2017

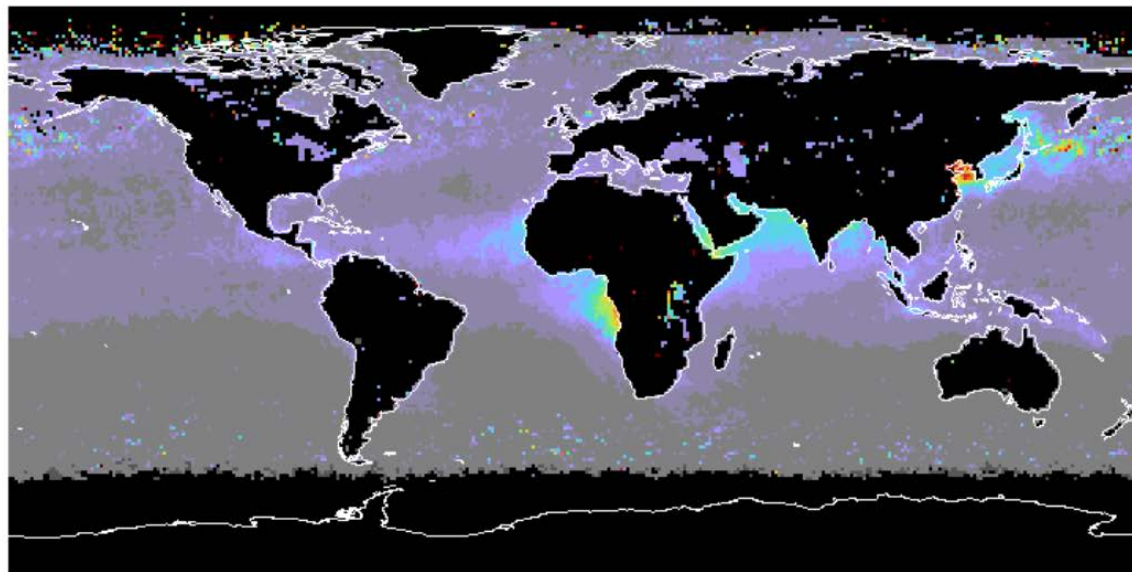
0.80

0.60

0.40

0.20

0.00



AOD 550 nm
Aqua MODIS
Monthly mean
July 2017

Fine mode only

MODIS/Aqua MYD08_M3.A2017182.006.2017213173821.hdf

none

Aerosol_Optical_Depth_Average_Ocean_Mean_Mean

01Jul2017

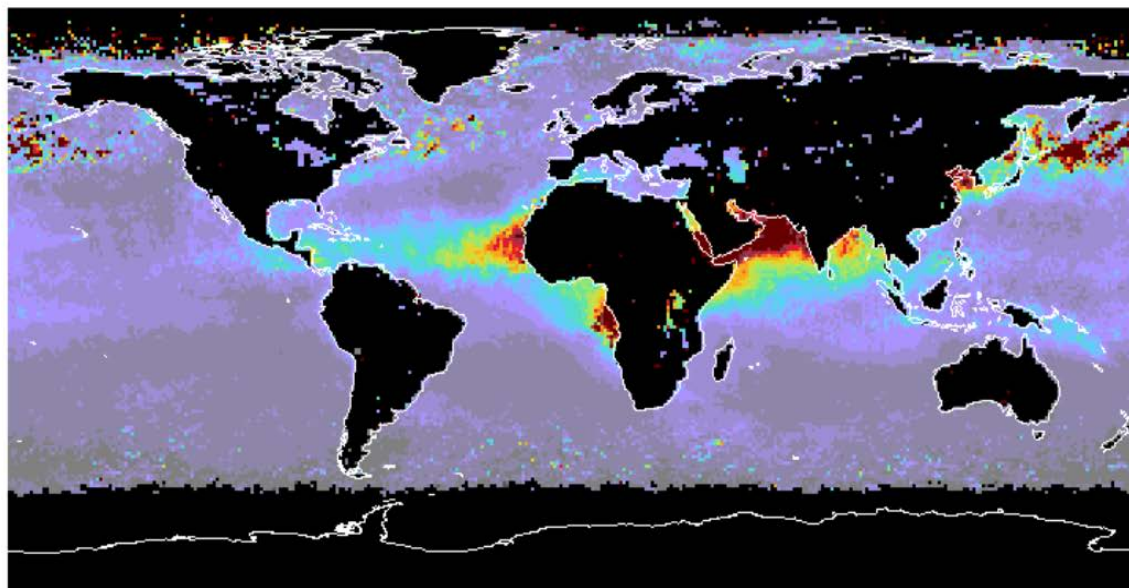
0.80

0.60

0.40

0.20

0.00

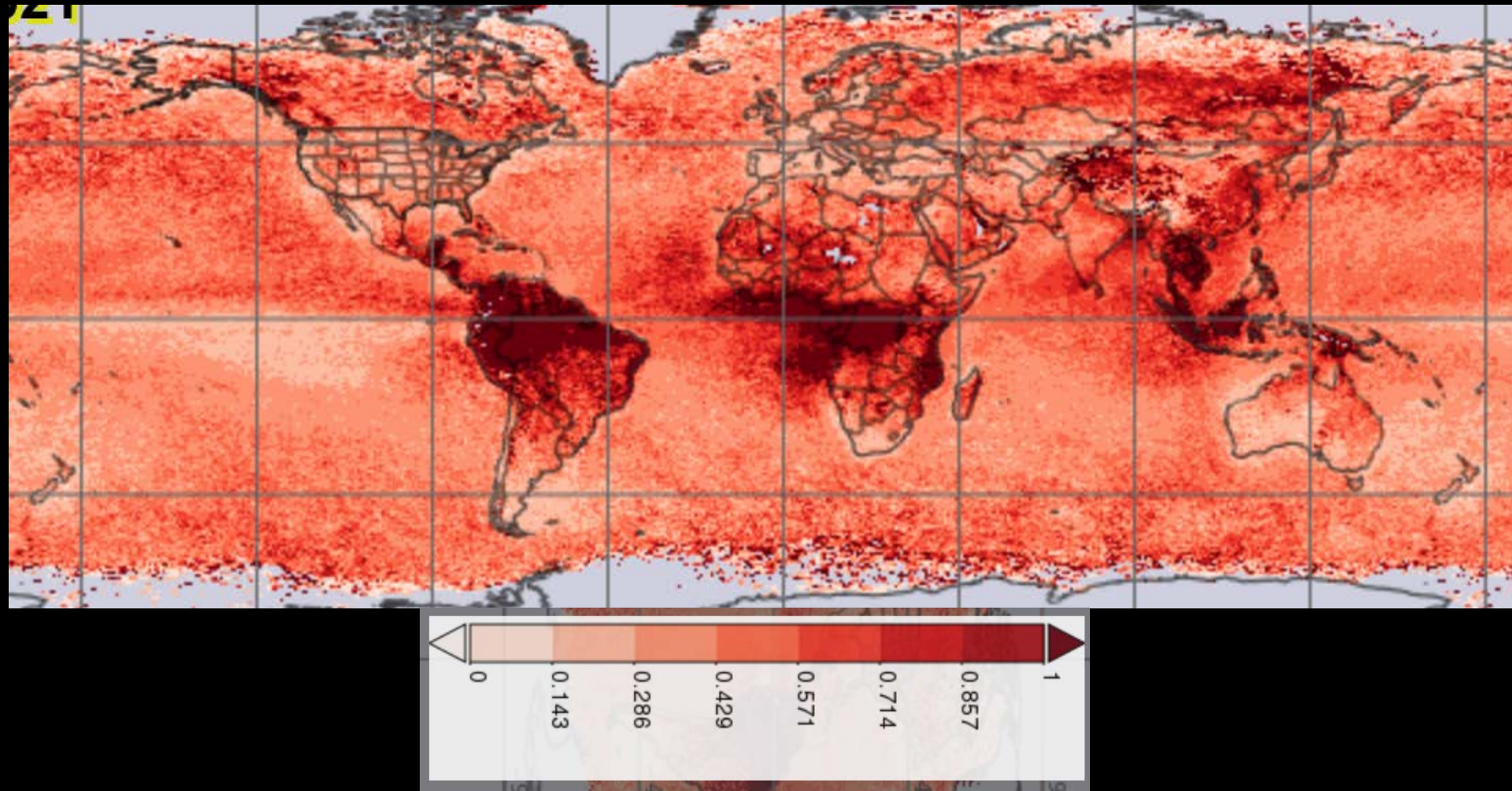


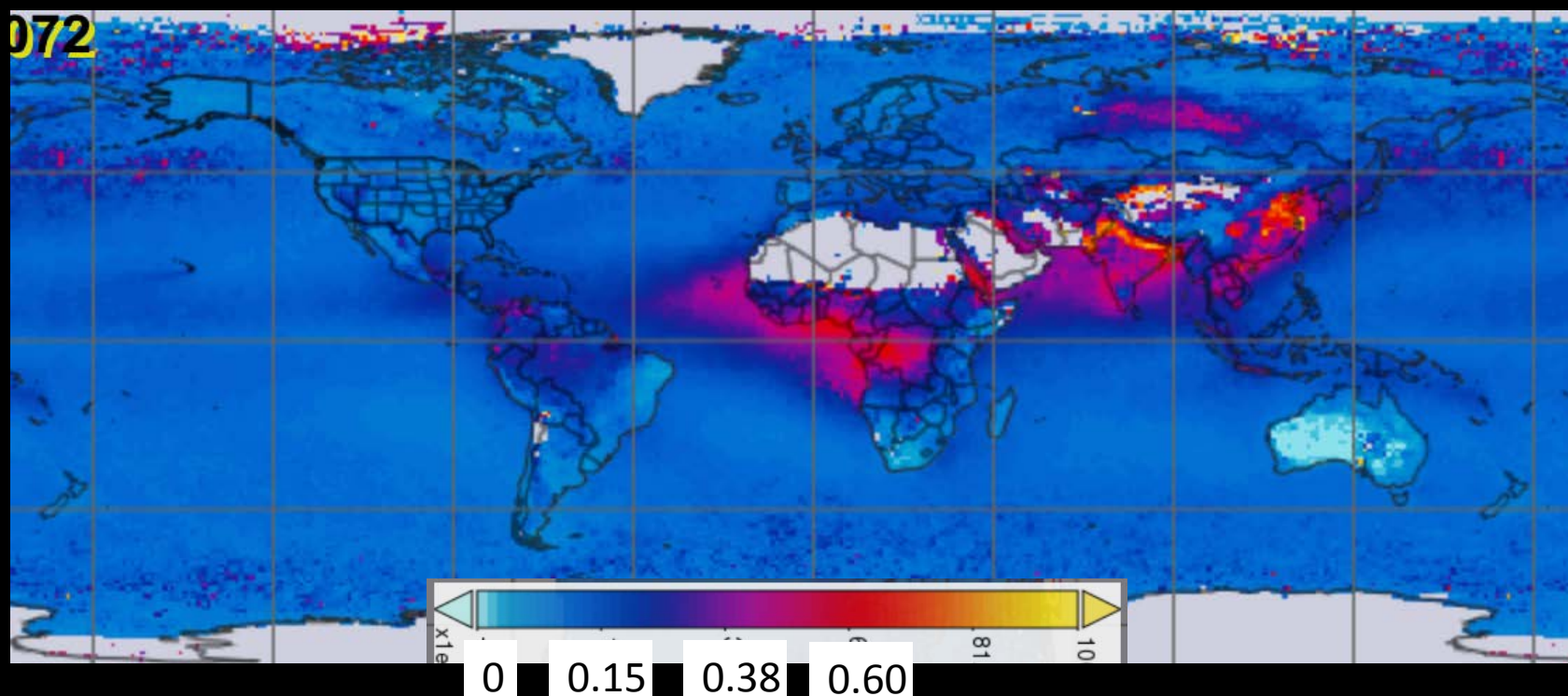
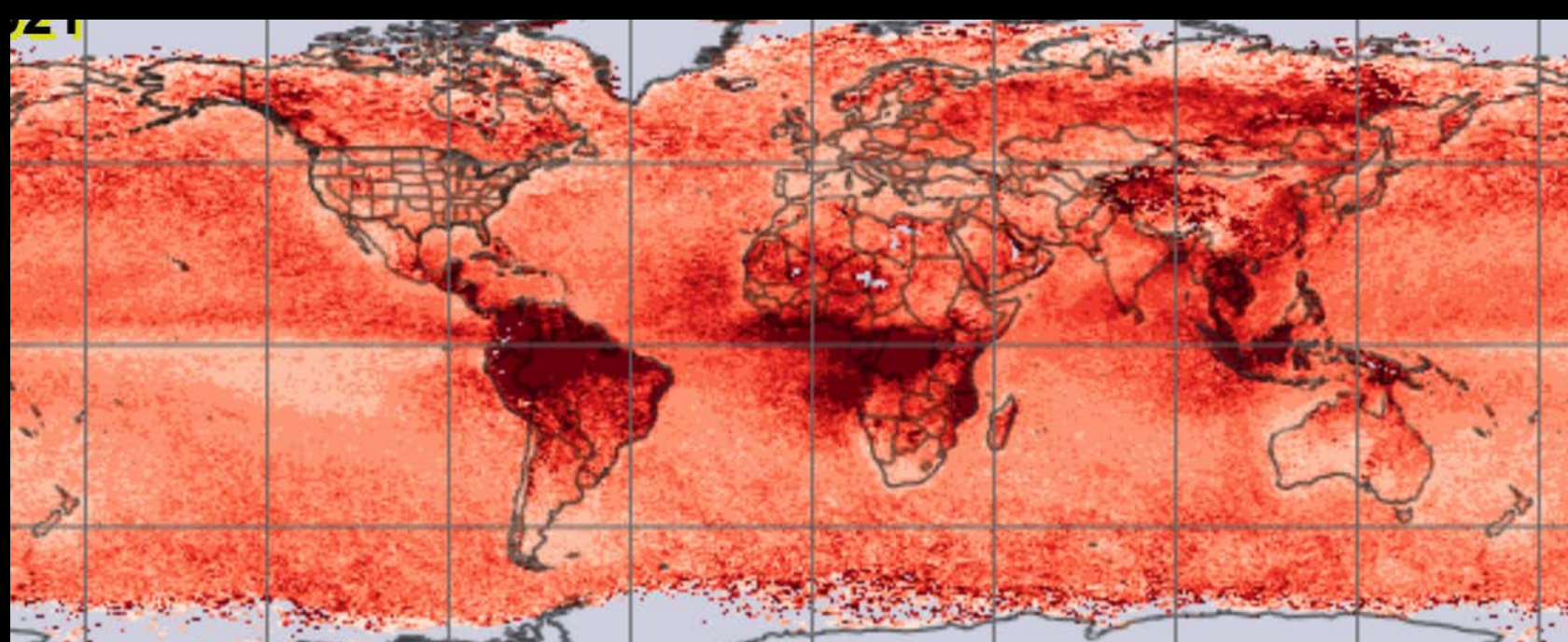
Total AOD

MODIS/Aqua MYD08_M3.A2017182.006.2017213173821.hdf

none

Global Aerosol Optical Depth at 483 nm from Aura OMI 2016 Annual Mean





Radiative transfer in the near UV

$$L^*(\Omega, \mu, \mu_0, \varphi, p_0) = L^0(\Omega, \mu, \mu_0, \varphi, p_0) + \frac{RT_t(\Omega, \mu, \mu_0, p_0)}{1 - RS(\Omega, p_0)}$$

Radiance measured at satellite

Radiance from atmosphere

Radiance from surface

Ω = ozone content
 p_0 = surface pressure

Note: no dependence on aerosol in the equation

Radiative transfer in the near UV

$$L^*(\Omega, \mu, \mu_0, \varphi, p_0) = L^0(\Omega, \mu, \mu_0, \varphi, p_0) + \frac{RT_t(\Omega, \mu, \mu_0, p_0)}{1 - RS(\Omega, p_0)}$$

$$R_{\lambda_0} = \frac{L_{\lambda_0}^* - L_{\lambda_0}^0}{T_{t_ \lambda_0} + S_{\lambda_0} (L_{\lambda_0}^* - L_{\lambda_0}^0)}$$

Reflectance of the lower surface in one wavelength.

If no aerosol, and ozone absorption is minimal (330-390 nm), then just Rayleigh scattering.

Radiative transfer in the near UV

L^0 , T_t and S are obtained from Rayleigh scattering calculations

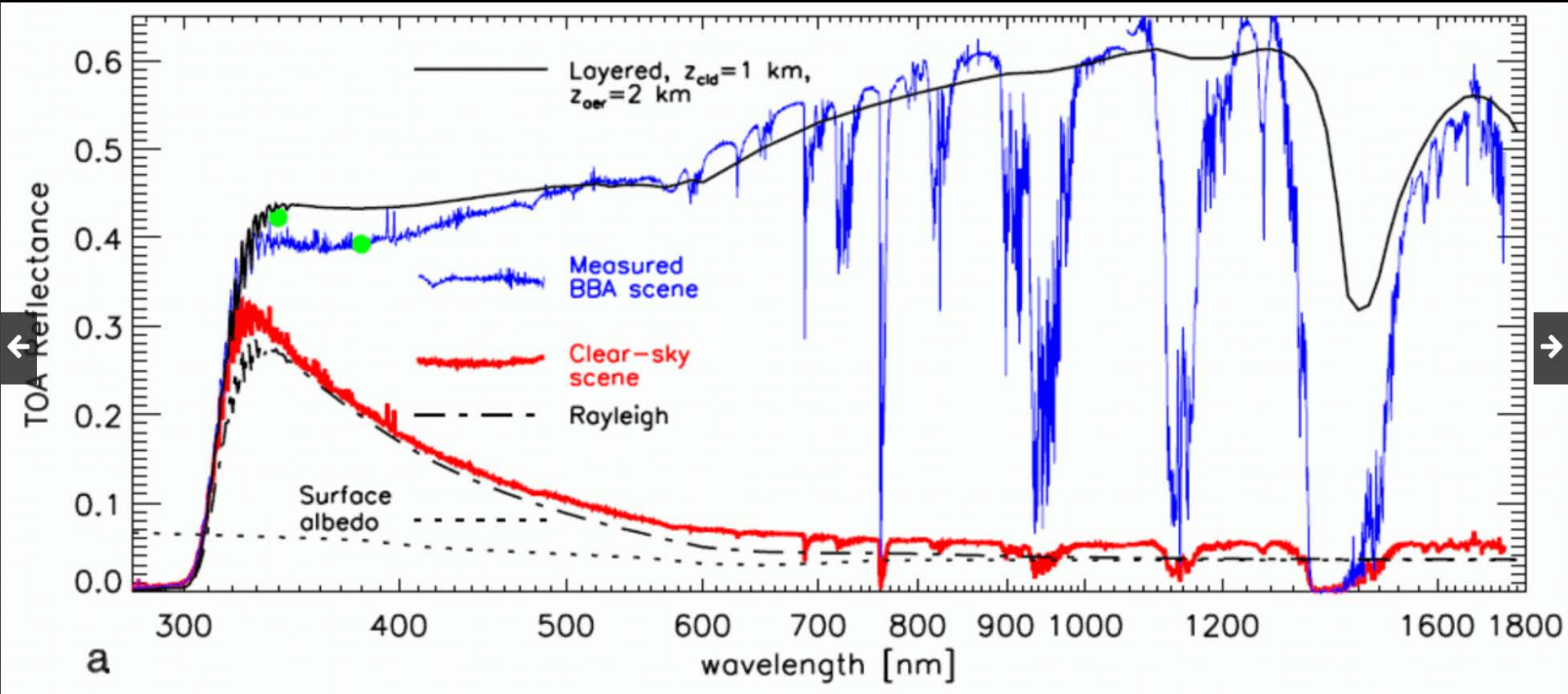
$$R_{\lambda_0} = \frac{L_{\lambda_0}^* - L_{\lambda_0}^0}{T_{t_ \lambda_0} + S_{\lambda_0} (L_{\lambda_0}^* - L_{\lambda_0}^0)}$$

Assume lower surface reflectance has NO spectral dependence.

Calculate R at two wavelengths.

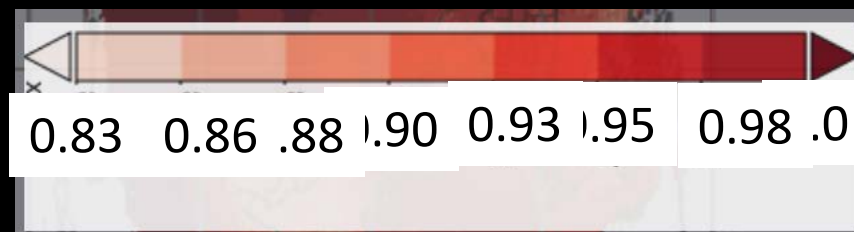
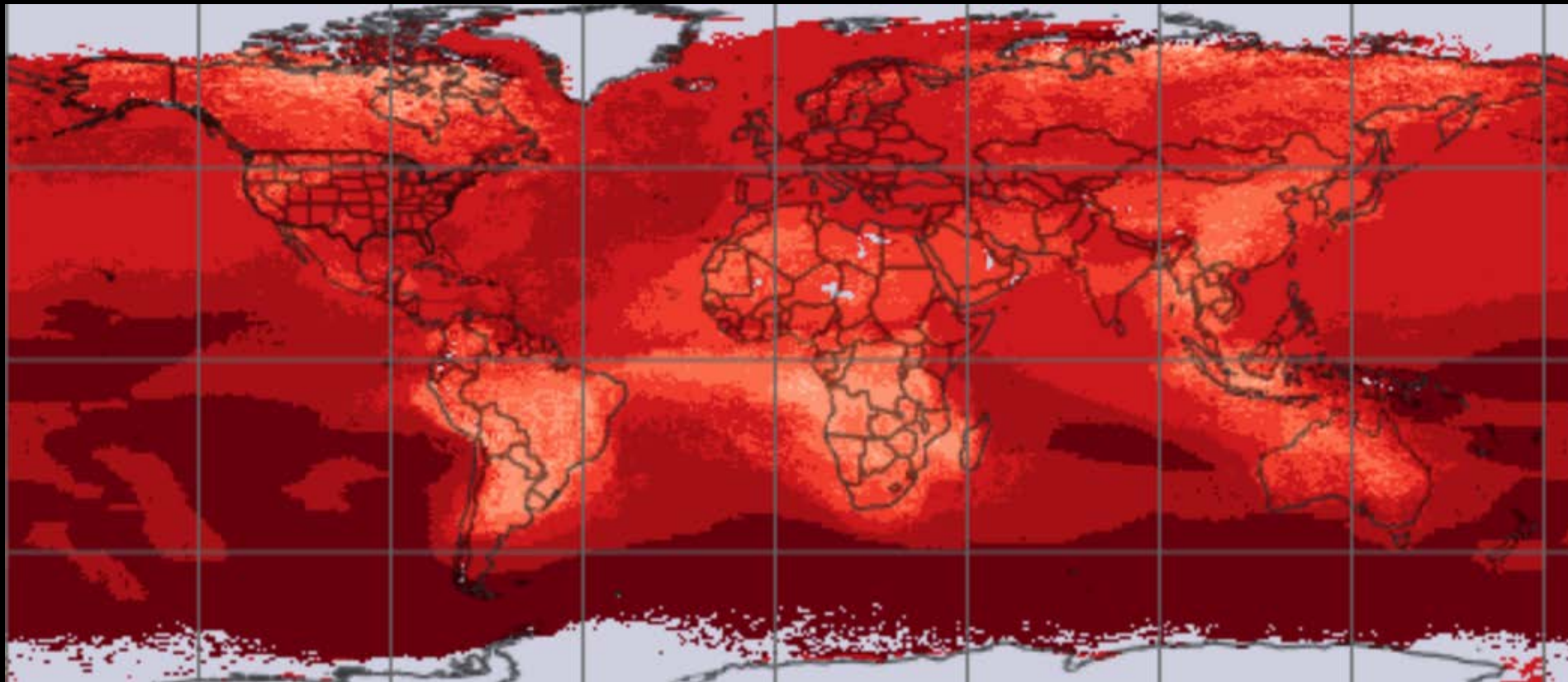
All spectral dependence should match Rayleigh expectations. If not then, **AEROSOL**.

Another SCIAMACHY scene of smoke over broken clouds over ocean



Measurements deviate from Rayleigh-only expectations, In magnitude and in spectral dependence.

Global Aerosol Single Scattering albedo at 483 nm from Aura OMI 2016 Annual Mean



One additional problem with the UV approach...

In the UV, deviation from Rayleigh depends on the height of the aerosol.

2 pieces of information/ 3 important parameters:

- Loading (AOD)
- Absorption (SSA)
- Height (h)

The dark target VNIR-SWIR approach...

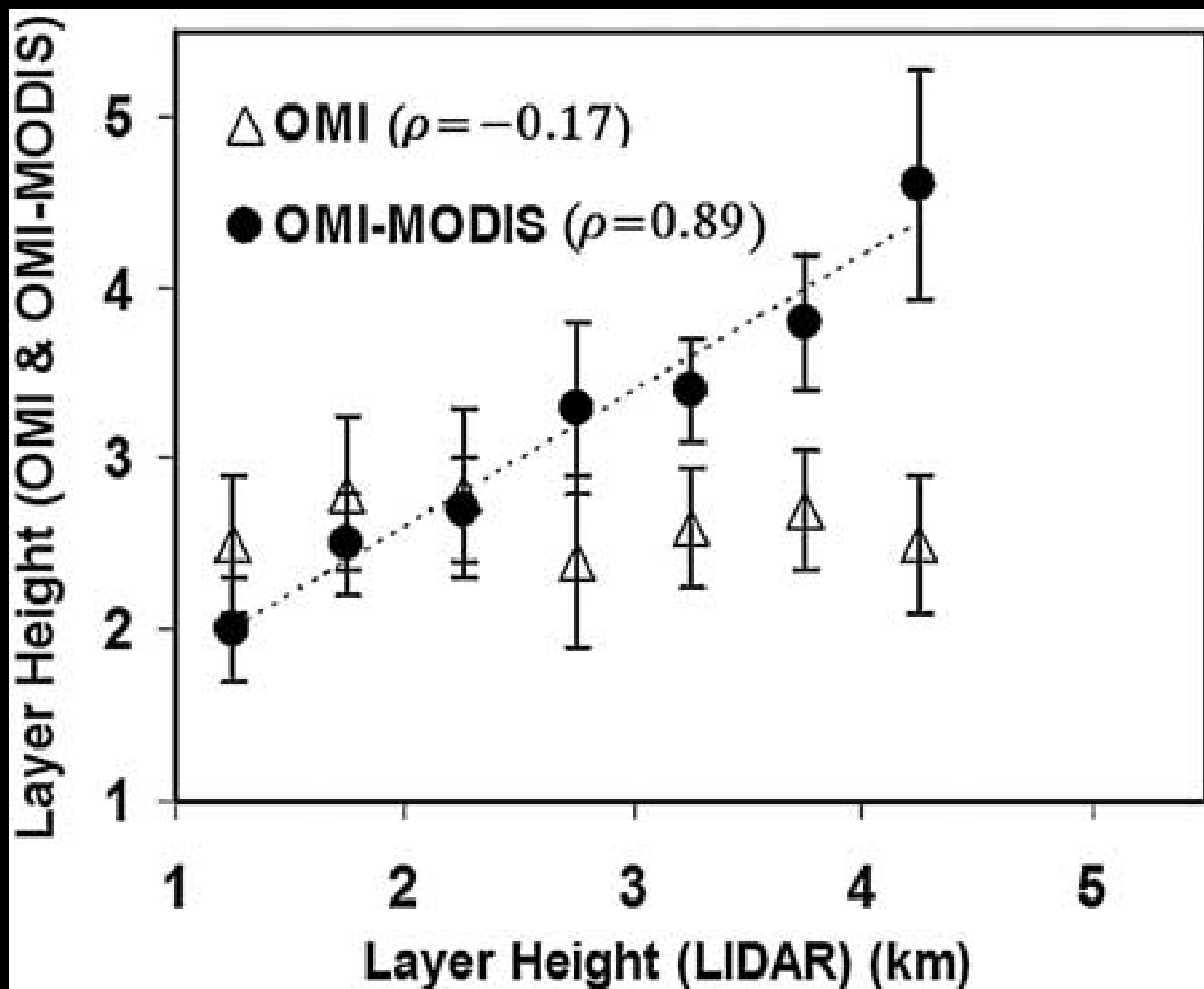
- Quantify the deviation from background radiance
- Spectral dependence gives size.

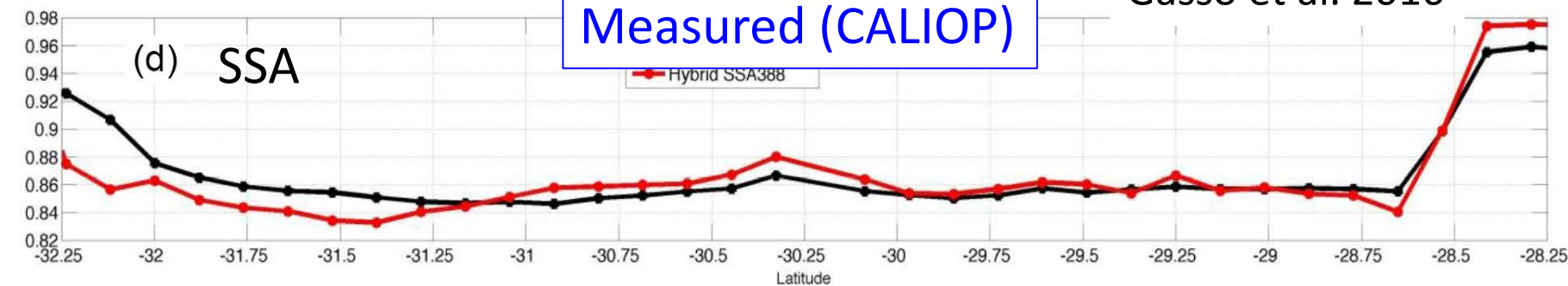
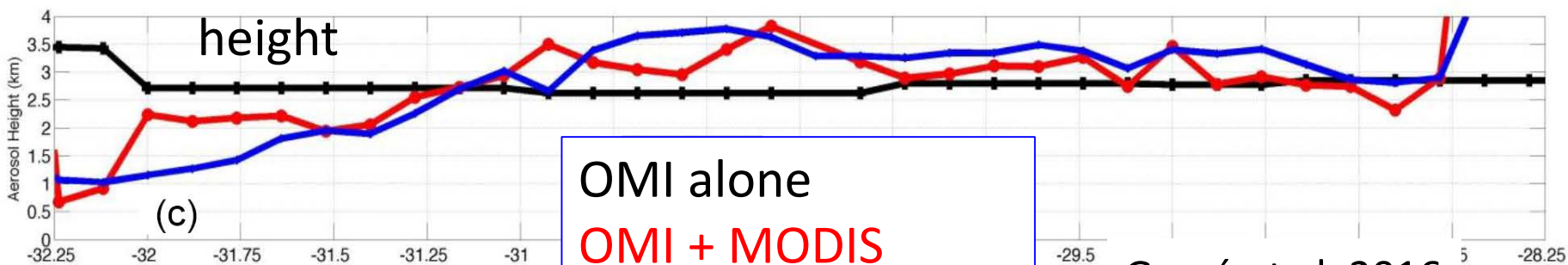
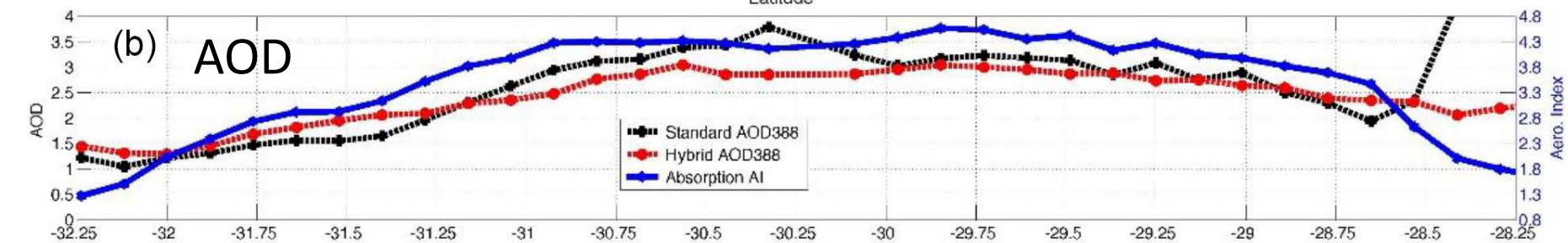
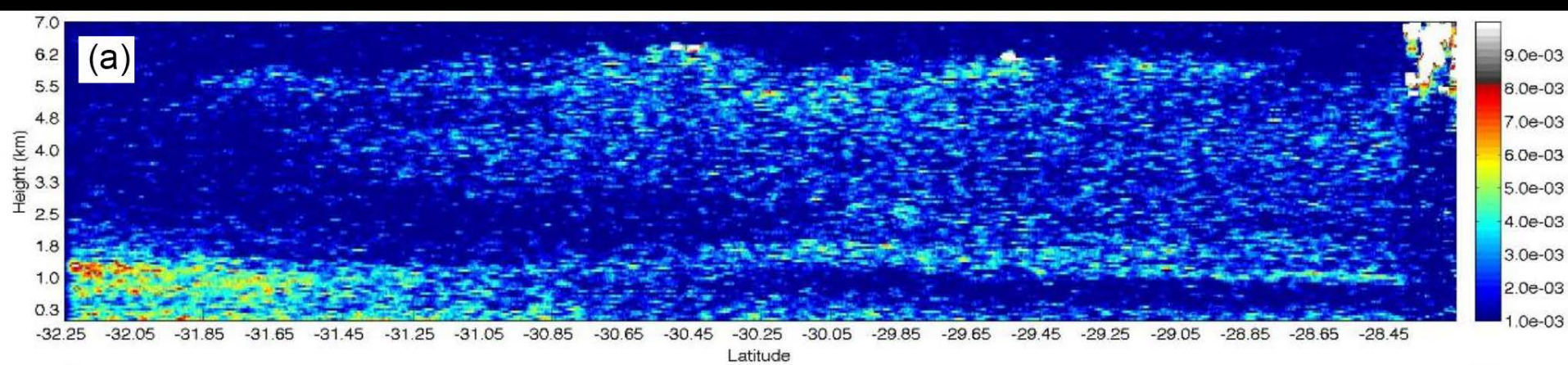
The UV approach...

- Quantify the deviation from Rayleigh scattering
- Spectral dependence gives absorption

Combining approaches (MODIS + OMI) we should be able to retrieve **all 3 parameters: AOD, SSA and h**

Retrieval of aerosol height (combined L2 products, not radiances)



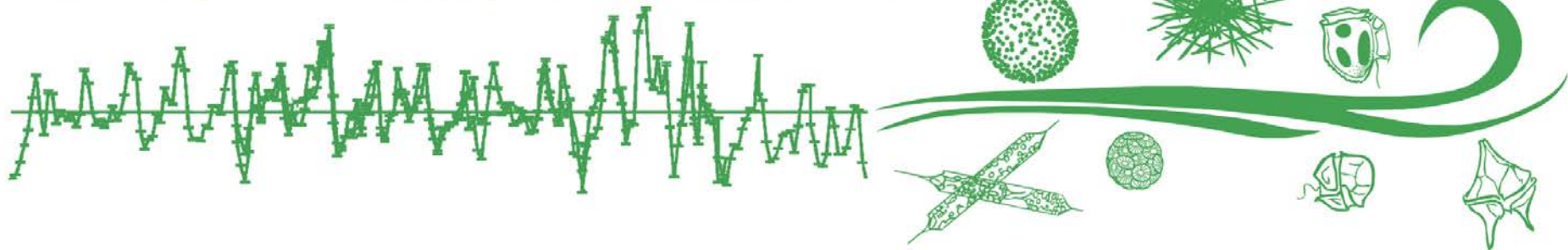


Gassó et al. 2016

Plankton, Aerosol Cloud ocean Ecosystems NASA mission for 2022



NASA's long-term chlorophyll record is *unparalleled*



PACE will show *all chlorophyll is not created equal*

Primary instrument : Ocean Color Instrument (OCI)

OCI Specifics:

- Single detector, rotating telescope scanner (like SeaWiFS)
- 20-degree tilt to avoid sun glint
- Monthly lunar calibration of all science detectors
- Ground sample distance ~ 1 square kilometer at nadir
- 5 nanometer (nm) resolution from 350 to 890 nm
- Plus short-wave infrared (SWIR) bands centered on 940, 1240, 1380, 1640, 2130 & 2250 nm

Primary instrument : Ocean Color Instrument (OCI)

OCI Specifics:

- Single detector, rotating telescope scanner (like SeaWiFS)
- 20-degree tilt to avoid sun glint
- Monthly lunar calibration of all science detectors
- Ground sample distance ~ 1 square kilometer at nadir
- 5 nanometer (nm) resolution from 350 to 890 nm
- Plus short-wave infrared (SWIR) bands centered on 940, 1240, 1380, 1640, 2130 & 2250 nm

Primary instrument : Ocean Color Instrument (OCI)

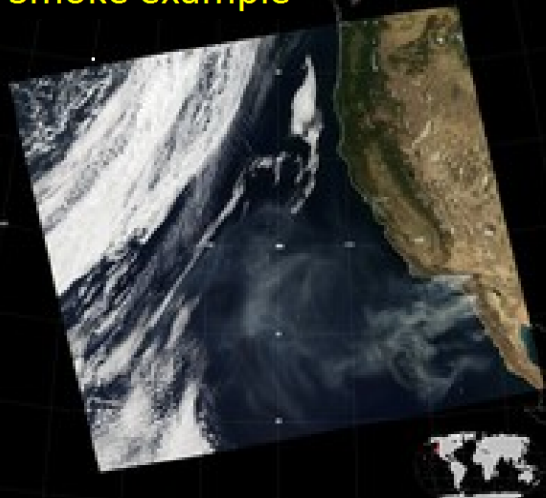
OCI Specifics:

- Single detector, rotating telescope scanner (like SeaWiFS)
- 20-degree tilt to avoid sun glint
- Monthly lunar calibration of all science detectors
- Ground sample distance ~ 1 square kilometer at nadir

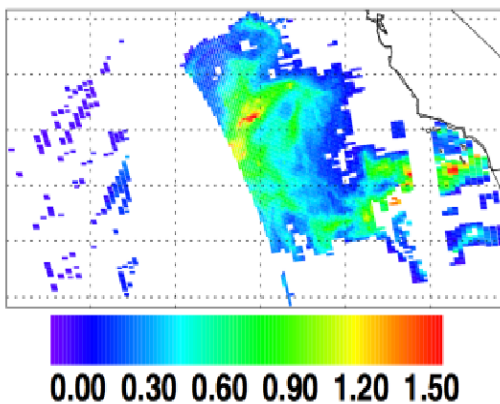
1 km

- 5 nanometer (nm) resolution from 350 to 890 nm
- Plus short-wave infrared (SWIR) bands centered on 940, 1240, 1380, 1640, 2130 & 2250 nm

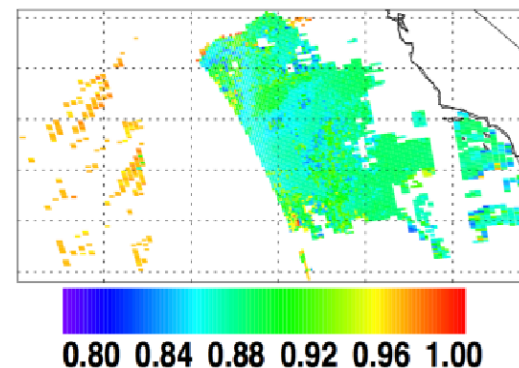
Smoke example



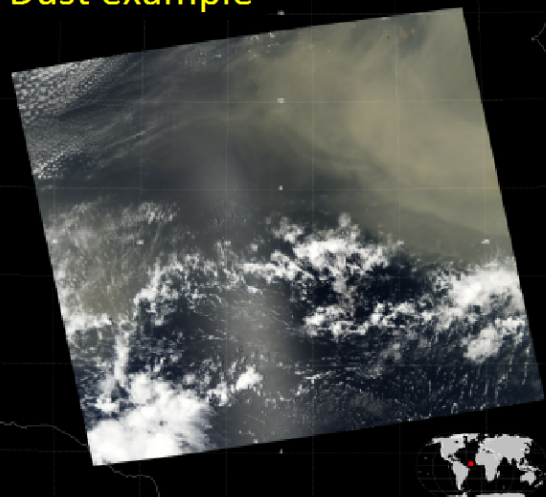
AOT 550 nm



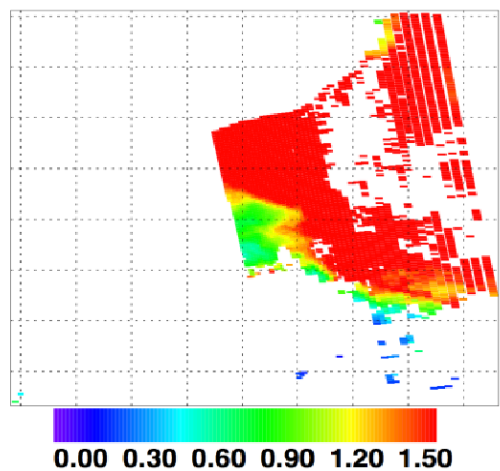
Single sca+ ering albedo 388 nm



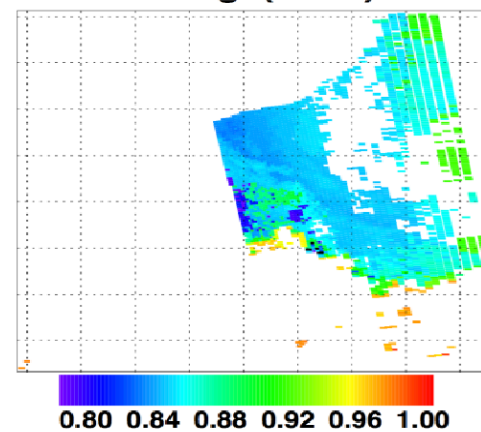
Dust example



AOT 550 nm



Single sca+ ering albedo 388 nm



Expected for PACE from OCI

Spectral AOD, SSA and height over oceans
(when AOD₅₅₀ is sufficiently high ~ 0.30)

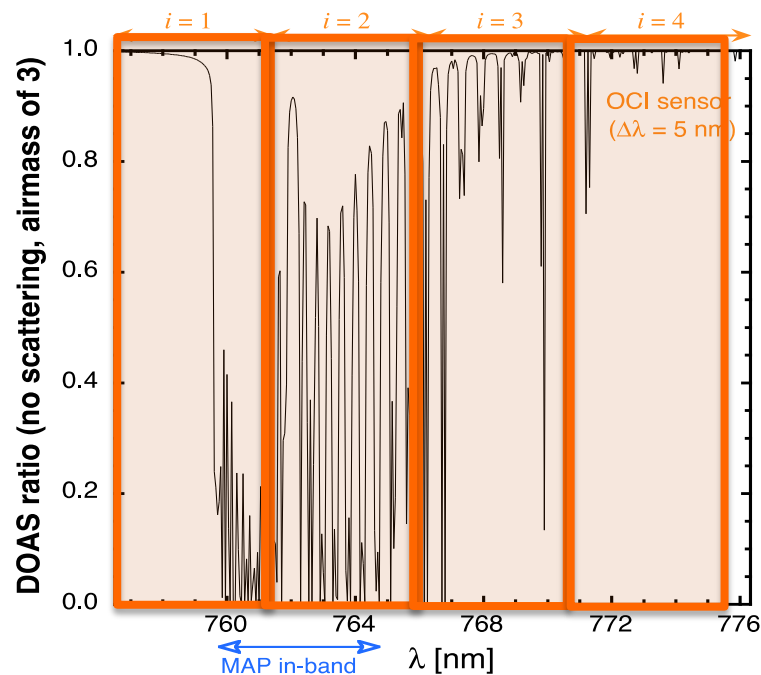
Land not yet explored.

In forward processing, at 3 to 10 km,
Across the OCI swath (2-day coverage)

Primary instrument : Ocean Color Instrument (OCI)

OCI Specifics:

- Single detector, rotating telescope scanner (like SeaWiFS)
- 20-degree tilt to avoid sun glint
- Monthly lunar calibration of all science detectors
- Ground sample distance ~ 1 square kilometer at nadir
- 5 nanometer (nm) resolution from 350 to 890 nm
- Plus short-wave infrared (SWIR) bands centered on 940, 1240, 1380, 1640, 2130 & 2250 nm



Using Oxygen A-band to retrieve aerosol height

DOAS = differential optical absorption spectroscopy

O₂ : both the amount and cross-section of the gas are accurately known.

DOAS then tells us about the height of the scattering layer (0-2 km vs. 3-5 km)

Plankton, Aerosol Cloud ocean Ecosystems NASA mission for 2022



Primary instrument: OCI for ocean color,

but also **an excellent aerosol instrument**:

- Everything for aerosol that MODIS and VIIRS offers
- Except the thermal channels for cloud mask
- Plus, UV channels at 1 km
- And Oxygen A-band at 5 nm

New opportunities for aerosol absorption and height

Secondary instrument: Multi-angle imaging polarimeter

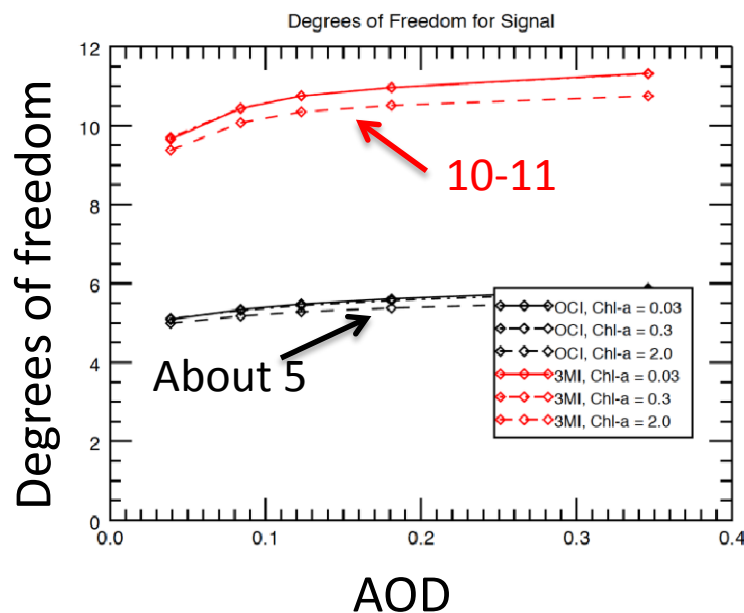
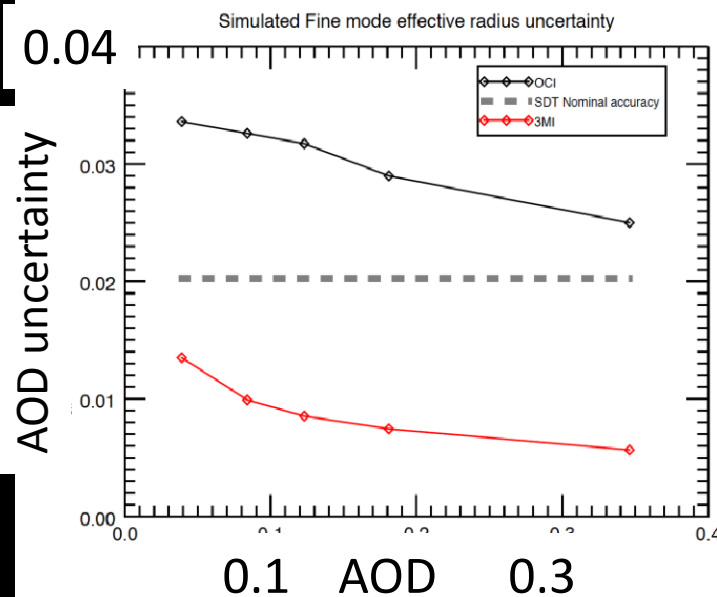
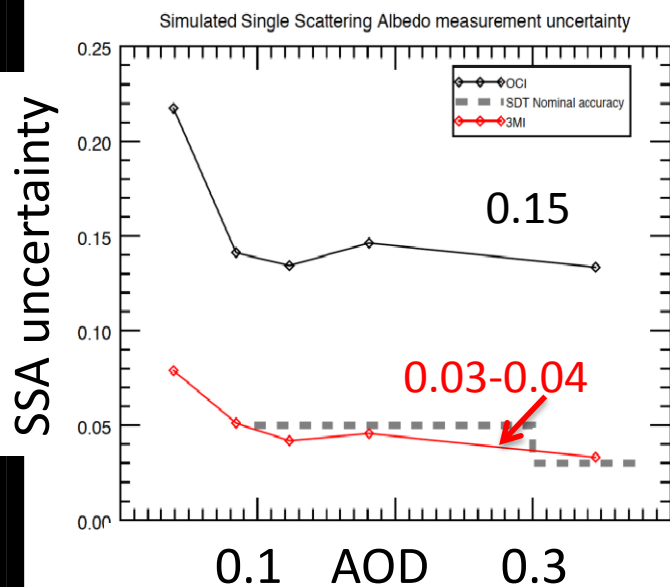


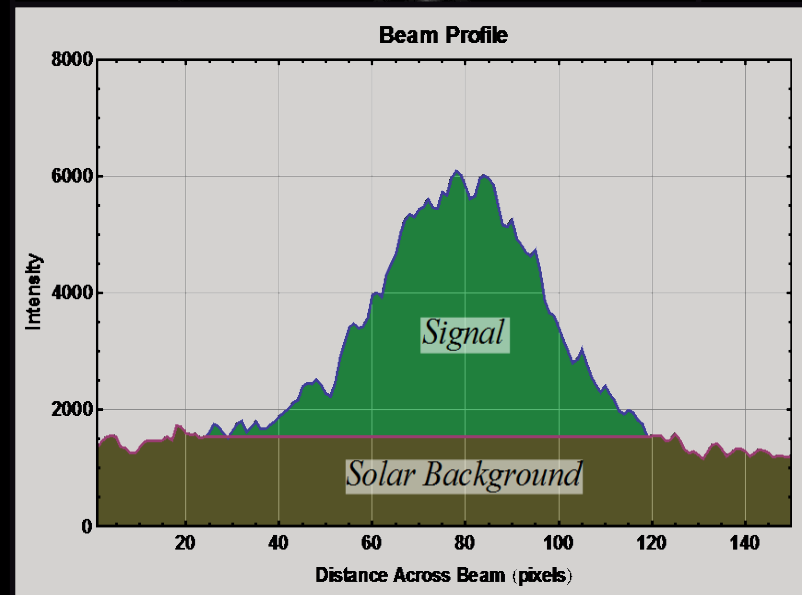
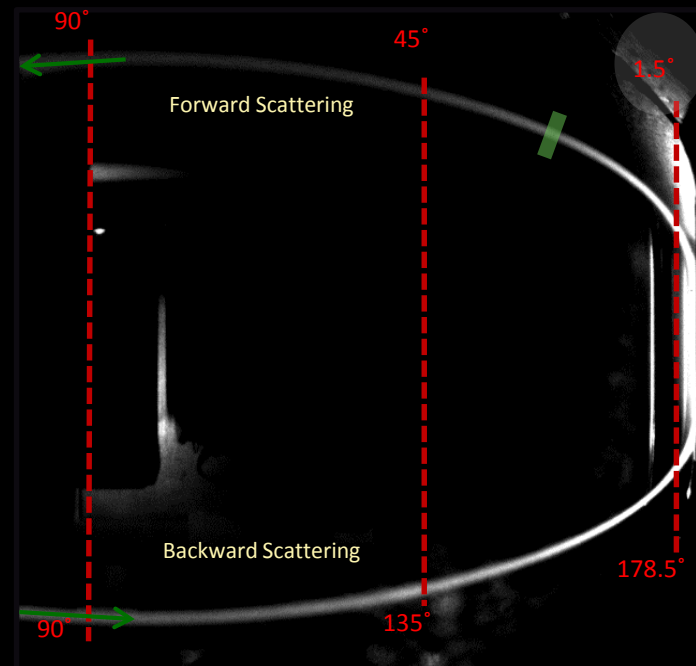
Figure 6. Left. Calculated degrees of freedom (information content) from K. Knobelspiesse candidate multi-angle polarimeter, the European 3MI instrument (red), as function of calculated degrees of freedom. Theoretical calculations

OCI (single angle radiometer) in black
3MI (multiangle polarimeter) in red

Bottom. Calculated uncertainties in retrievals of single scattering albedo (bottom left) and fine mode effective radius (bottom right) for the two instruments, following the same color scheme. The dashed line indicates the uncertainty requirements of these parameters, defined by the PACE Science Definition Team report.



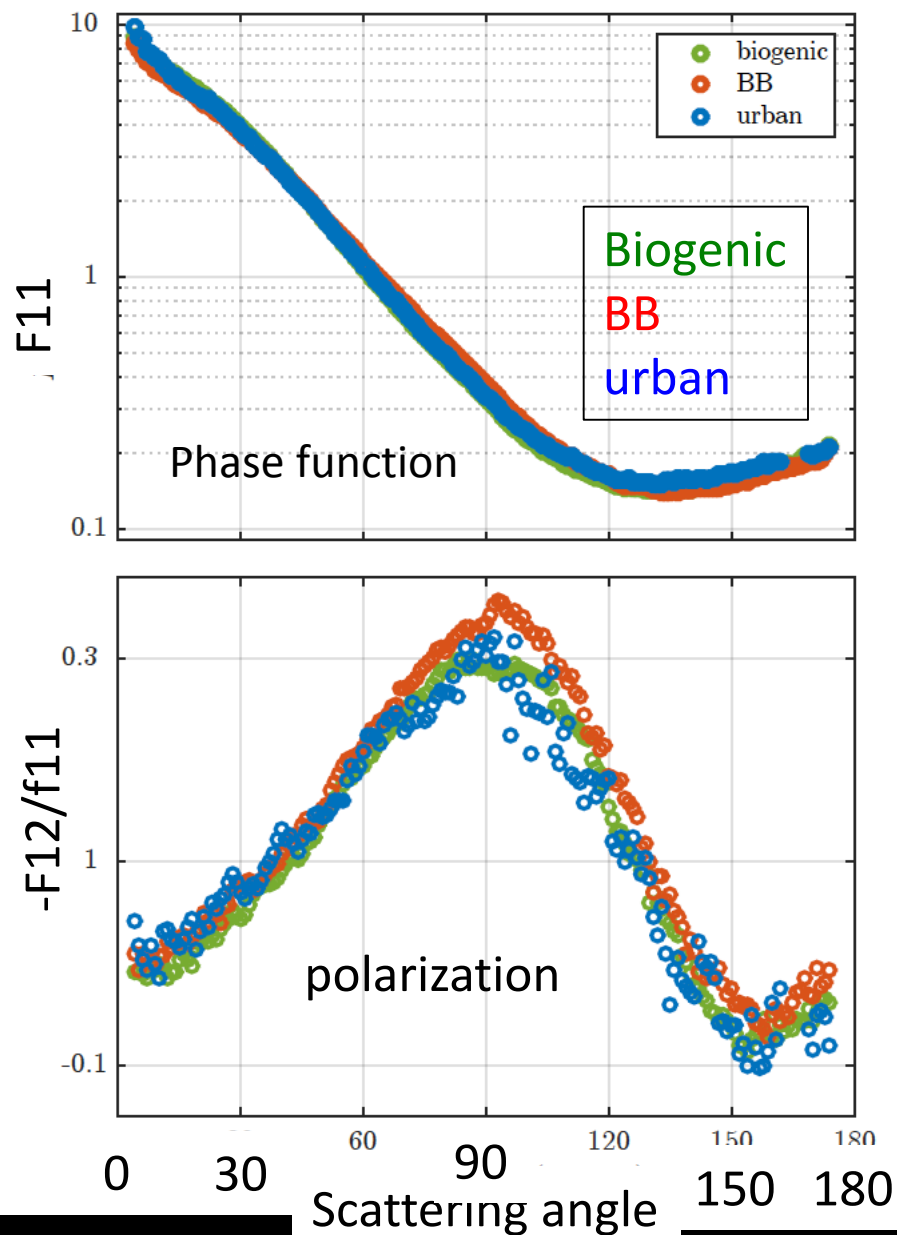
UMBC PI-Neph



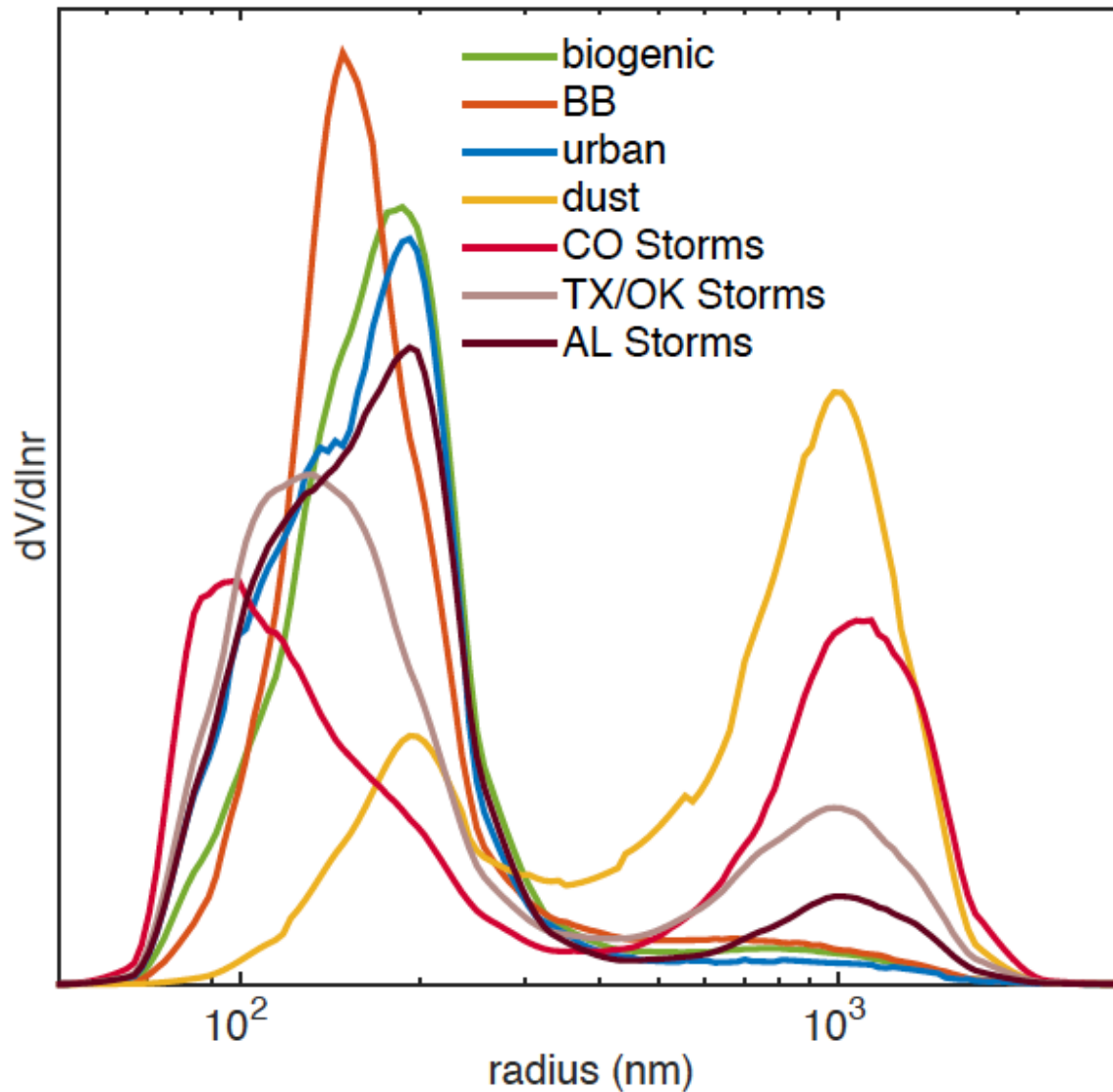
Espinosa, Dolgos and the UMBC team

UMBC PI-Neph measurements of 3 different fine mode aerosols from SEAC4RS

Espinosa et al., 2017



Volume size distribution



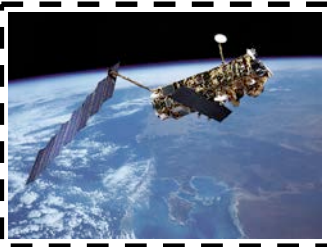
GRASP retrieval
applied to
PI-Neph
measurements

Espinosa et al. (to be
submitted)

GRASP: Generalized Retrieval of Aerosol and Surface Properties

Dubovik et al.

MERIS



AERONET



POLDER



lidar



AERONET

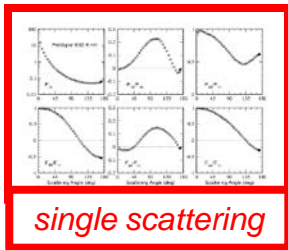


Sentinel -

4

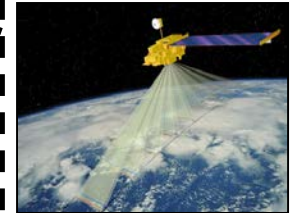


laboratory

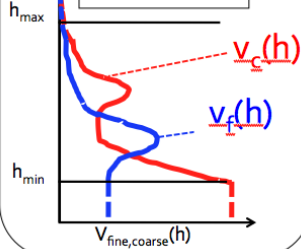


GRASP
open source

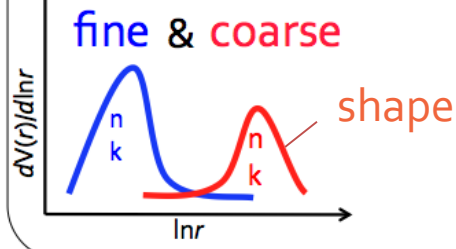
MISR



PROFILES of
AEROSOL

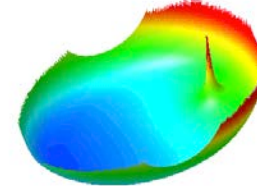


COLUMNAR AEROSOL

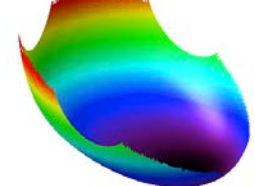


Surface reflectance

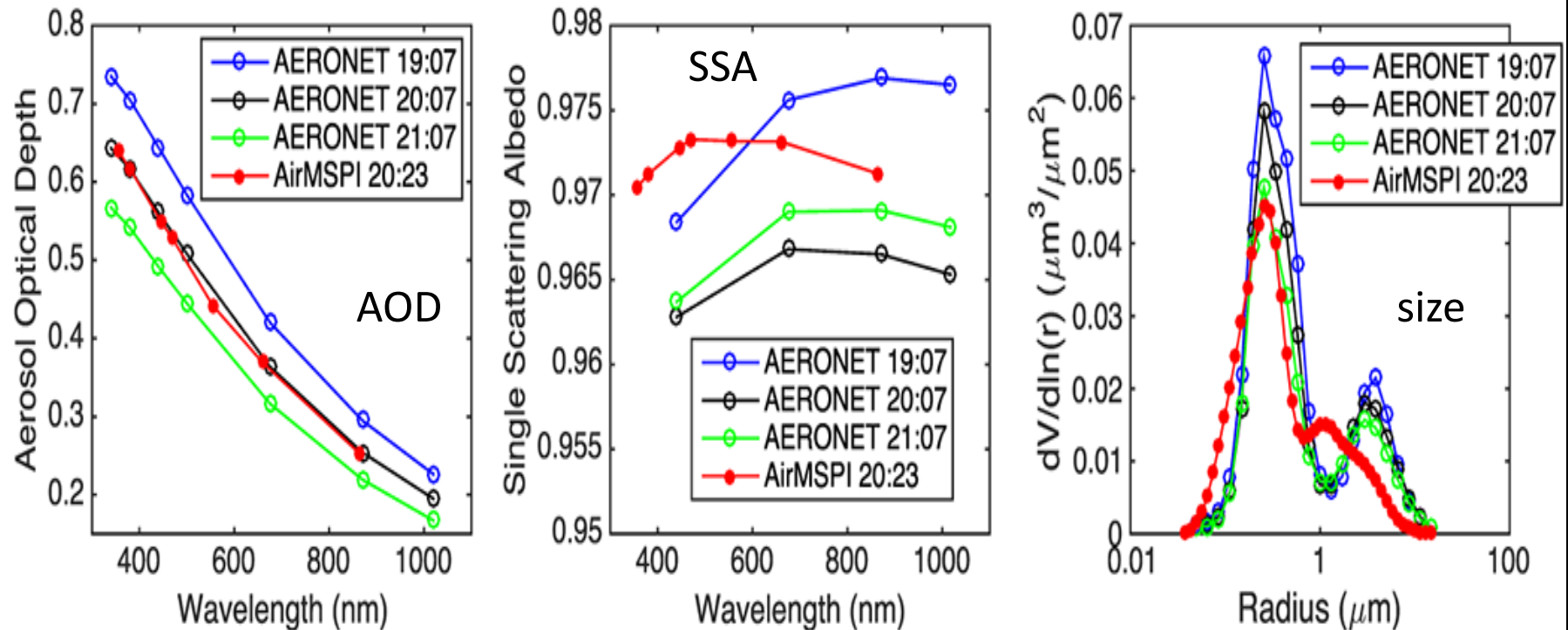
BRDF



BPDF



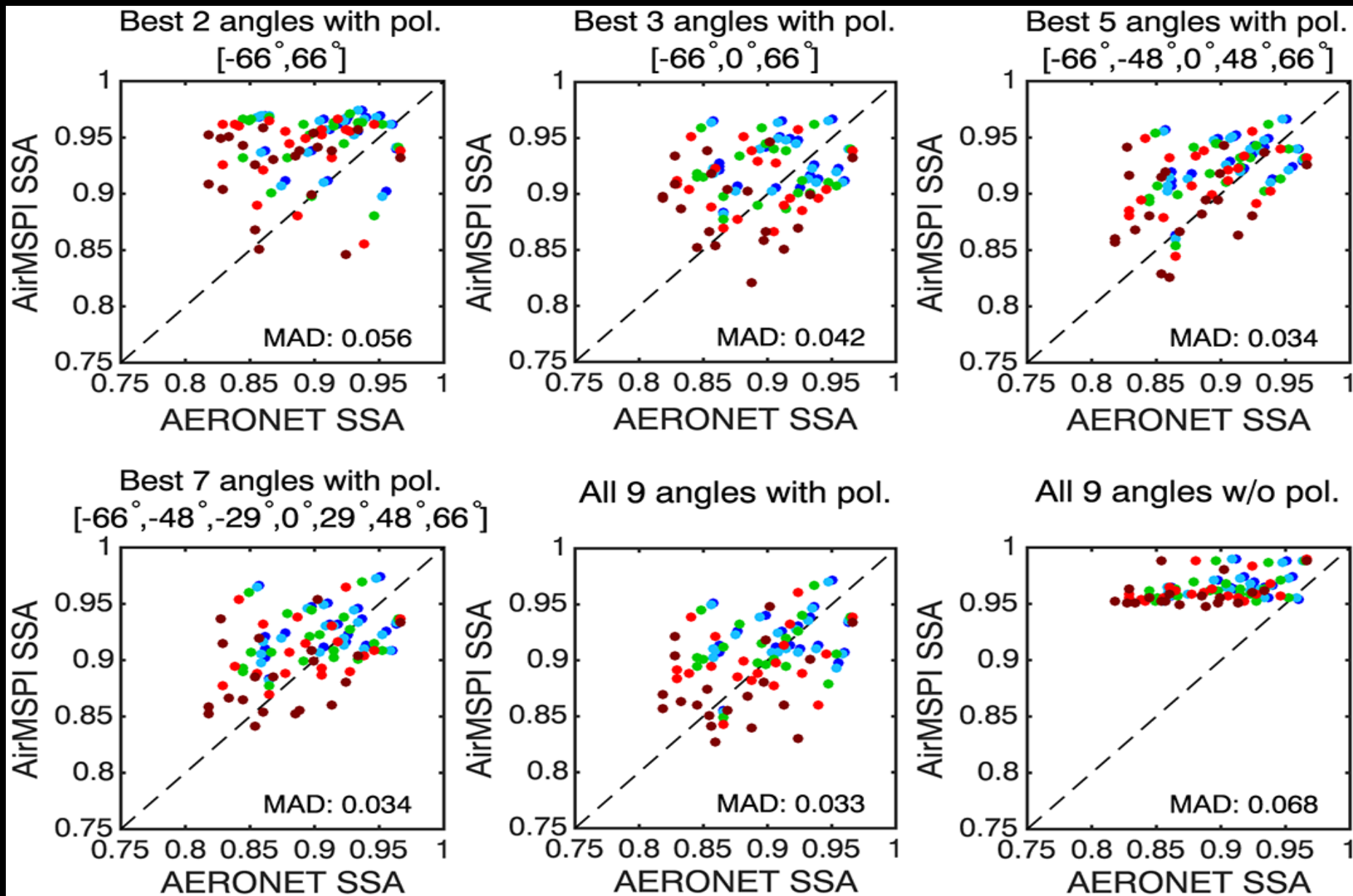
Aerosol retrievals from airborne multi-angle polarimeter (AirMSPI)



AirMSPI on NASA ER-2 over Fresno CA (in red)

Near-time AERONET retrievals at Fresno station (other colors)

Xu et al. (2017)



Where are we heading?

Towards broader aerosol-relevant spectra;

Finer spectral resolution;

Finer spatial resolution for UV;

Multi-angle polarimeters;

Retrievals of more aerosol properties;

With better accuracy;

Expanding retrievals to over clouds and difficult surfaces;

Simultaneous retrievals of aerosol + surface;

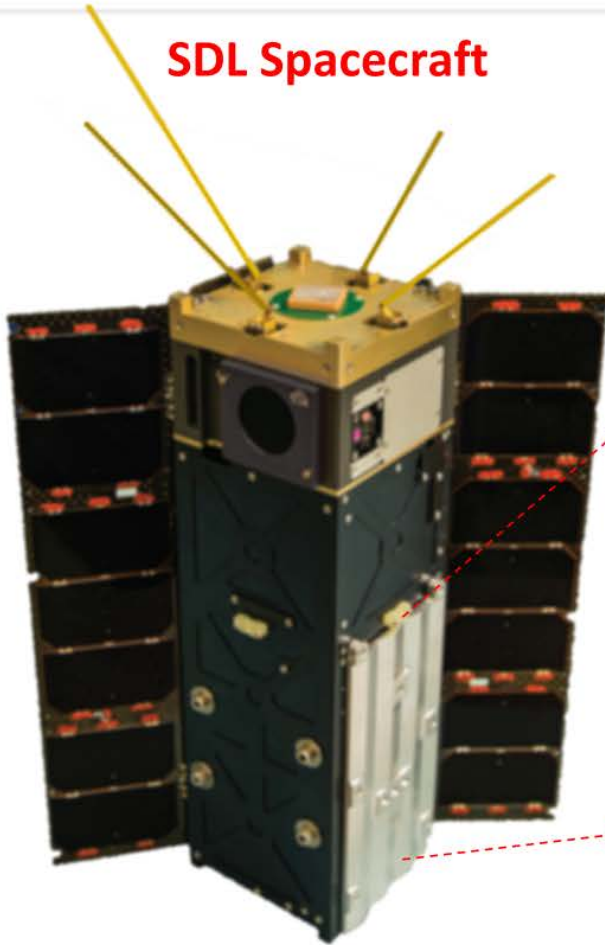
Advanced retrieval algorithms that can handle all this
information

How will we get there?

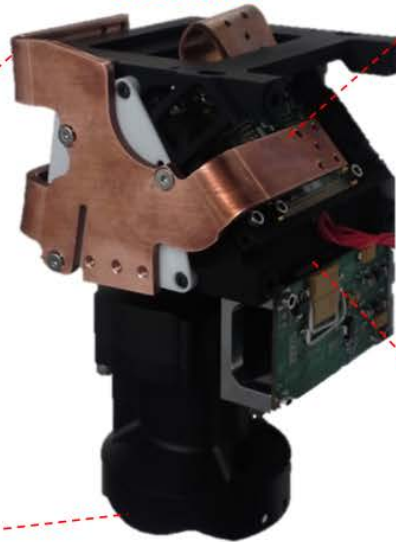
- PACE OCI: 2022, but in political limbo
- PACE polarimeter: even less assured
- MetOP 3MI: 2018 and continuing
- MAIA: an instrument without a launch date
- HARP Cubesat: early 2018

Photos of Actual Instrument & Spacecraft

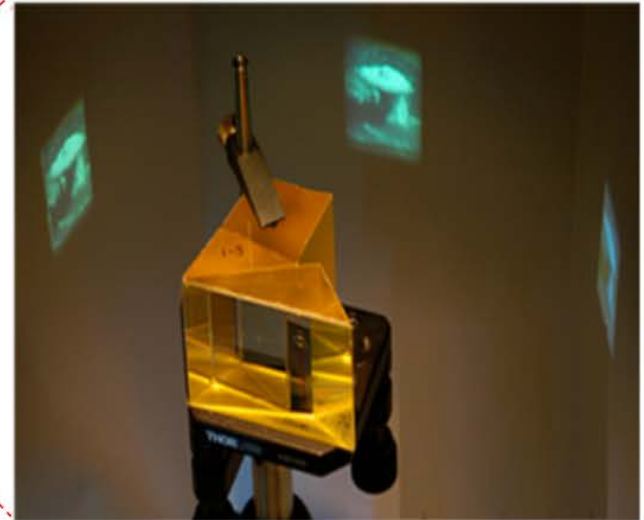
SDL Spacecraft



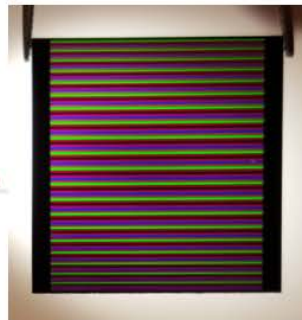
UMBC
Sensor



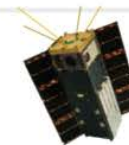
HARP Prism



HARP
Stripe
Filter

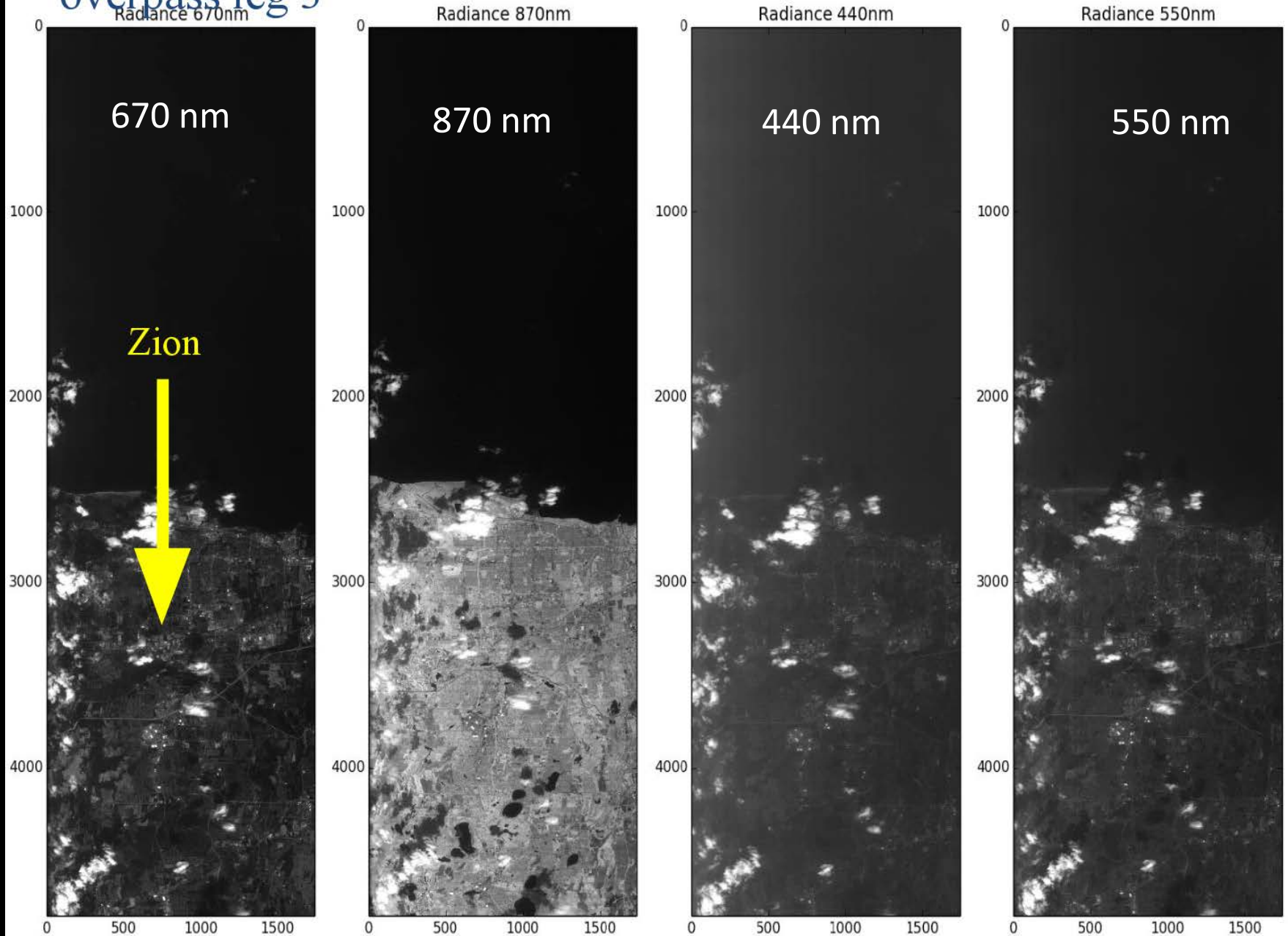


UMBC
Martins et al.

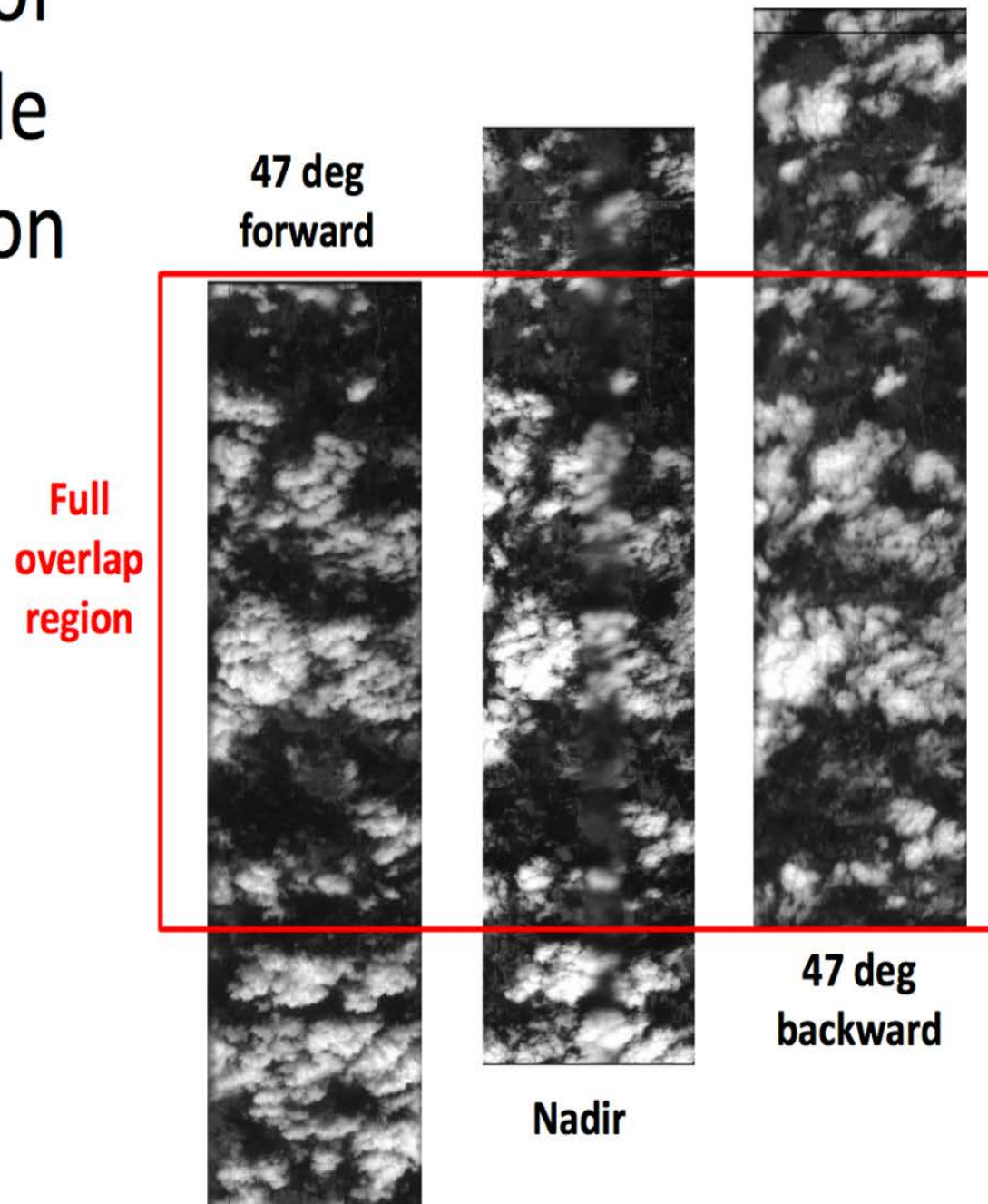


HARP

Preliminary Results from LMOS, 12 June 2017 – AirHARP Zion overpass leg 3



Example of Multiangle observation



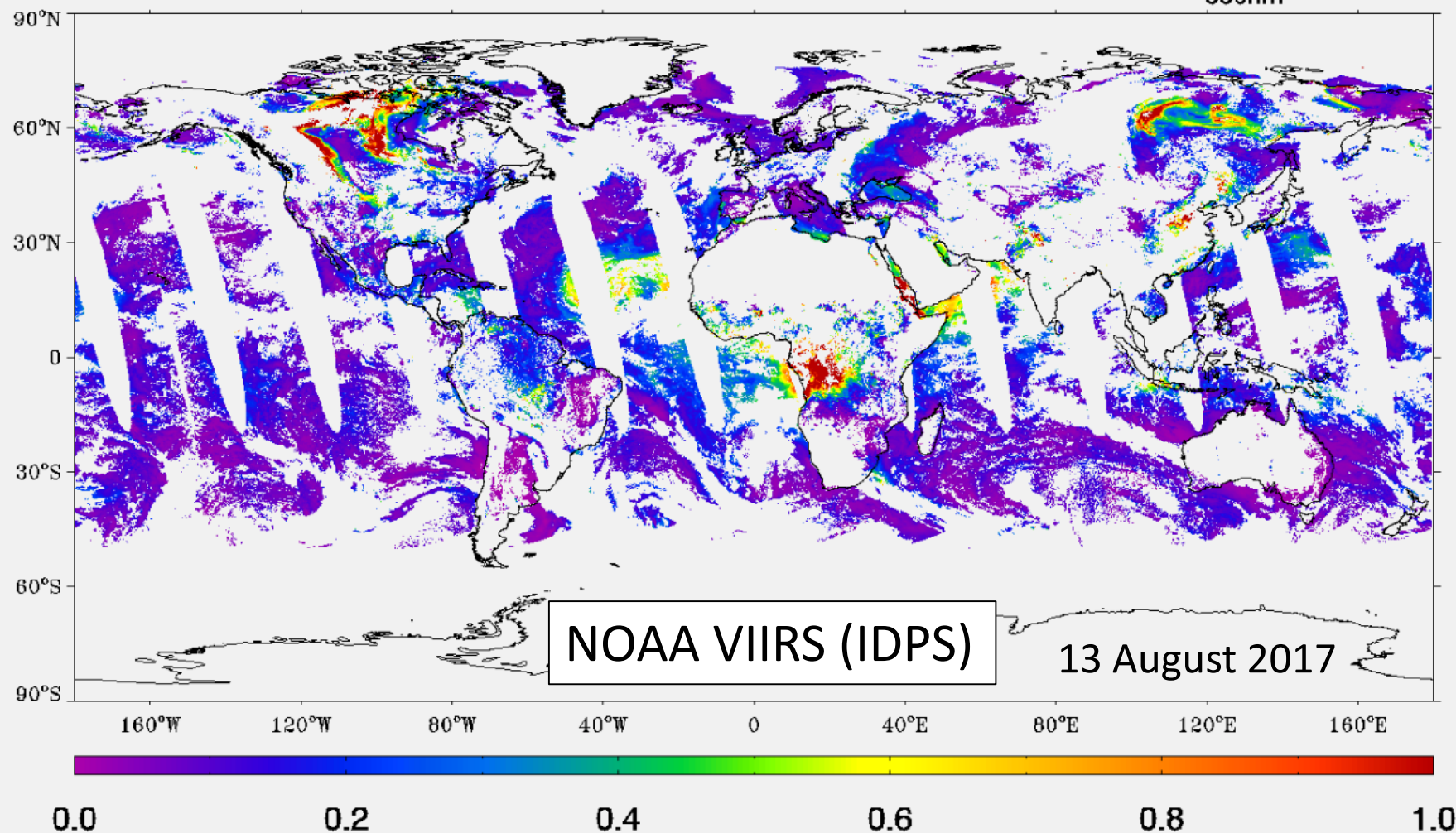
Comparison of NOAA VIIRS and NASA MODIS Aerosol Products

Lorraine A. Remer¹, Jennifer Christhilf^{1,2}, Robert C. Levy²

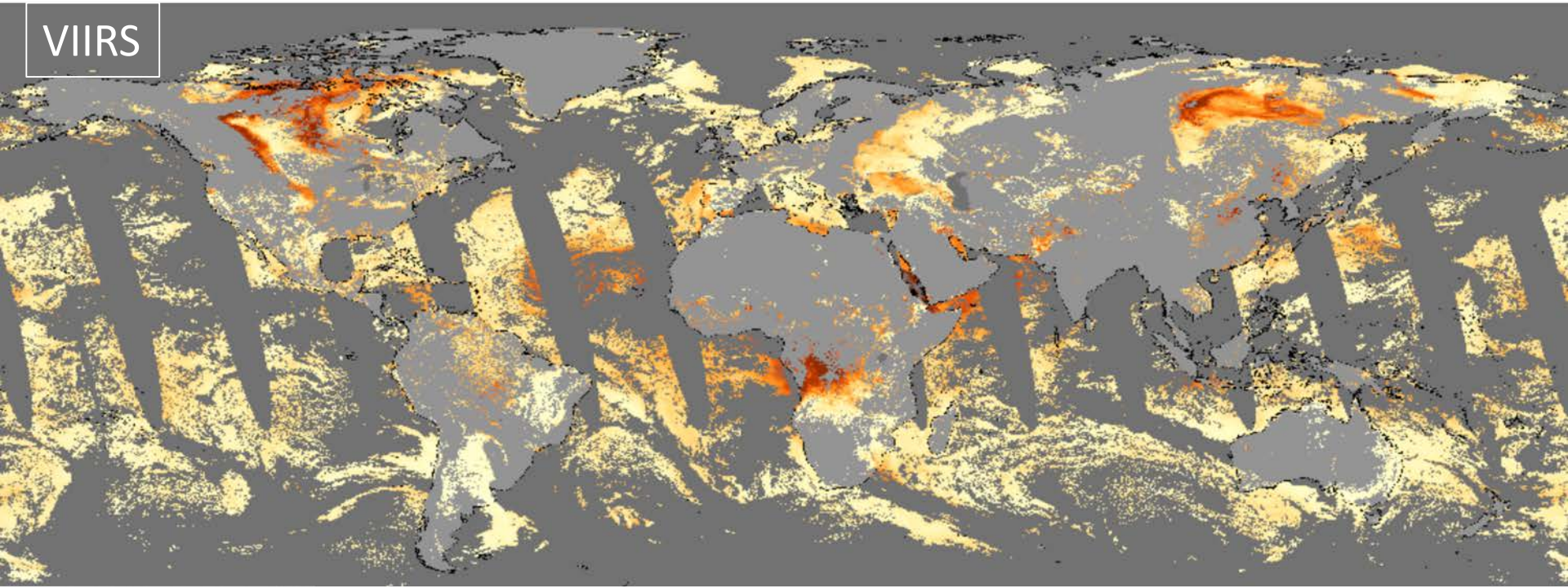
¹UMBC, ²NASA/GSFC



20170813 0.25°x0.25° Gridded High Quality EDR AOT_{550nm}



VIIRS

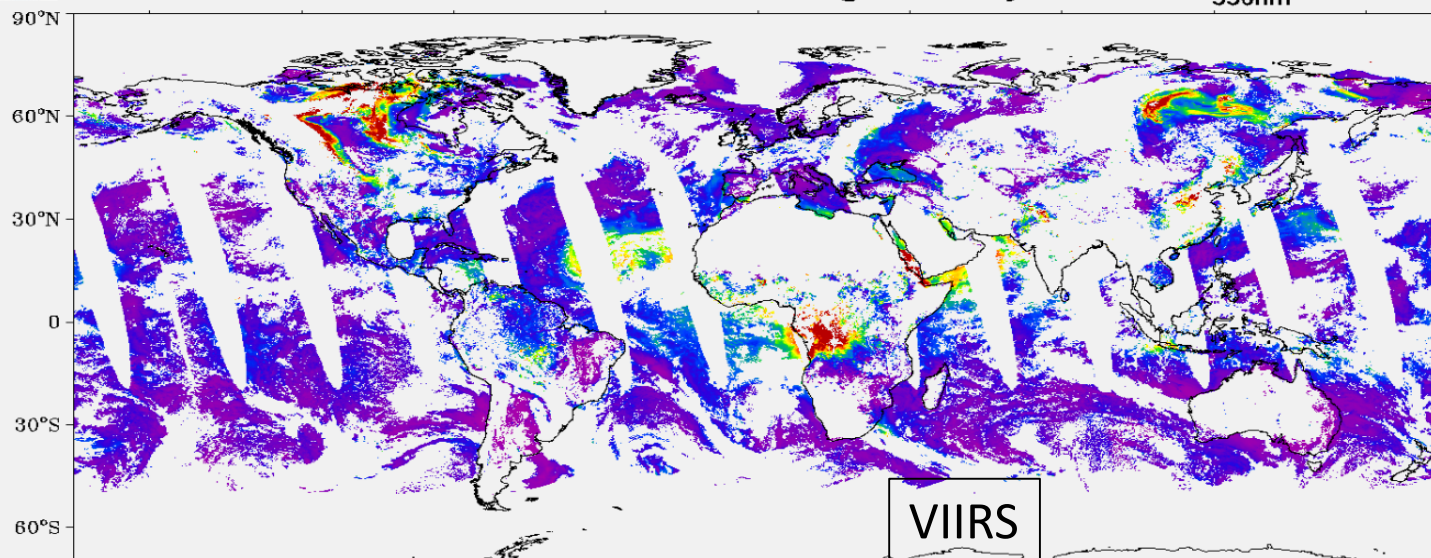


MODIS



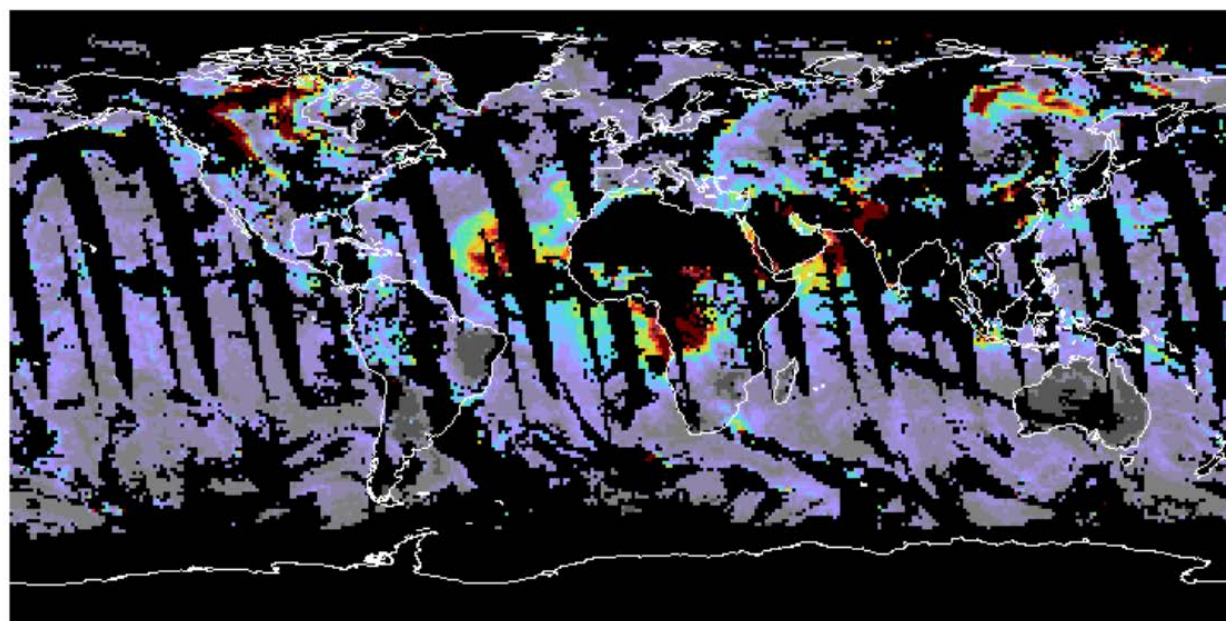


20170813 0.25°x0.25° Gridded High Quality EDR AOT_{550nm}



Aerosol_Optical_Depth_Land_Ocean_Mean

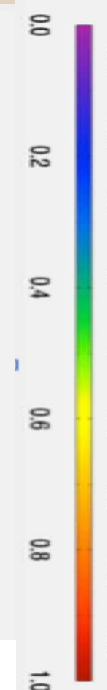
13Aug2017
0.80



MODIS/Aqua

MYD08_D3.A2017225.006.2017226175038.hdf

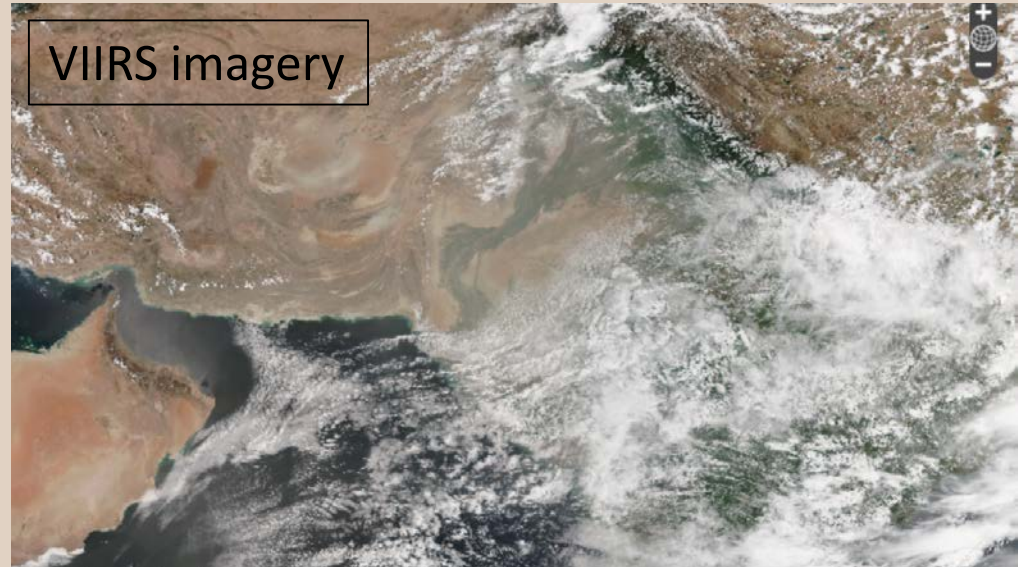
none



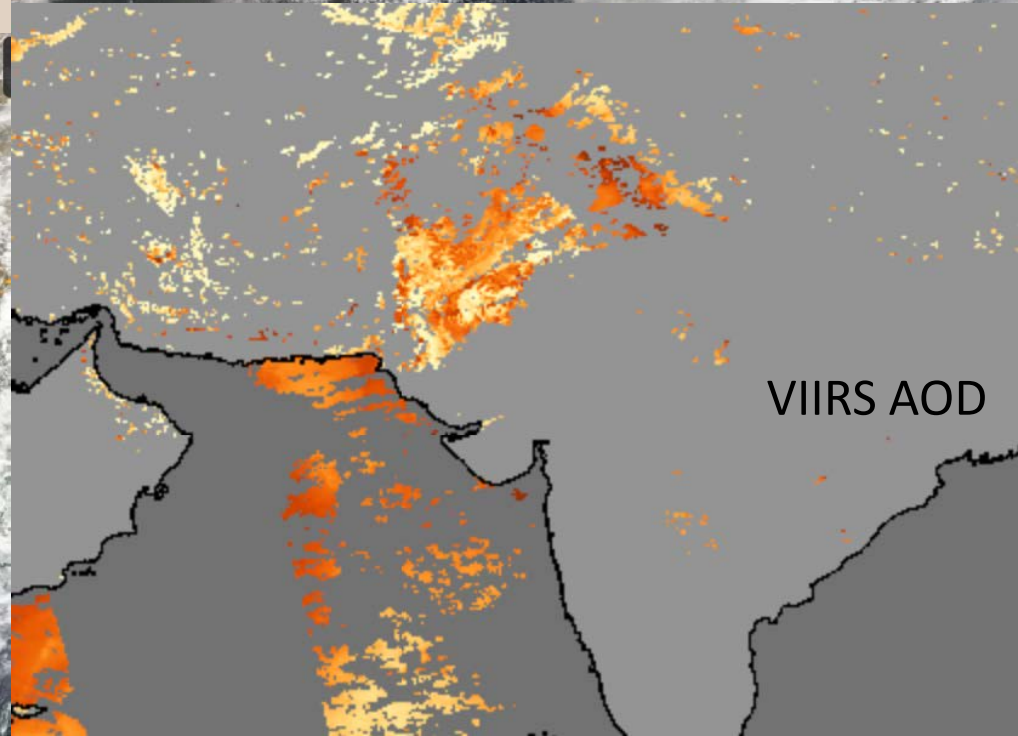
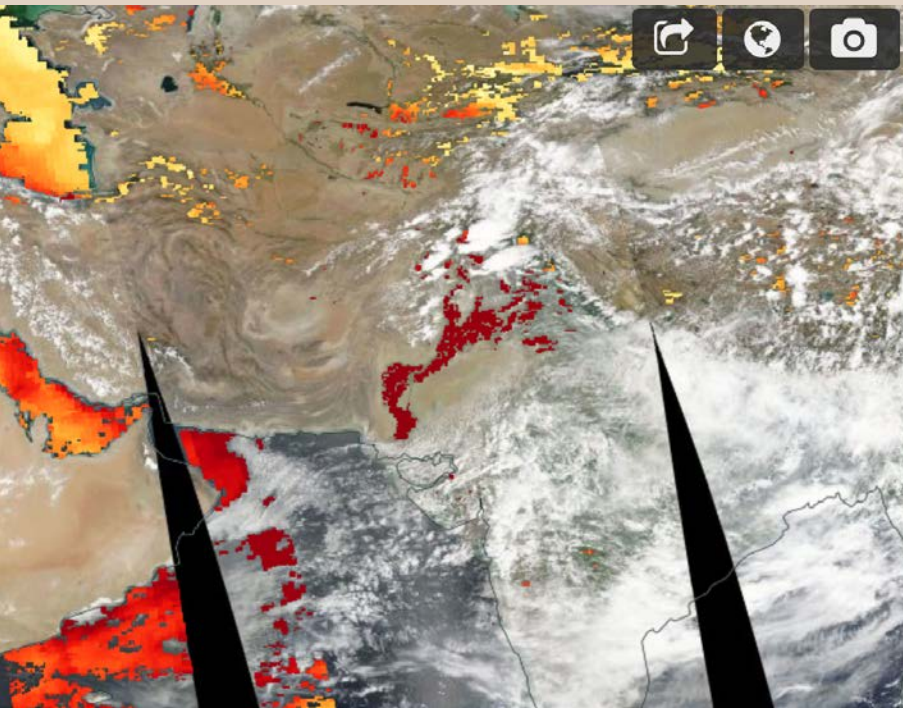
IDPS
Daily
0.25 deg
Gridded
From 6 km
High QA

DT
Daily
1 deg
Gridded
From 10 km
High QA

Real color imagery and
native resolution AOD
13 August 2017



MODIS Aqua AOD and imagery



Wavelength differences

Swath differences

Orbit differences

Spatial resolution differences

Calibration differences

Algorithm differences

>>>> Sampling differences

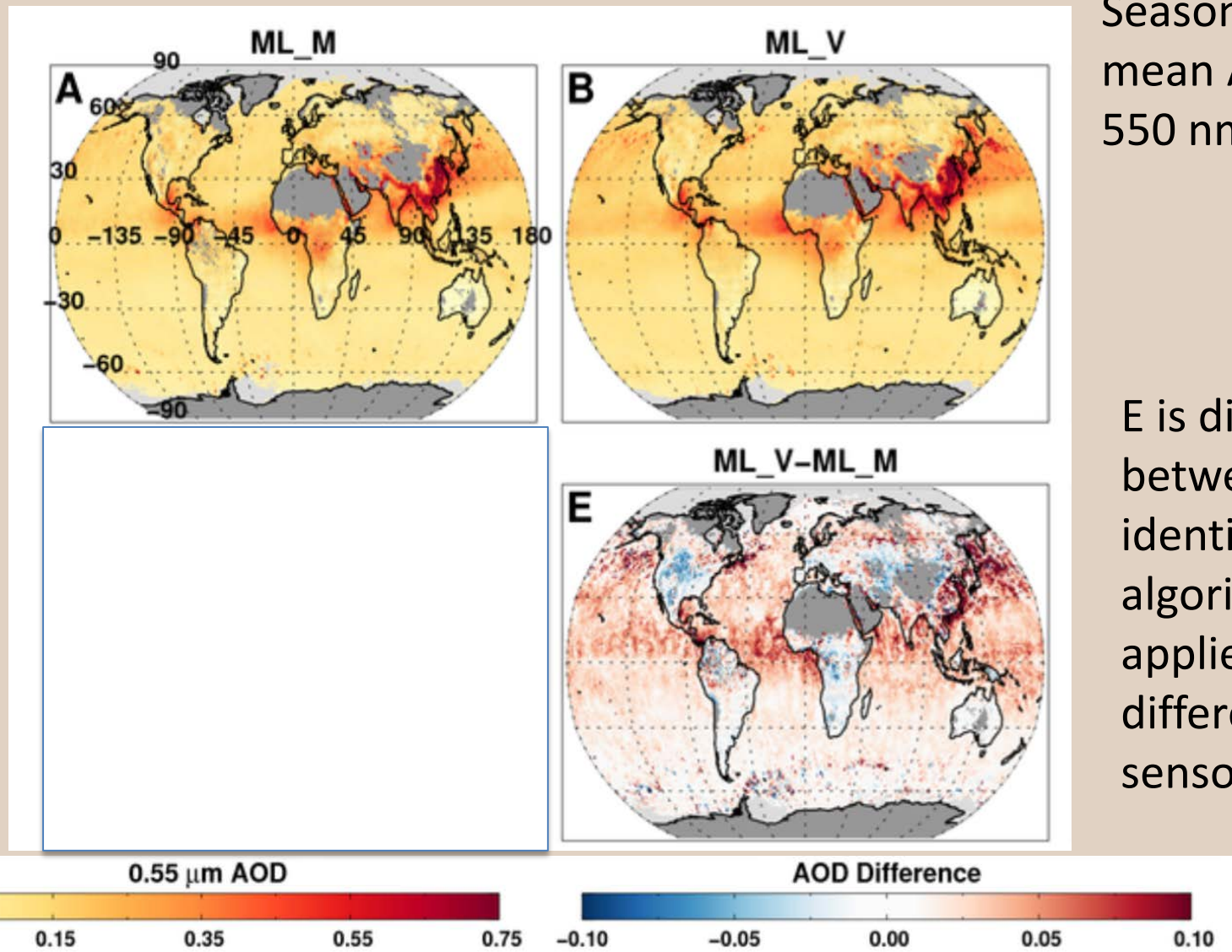
>>>> Retrieval differences

>>>> Differences in means

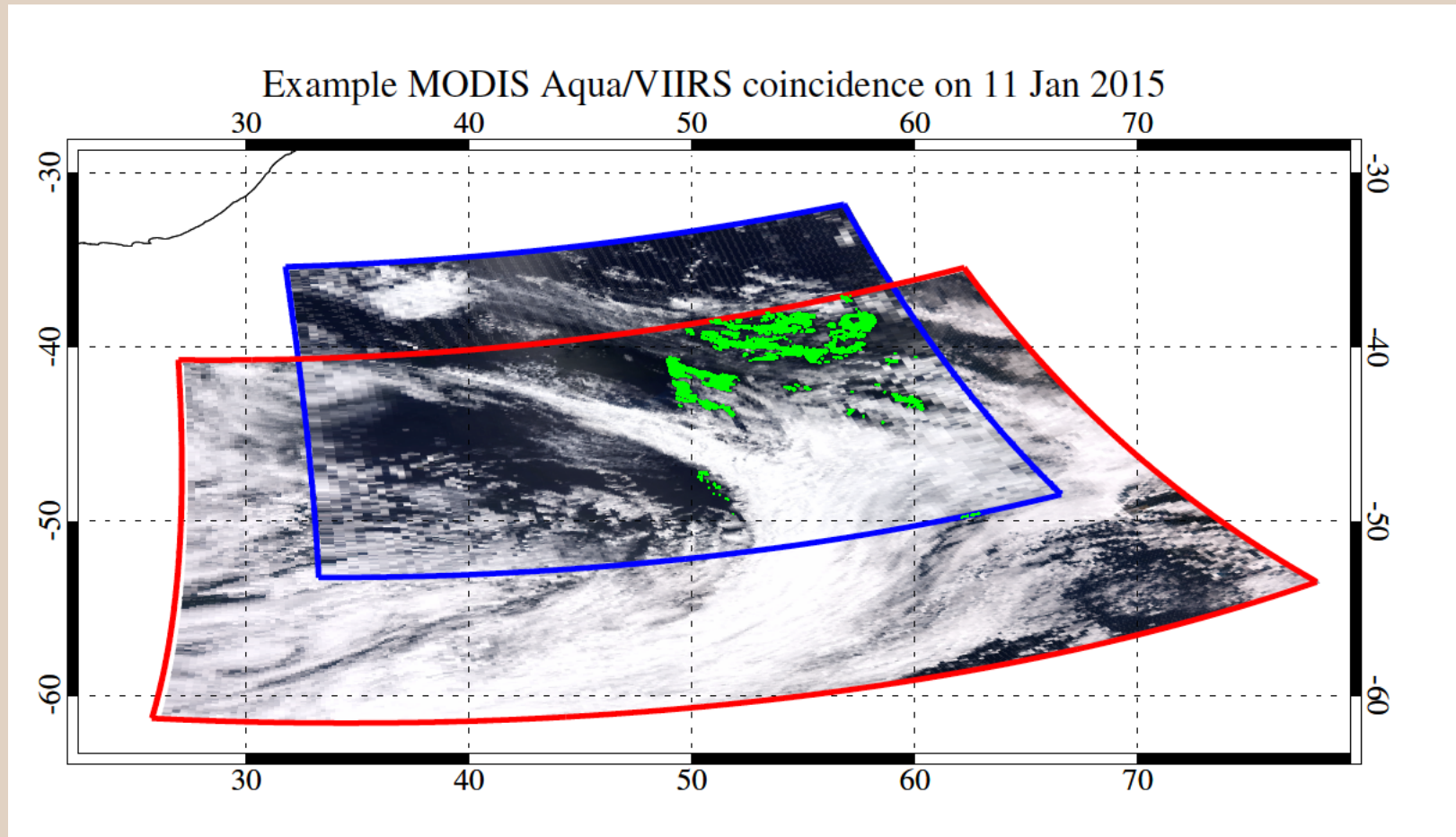
A & B are identical algorithms

Seasonal (MAM)
mean AOD at
550 nm

E is difference
between
identical
algorithms
applied to
different
sensors (B-A)

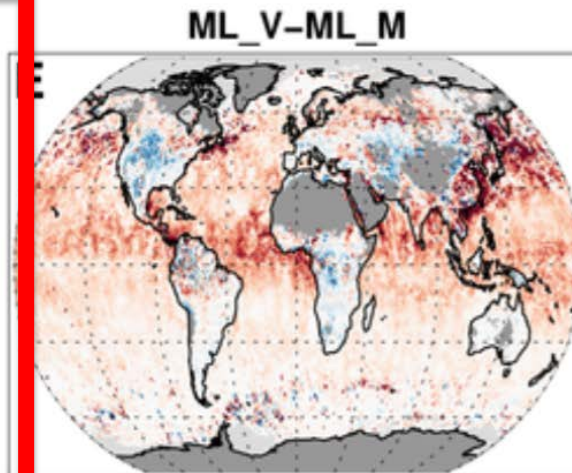
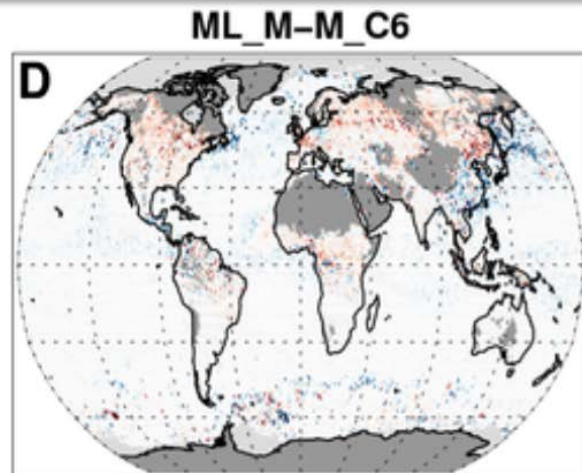
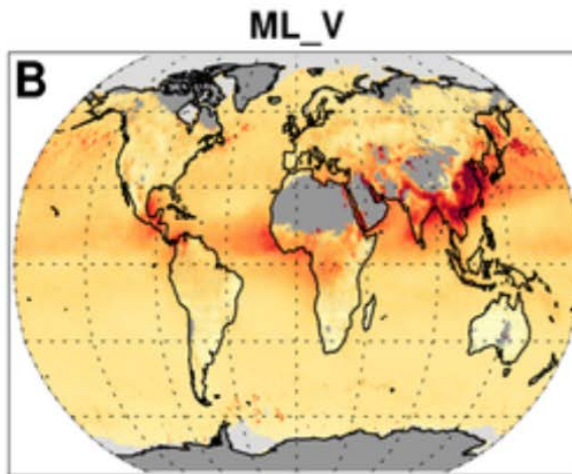
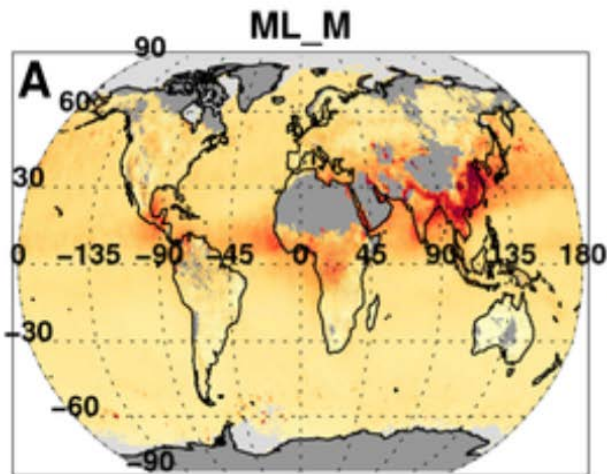


A calibration investigation using “match files” (Sayer et al., 2017)



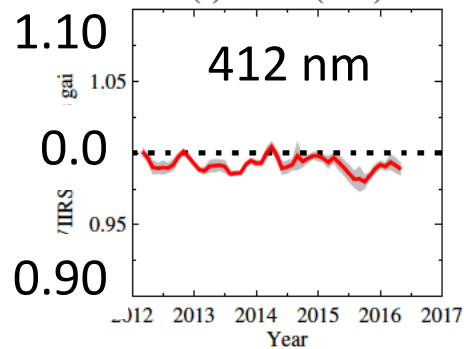
From SIPS:

MCST MODIS Aqua Collection 6 data (at 1 km pixel size, the MYD021KM product)
VCST VIIRS Version 1.1 data with Version 1.0.1 calibration (the VL1BM product).

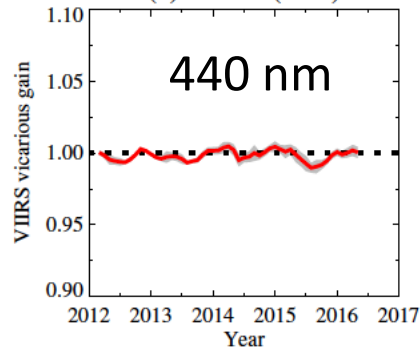


Red box outlines the difference between using the SIPS MODIS input and the operational MODIS product.

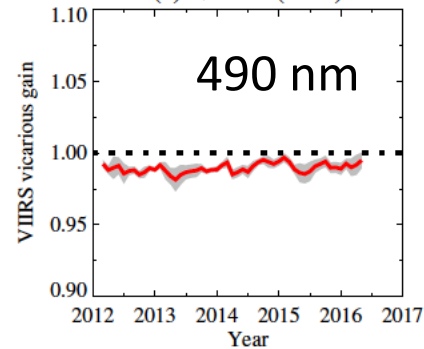
(a) 412 nm (M01)



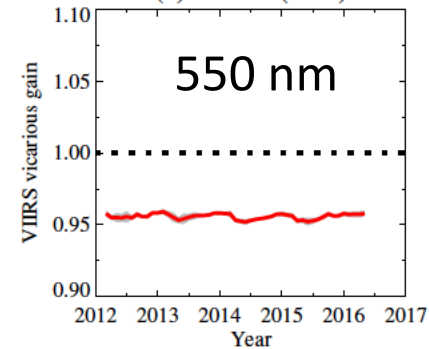
(b) 440 nm (M02)



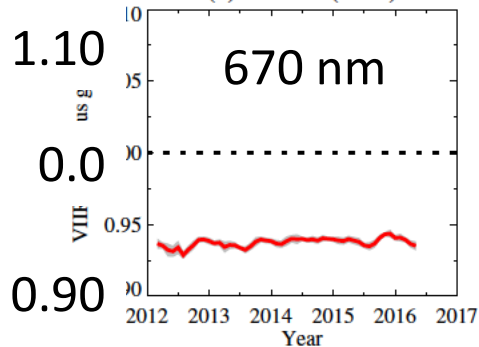
(c) 490 nm (M03)



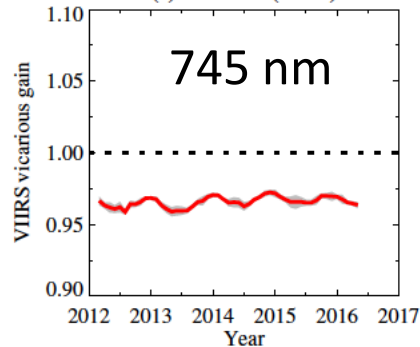
(d) 550 nm (M04)



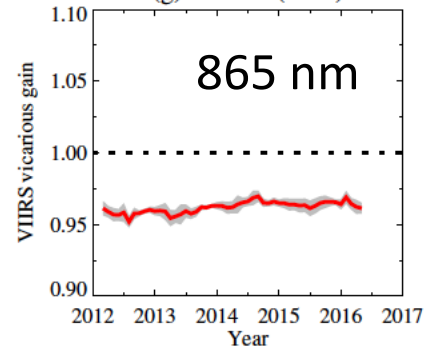
(e) 670 nm (M05)



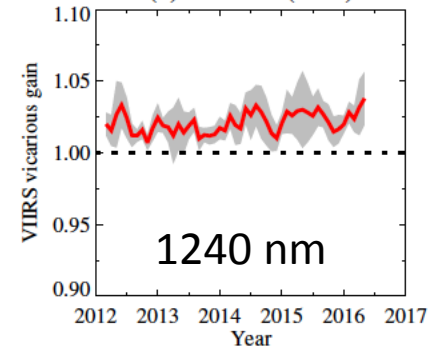
(f) 745 nm (M06)



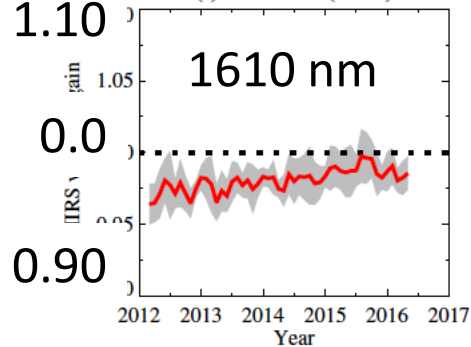
(g) 865 nm (M07)



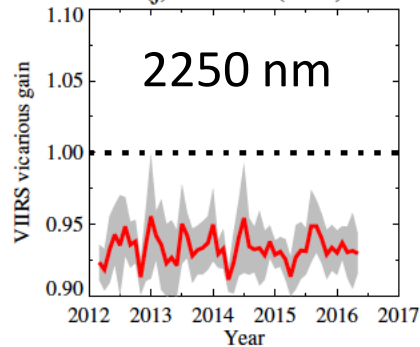
(h) 1240 nm (M08)



(i) 1610 nm (M10)



(j) 2250 nm (M11)



VIIRS Vicarious Gain

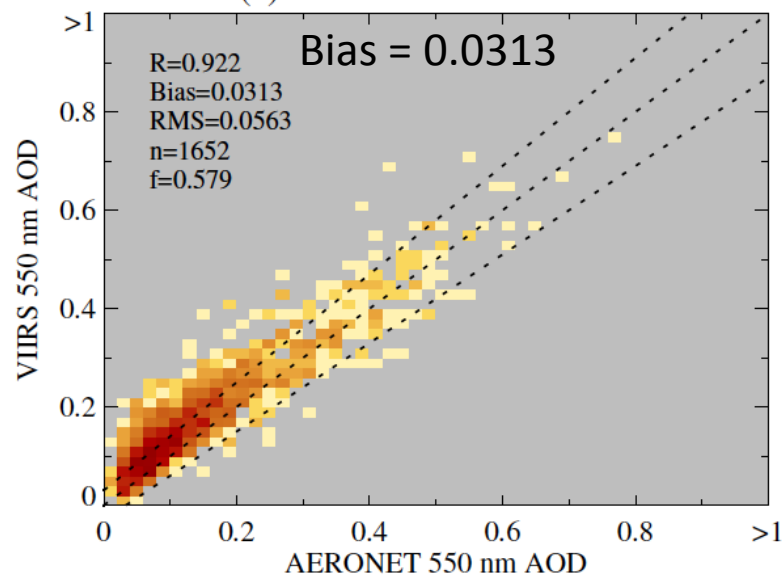
Sayer et al., 2017

Site	Latitude, °	Longitude, °	Number of matchups
ARM Graciosa	39.091	-28.029	149
Ascension Island	-7.976	-14.415	414
Ersa	43.004	9.359	624
Manus	-2.060	147.425	105
MCO Hanimaadhoo	6.776	73.183	268
Midway Island	28.210	-177.378	89

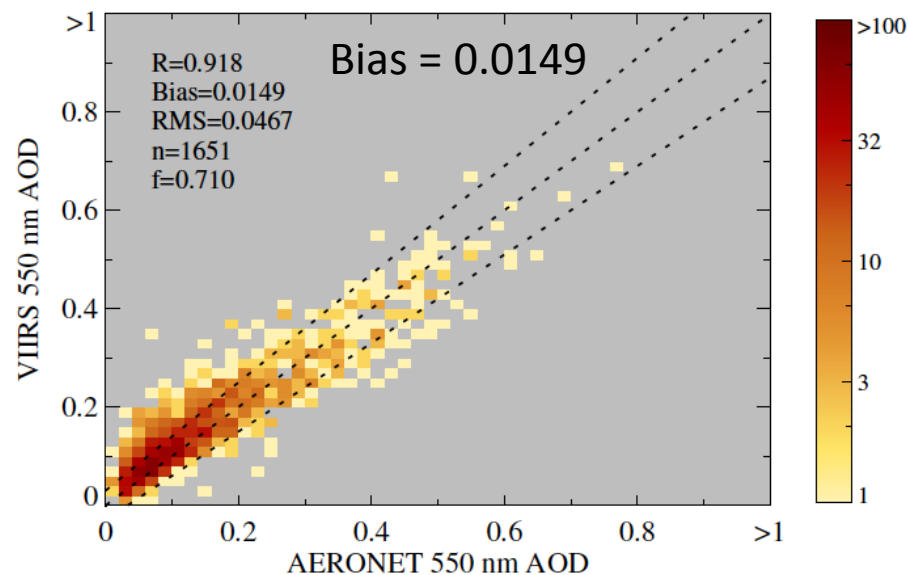
AOD validation at 6 AERONET island sites

Standard

(a) Standard L1 calibration



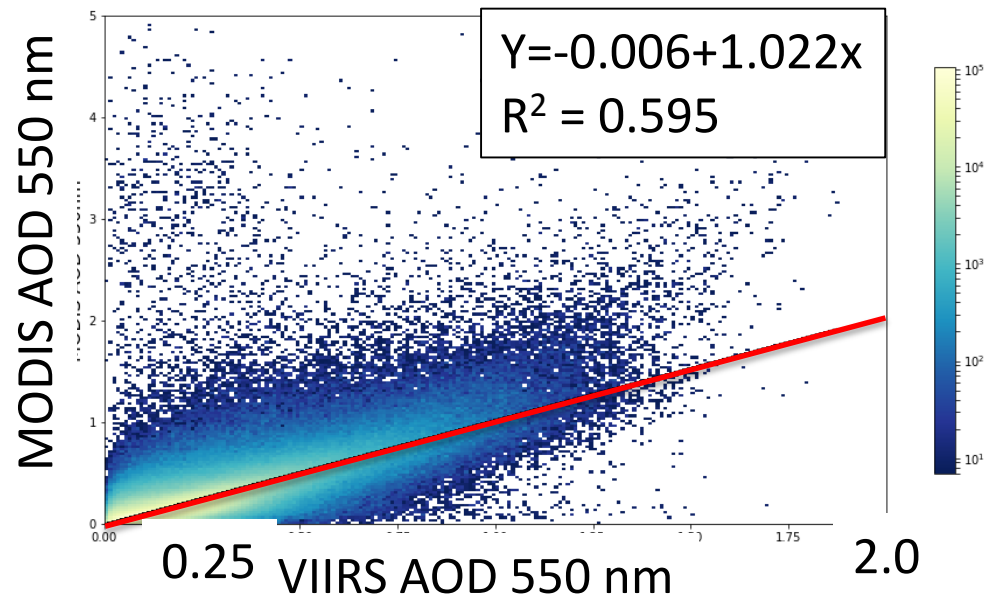
With vicarious corrections



Characterizing MODIS – VIIRS differences

- MODIS Collection 6 Level 3 AOD 550,
 - DT land and ocean,
 - 1 degree gridded
-
- VIIRS IDPS AOD550
 - 0.25 degree gridded (from VIIRS team web page).
 - Aggregated up to 1 degree (if any one of the 0.25 deg squares is populated, the 1 deg square will have a value
-
- 8-day means created from each.
 - Sync-ed
 - Start 25 January 2013
 - End 24 January 2017

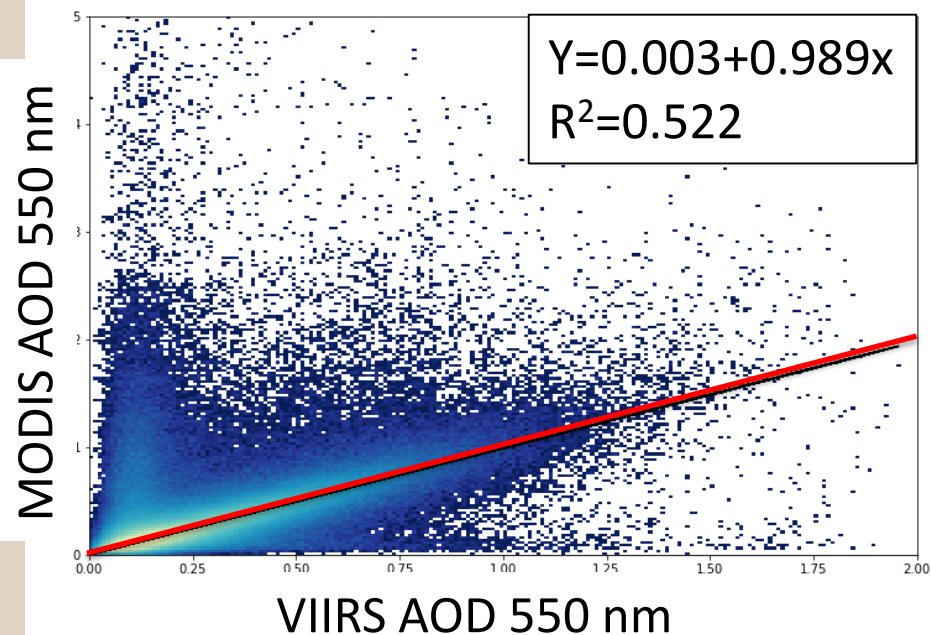
Land Scatter Jan 25, 2013 - Jan 24, 2017



Each ordered pair is an 8-day mean of a 1-degree grid box.

Red line is 1:1 line.

Ocean Scatter Jan 25, 2013 - Jan 24, 2017

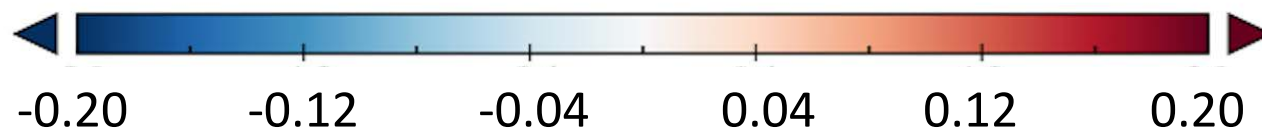
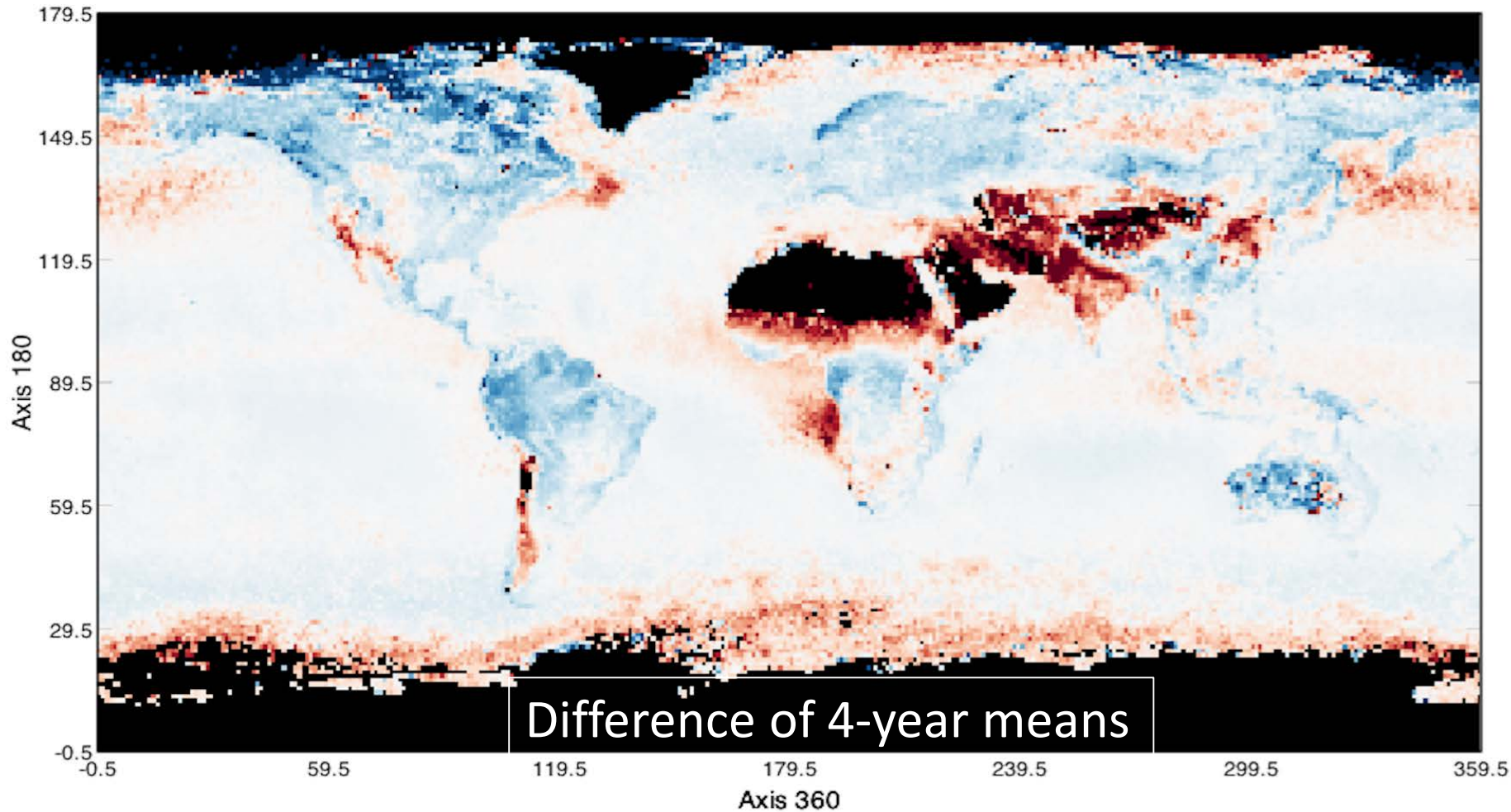


MODIS - VIIRS

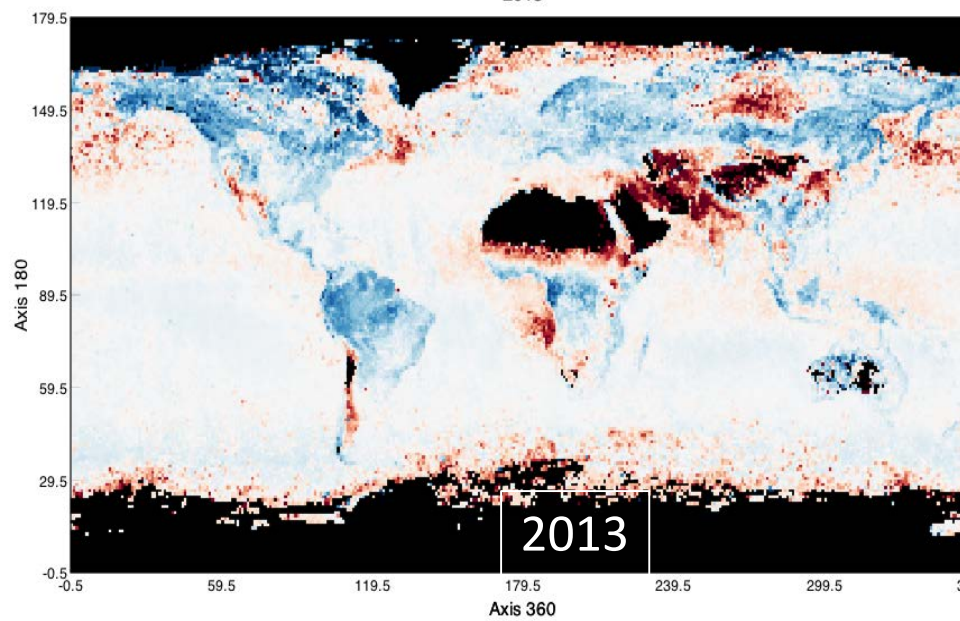
2013-2017

Feb. 2013 – Jan. 2017

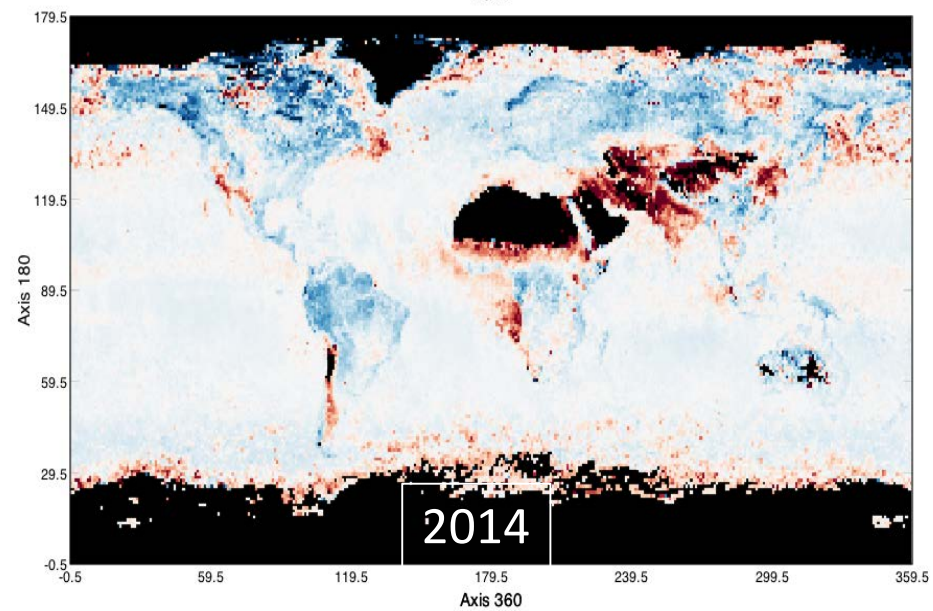
AOD 550 differences



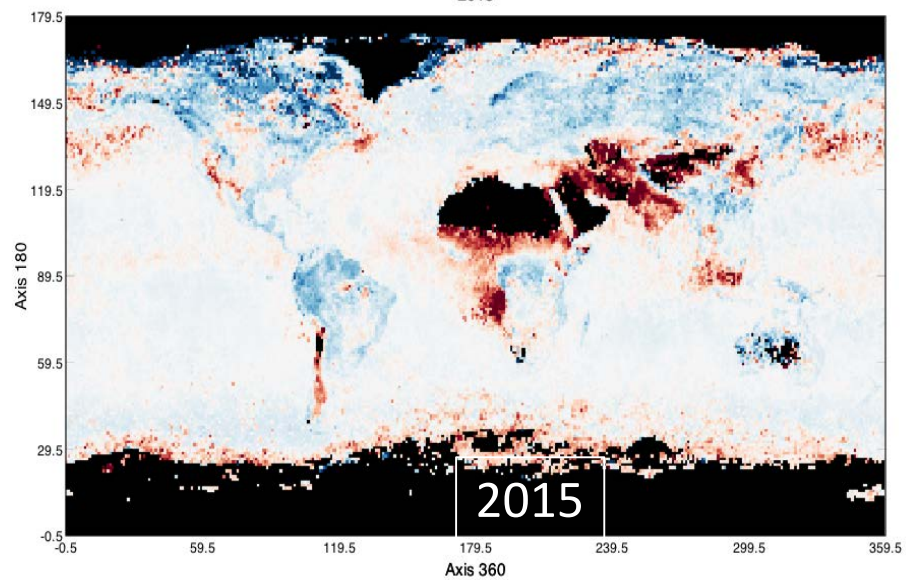
MODIS - VIIRS
2013



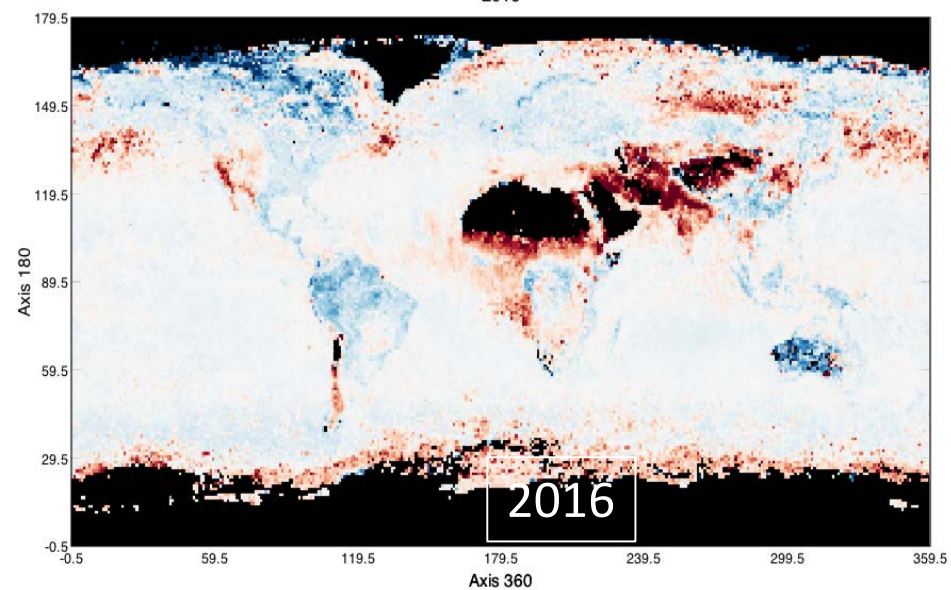
MODIS - VIIRS
2014

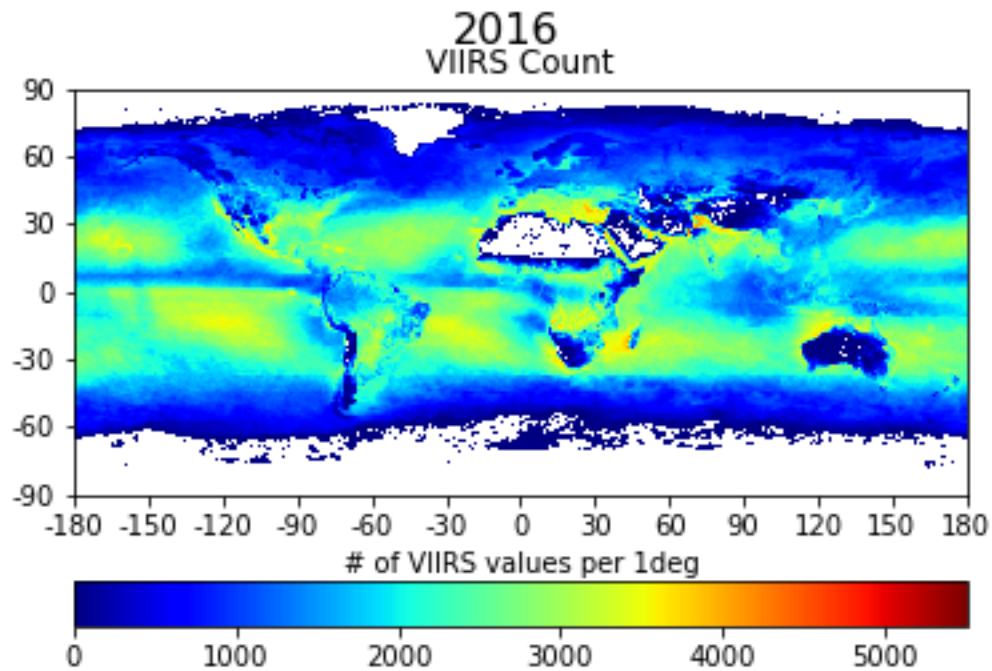


MODIS - VIIRS
2015



MODIS - VIIRS
2016

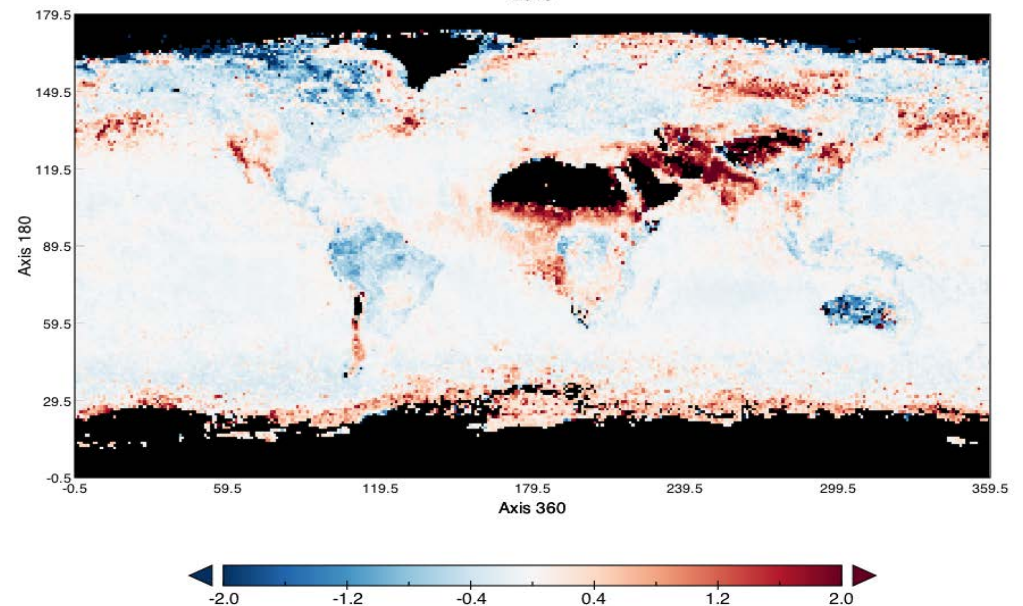


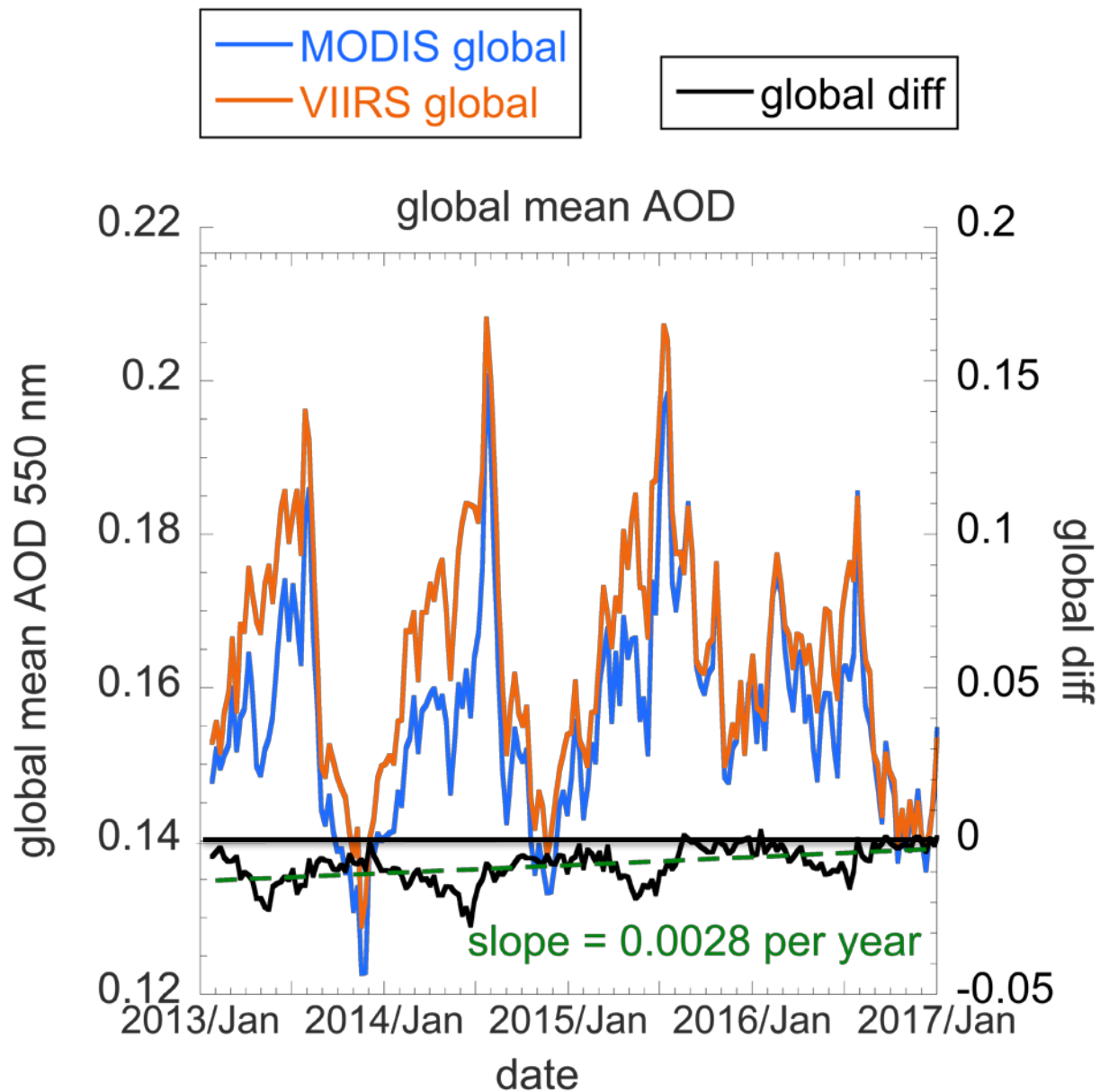


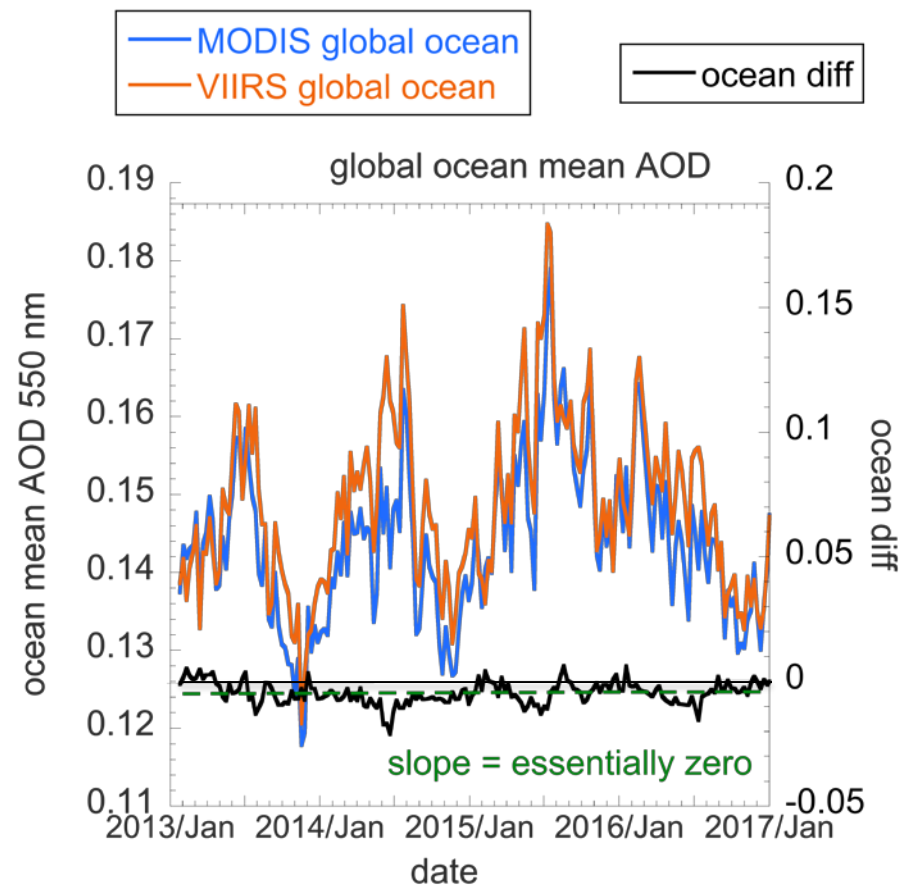
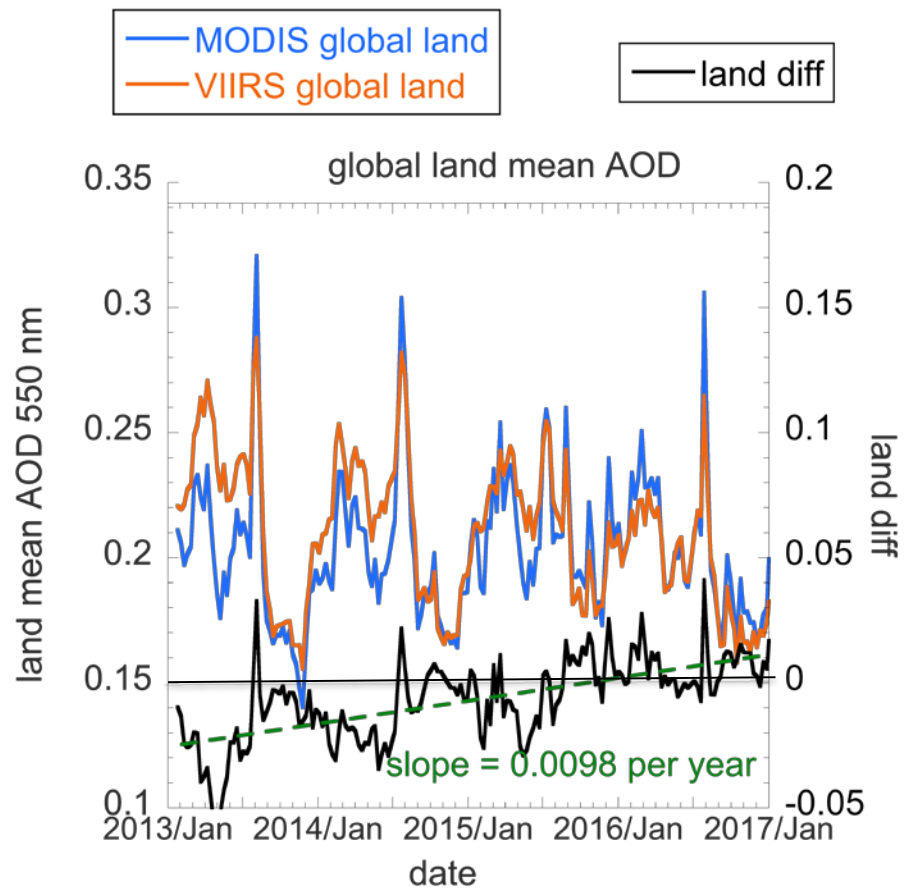
VIIRS count is the number of 0.25 deg squares in each 1 degree box for the entire period. (5840 max for 1 year).

Shown are 2016 counts and differences.

MODIS - VIIRS
2016





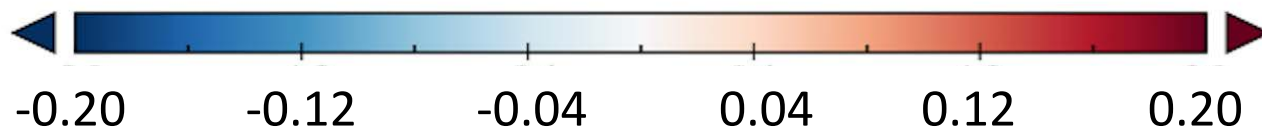
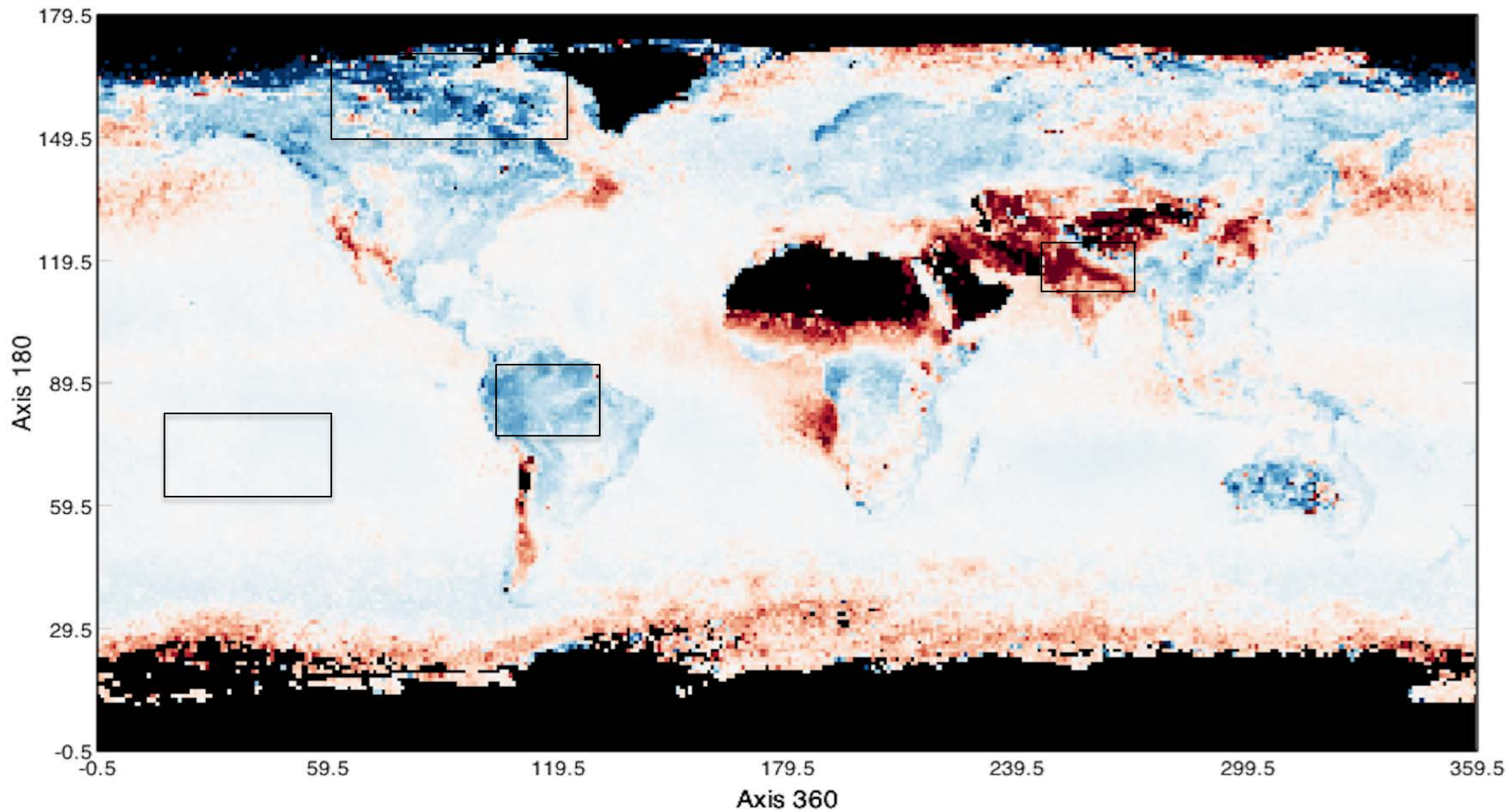


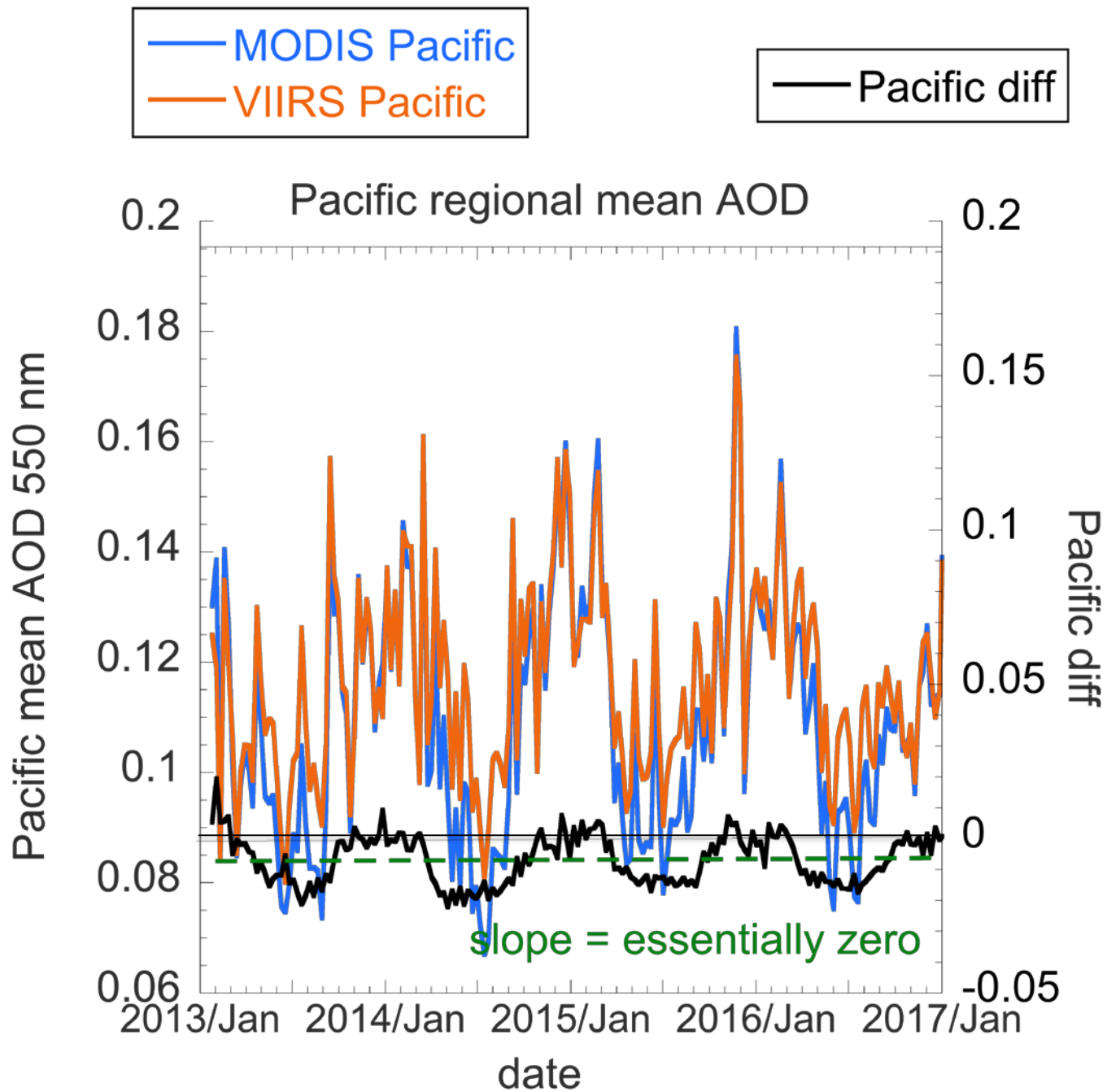
AOD 550 differences

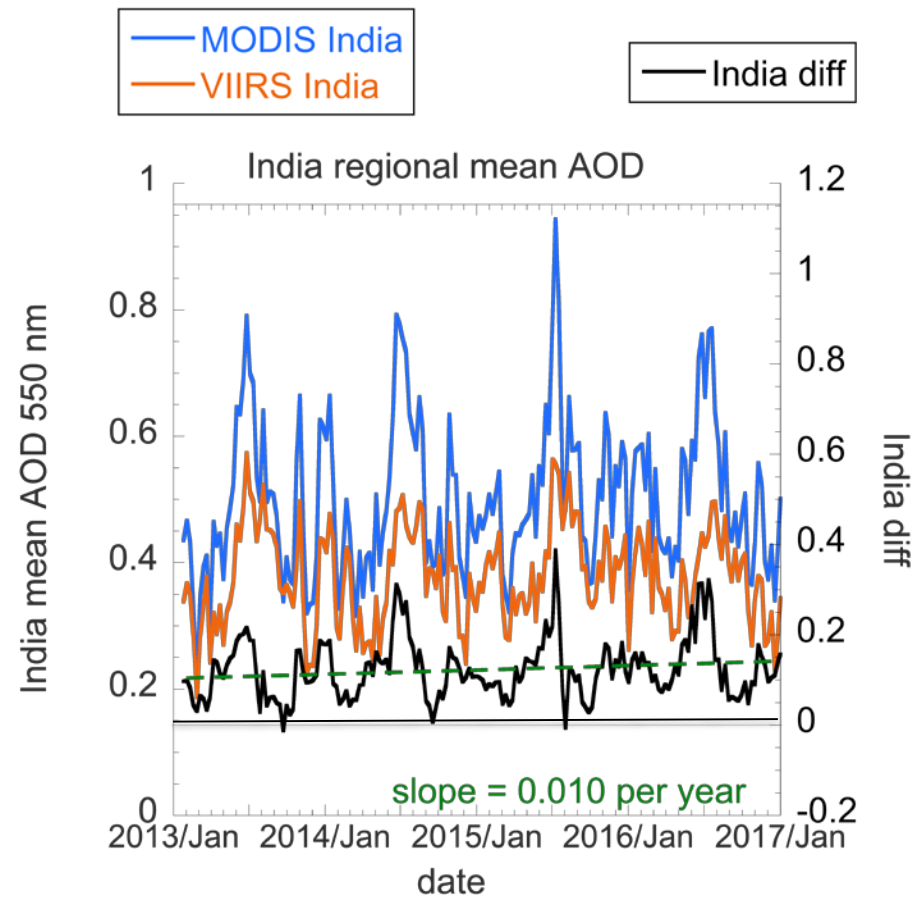
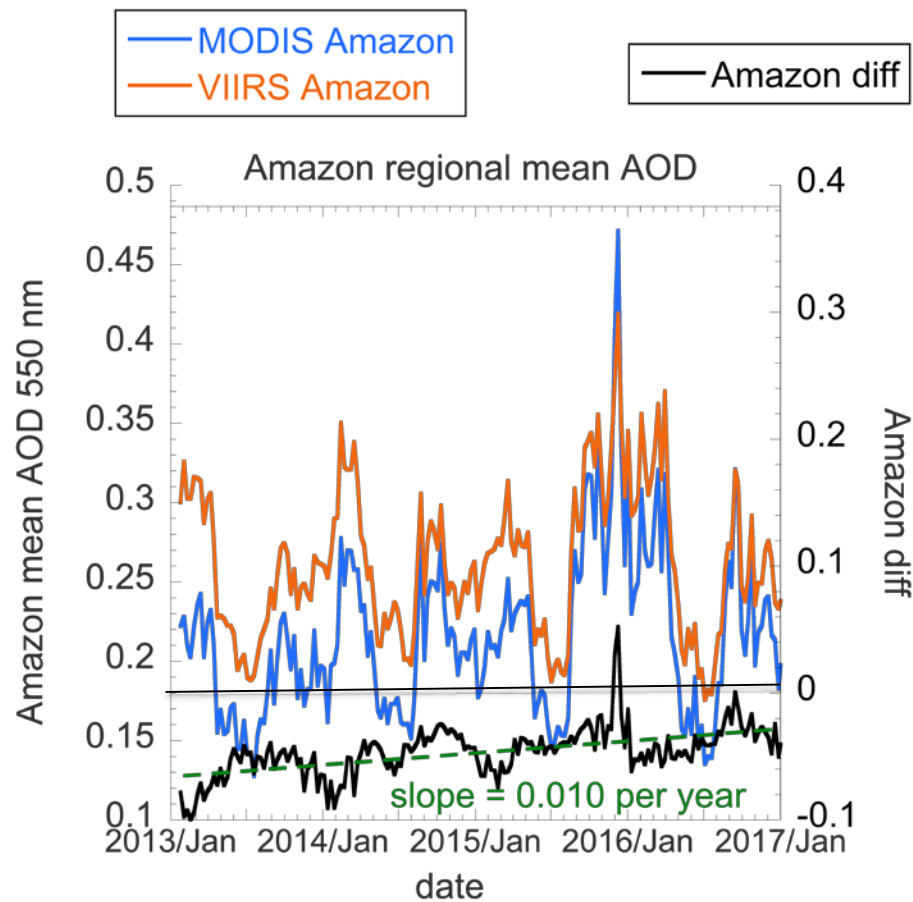
MODIS - VIIRS

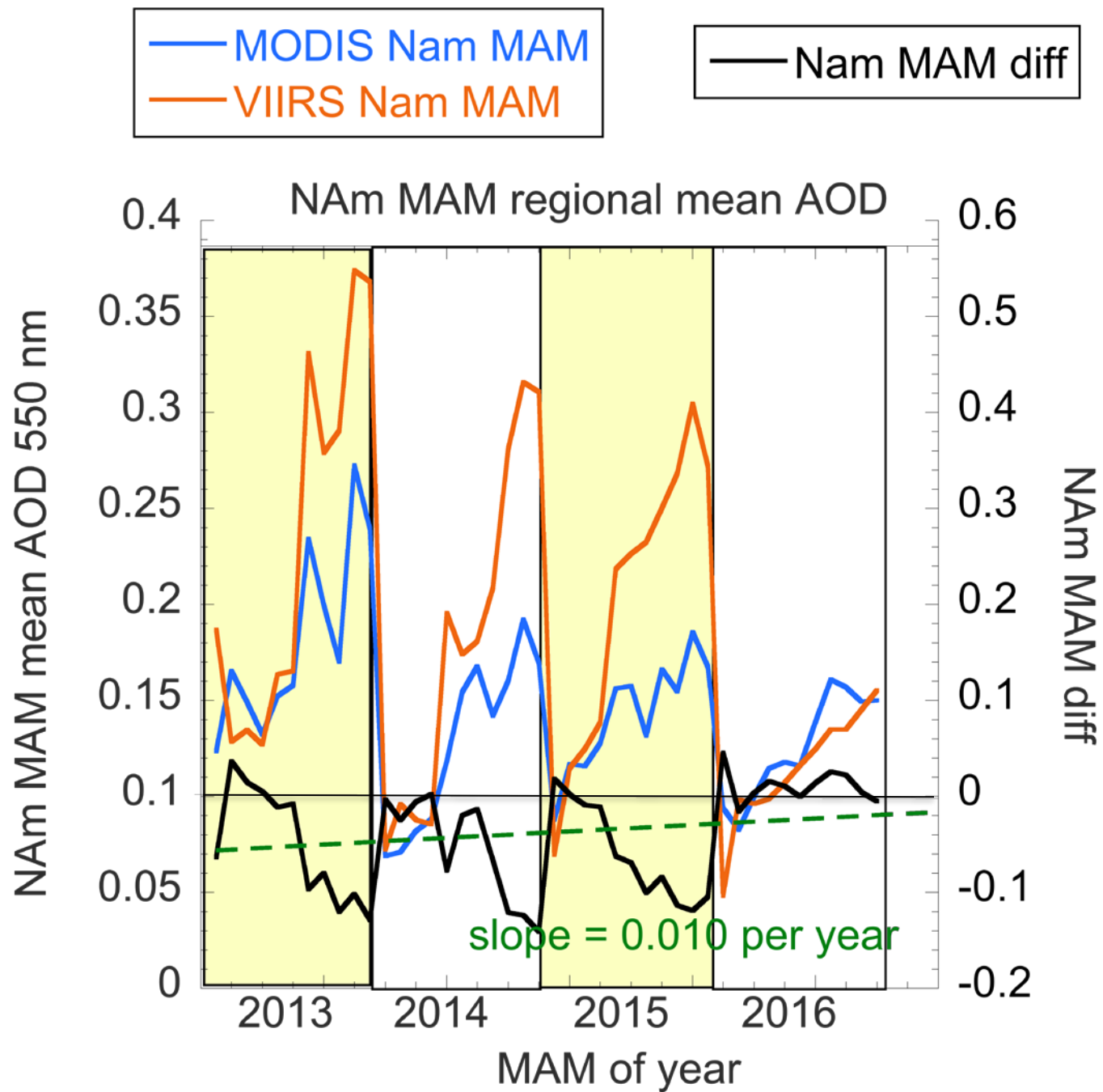
2013-2017

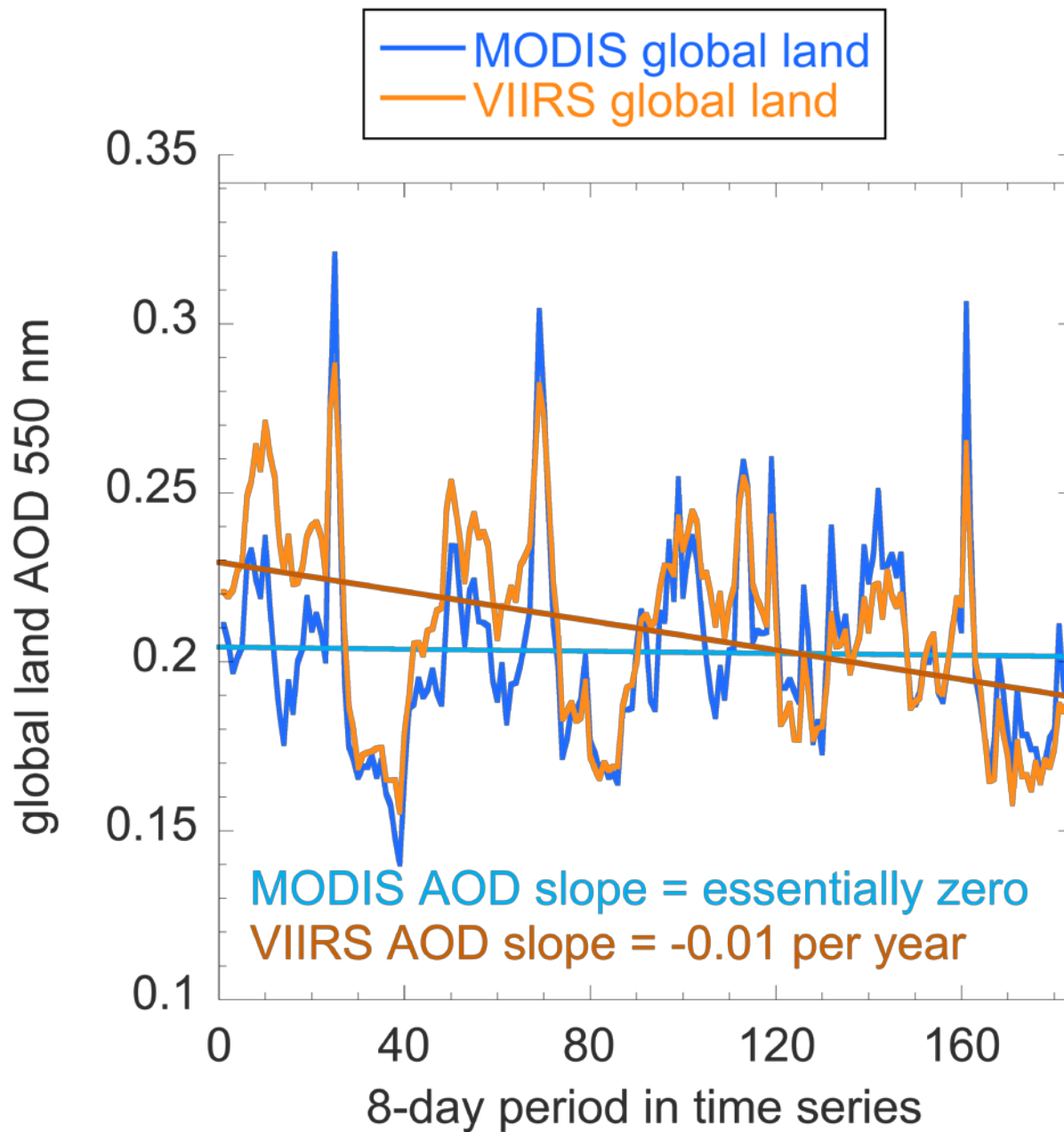
Feb. 2013 – Jan. 2017











Something happened to VIIRS in 2015 that caused land AODs to decrease.

Translates to 0.01 per year, but is really a jump, not linear.

Result over all is to bring VIIRS closer to MODIS.

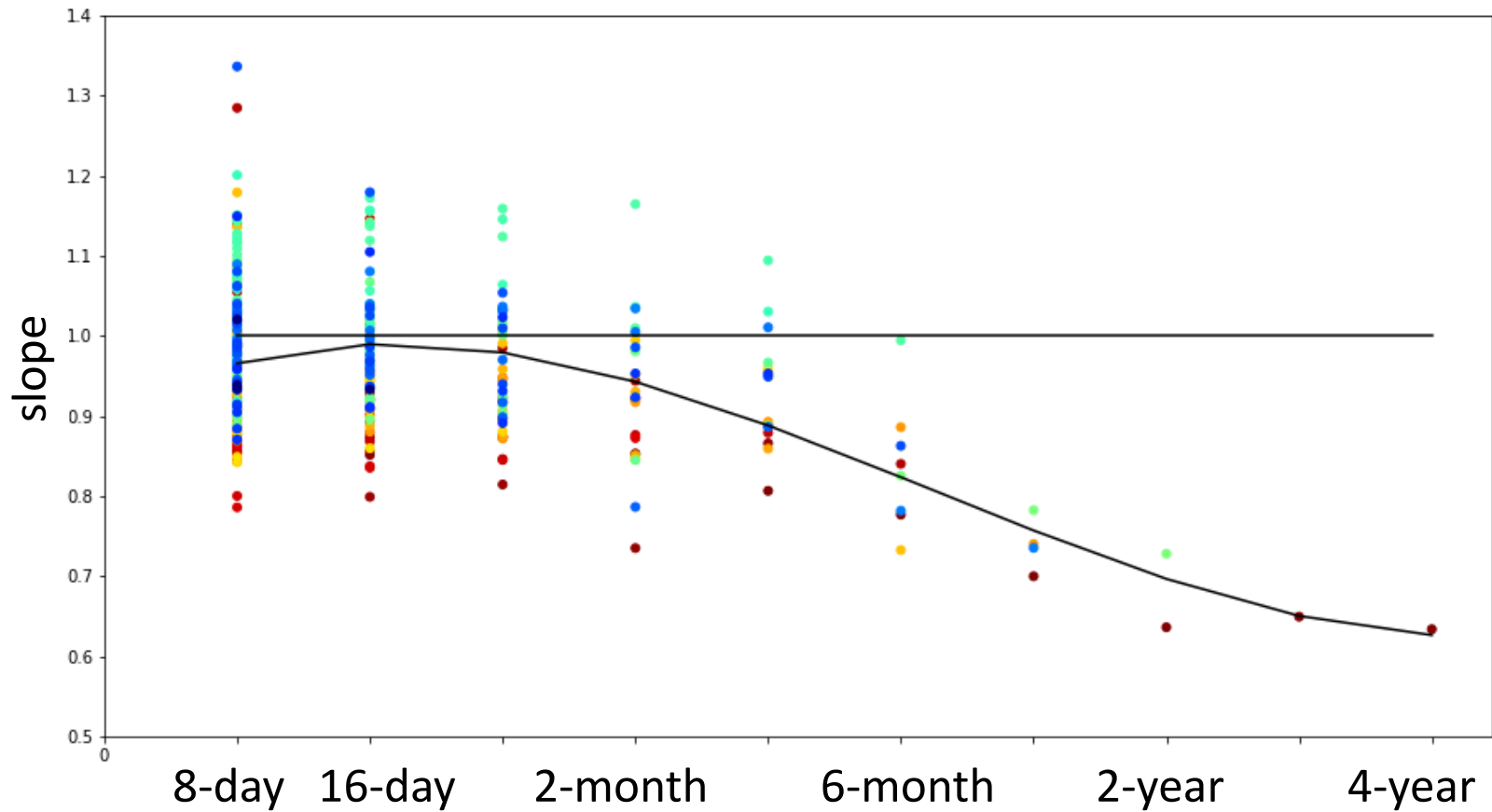
But not in India, and other land locations where VIIRS is higher than MODIS.

No temporal change to ocean AODs.

VIIRS background ocean AOD still 0.005 higher than MODIS.

Global

4 Years, Slope



Averaging interval

Each ordered pair
is 8-day mean

Each ordered
pair is a 4-year mean

Potential Solution to Resolving Data Artifacts in VIIRS Aerosol Detection Product over Land

Hai Zhang¹, Pubu Ciren¹, Shobha Kondragunta², Istvan Laszlo², Lorraine A. Remer³,
Hongqing Liu¹, Jingfeng Huang⁴, Mi Zhou¹, Ivan Valerio¹

1. IMSG; 2. NOAA; 3. UMBC; 4. UMD



Outline

- VIIRS Aerosol Detection Product (ADP)
- Demonstration and analysis of the data artifacts in ADP dust detection
- Dust RGB images using IR bands
- Dust detection using IR bands based on dust RGB method

VIIRS Aerosol Detection Product (ADP)

- Detect smoke and dust using two aerosol indices:

- Absorbing Aerosol Index (AAI)

$$AAI = -100 \left[\log_{10} \left(\frac{R_{412}}{R_{440}} \right) - \log_{10} \left(\frac{R'_{412}}{R'_{440}} \right) \right]$$

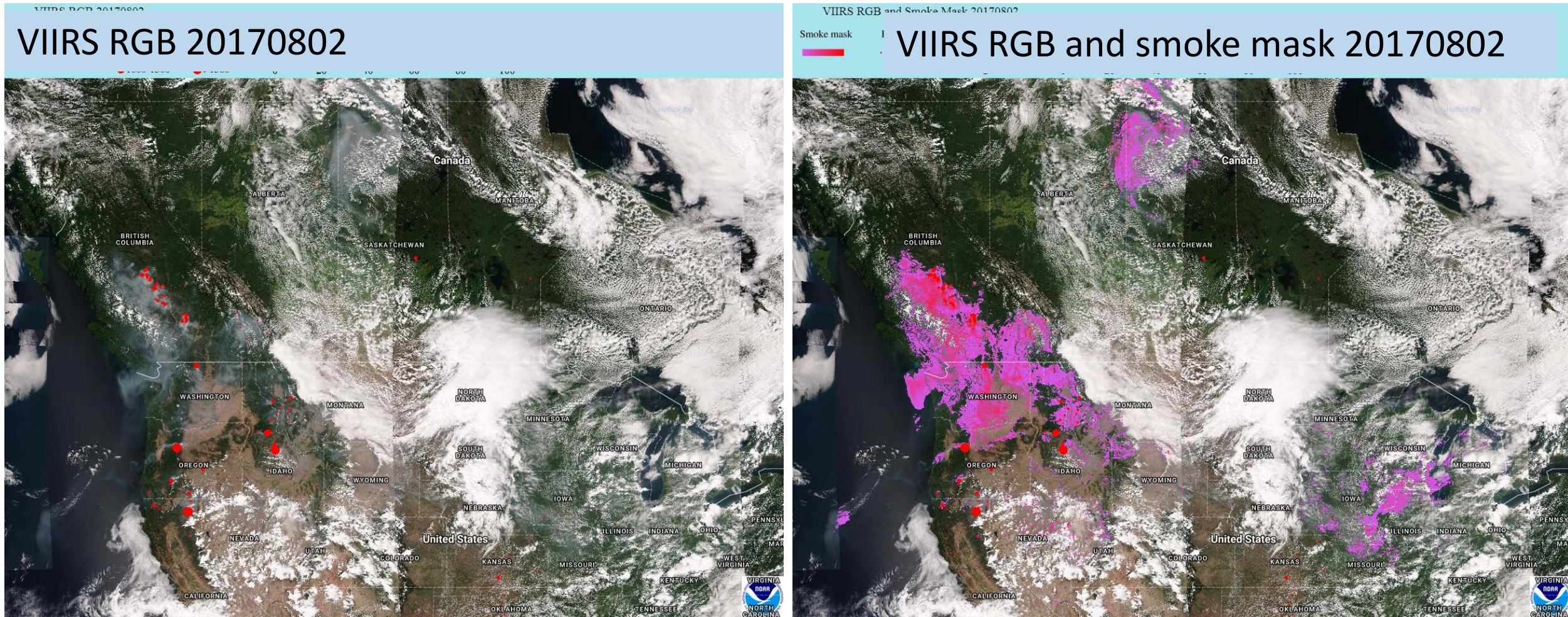
- R_{412} and R_{440} : TOA reflectance at 412nm and 440nm bands
 - R'_{412} and R'_{440} : Rayleigh reflectance at 412nm and 440nm bands
 - Dust Smoke Discrimination Index (DSDI)
 - $DSDI = -10 \log_{10} \left(\frac{R_{412}}{R_{2130}} \right)$
 - R_{412} and R_{2130} : TOA reflectance at 412nm and 2130nm bands

VIIRS Aerosol Detection Product (ADP)

- The detection is based on thresholds of AAI and DSDI, which are different over land and ocean

Surface type	Aerosol type	AAI thresholds	DSDI thresholds	Other
Land	Dust	> 10	≥ 0.0	
	Smoke	≥ 5.0 thin ≥ 9.0 thick	≤ -3.0 thin ≤ -2.0 thick	$0.2 < R_{412} < 0.4$ thick
Ocean	Dust	> 4.0	≥ -10.0	
	Smoke	≥ 4.5 thin ≥ 10.0 thick	≤ -10.0 thin ≤ -4.0 thick	$R_{2130} < 0.1$ thin

An example of smoke mask shown on eIDEA
(<https://www.star.nesdis.noaa.gov/smcd/spb/aq/eidea/>)



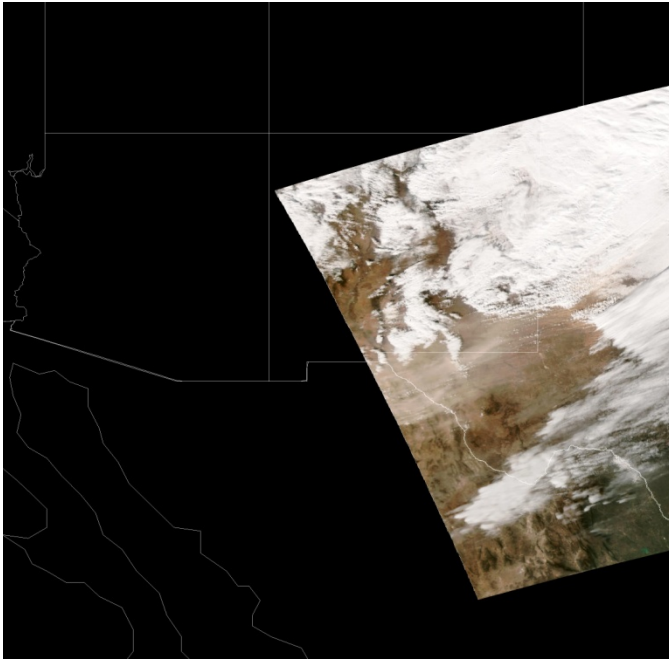
The dust mask is not shown on eIDEA because of the problems in the following slides

Problems in dust detection over land

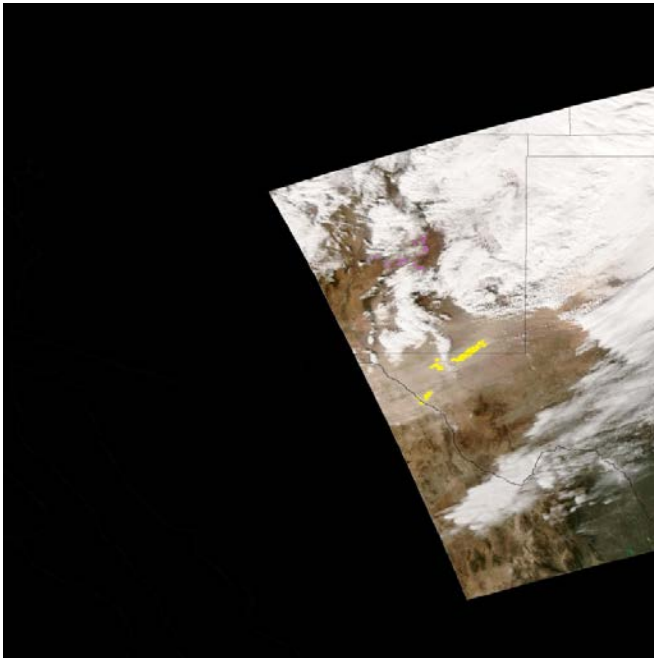
- False detection
- Undetected dust
- Geometry dependent
- Demonstrated in the following cases

1902 UTC

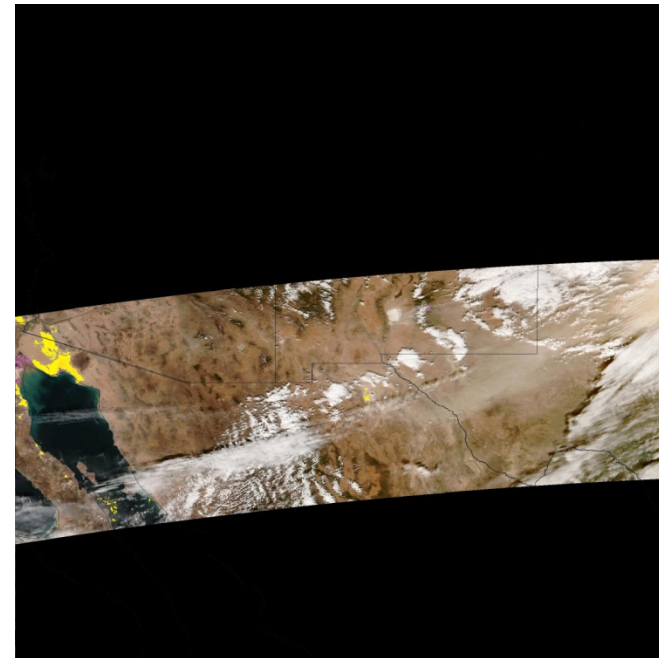
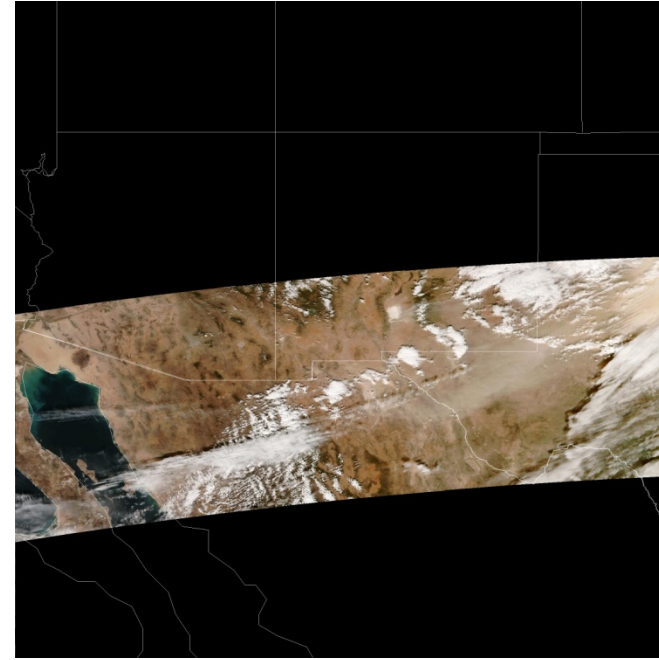
RGB



RGB and
dust mask
(yellow)



2043 UTC



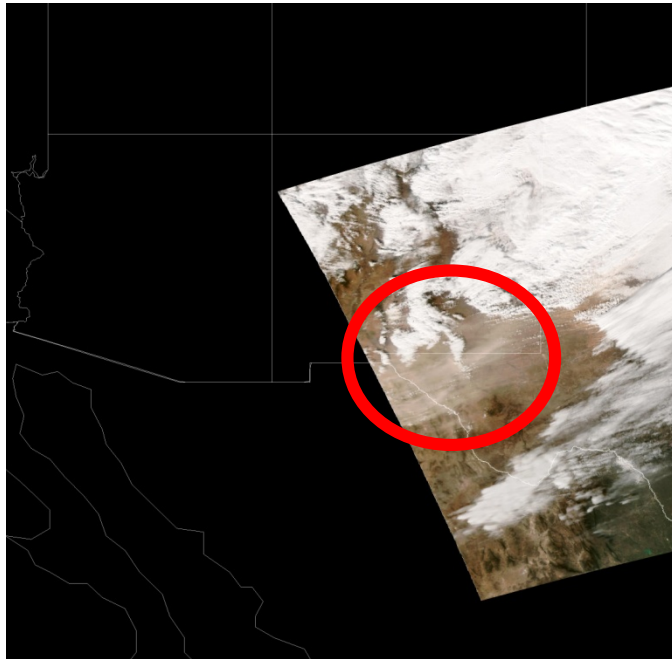
VIIRS 20161217

Dust storm near
Texas/Mexico
boundary

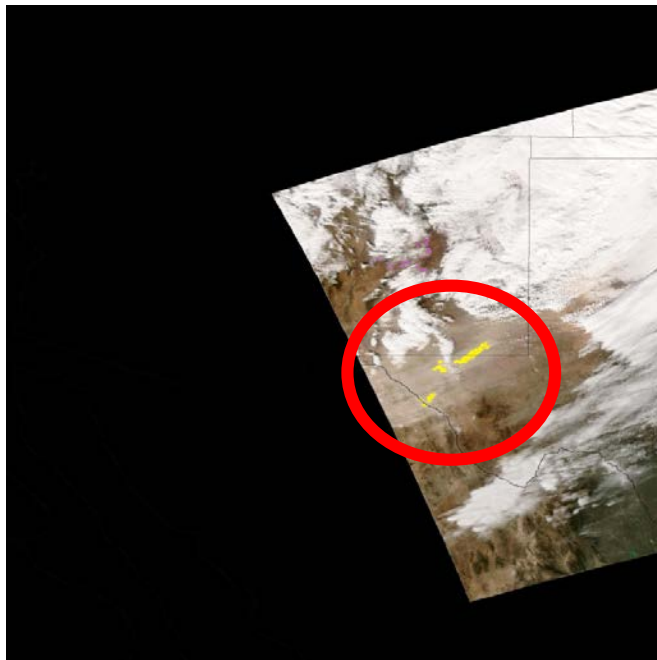
Two overpasses

1902 UTC

RGB



RGB and
dust mask
(yellow)



2043 UTC



VIIRS 20161217

Dust storm near
Texas/Mexico
boundary

Two overpasses

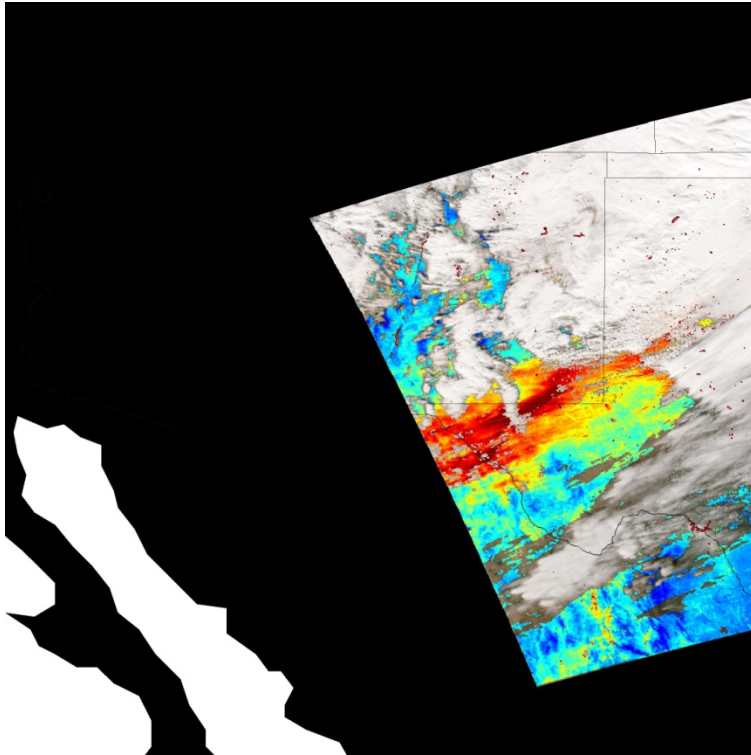
NPP track for 20161217

Since the sun is to the west of the nadir, the overpass at 1902 is in forward reflection geometry and the overpass at 2043 is in backward reflection geometry.

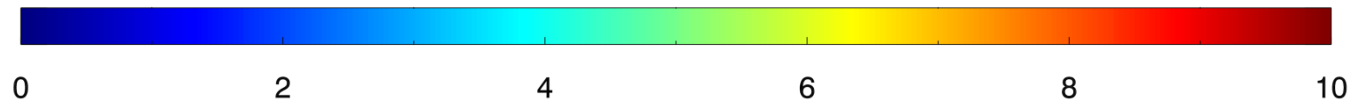
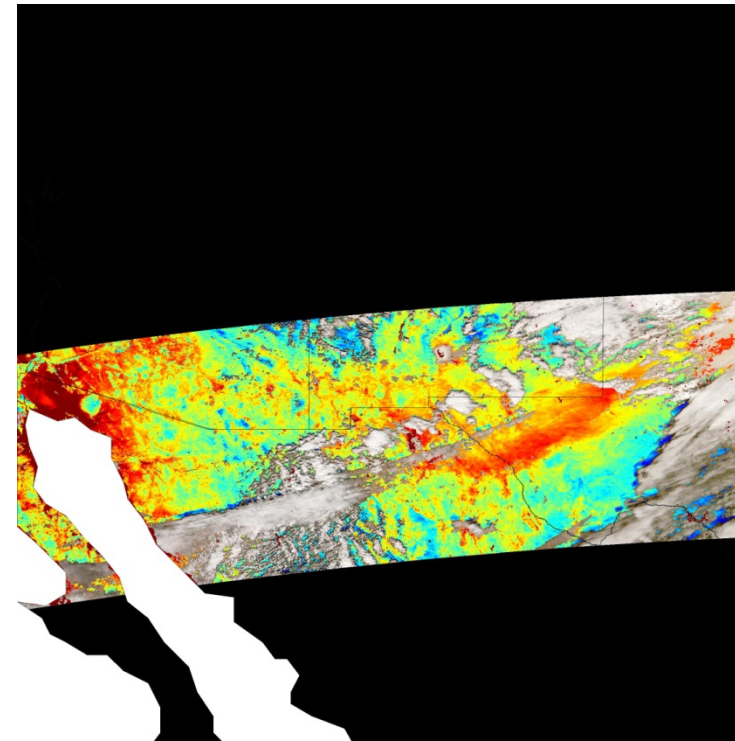


VIIRS AAI 20161217

1902 UTC

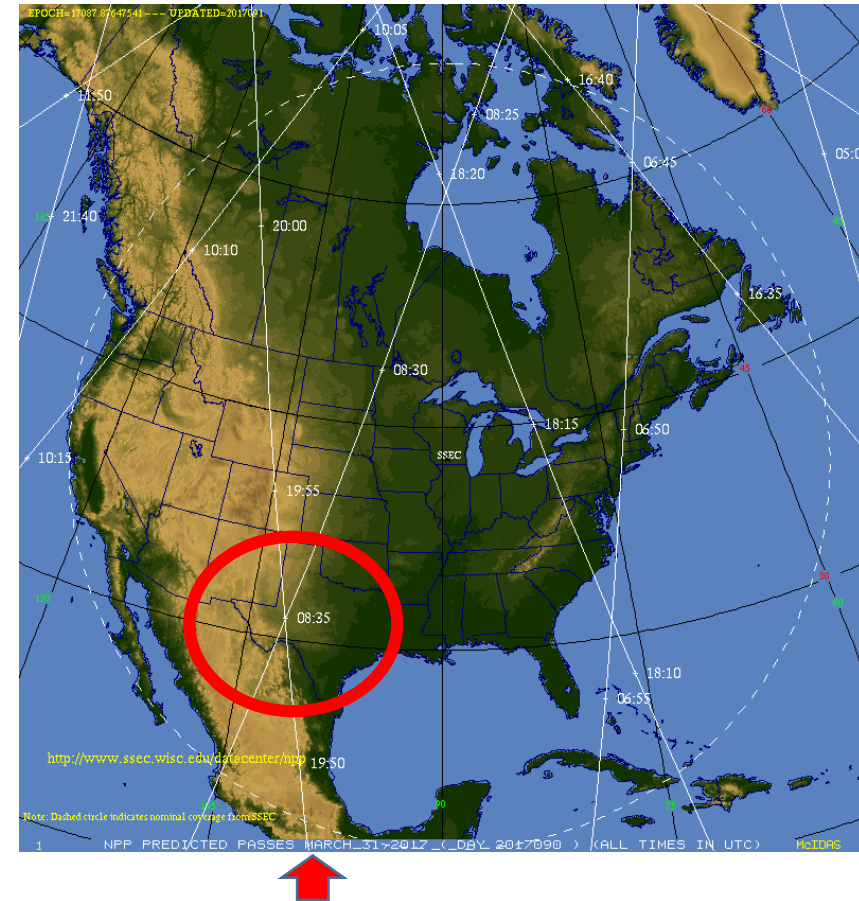
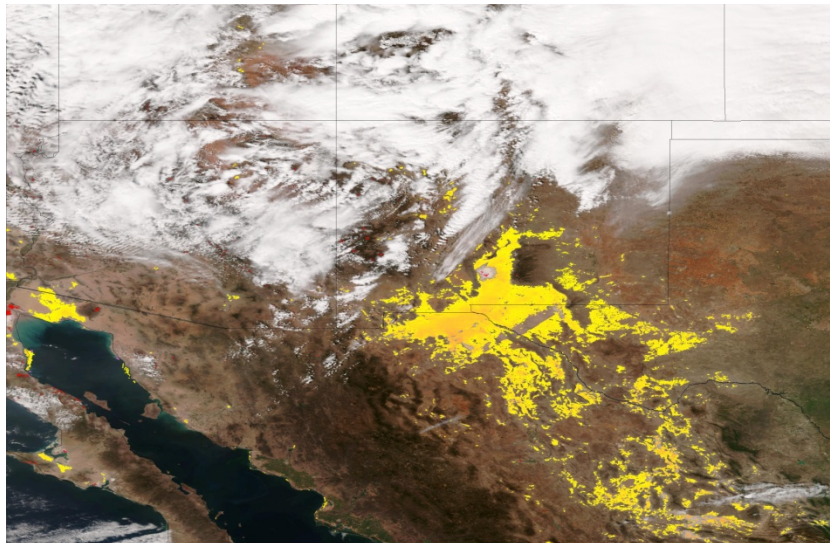
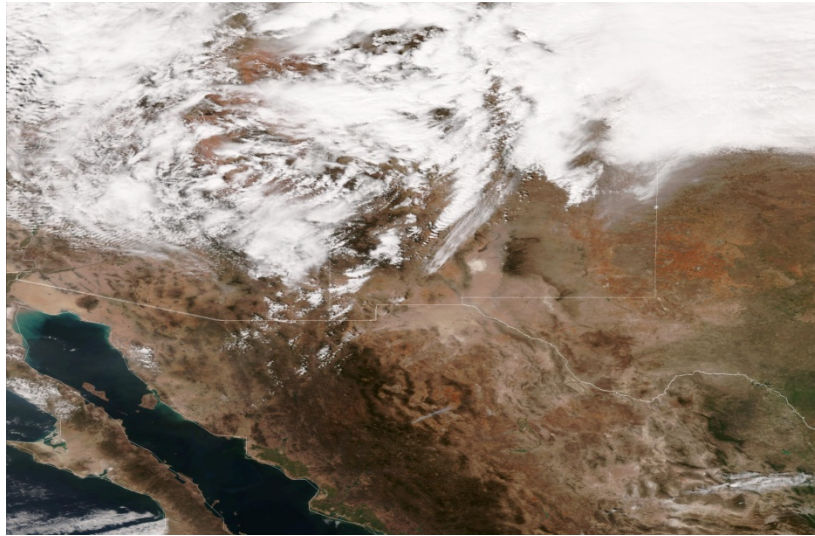


2043 UTC



- AAI is lower in the backward reflection geometry than that in the forward reflection geometry

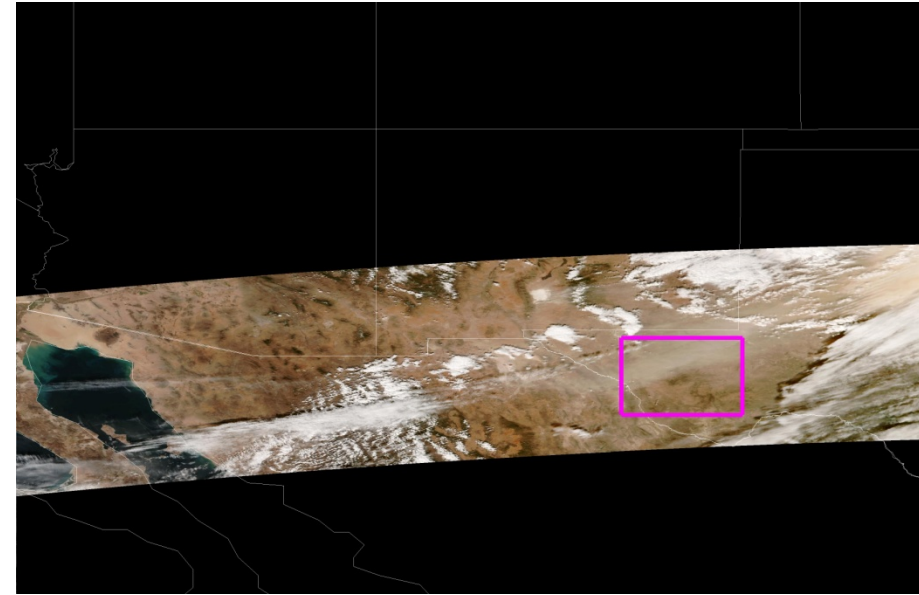
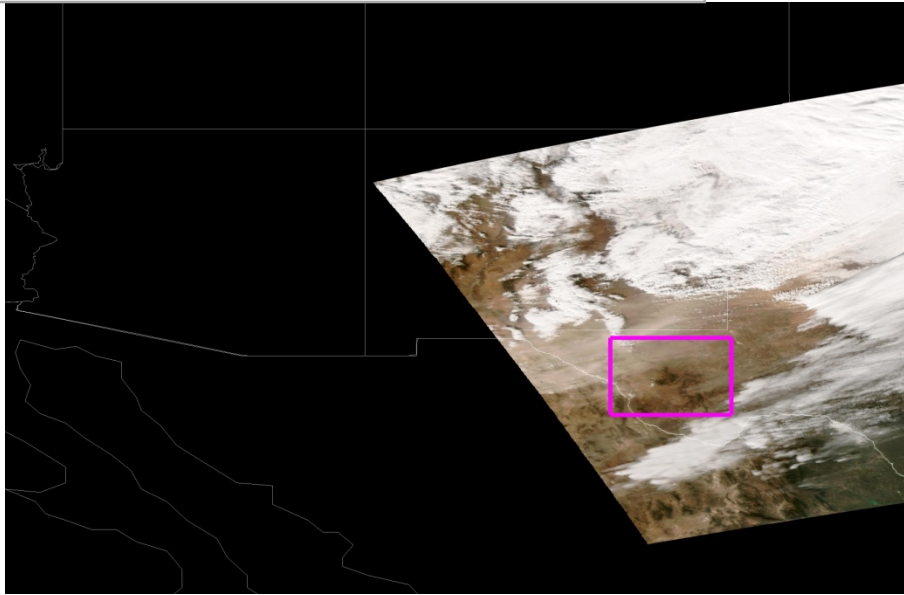
An example with the area close to the center of the granule (20170331)



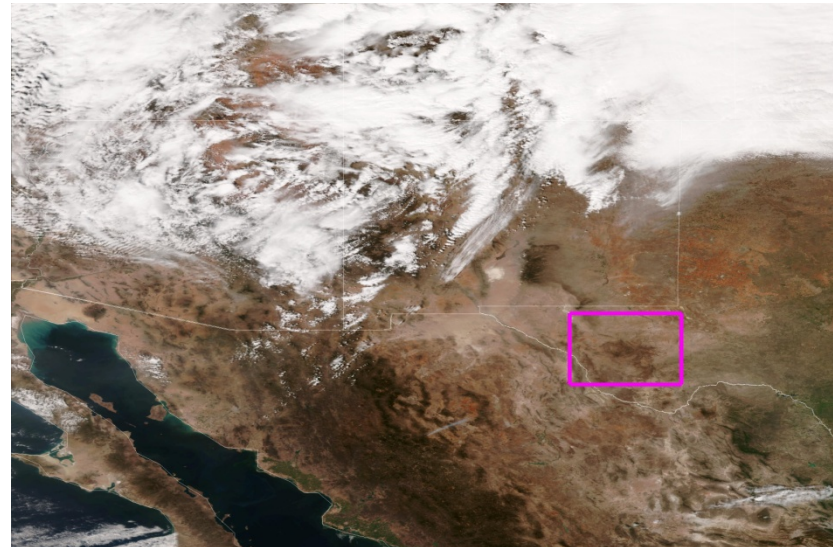
The false detection is more serious in the areas close to the nadir

Simulation study of AAI vs aerosol load in the three geometries

20161217



20170331



- Obtain the geometries in the boxes (same area in the three cases)
- Obtain the surface reflectance from surface reflectance database (built from multi-year VIIRS data)

Parameters for the three cases

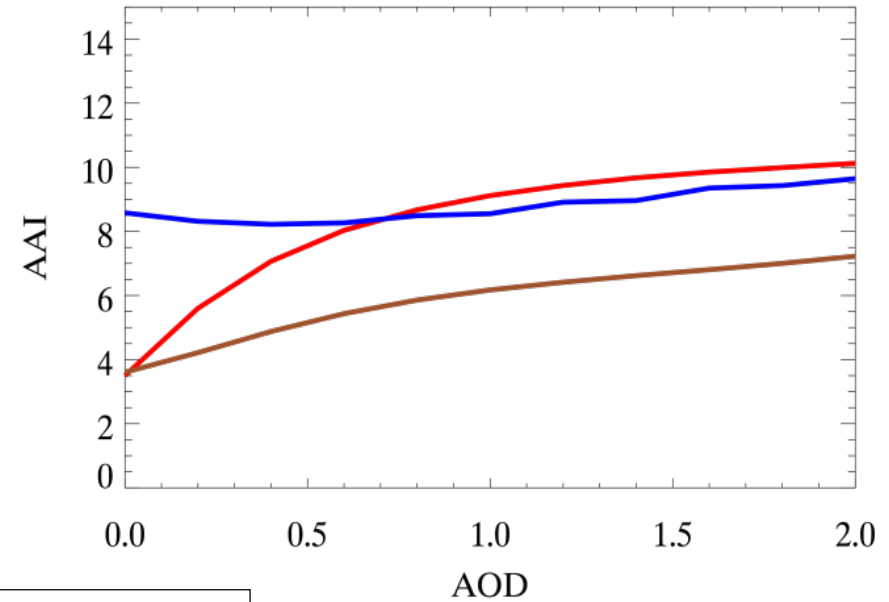
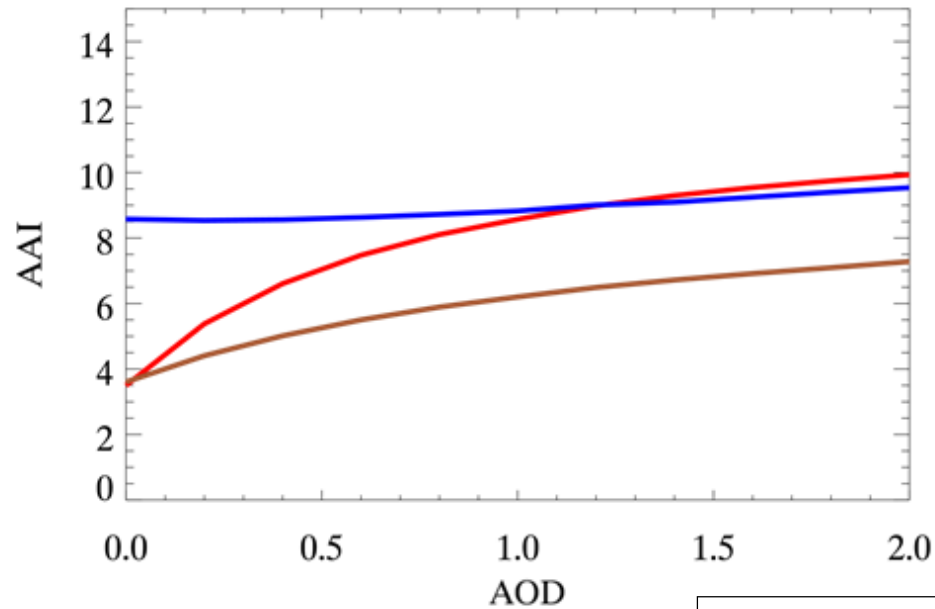
Case number	description	Lat,lon bound	geometry (sza, vza,azi)	Surface reflectance M1,M2, M3, M5, M11
1	20161217 overpass 1	Lat 29.8N-31.8N Lon 105W-103W	forward (54.27, 65.26, 110.86)	0.05, 0.056, 0.067, 0.126, 0.196
2	20161217 overpass2		backward (60.37, 57.52, 55.80)	0.070, 0.081, 0.098, 0.185, 0.275
3	20170331		nadir (29.11, 13.29, 128.71)	0.076, 0.087, 0.103, 0.182, 0.269

Simulated AAI vs AOD (using LUT in Enterprise AOD algorithm)

$$AAI = -100 \left[\log_{10} \left(\frac{R_{412}}{R_{440}} \right) - \log_{10} \left(\frac{R'_{412}}{R'_{440}} \right) \right]$$

Dust

Smoke



Red: forward (20161217 p1)
Brown: backward (20161217 p2)
Blue : nadir (20170331)

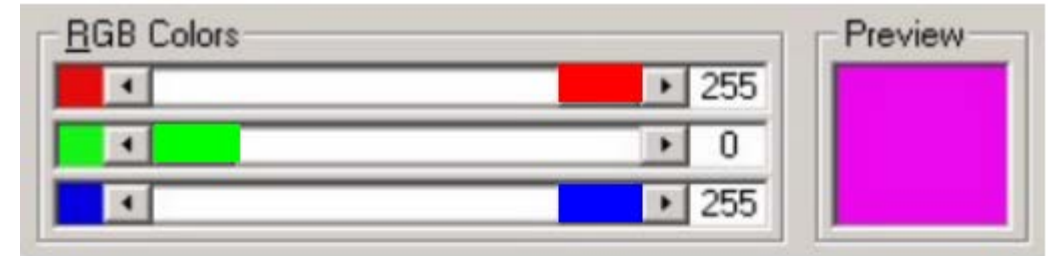
- Good sensitivity in forward direction, some sensitivity in backward direction, no sensitivity near nadir
- Dust and smoke are similar in AAI

Dust RGB

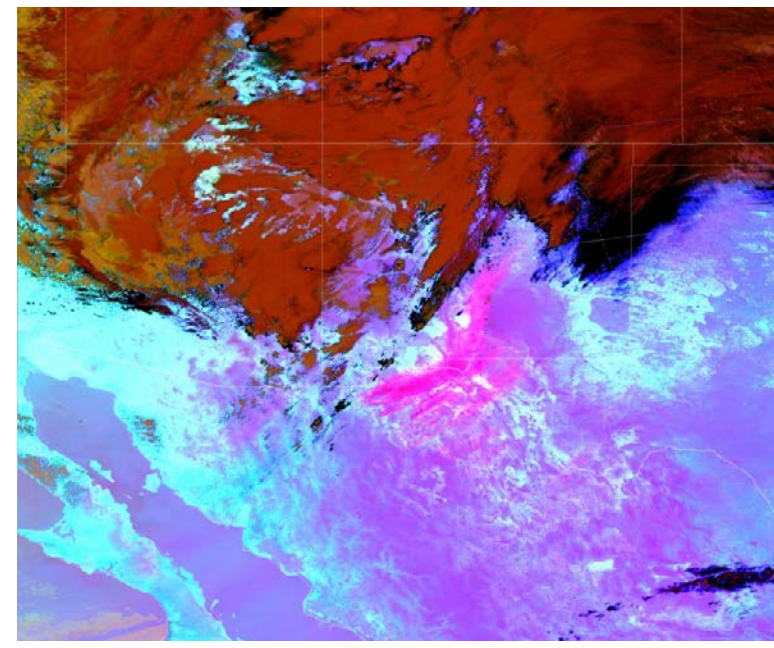
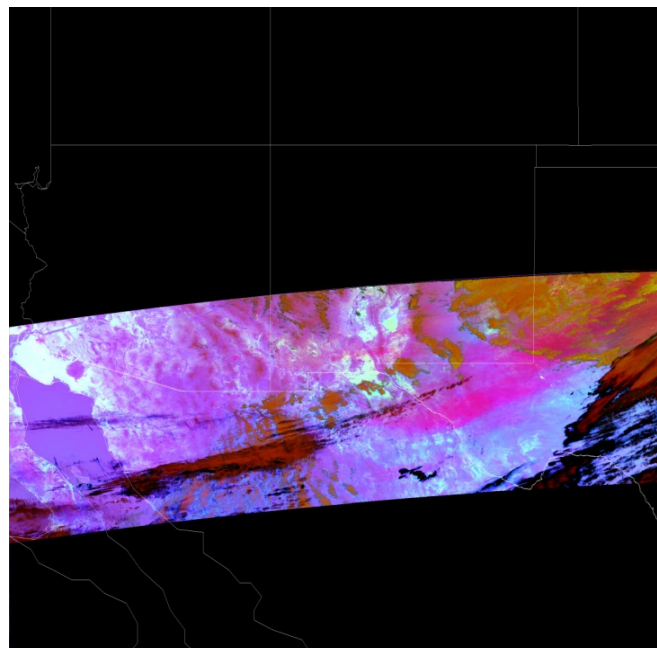
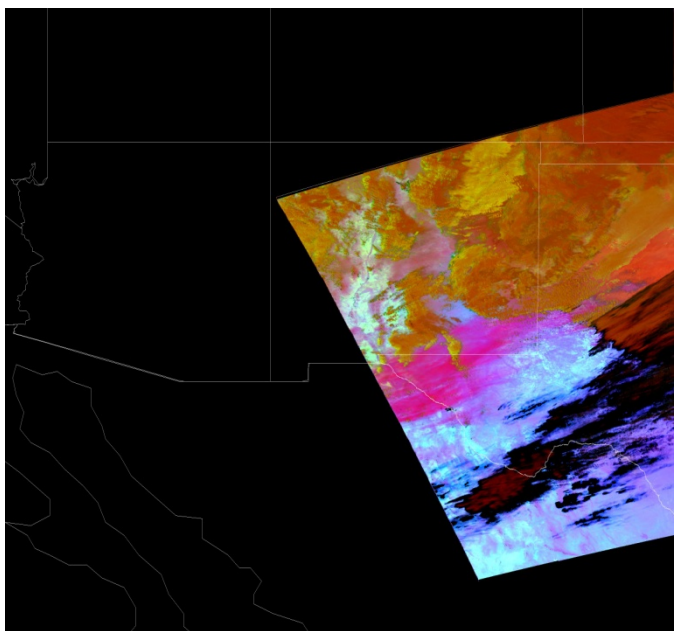
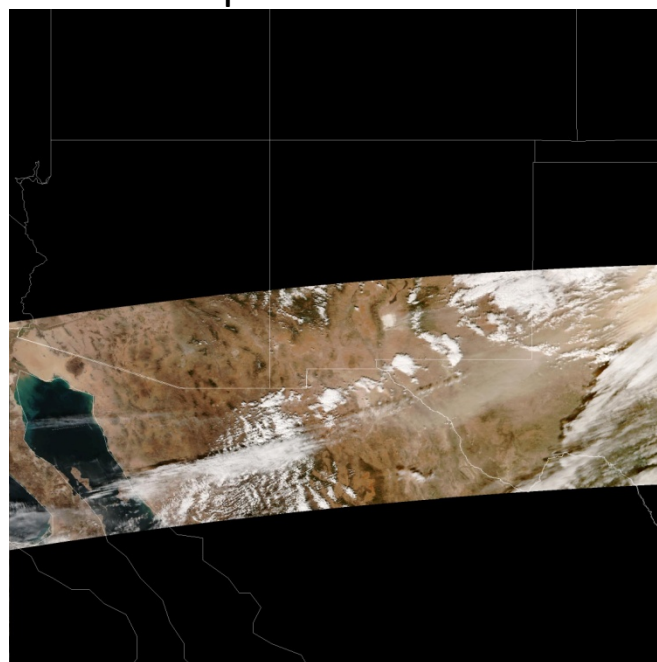
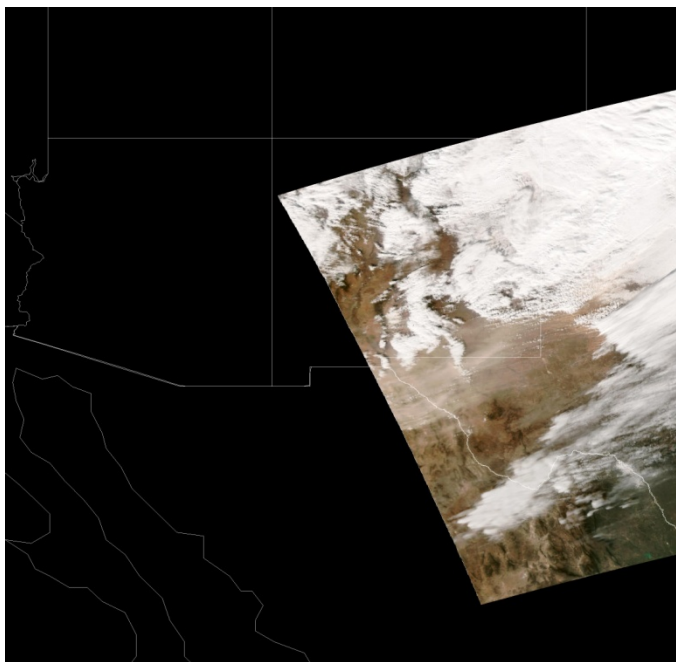
- Used by EUMETSAT (European Organization for Meteorological Satellites) on MSG (Meteosat Second Generation)
(https://www.eumetsat.int/website/home/Data/Training/TrainingLibrary/DAT_2042669.html?lang=EN)
- Three IR bands are used: IR8.7, IR10.8 and IR12.0
 - Brightness temperature at IR10.8 is less than that at IR12.0
 - Surface emissivity in 10.8 μm is similar to that in 12 μm
 - More absorption for dust in 10.8 μm than in 12 μm
 - Brightness temperature is close in IR10.8 and in IR8.7
 - Surface emissivity in 10.8 μm is higher than that in 8.7 μm
 - More absorption for dust in 8.7 μm than in 10.8 μm

Dust RGB

- R: $bt_{12} - bt_{10.8}$ (bt– brightness temperature)
- G: $bt_{10.8} - bt_{8.7}$
- B: $bt_{10.8}$
- Using this method, dust shows as magenta color over desert



The three cases plotted in dust RGB image

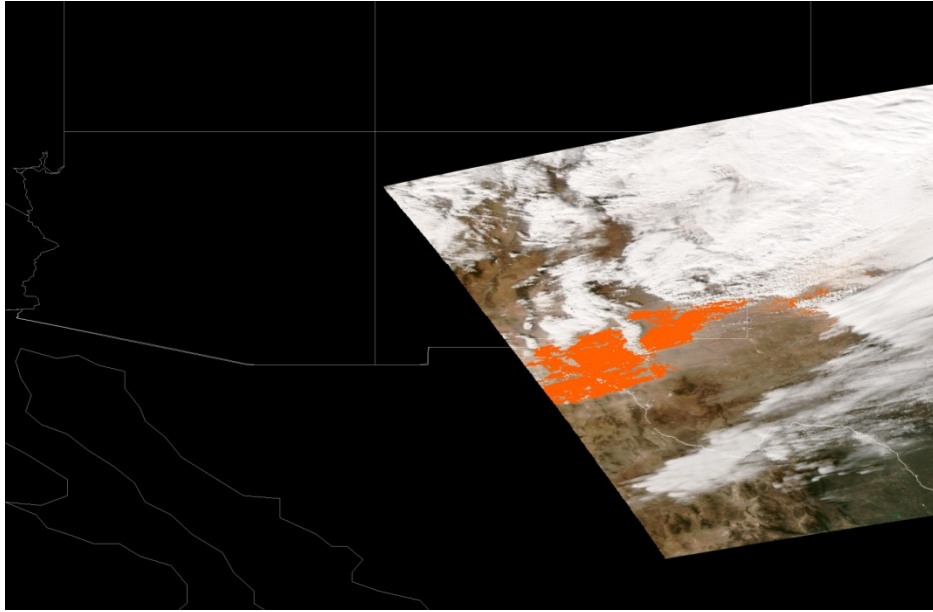


Use thresholds to detect dust in IR bands

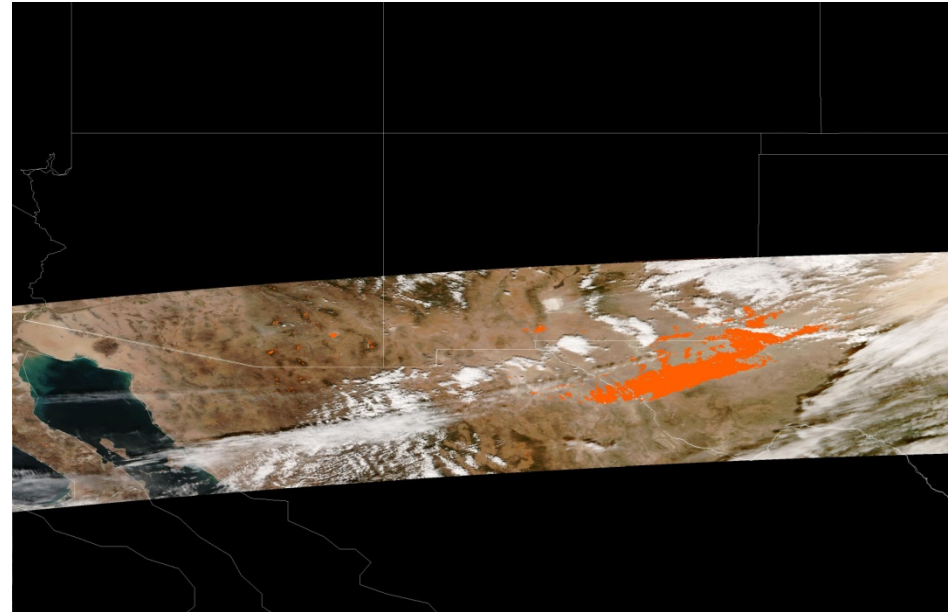
Determine thresholds through visual inspection of the dust cases

	thresholds
R: $bt_{12} - bt_{10.8}$	> 0
G: $bt_{10.8} - bt_{8.7}$	< 0.5 in North America < 4 in North Africa and Arabian Peninsula
B: $bt_{10.8}$	> 273

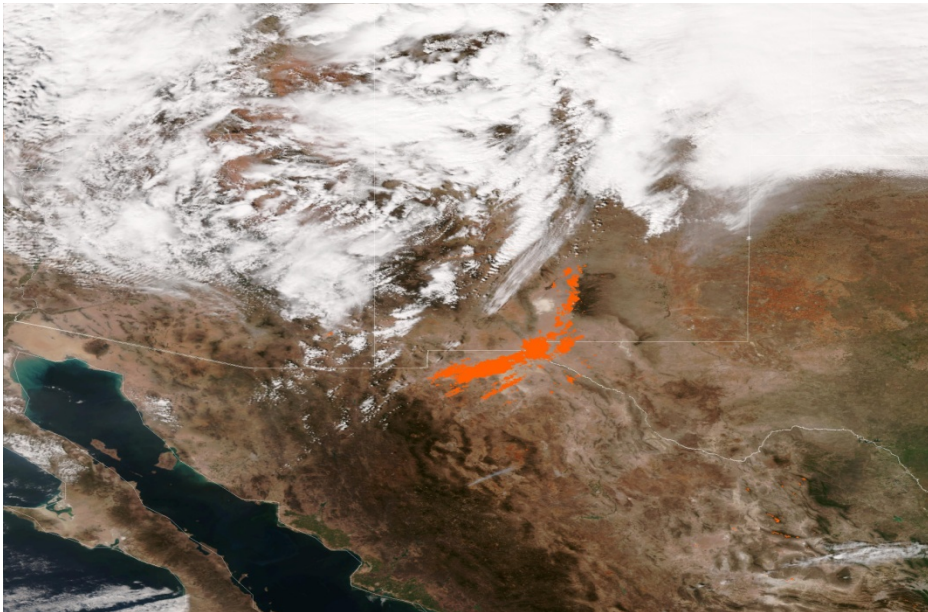
20161217 1902



20161217 2043

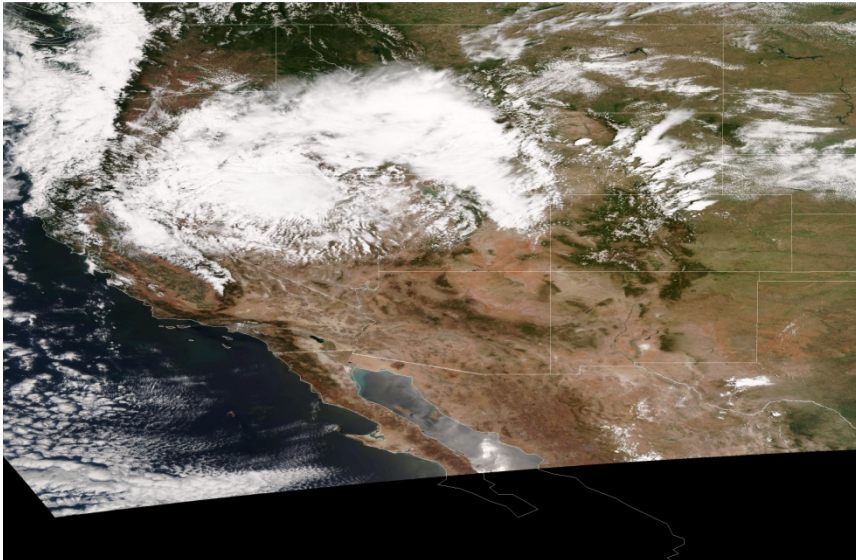


20170331

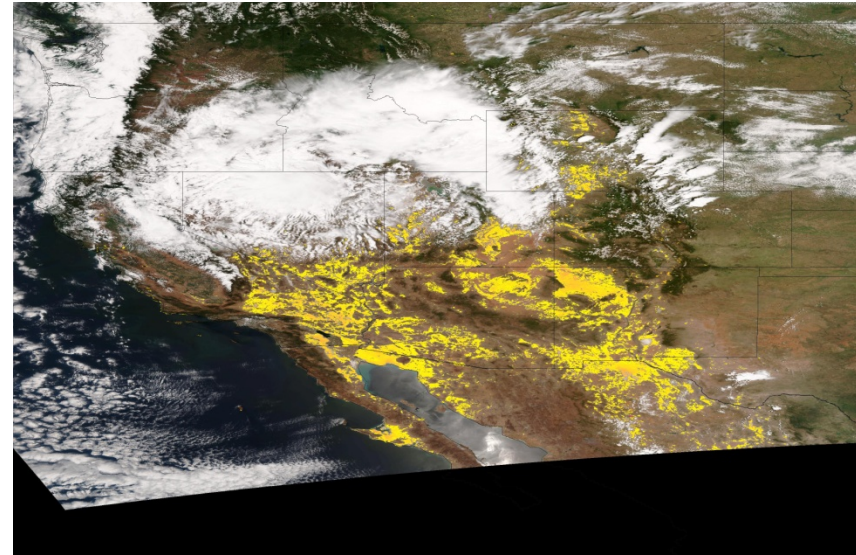


Dust mask (brown color regions) using
IR bands for the three cases

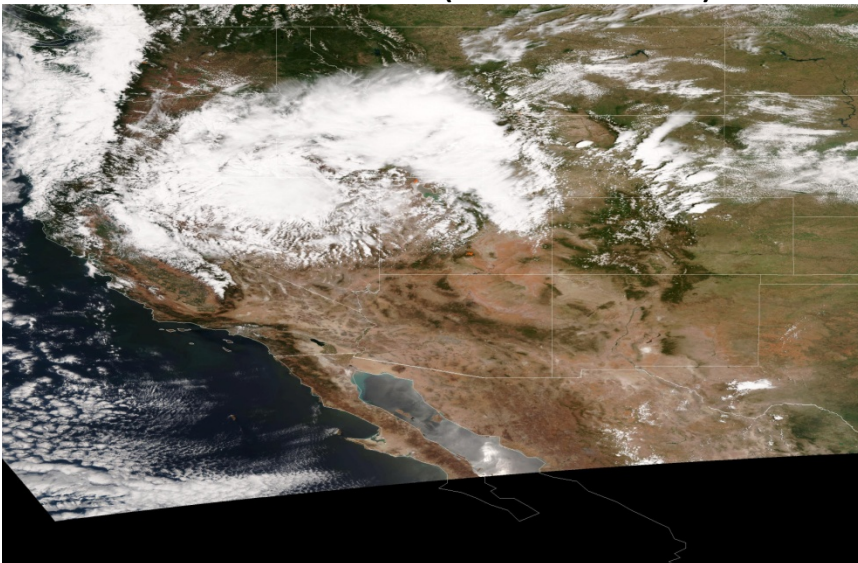
20170612 RGB



20170612 RGB ADP



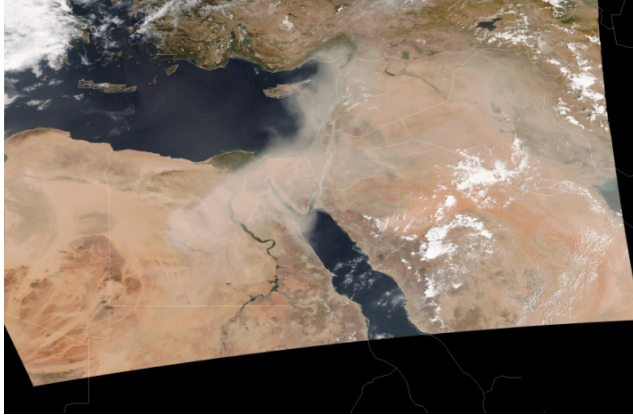
20170612 RGB IRDM (IR dust mask)



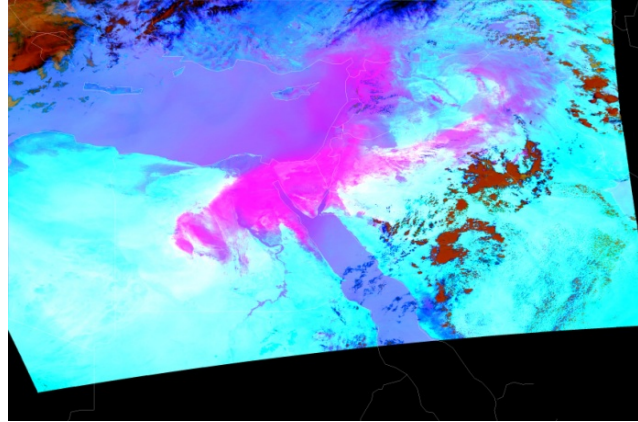
Another case with no dust

20150909 North Africa and Arabian Peninsula

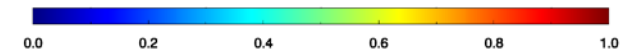
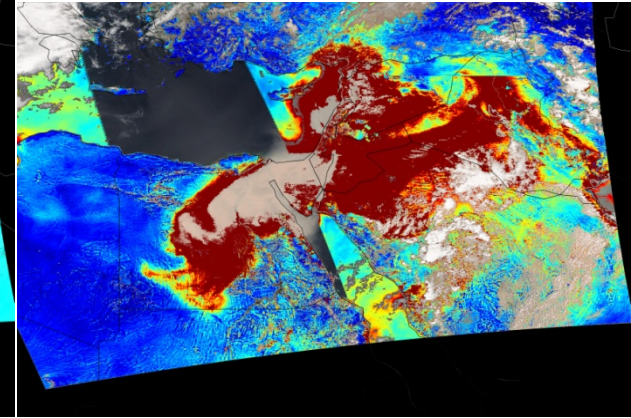
RGB



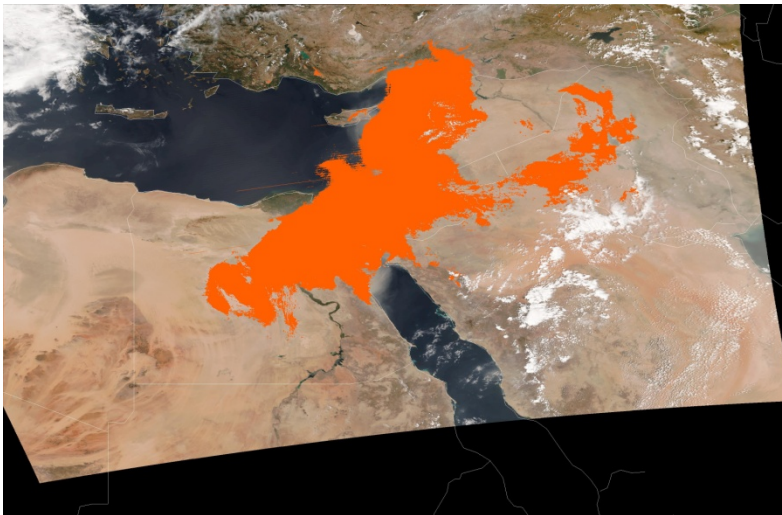
Dust RGB



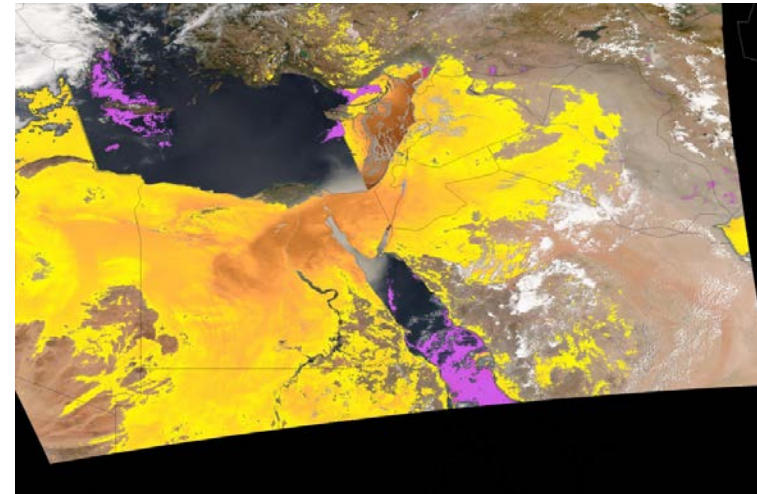
AOD



IRDM

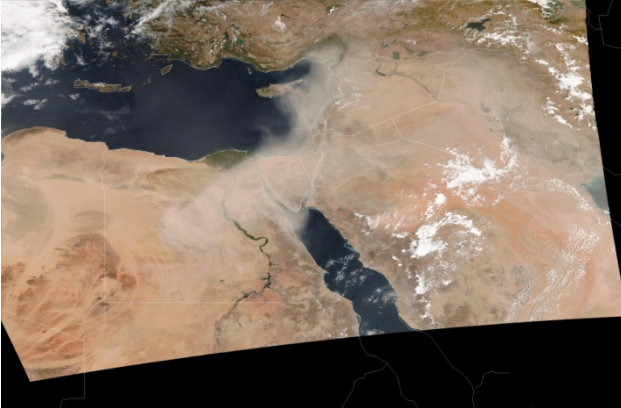


ADP

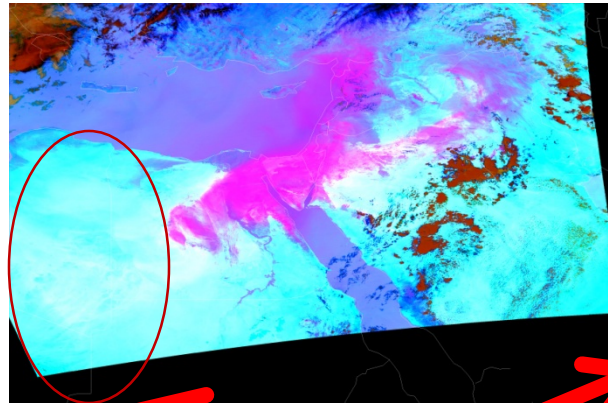


20150909 North Africa and Arabian Peninsula

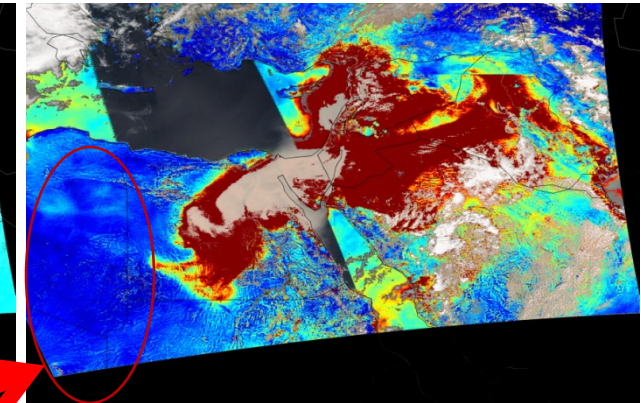
RGB



Dust RGB

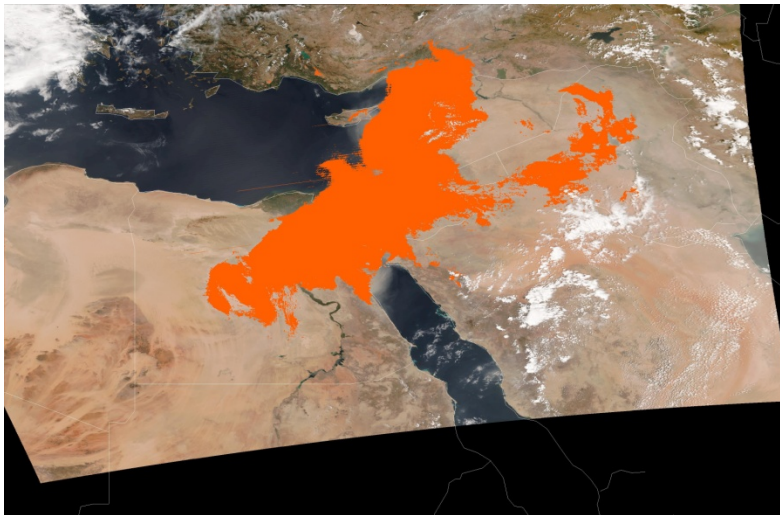


AOD

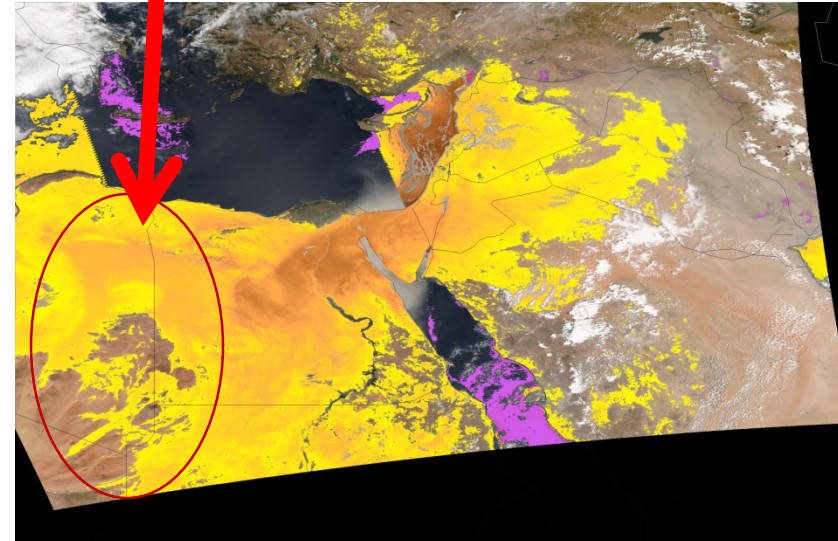


False detection in ADP

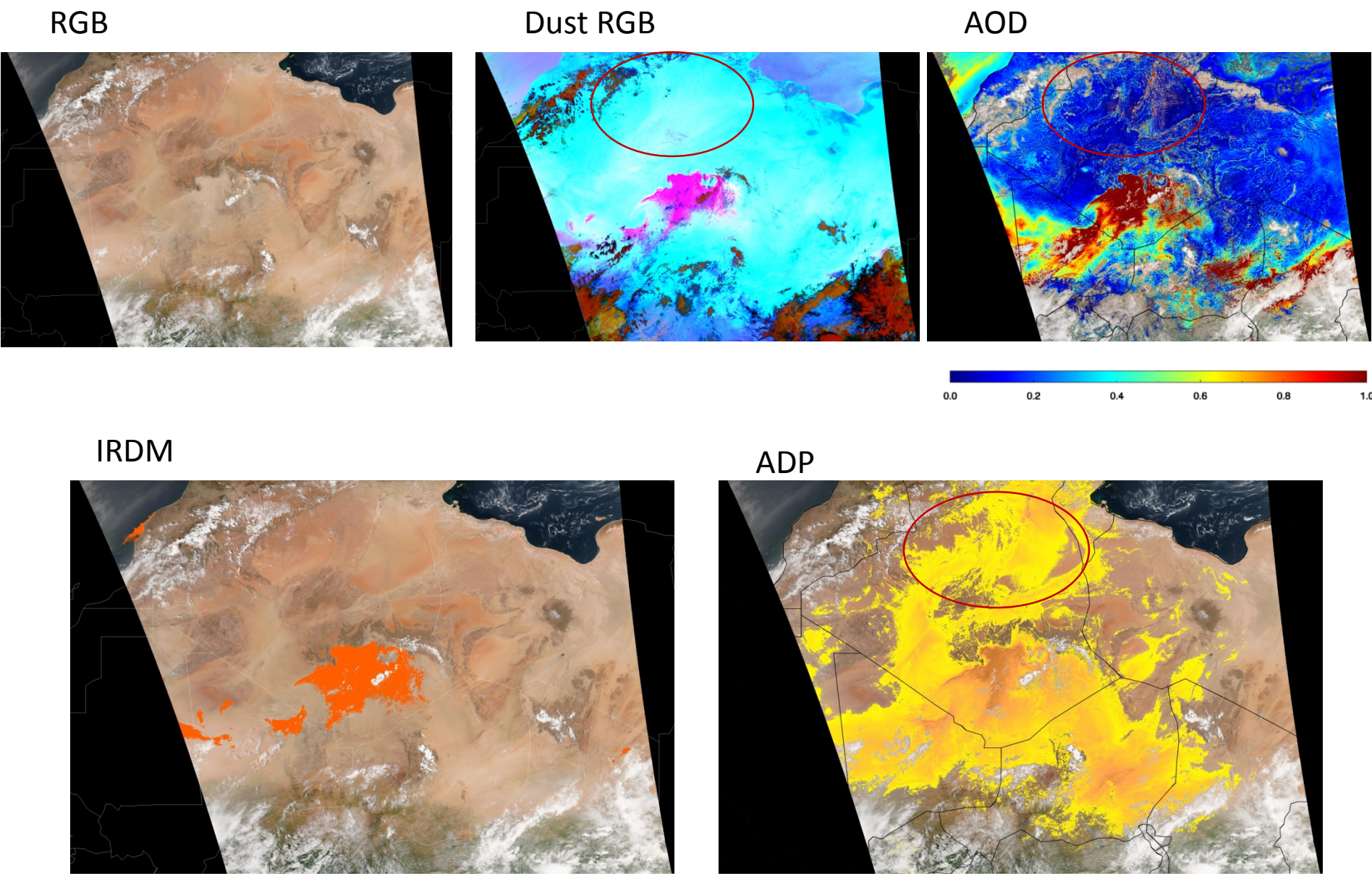
IRDM



ADP



Another case in North Africa 20130823



Summary

- Current ADP dust detection over land using deep blue bands has many areas of false detections
 - Less or no sensitivity of AAI to the aerosol load in some geometries and surface conditions
- An alternative dust detection method based on IR bands is proposed
- Case studies show that using IR bands for dust detection can greatly reduce false detections



STAR JPSS



2017 Annual Science Team Meeting

14-18 August 2017 • NCWCP • College Park, MD

The Future with JPSS

NOAA Center for Weather and Climate Prediction

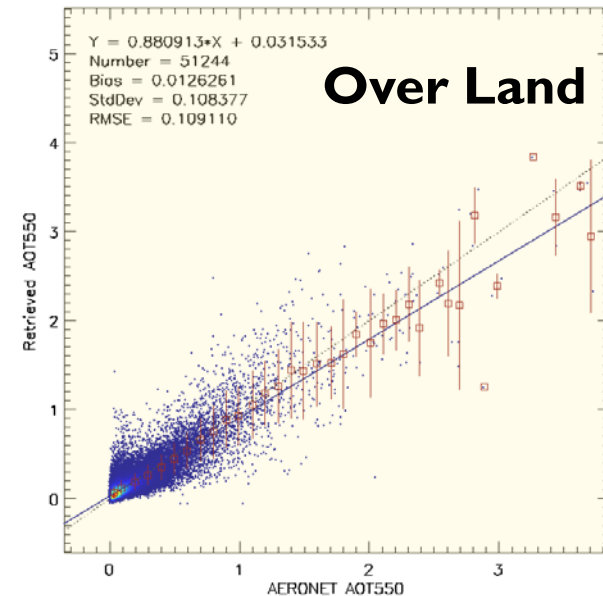
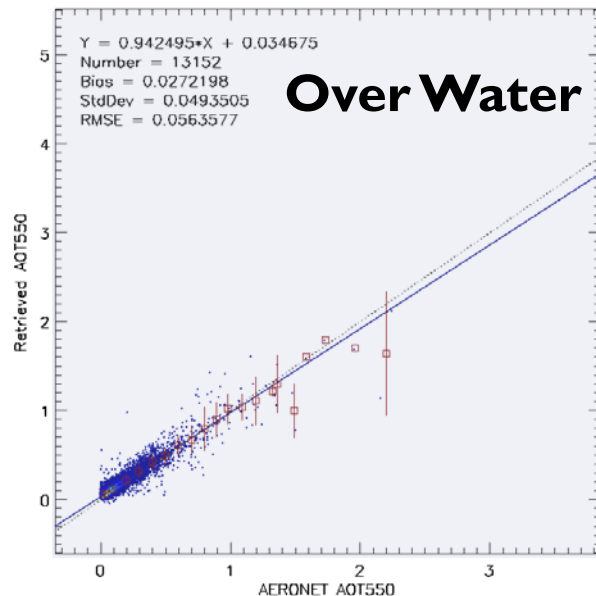
Conference Center • 5830 University Research Court • College Park, MD 20740

Evaluation of the VIIRS Enterprise Processing System AOD using AERONET over Different Geographic Regions

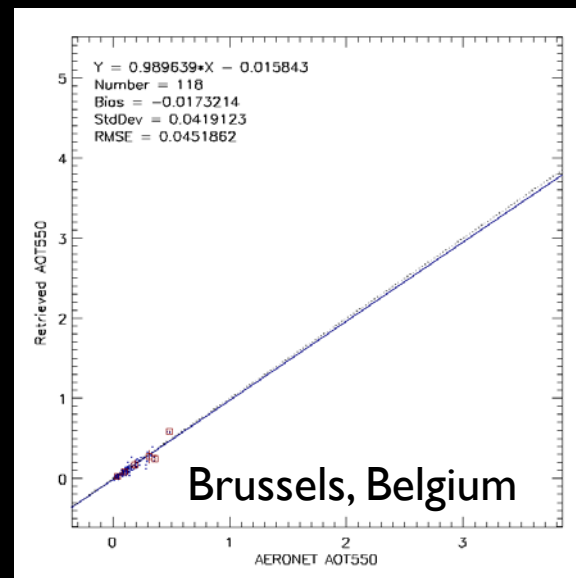
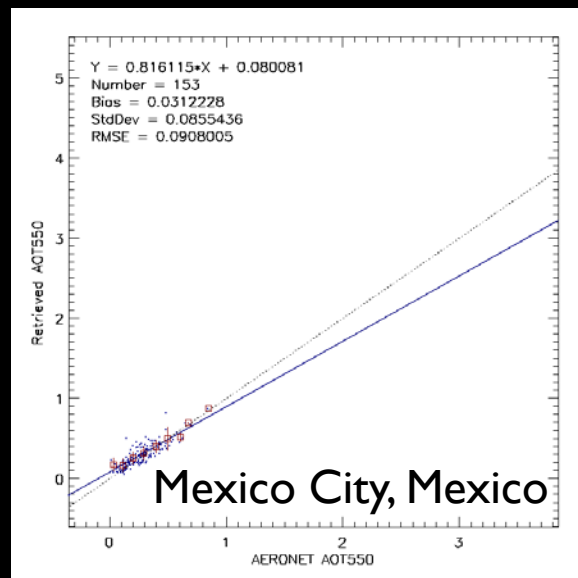
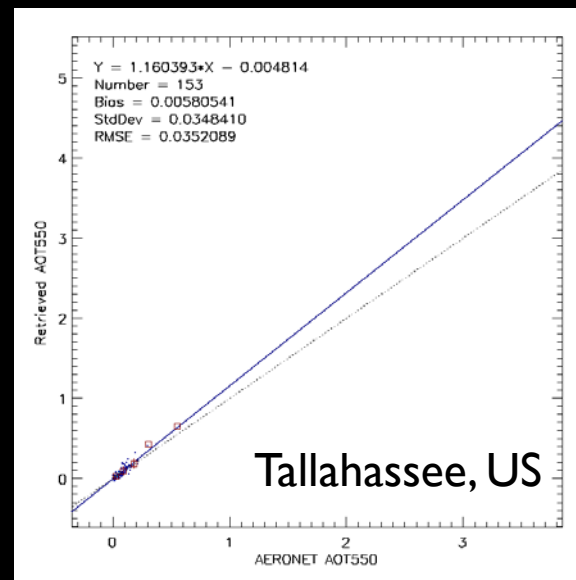
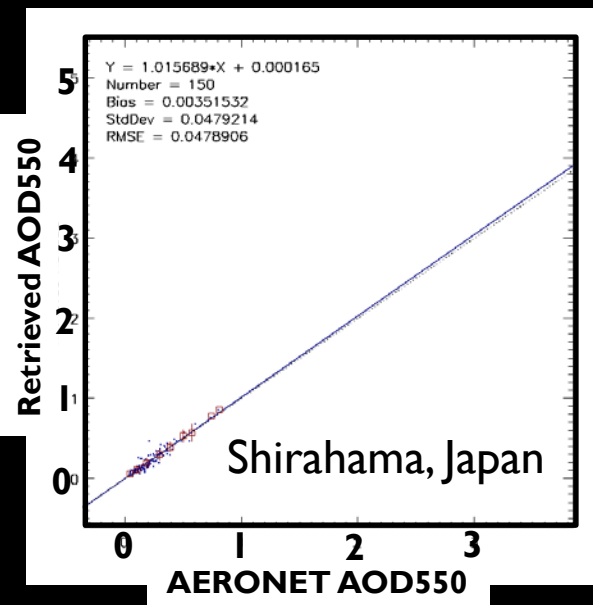
**Hongqing Liu
and NOAA STAR Aerosol Cal/Val Team**

EPS AOD Algorithm

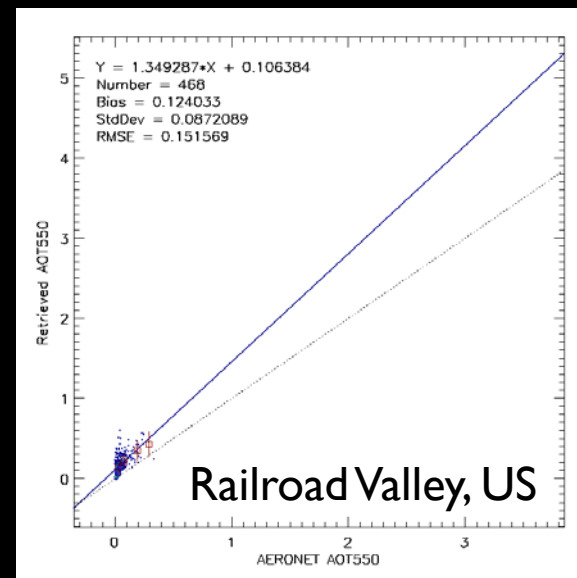
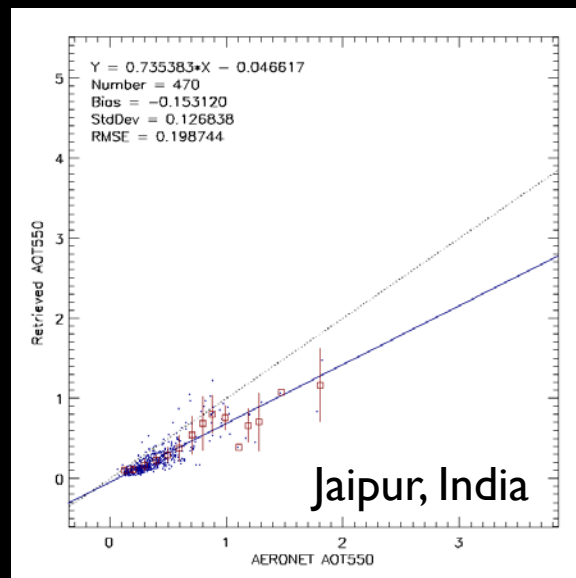
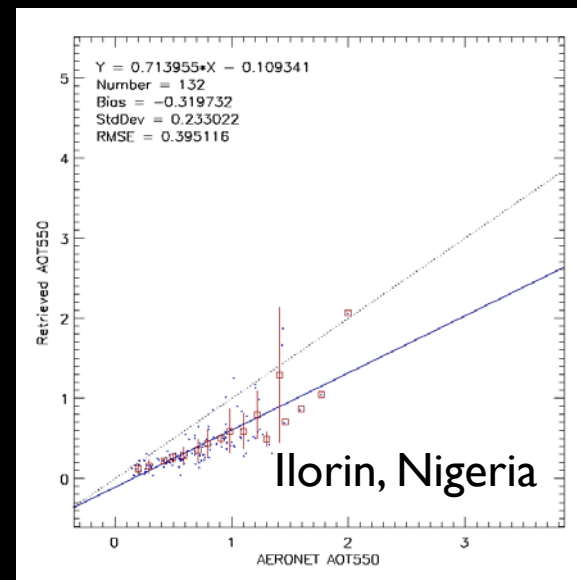
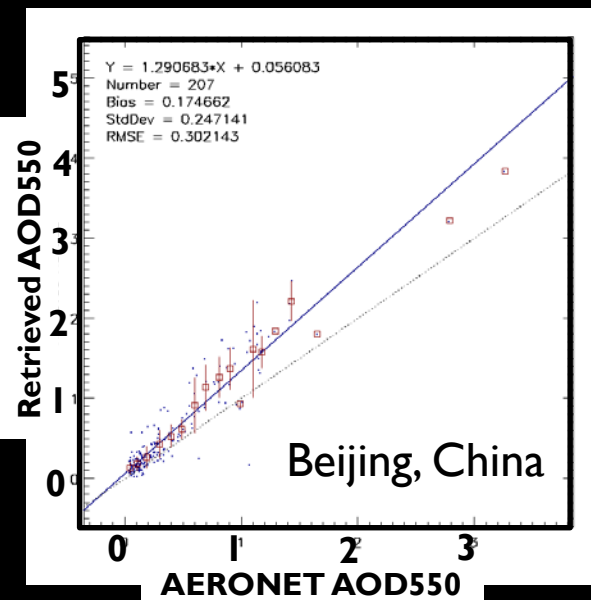
- **Multi-spectral aerosol retrieval**
- **Applied to VIIRS and ABI/AHI at pixel level**
- **Retrieval Coverage**
 - **Daytime cloud and snow/ice-free areas**
 - **Land: dark and bright**
 - **Ocean: non-glint deep water**
 - **AOD at 0.55 μ m: from -0.05 to 5.0**
- **High-quality retrievals meet requirement**
 - **Larger RMSE over land**



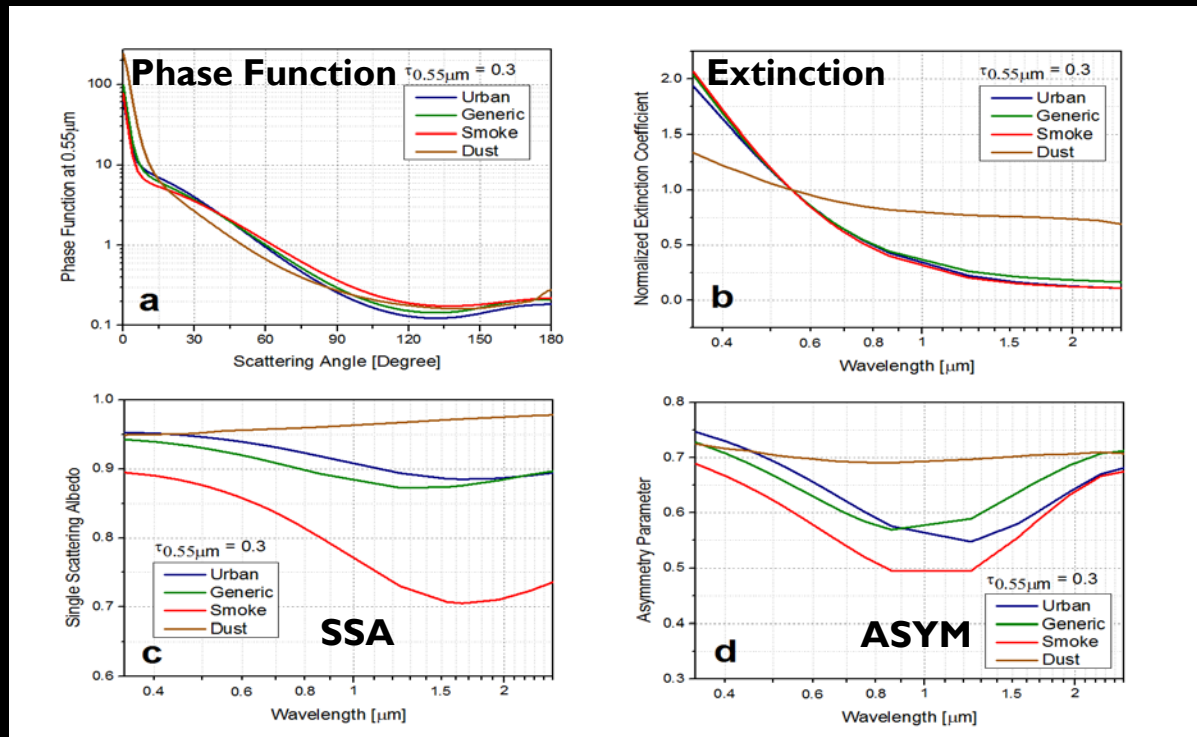
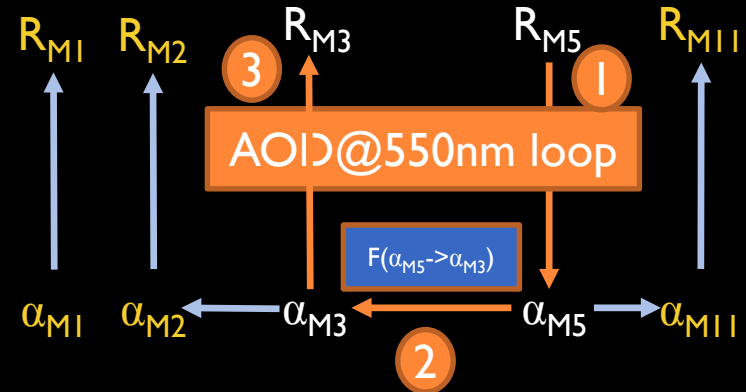
Example of Accurate Regional Retrievals



Example of Biased Regional Retrievals

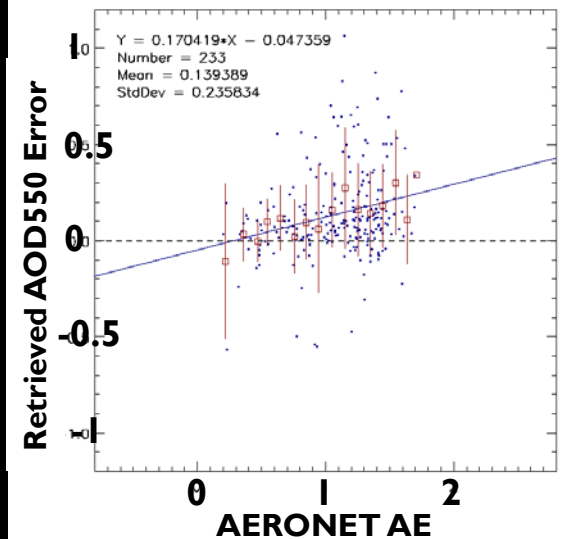
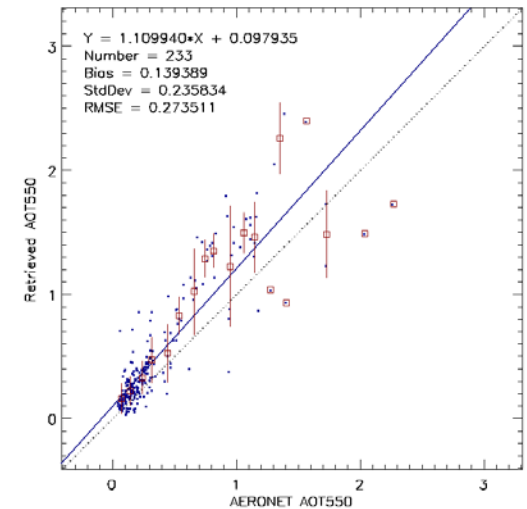
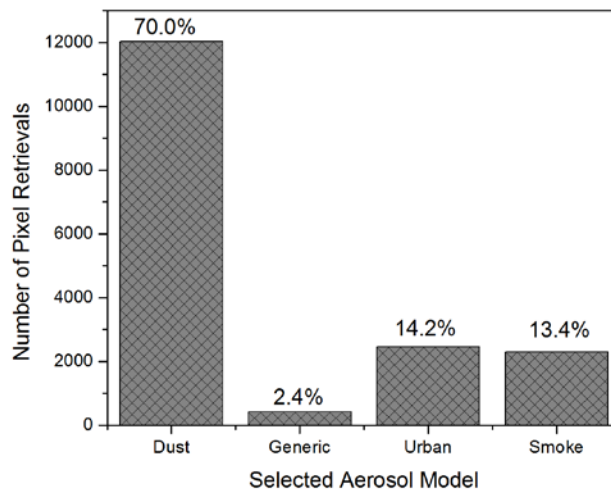


- Surface Reflectance
 - Simultaneous retrieval of AOD@550nm and surface reflectance with two reference channels
- Aerosol Models
 - Once AOD and surface reflectance are determined, difference between calculated and observed reflectance at residual channels are used to select optimal aerosol model from four candidates (urban, generic, smoke and dust)

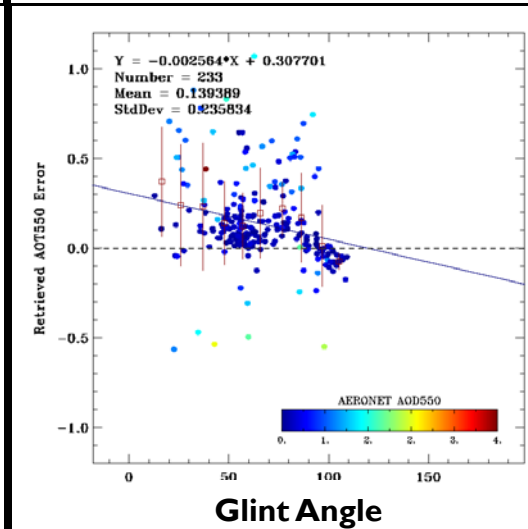
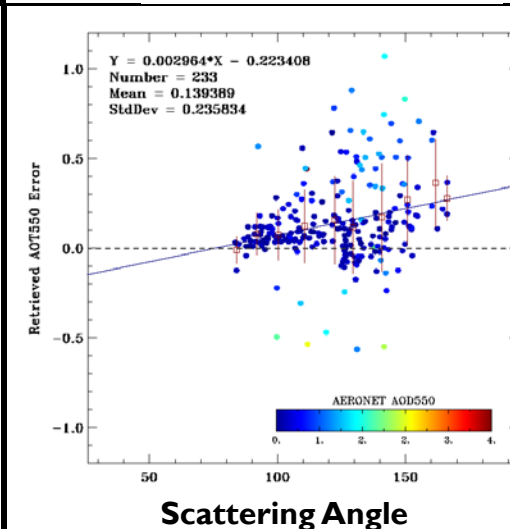
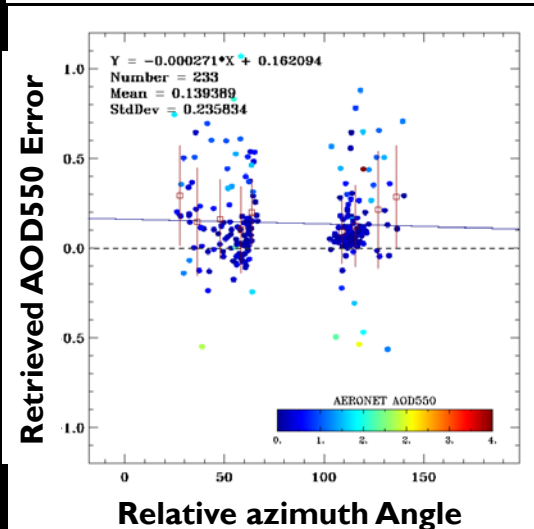
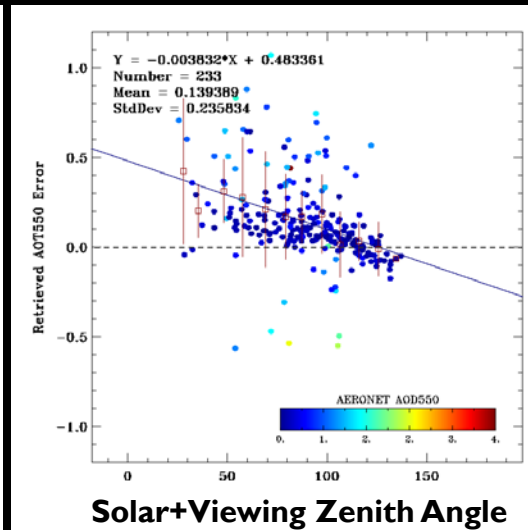
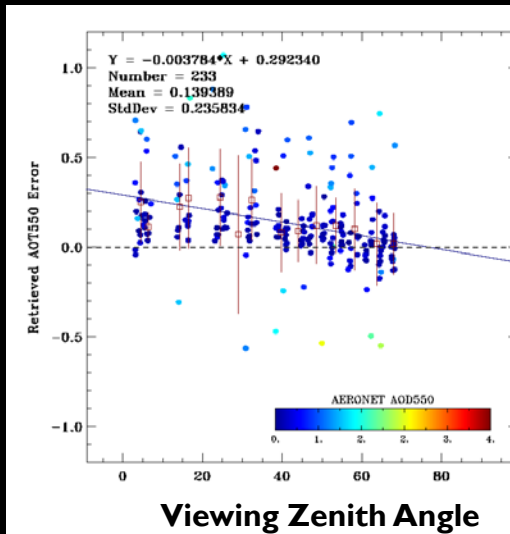
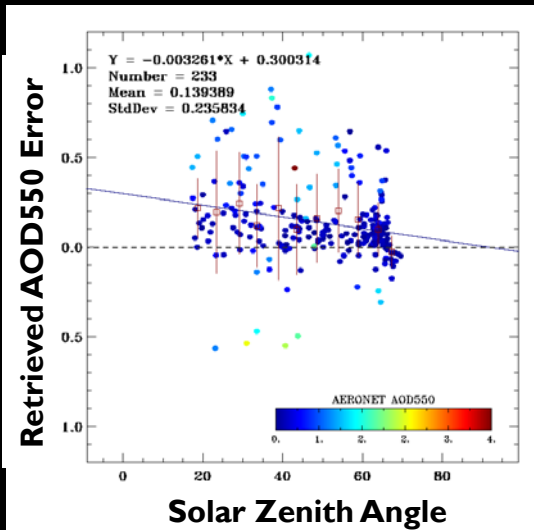


Beijing (I)

- AOD over-estimation
- Higher positive bias for fine-mode aerosol dominated cases (high AERONET AE)
- Majority (70%) of retrievals pick dust model

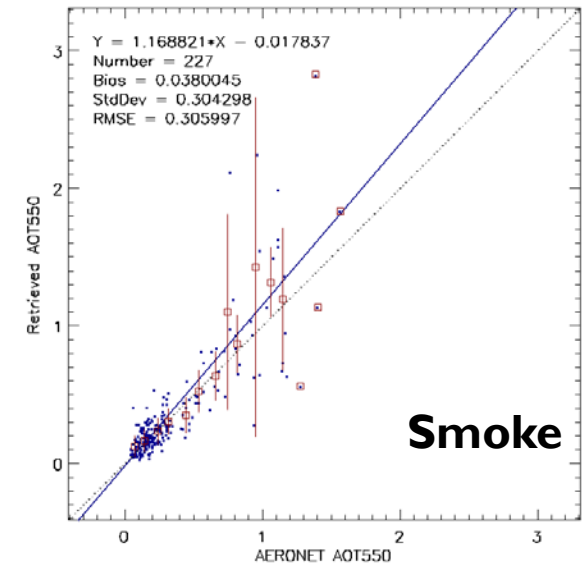
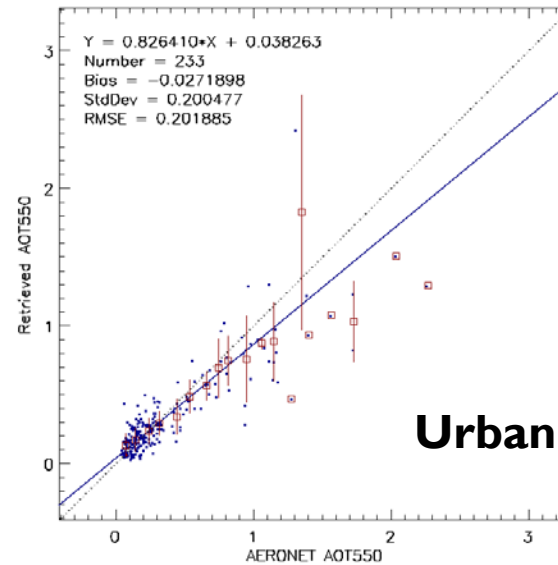
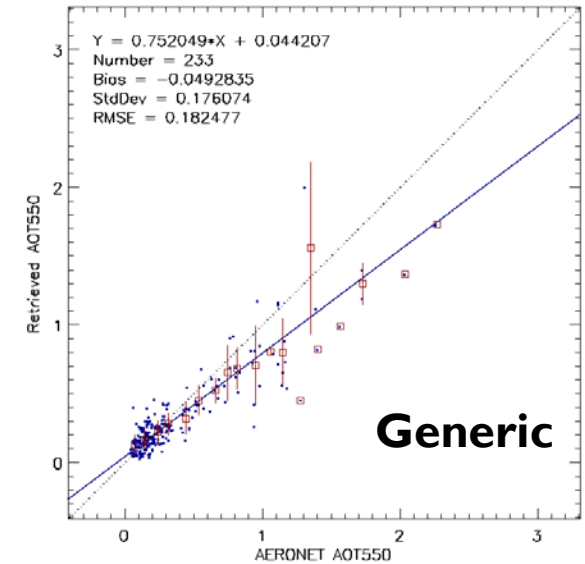
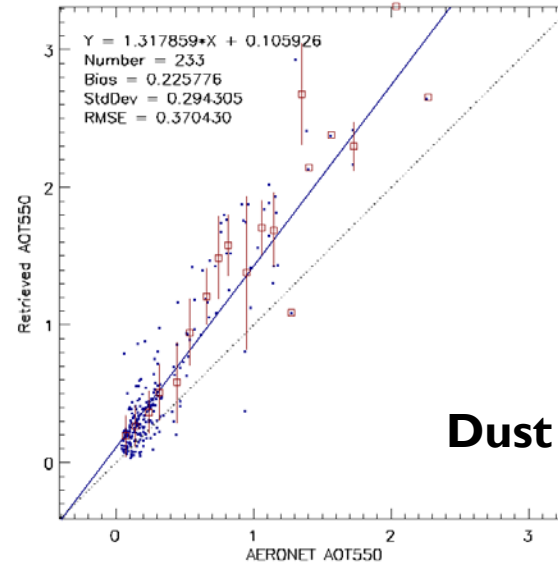


- Angular Dependence
 - Retrieval error against zenith, azimuth, scattering and glint angles

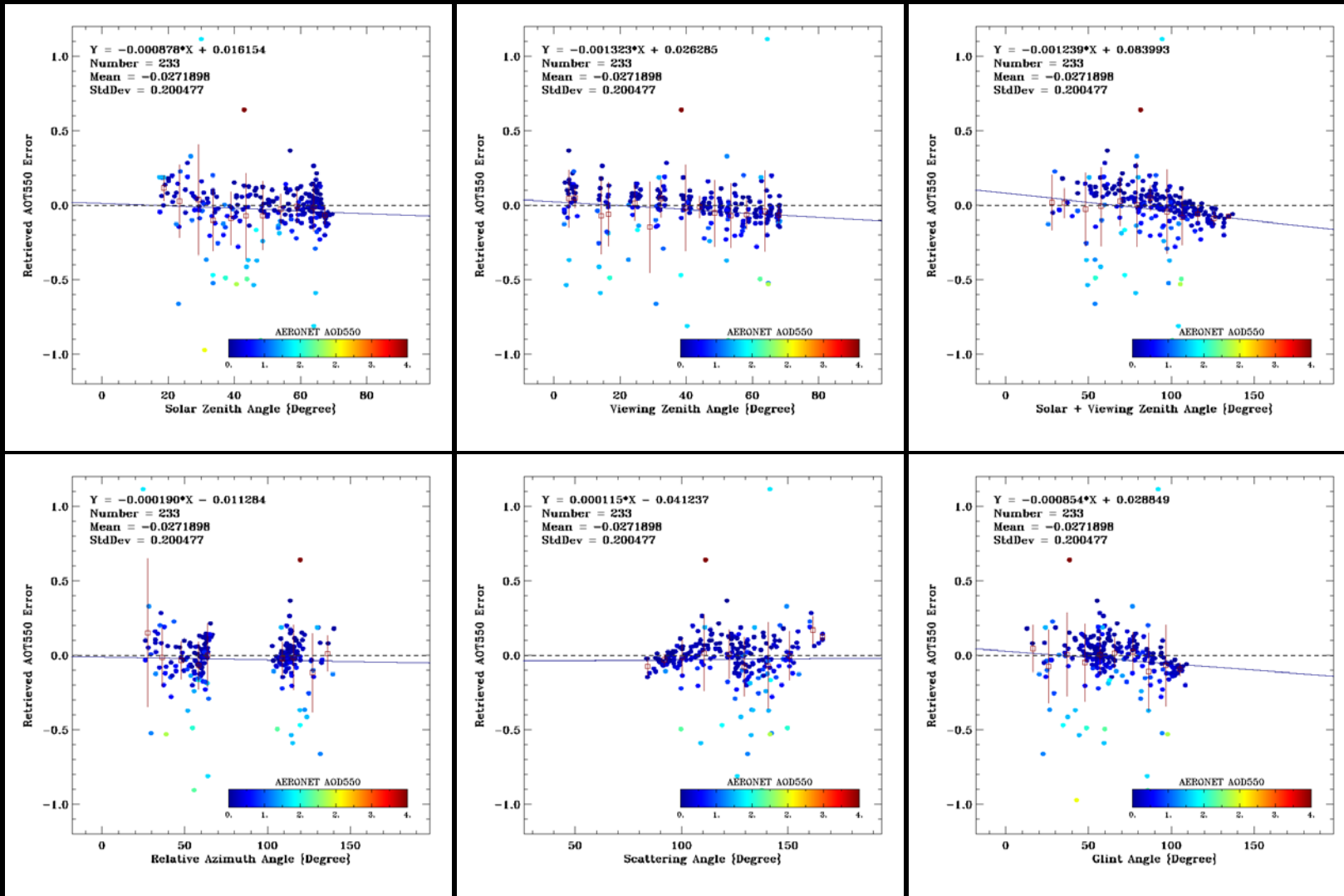


Beijing (3)

- Retrievals with fine-mode dominated aerosols would generate better results
- Problem in aerosol model selection



- Retrieval with urban aerosol model
 - Insignificant angular dependence of retrieval errors



• Case Study (04/17/2013 05:57GMT)

Inputs:

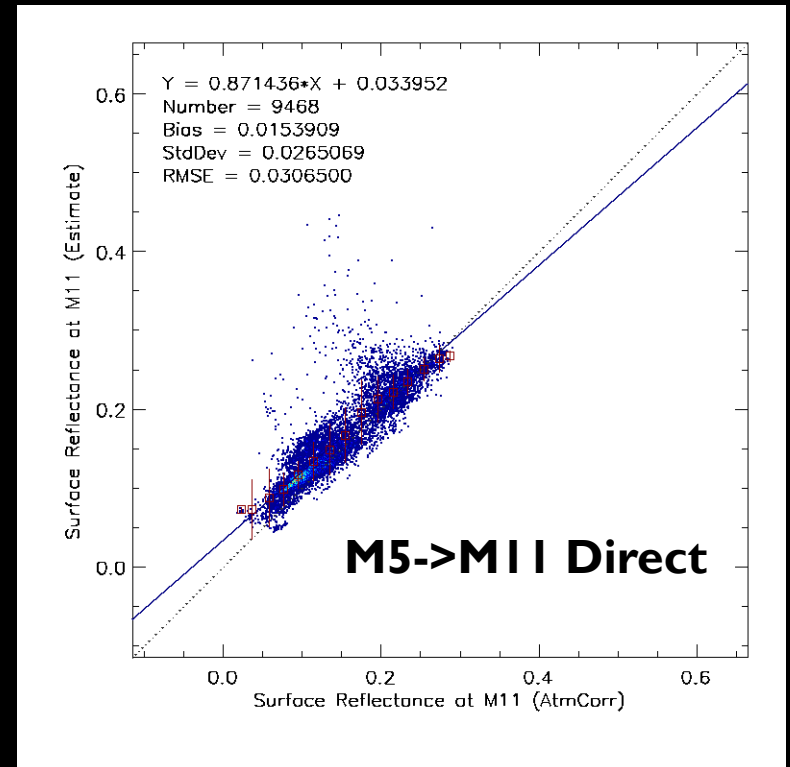
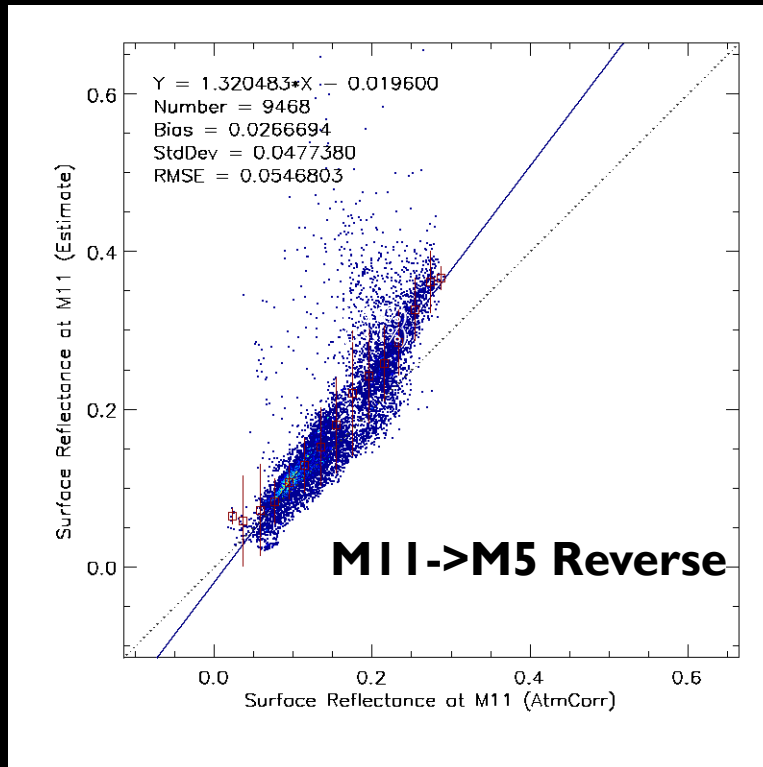
PW 1.14337 cm
 OZCONC 0.350851 atm-cm
 PSL 1004.41 hpa
 SFCTEMP 290.059 K
 HGT 13.8458 m
 WNDDIR 325.130 degree
 WNDSPD 3.28555 m/s
 REFLM1 0.322285
 REFLM2 0.289493
 REFLM3 0.258971
 REFLM4 0.227863
 REFLM5 0.235482
 REFLM6 0.176977
 REFLM7 0.282510
 REFLM8 0.299651
 REFLM9 0.00642178
 REFLM10 0.299211
 REFLM11 0.243100
 BTM12 313.225 K
 BTM15 292.967 K
 BTM16 291.786
 LAT 39.7449
 LON 116.487
 SOLZEN 37.2535 degree
 SATZEN 57.5084 degree
 SOLAZI -134.700 degree
 SATAZI -93.8151 degree
 HEIGHT 30.4856 m

AERONET AOD550 = **0.727** AE=1.25

	Dust	Generic	Urban	Smoke
AOD550	1.079	0.498	0.507	0.769
Resi@M1	0.035	0.070	0.071	0.021
Resi@M2	0.016	0.038	0.038	0.021
Resi@M11	0.137	0.528	0.527	0.700
Residual	0.082	0.309	0.308	0.404
SfcR@M1	0.0929	0.1318	0.1304	0.1547
SfcR@M2	0.1030	0.1436	0.1421	0.1675
SfcR@M3	0.1160	0.1577	0.1561	0.1822
SfcR@M5	0.1786	0.2304	0.2285	0.2609
SfcR@M11	0.3202	0.4434	0.4389	0.5160

Residual dominated by M11 (2.13μm)

- Revise the estimation of surface reflectance at M11
 - Current scheme uses the reverse of M11->M5 relationship
 - Derive a new direct relationship from M5 to M11



• Case Study - Revisit

AERONET AOD550 = **0.727** AE=1.25

- Compared with current EPS retrieval, estimated surface reflectance at M11 for fine mode aerosols is much closer to the correct value, and the residual is not significantly biased to M11 band.

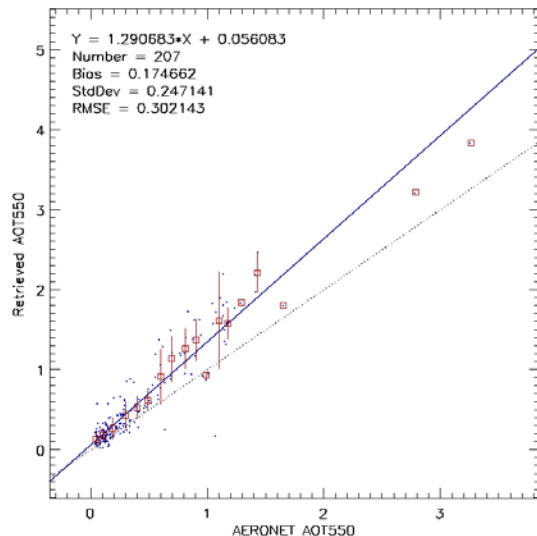
- Dust is still the best solution.

- Average of two best solutions (dust and generic weighed by residual) 0.794 is closer to the AERONET measurement.

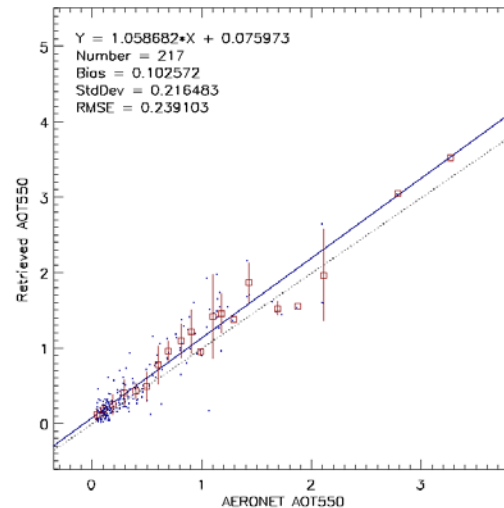
	Dust	Generic	Urban	Smoke
AOD550	1.079	0.498	0.507	0.769
Resi@M1	0.035	0.070	0.071	0.021
Resi@M2	0.016	0.038	0.038	0.021
<i>Resi@M11</i>	<i>0.056</i>	<i>0.038</i>	<i>0.041</i>	<i>0.087</i>
Residual	0.049	0.051	0.052	0.053
SfcR@M1	0.0929	0.1318	0.1304	0.1547
SfcR@M2	0.1030	0.1436	0.1421	0.1675
SfcR@M3	0.1160	0.1577	0.1561	0.1822
SfcR@M5	0.1786	0.2304	0.2285	0.2609
SfcR@M11	0.2472	0.2952	0.2934	0.3234

- Retrieval with new M5->MI I surface relationship
 - Retrieval over Beijing is slightly improved by using new M5->MI I surface reflectance relationship
 - With modification, less dust retrievals are picked as the best solution: dust 36% (70%); generic 2% (2%); urban 30% (14%); smoke 32% (14%)
 - More improvement is achieved if best two solutions are weighted averaged by the residual

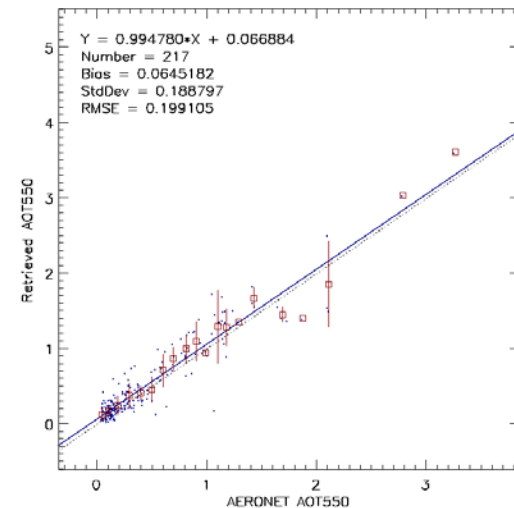
EPS Original Retrieval



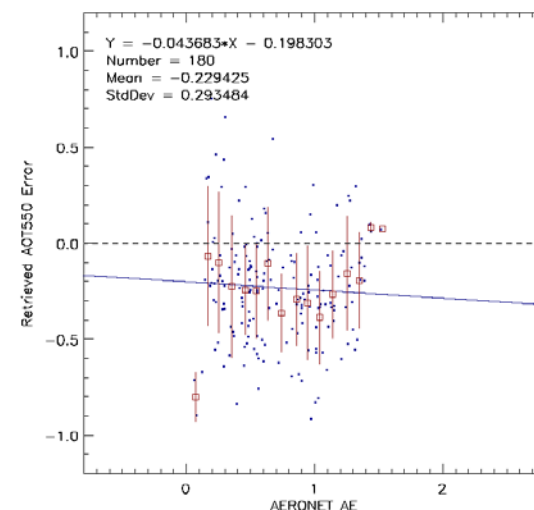
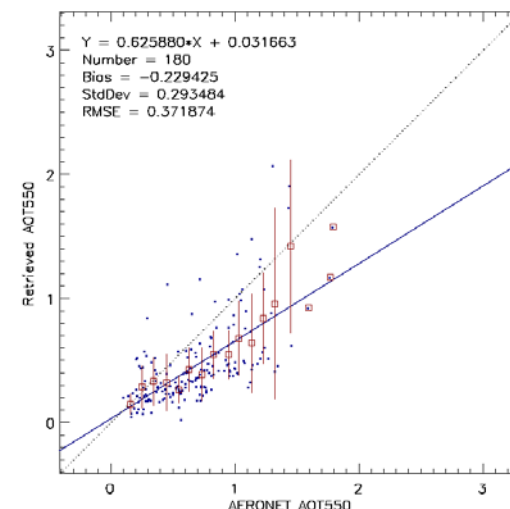
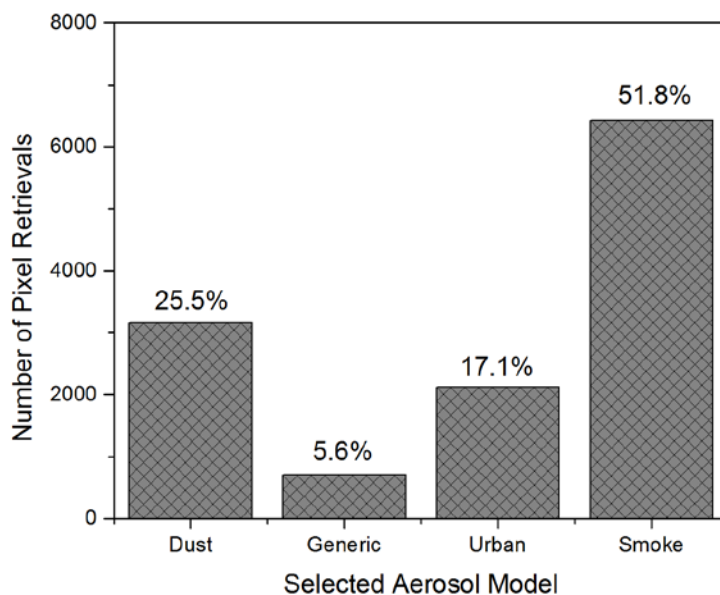
New M5->MI I Relationship



New M5->MI I Relationship
Average of best two solutions

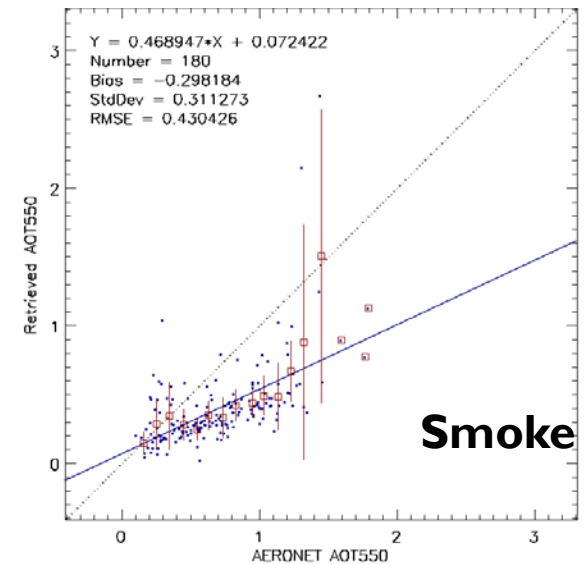
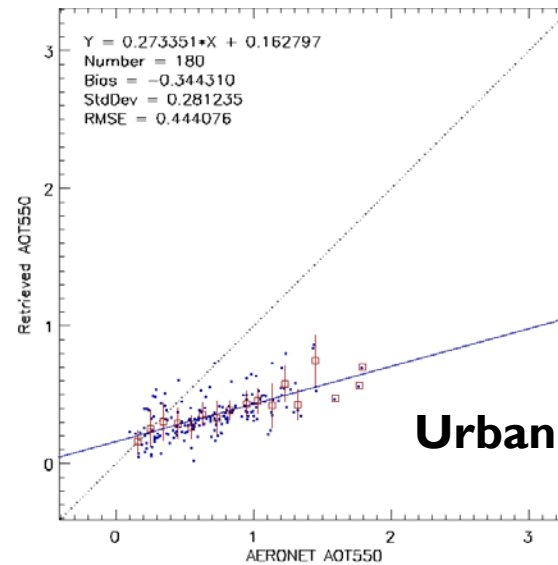
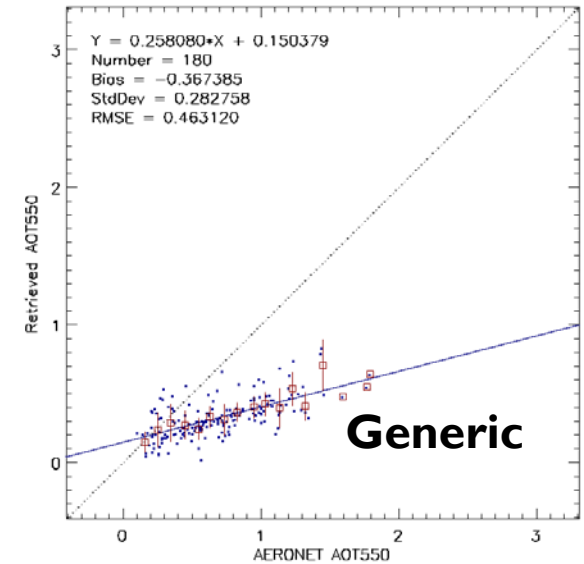
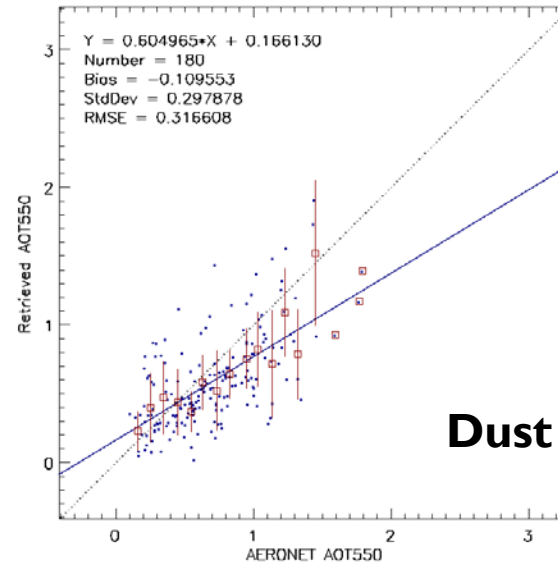


- AOD under-estimation
- Majority (52%) of retrievals pick smoke model, while AERONET Angstrom Exponent shows many dust cases dominated by low AE



Ilorin (2)

- Retrievals with dust model would generate better results
- Problem in aerosol model selection



- Case Study (12/18/2012)

Inputs:

PW 1.51776 cm
OZCONC 0.253983 atm-cm
PSL 966.612 hpa
SFCTEMP 306.494 K
HGT 331.854 m
WNDDIR 212.892 degree
WINDSPD 3.59268 m/s
REFLM1 0.262927
REFLM2 0.229963
REFLM3 0.200540
REFLM4 0.177515
REFLM5 0.165452
REFLM6 0.175586
REFLM7 0.270887
REFLM8 0.329367
REFLM9 0.0115250
REFLM10 0.285928
REFLM11 0.195022
BTM12 316.778 K
BTM15 304.850 K
BTM16 303.218 K
LAT 8.28619
LON 4.16135
SOLZEN 40.53 degree
SATZEN 40.63 degree
SOLAZI -141.99 degree
SATAZI -98.14 degree
HEIGHT 371.975 m

AERONET AOD550 = **1.186** AE = 0.34

	Dust	Generic	Urban	Smoke
AOD550	1.254	0.570	0.606	0.769
Resi@M1	0.023	0.035	0.036	0.009
Resi@M2	0.006	0.019	0.019	0.005
<i>Resi@M11</i>	<i>0.201</i>	<i>0.194</i>	<i>0.193</i>	<i>0.198</i>
Residual	0.1167	0.1141	0.1139	0.1143
SfcR@M1	0.0269	0.0739	0.0738	0.0810
SfcR@M2	0.0289	0.0812	0.0811	0.0891
SfcR@M3	0.0364	0.0921	0.0919	0.1005
SfcR@M5	0.0677	0.1355	0.1353	0.1457
SfcR@M11	0.1320	0.1728	0.1726	0.1789

Residual dominated by M11, difference is very small, hard to select correct model; dust high AOD associated with low surface reflectance

- Case Study (1/9/2013)

Inputs:

AERONET AOD550 = **1.273** AE = 0.578

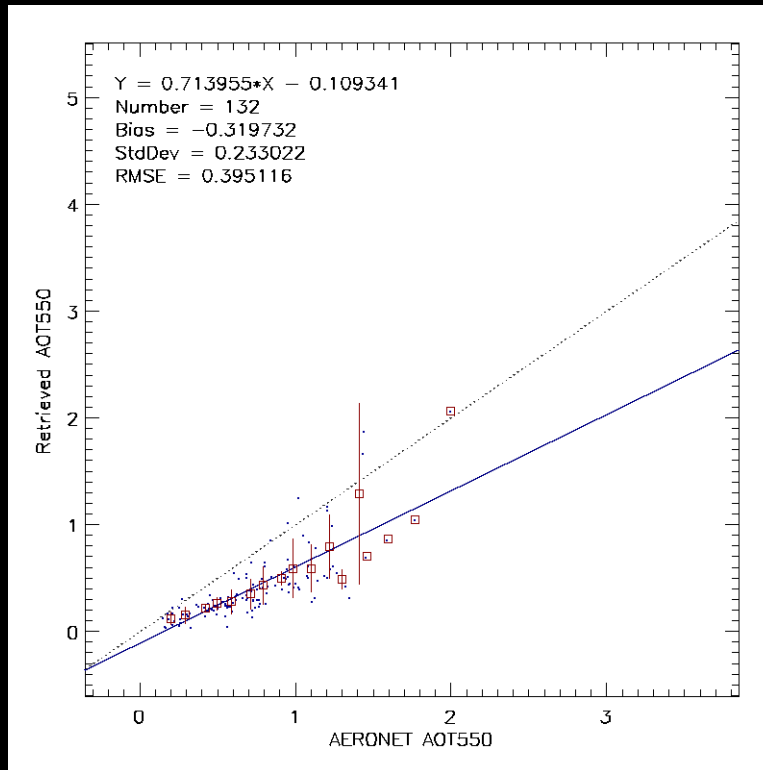
PW 2.16383
OZCONC 0.246923
PSL 965.934
SFCTEMP 308.135
HGT 357.818
WNDDIR 217.665
WINDSPD 2.76619
REFLM1 0.206205
REFLM2 0.180127
REFLM3 0.156760
REFLM4 0.141377
REFLM5 0.127727
REFLM6 0.164988
REFLM7 0.249692
REFLM8 0.294279
REFLM9 0.00300334
REFLM10 0.228132
REFLM11 0.133368
BTM12 311.346
BTM15 303.350
BTM16 301.711
LAT 8.08027
LON 4.37263
SOLZEN 36.08
SATZEN 20.74
SOLAZI -146.94
SATAZI -97.84
HEIGHT 395.466

	Dust	Generic	Urban	Smoke
AOD550	1.232	0.620	0.679	0.700
<i>Resi@M1</i>	<i>0.065</i>	<i>0.098</i>	<i>0.096</i>	<i>0.056</i>
Resi@M2	0.017	0.039	0.037	0.026
Resi@M11	0.015	0.005	0.007	0.014
Residual	0.040	0.061	0.060	0.036
SfcR@M1	0.0115	0.0504	0.0499	0.0558
SfcR@M2	0.0136	0.0540	0.0535	0.0596
SfcR@M3	0.0207	0.0617	0.0612	0.0673
SfcR@M5	0.0463	0.0968	0.0962	0.1037
SfcR@M11	0.1139	0.1450	0.1446	0.1492

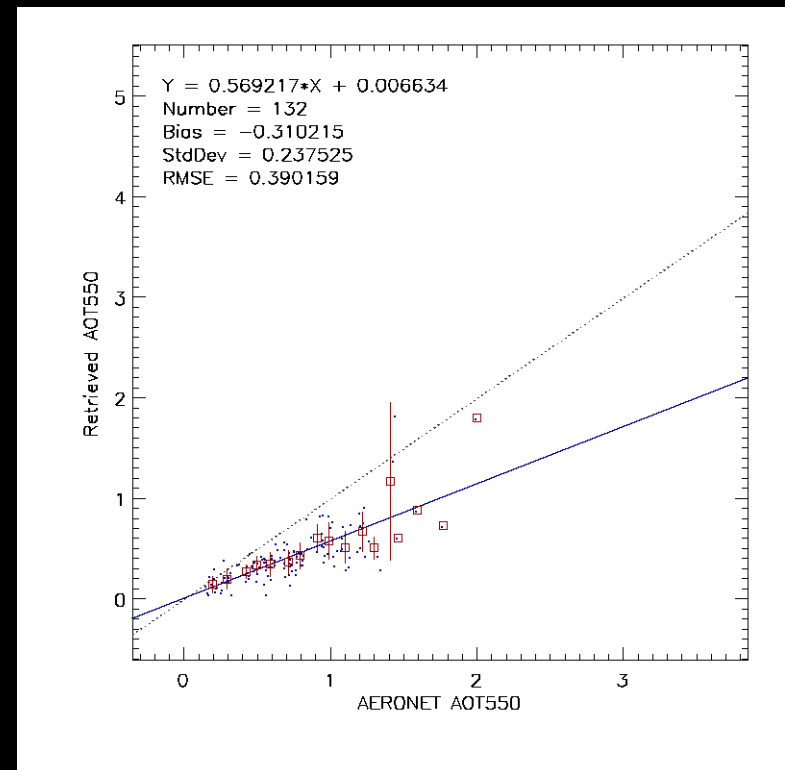
Residual dominated by M1, difference is very small, hard to select correct model; dust high AOD associated with low surface reflectance

- Retrieval with new M5->MI I surface relationship
 - No improvement

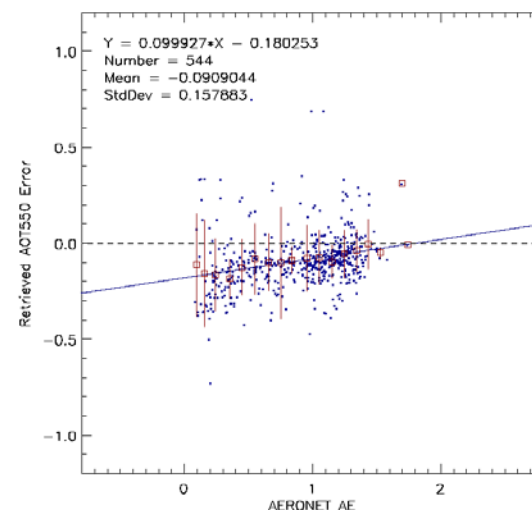
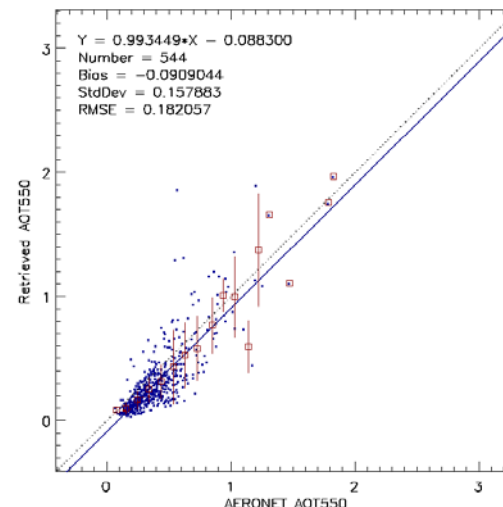
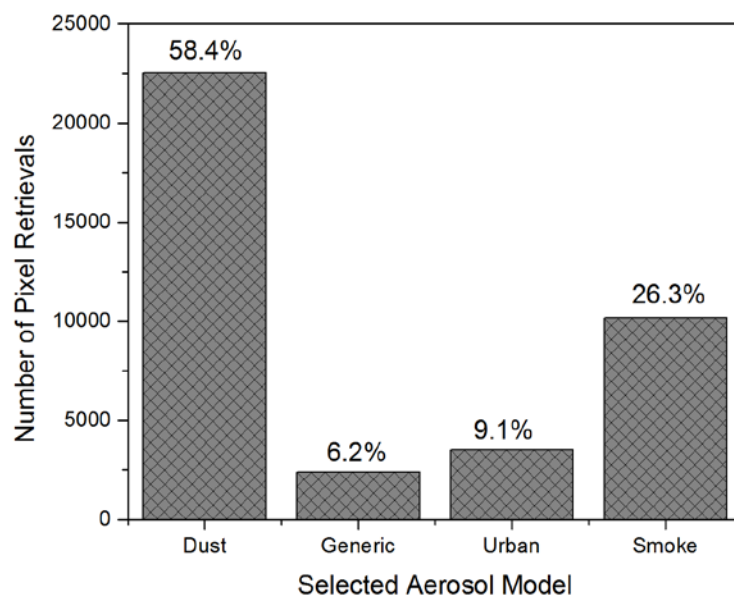
EPS Original Retrieval



New M5->MI I Relationship

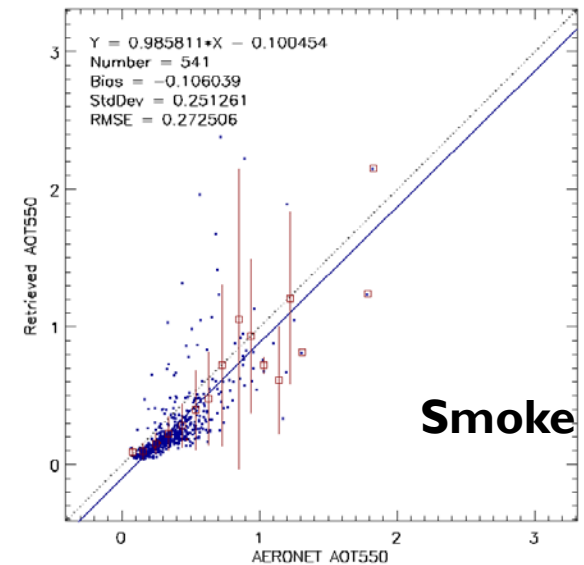
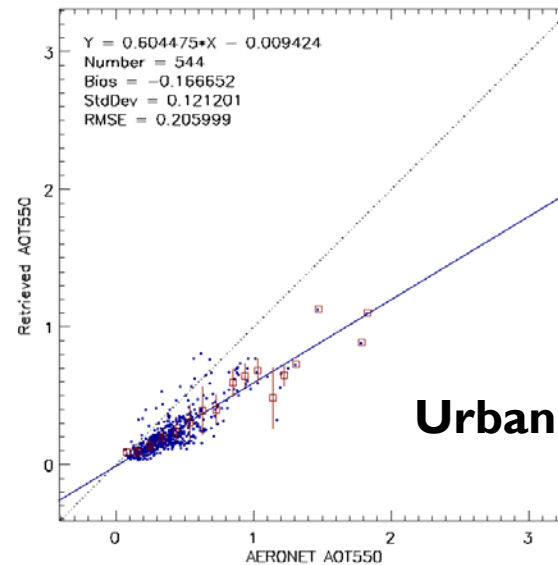
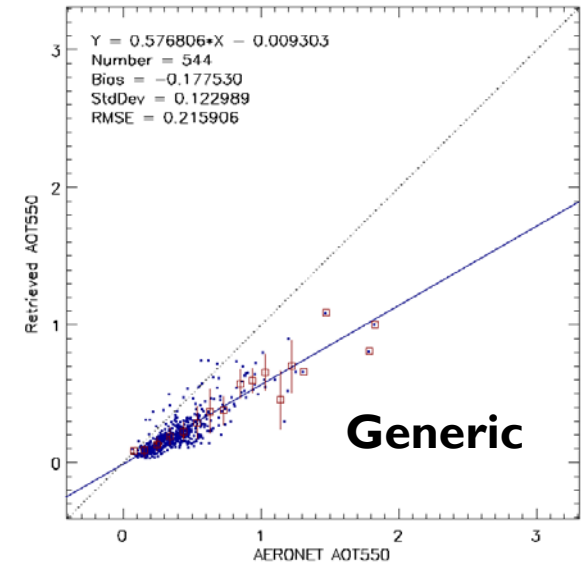
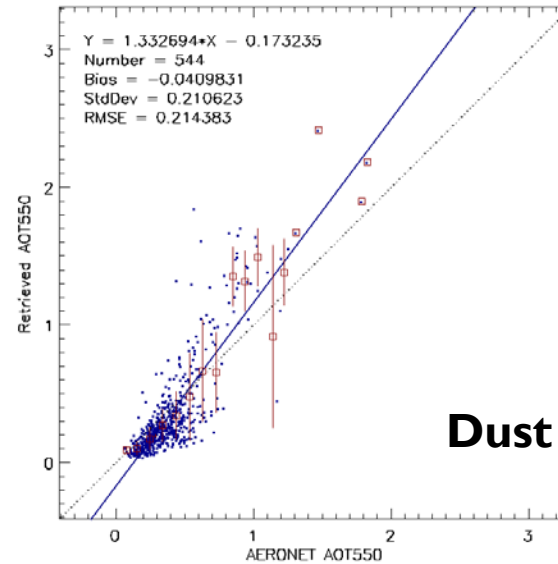


- AOD small under-estimation
- 58% of retrievals pick dust model and 26% of retrievals pick smoke.

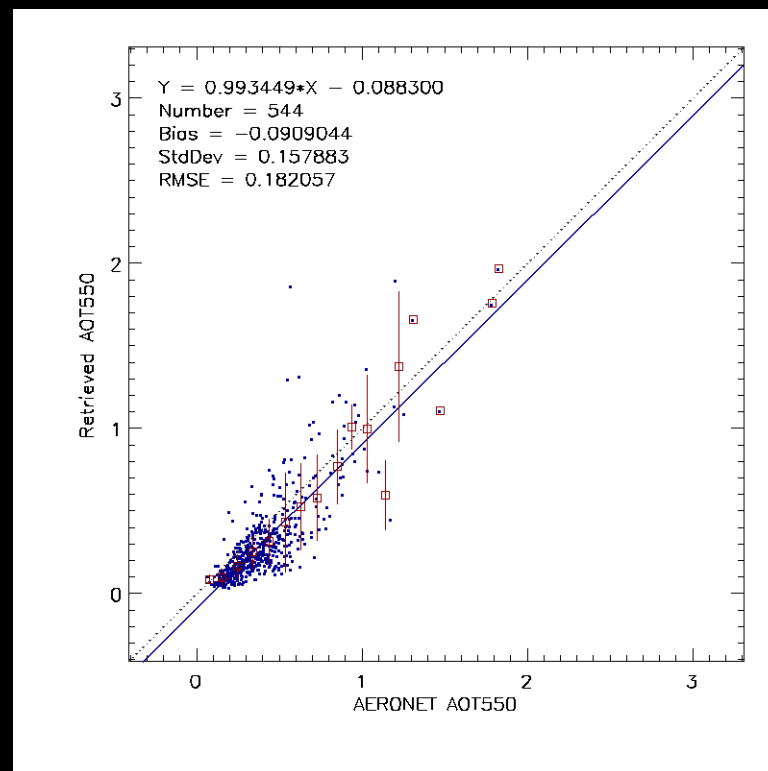
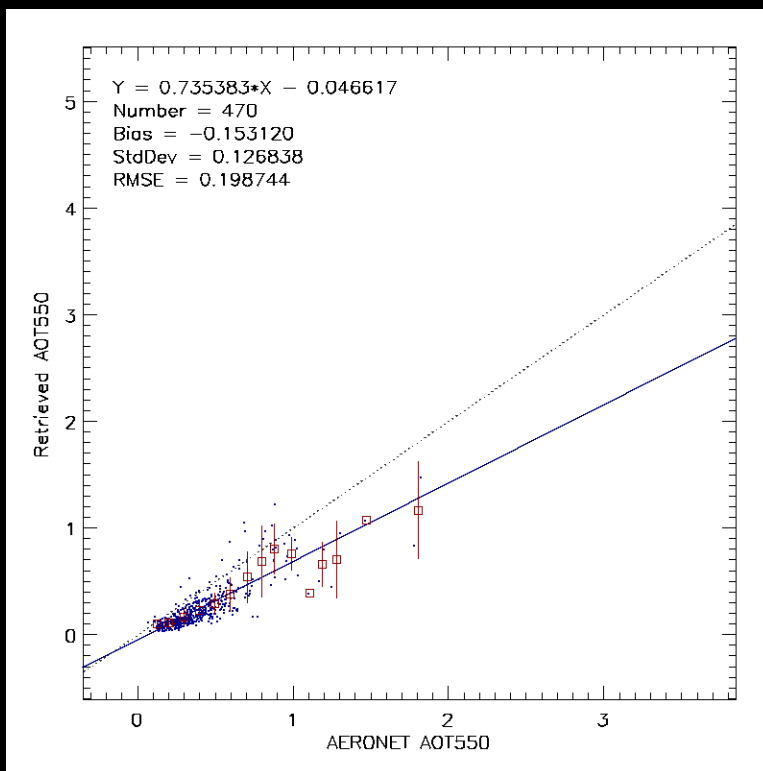


Jaipur (2)

- Dust and smoke models give better results than generic and urban models

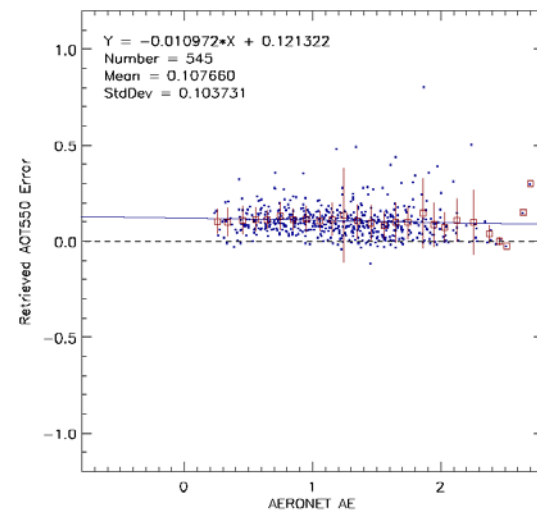
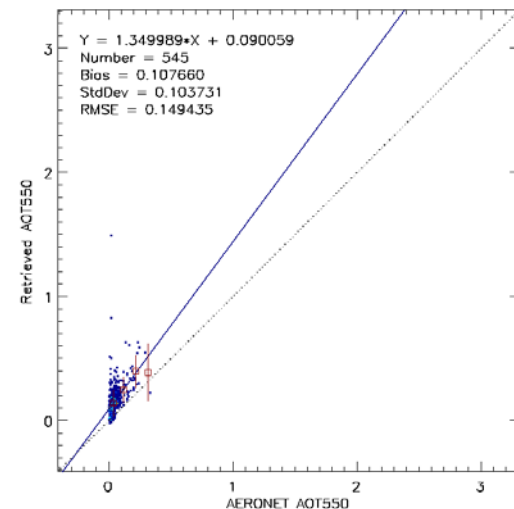
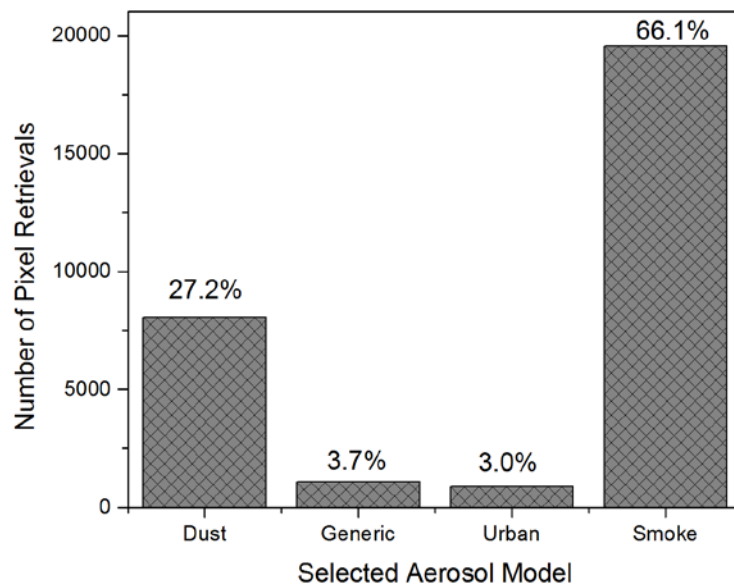


- Validation statistics depend on the satellite-ground matching method
 - **Left:** 27.5 km radius on satellite retrievals centered on the Jaipur station, at least 750 high quality pixel retrievals
 - **Right:** 5 km radius, at least 5 high quality retrievals

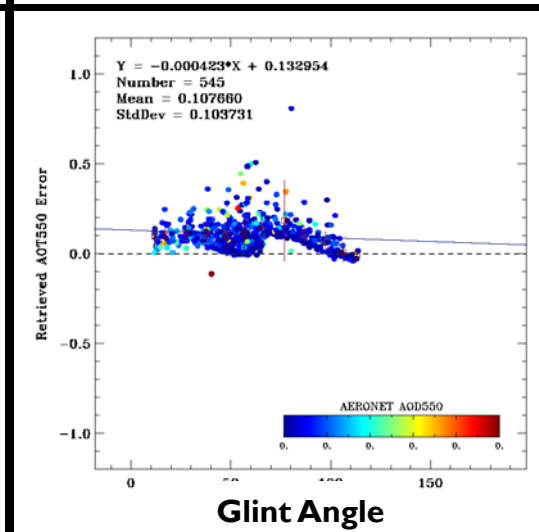
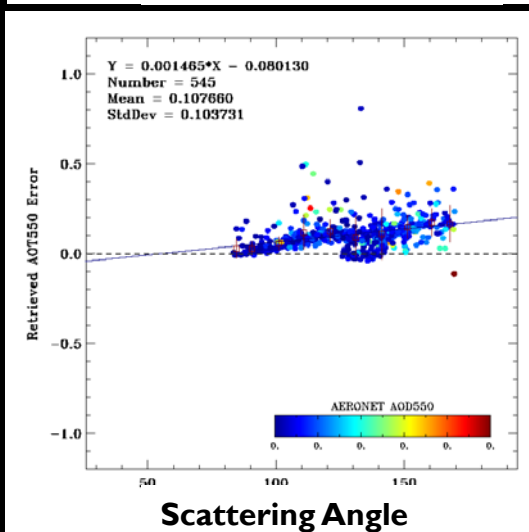
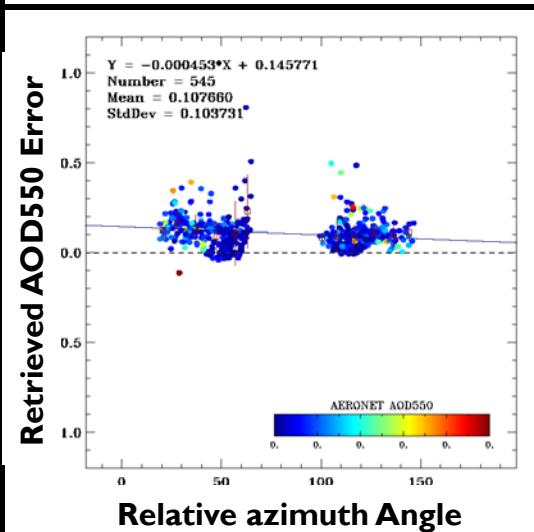
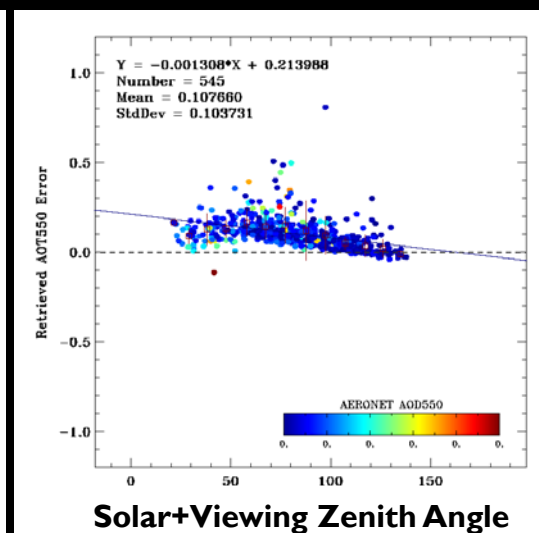
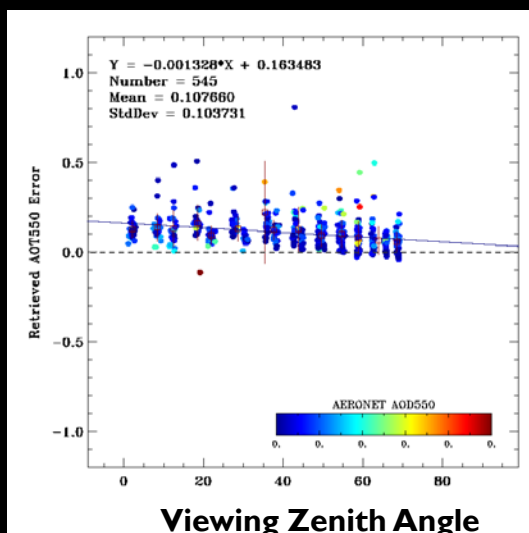
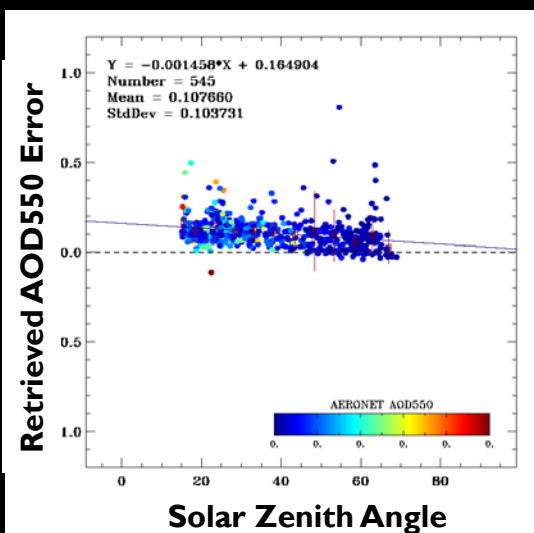


Railroad Valley (I)

- AOD over-estimation
- Low AOD dominated area
- 66% of retrievals pick smoke model and 27% of retrievals pick dust.

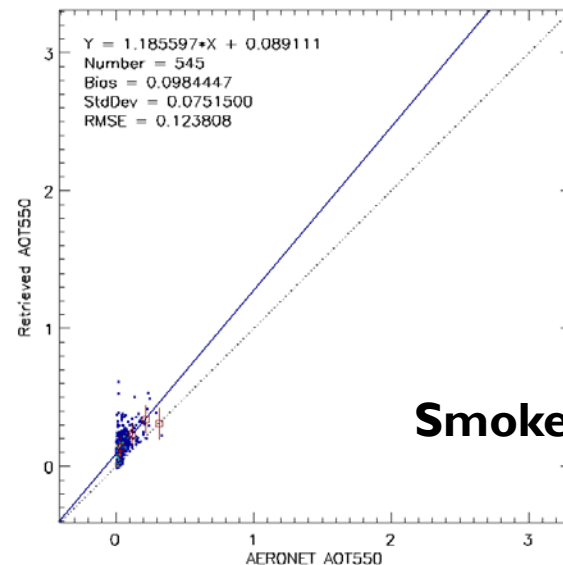
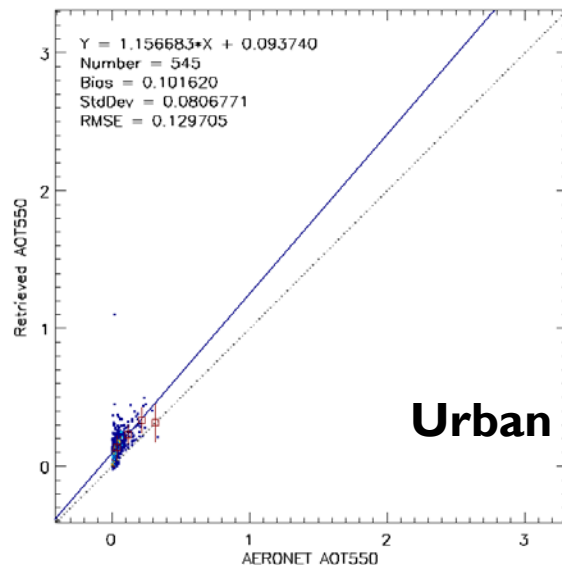
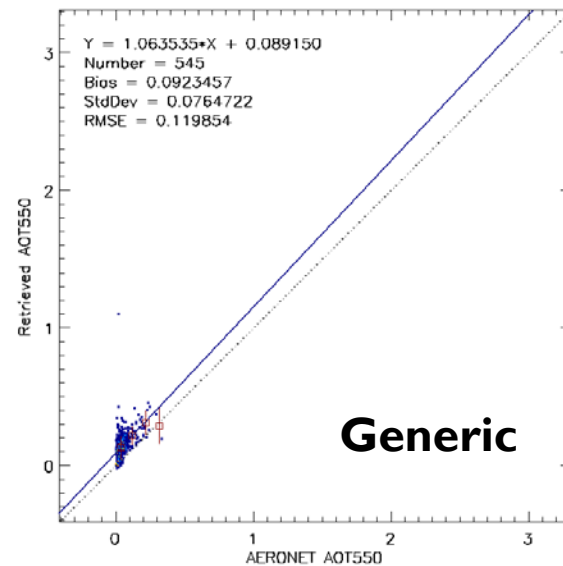
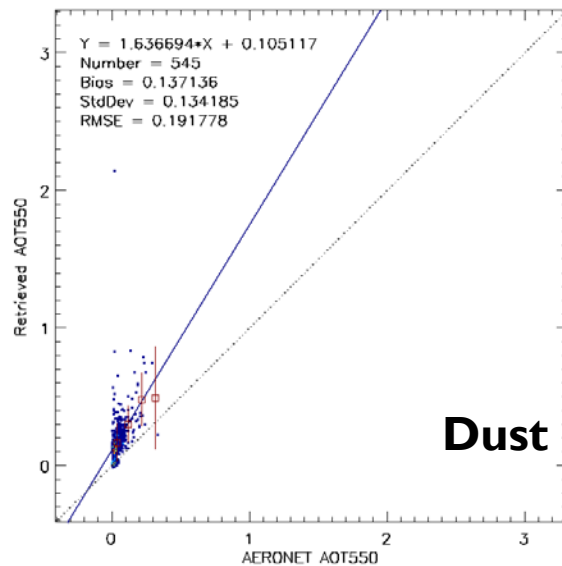


- Angular Dependence
 - Retrieval error against zenith, azimuth, scattering and glint angles



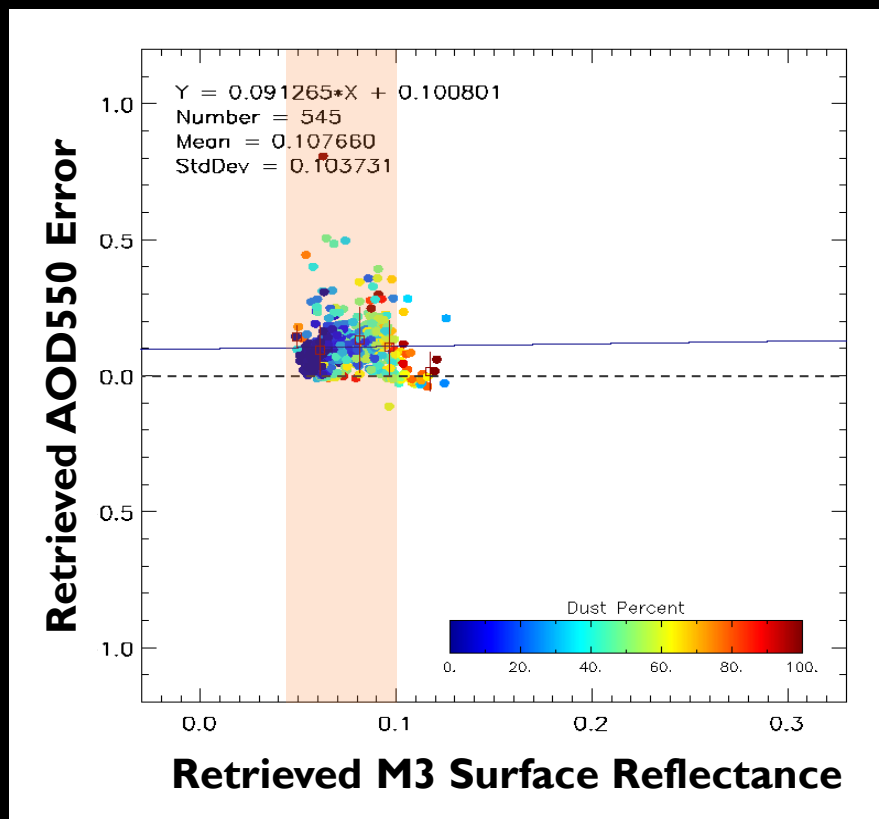
Railroad Valley (3)

- All aerosol models overestimate.

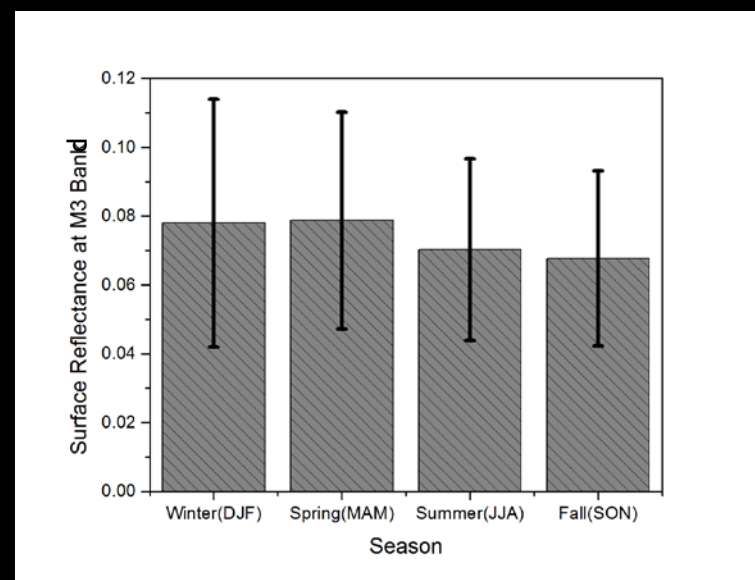
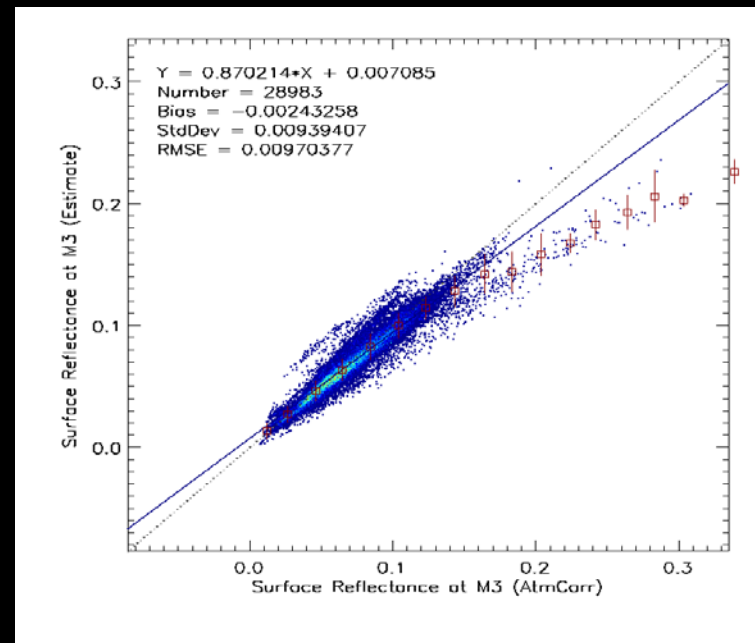


• Surface reflectance

- Retrieve surface reflectance from low AOD cased via atmospheric correction
- Evaluation of the surface reflectance relationship (M5->M3 derived globally) over this station does not reveal significant error
- SfcRef@M3 of majority retrievals fall within expected range
- No significant season variation



SfcRef@M3: 0.072 ± 0.029



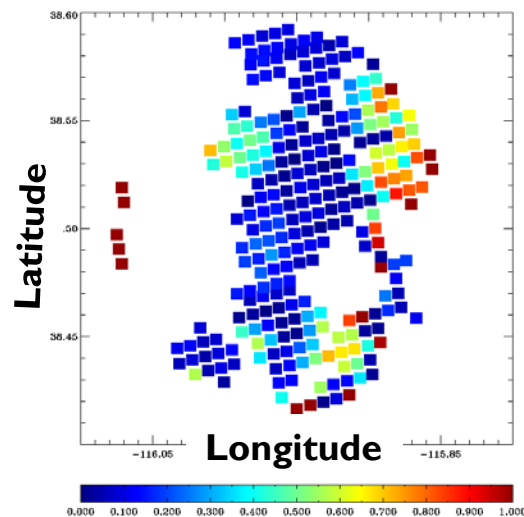
- Rugged terrain



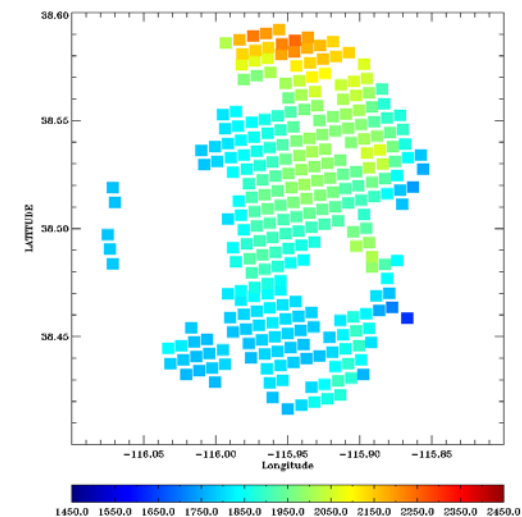
Case Study

Date: 2013.157
AERONET AOD550: 0.052
EPS Mean AOD550: 0.276
Solar Zenith Angle: 19.10°
Viewing Zenith Angle: 11.89°
Solar Azimuth Angle: -142.06°
Viewing Azimuth Angle: 78.16°
Scattering Angle: 150.83°
Glint Angle: 12.54°

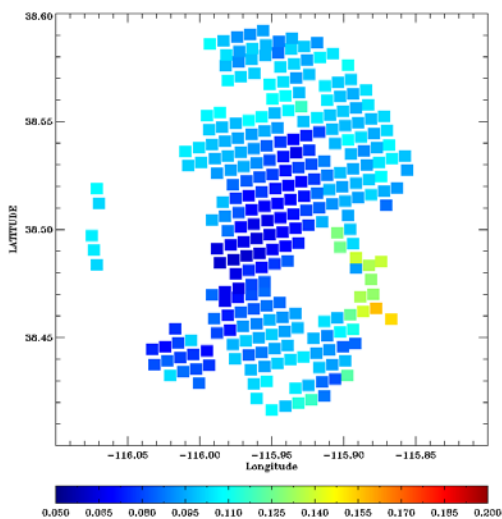
Retrieved AOD550



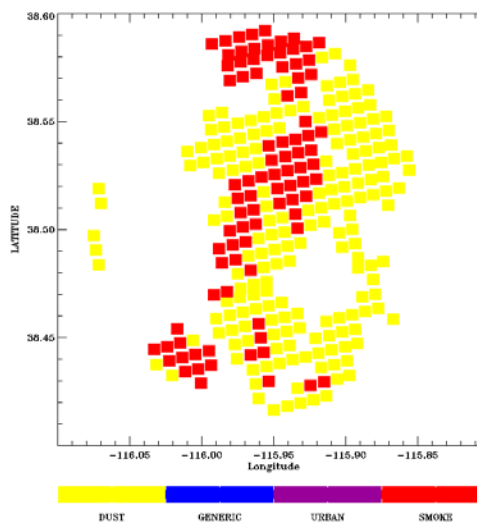
Input Surface Height



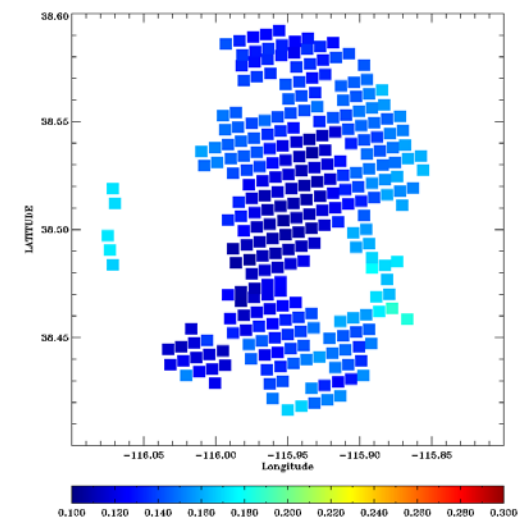
Retrieved SfcRef@M3



Selected Aerosol Model



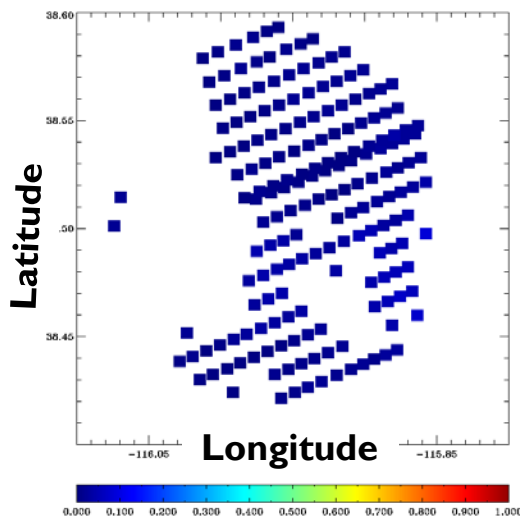
Input ToaRef@M3



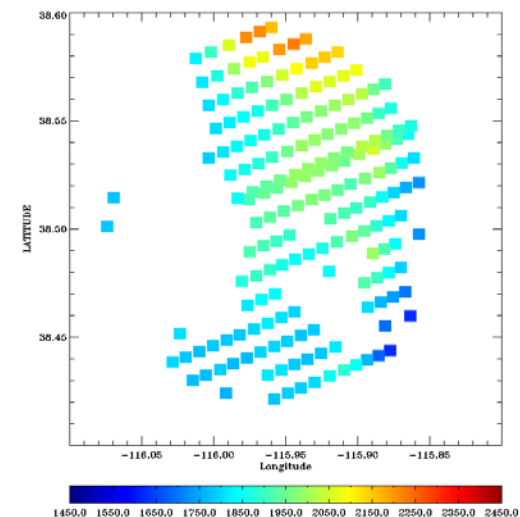
Case Study

Date: 2012.328
AERONET AOD550: 0.009
EPS Mean AOD550: 0.017
Solar Zenith Angle: 59.20°
Viewing Zenith Angle: 59.09°
Solar Azimuth Angle: -175.33°
Viewing Azimuth Angle: 70.62°
Scattering Angle: 87.87°
Glint Angle: 55.71°

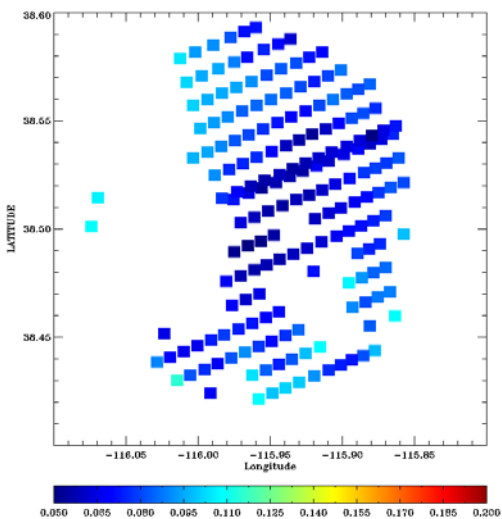
Retrieved AOD550



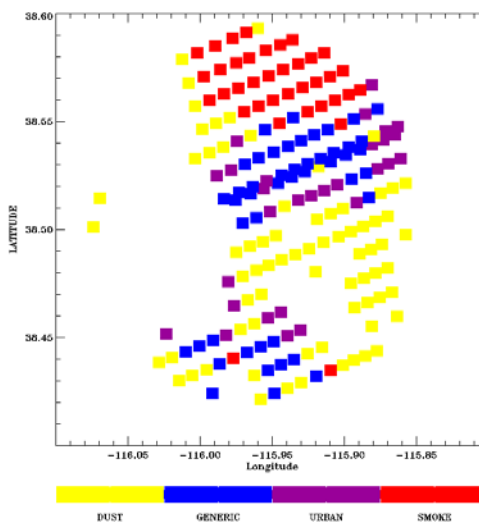
Input Surface Height



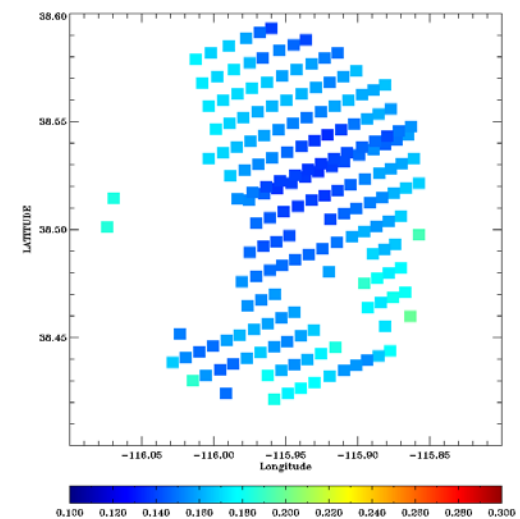
Retrieved SfcRef@M3



Selected Aerosol Model



Input ToaRef@M3



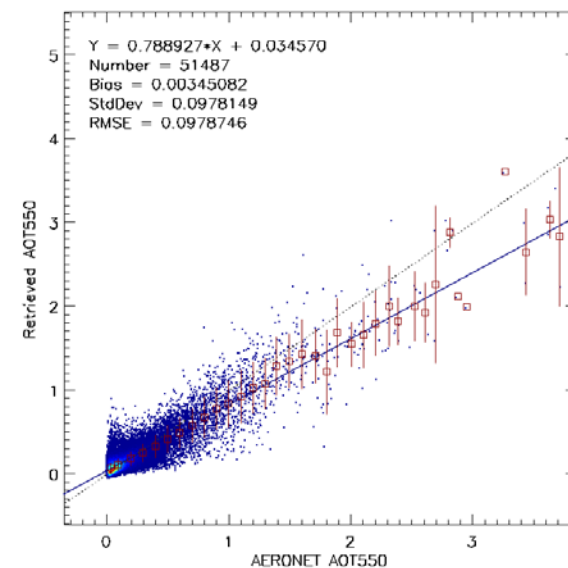
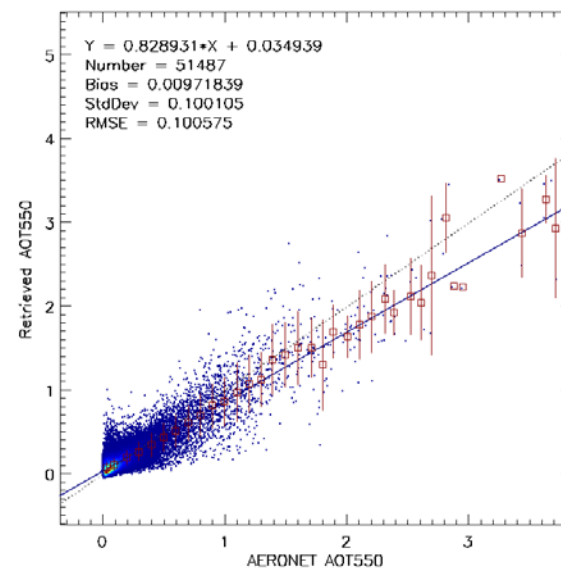
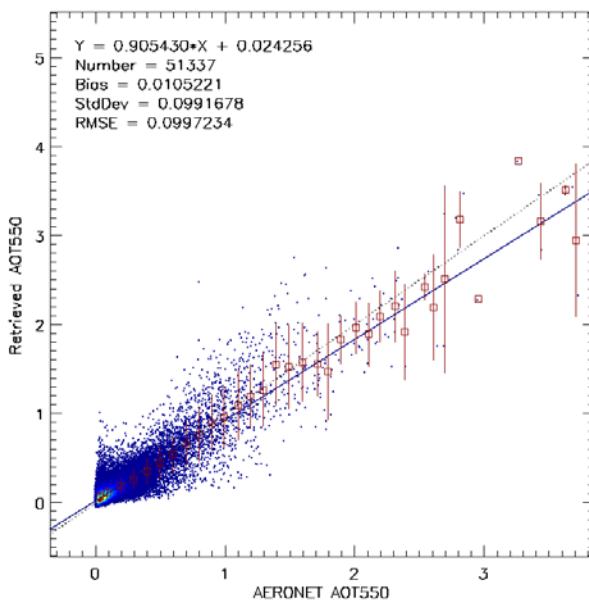
- VIIRS Enterprise Processing System AOD retrieval over land is evaluated using AERONET measurements over different geographic regions.
- Aerosol model selection can be improved by introducing a new set of surface reflectance relationship over East Asia.
- Lack a more absorbing dust model might be the cause of the negative bias over Africa.
- Evaluation of retrieval performance is sensitive to the validation domain selection over certain areas.
- Retrieval would have difficulty over rugged terrain areas.

Global Evaluation

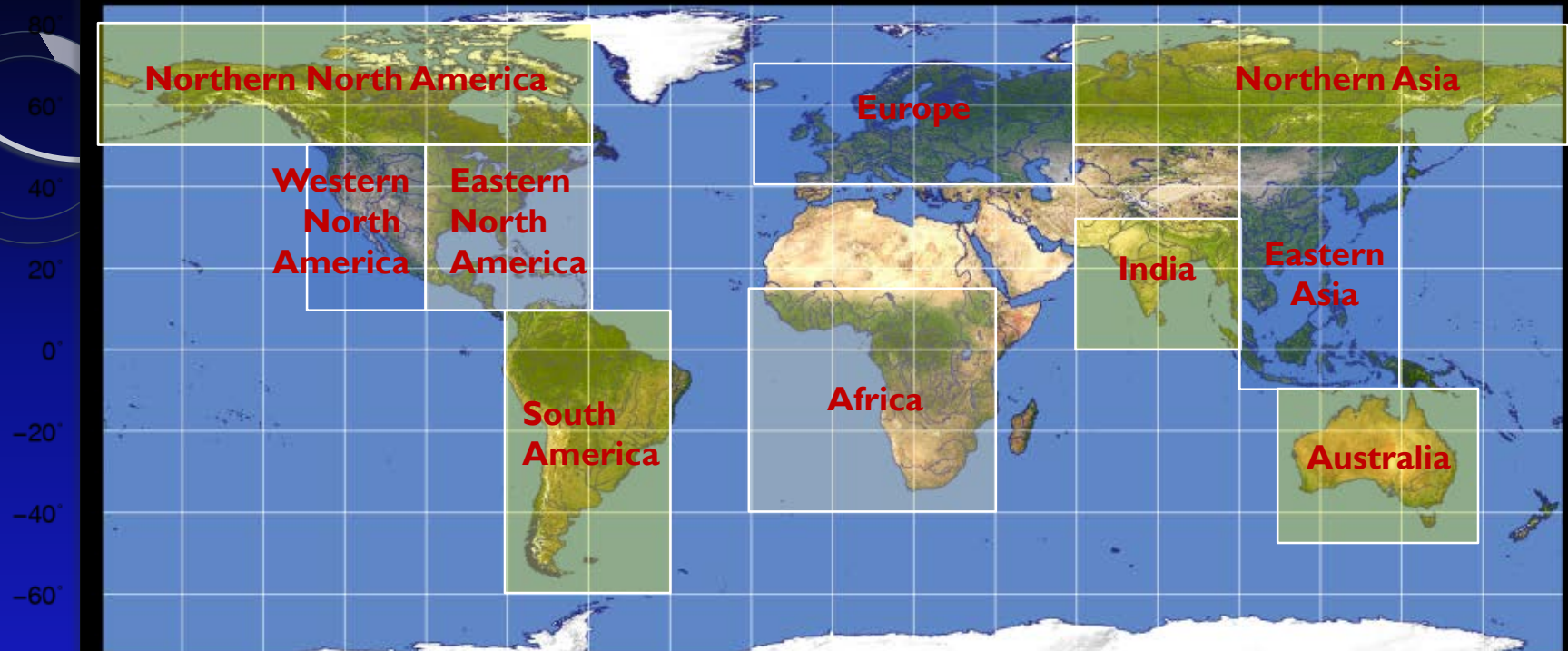
EPS Original Retrieval

New M5->M11 Relationship

New M5->M11 Relationship
Average of best two solutions



Regional Evaluation



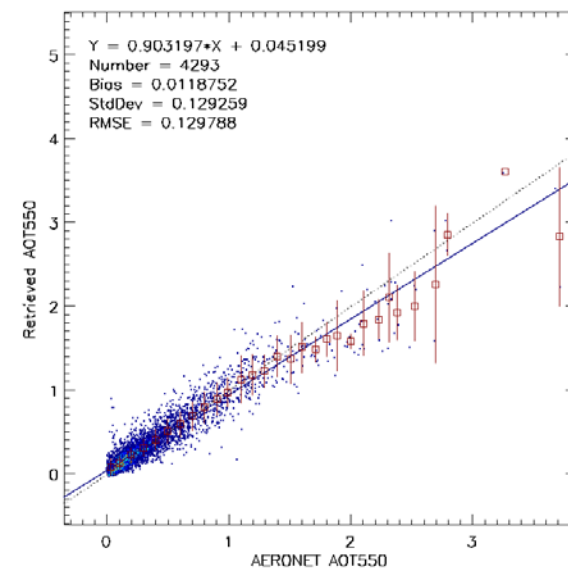
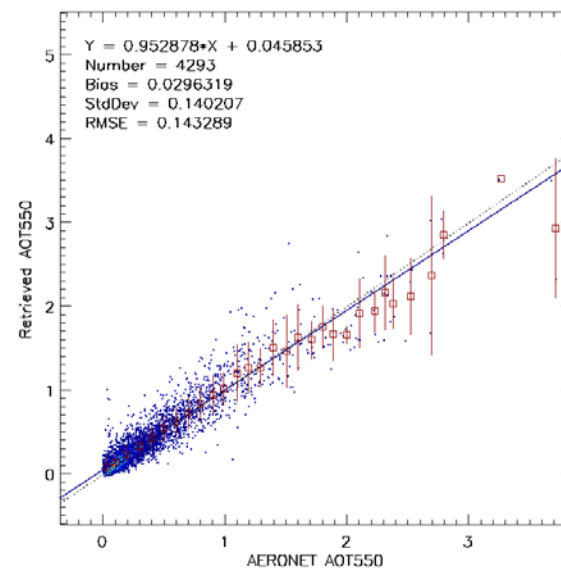
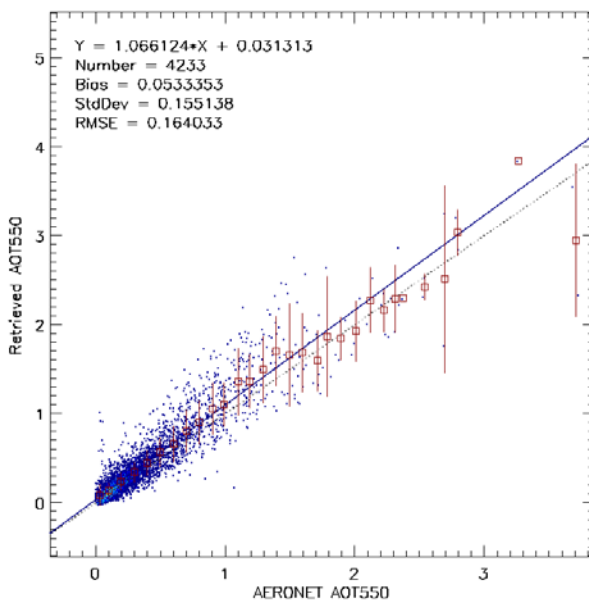
Domain	Longitude	Latitude
Northern North America	180° W - 60° W	50° N - 80° N
Northern Asia	60° E - 180° E	50° N - 80° N
Europe	20° W - 60° E	40° N - 70° N
Western North America	130° W - 100° W	10° N - 50° N
Eastern North America	100° W - 60° W	10° N - 50° N
South America	80° W - 40° W	60° S - 10° N
South Africa	20° W - 40° E	40° S - 15° N
India	60° E - 100° E	0° - 30° N
Eastern Asia	100° E - 140° E	10° S - 50° N
Australia	110° E - 160° E	50° S - 10° S

• Eastern Asia

EPS Original Retrieval

New M5->M11 Relationship

New M5->M11 Relationship
Average of best two solutions

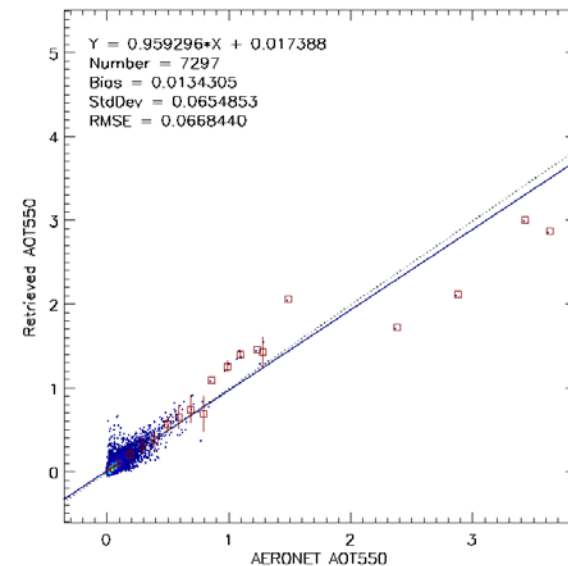
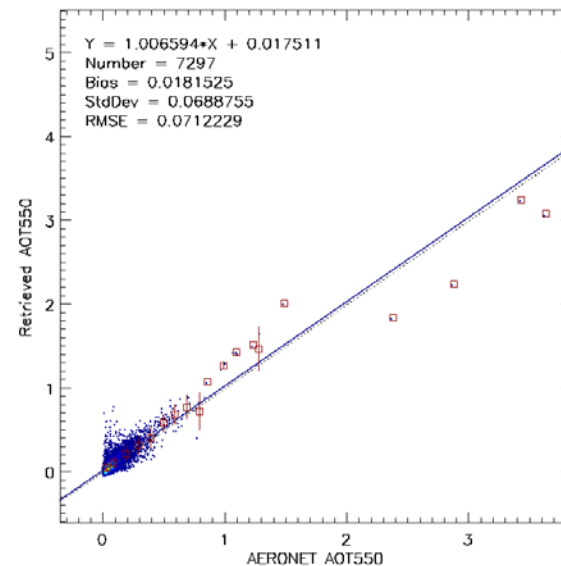
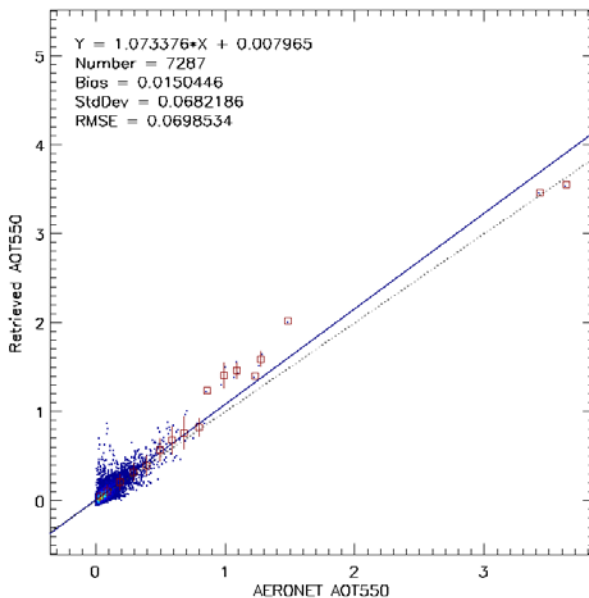


• Eastern North America

EPS Original Retrieval

New M5->M11 Relationship

New M5->M11 Relationship
Average of best two solutions

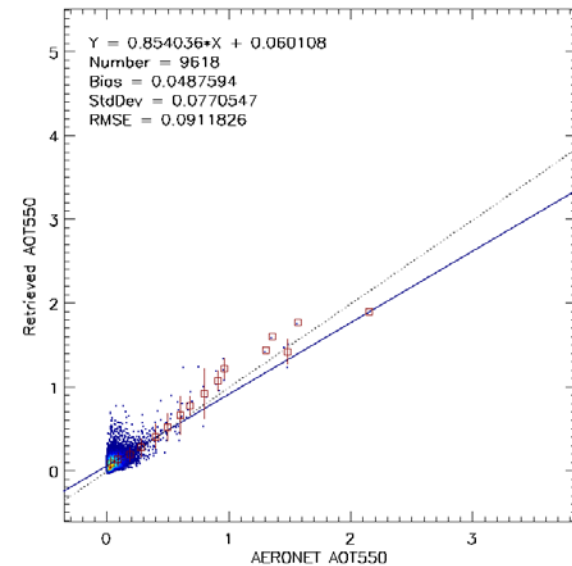
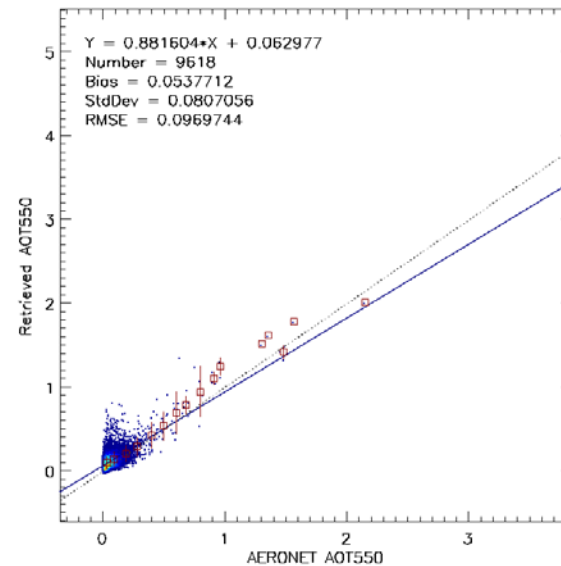
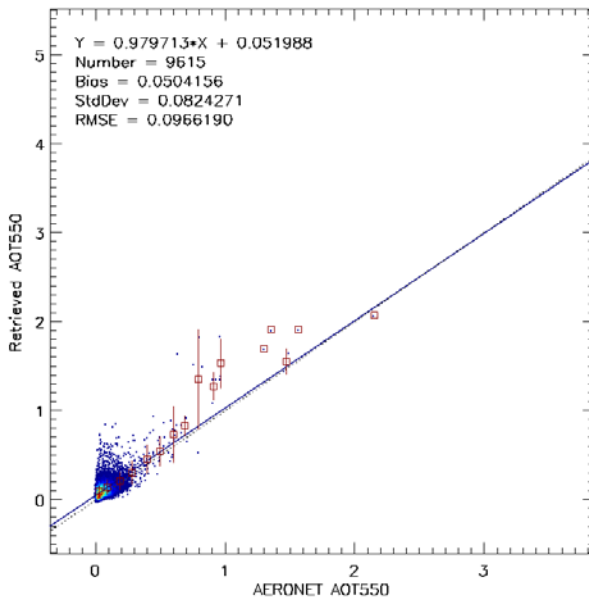


• Western North America

EPS Original Retrieval

New M5->M11 Relationship

New M5->M11 Relationship
Average of best two solutions

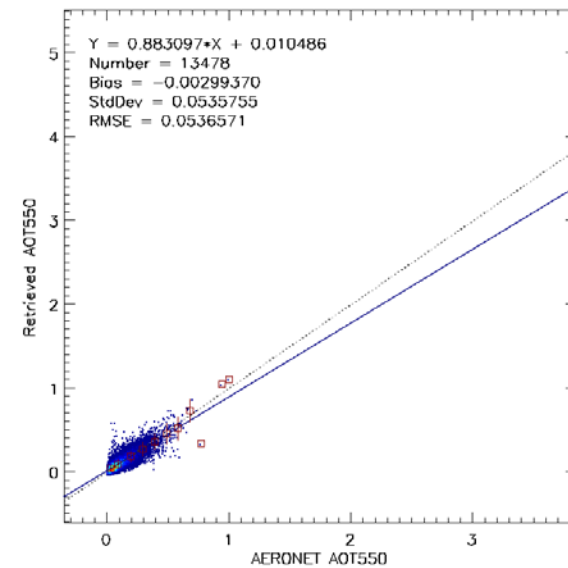
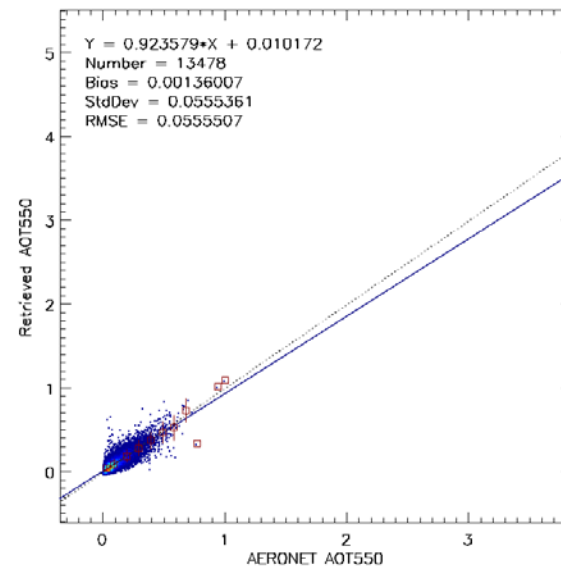
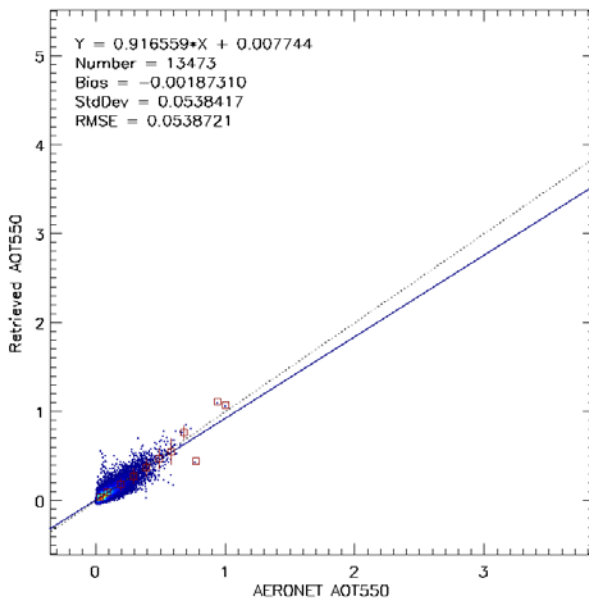


• Europe

EPS Original Retrieval

New M5->M11 Relationship

New M5->M11 Relationship
Average of best two solutions

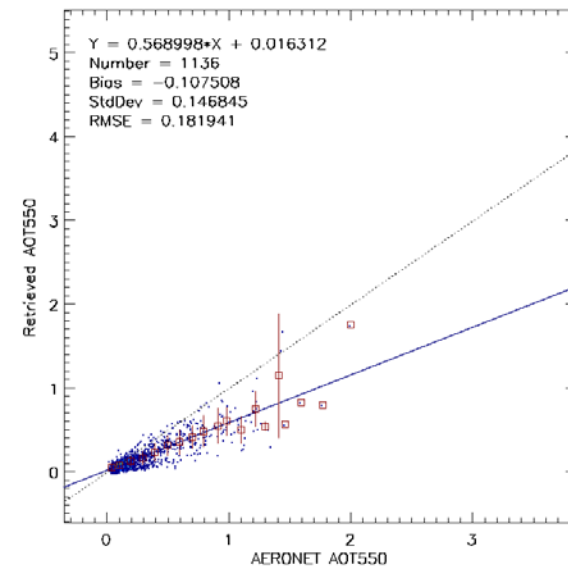
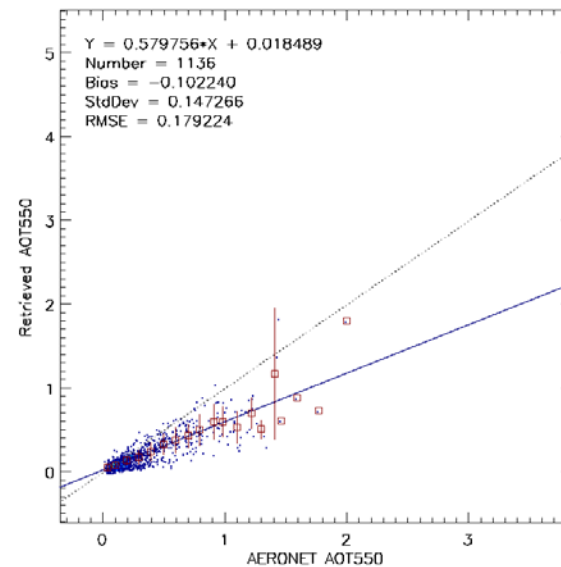
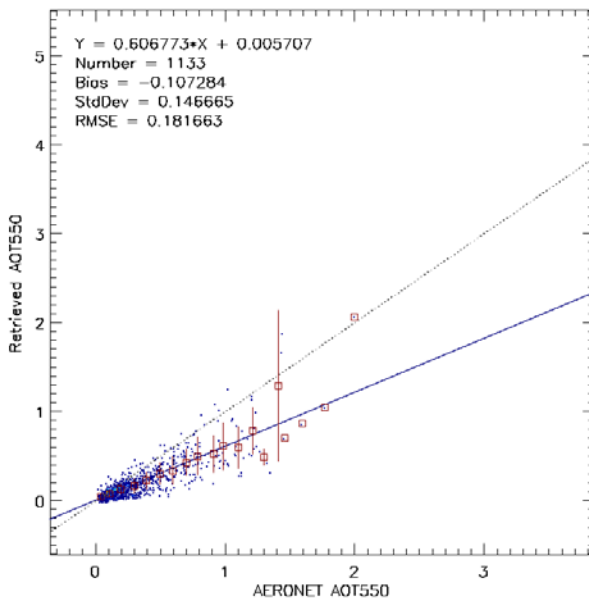


• Africa

EPS Original Retrieval

New M5->M1 I Relationship

New M5->M1 I Relationship
Average of best two solutions

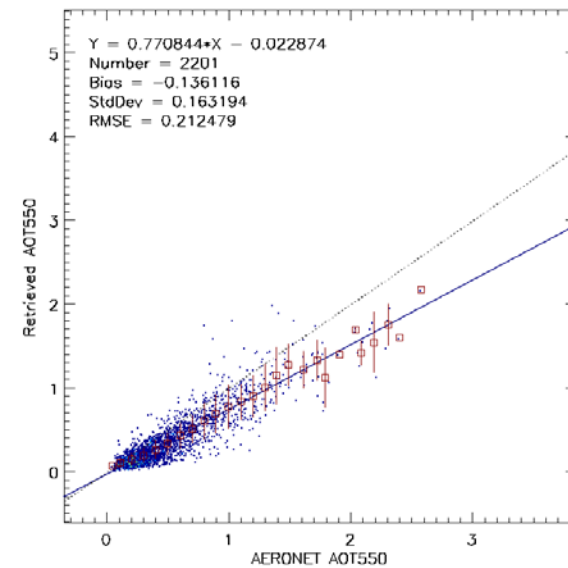
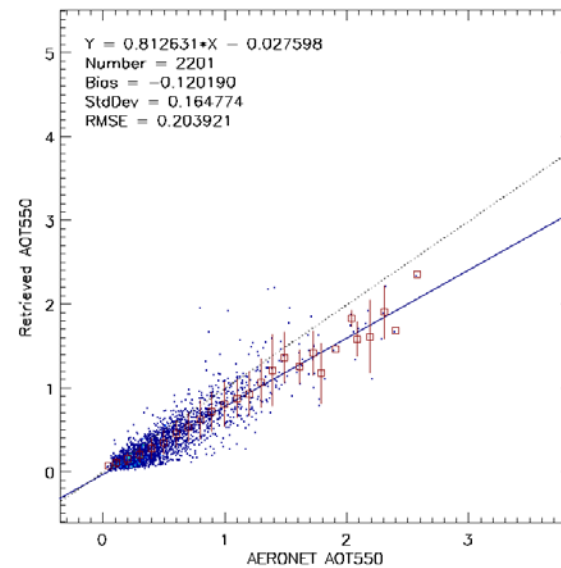
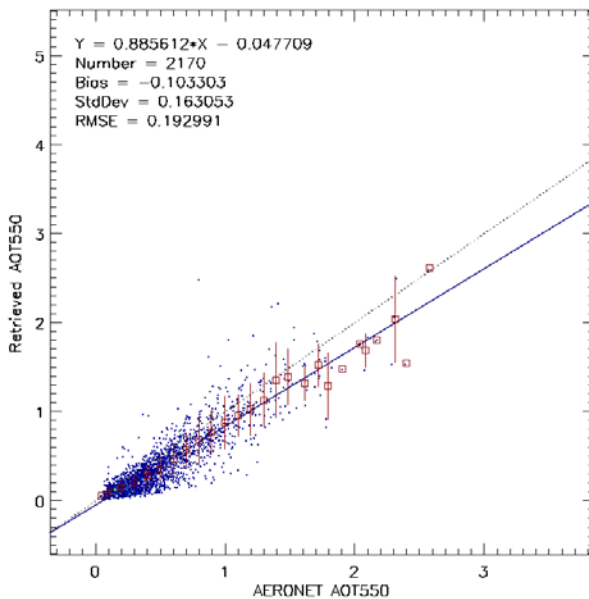


• India

EPS Original Retrieval

New M5->M1 I Relationship

New M5->M1 I Relationship
Average of best two solutions

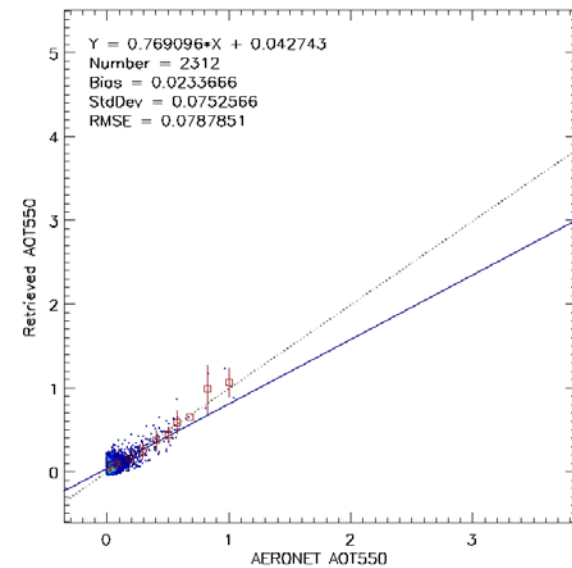
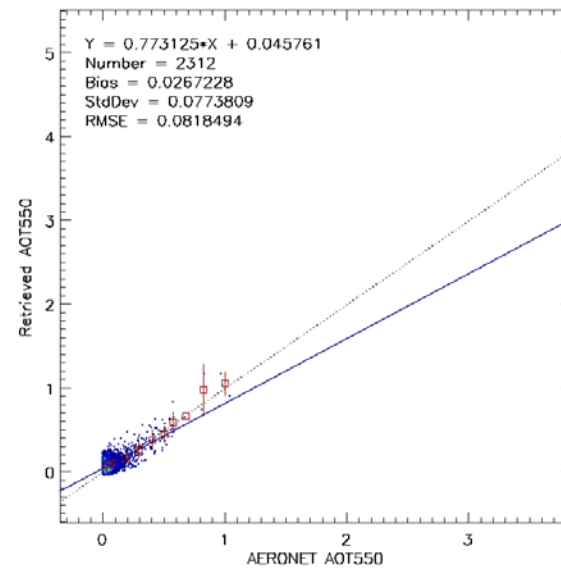
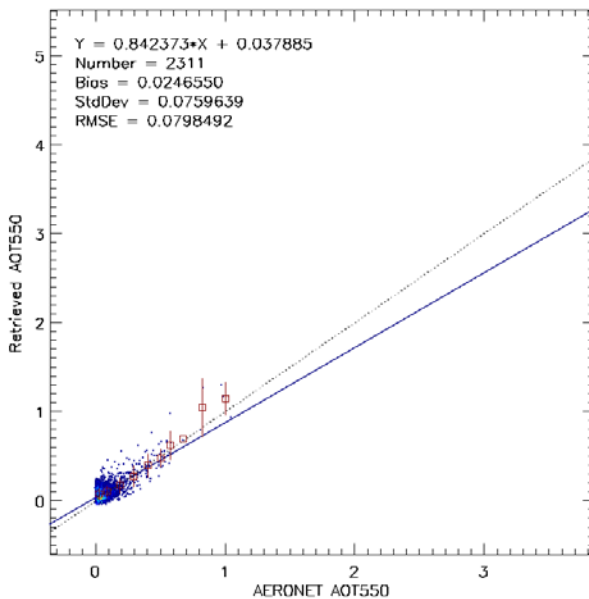


• South America

EPS Original Retrieval

New M5->M11 Relationship

New M5->M11 Relationship
Average of best two solutions

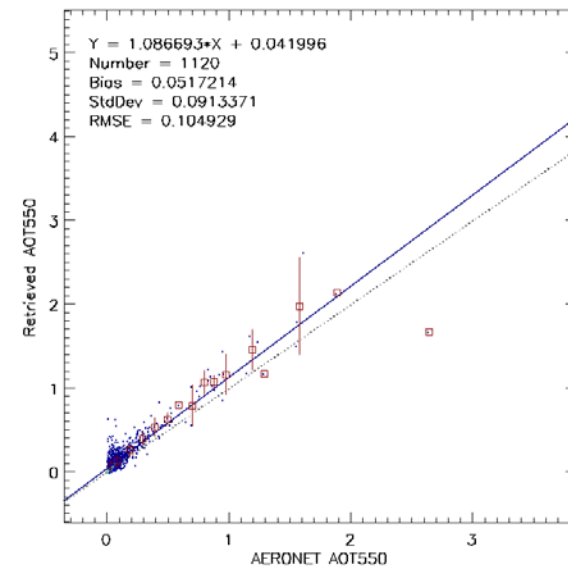
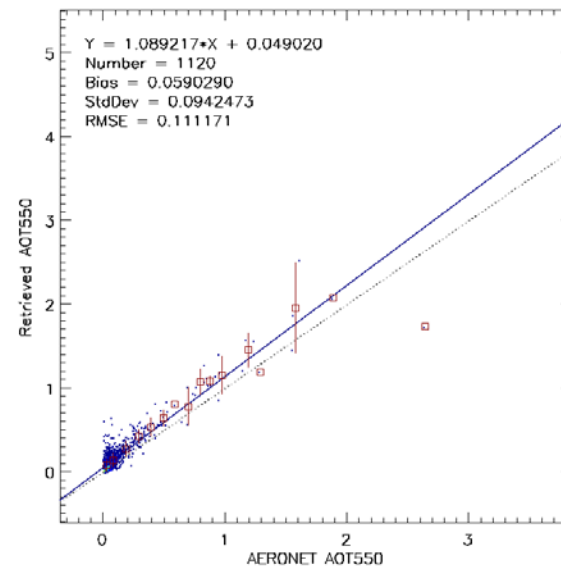
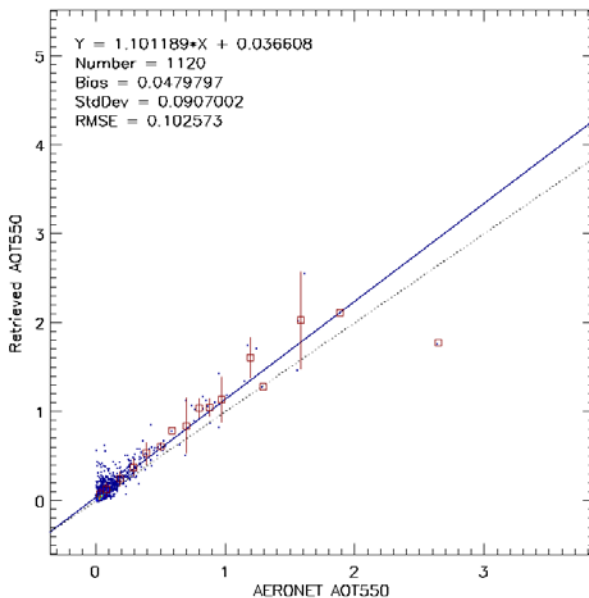


• Northern North America

EPS Original Retrieval

New M5->M11 Relationship

New M5->M11 Relationship
Average of best two solutions

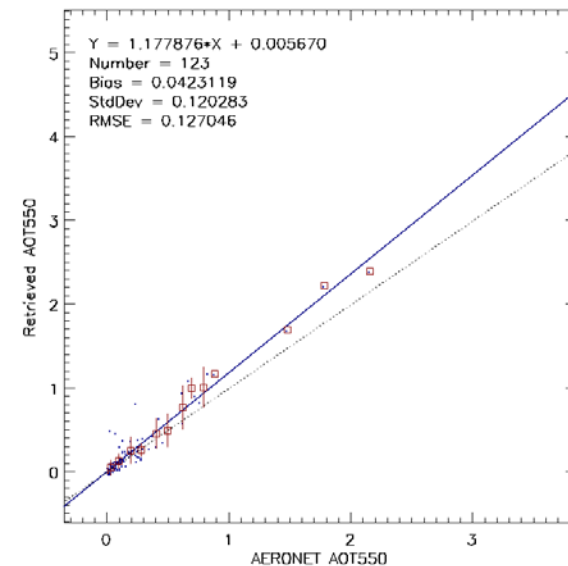
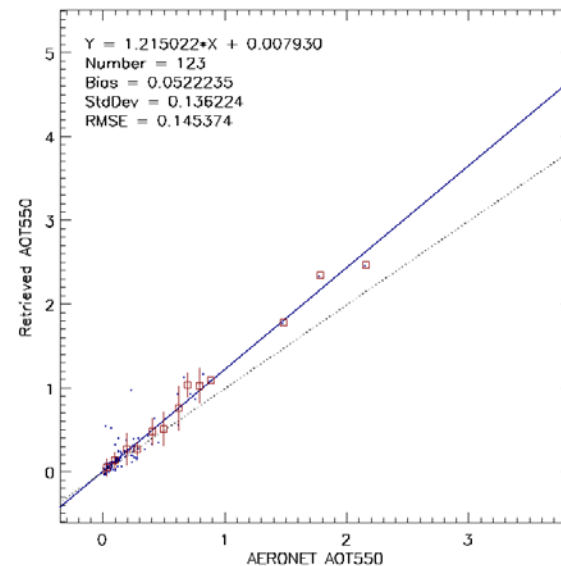
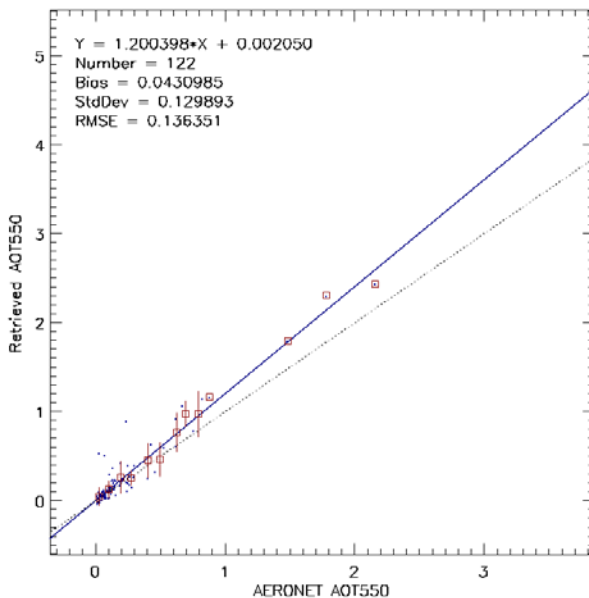


• Northern Asia

EPS Original Retrieval

New M5->M11 Relationship

New M5->M11 Relationship
Average of best two solutions

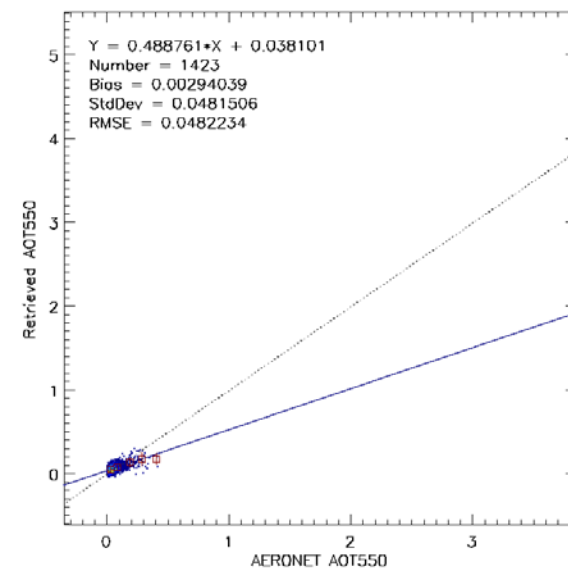
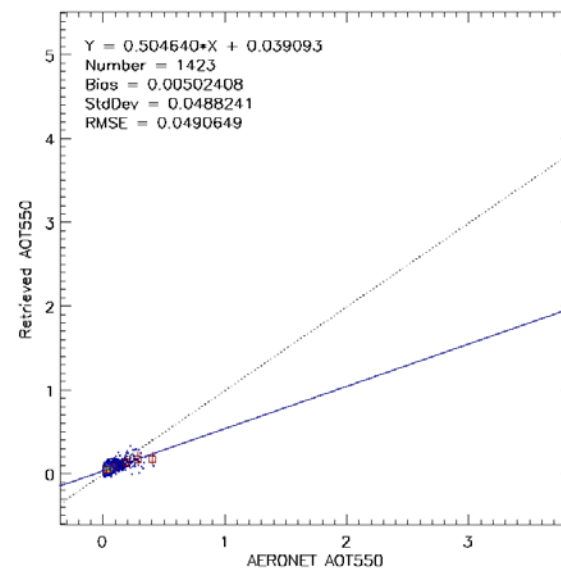
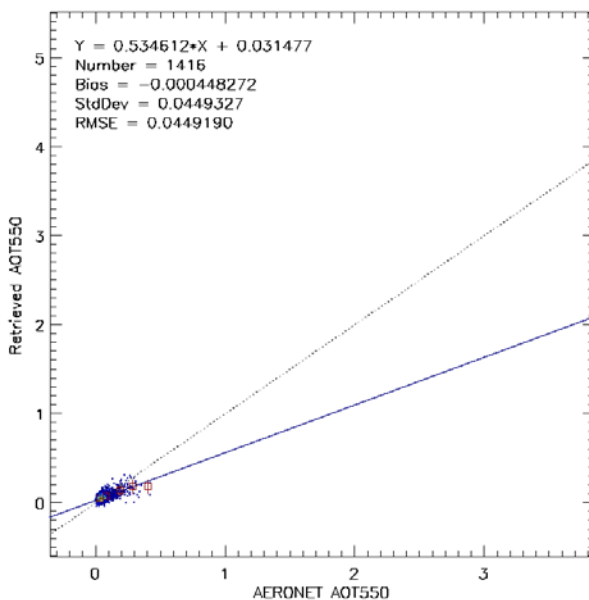


• Australia

EPS Original Retrieval

New M5->M11 Relationship

New M5->M11 Relationship
Average of best two solutions





STAR JPSS



2017 Annual Science Team Meeting

14-18 August 2017 • NCWCP • College Park, MD

The Future with JPSS

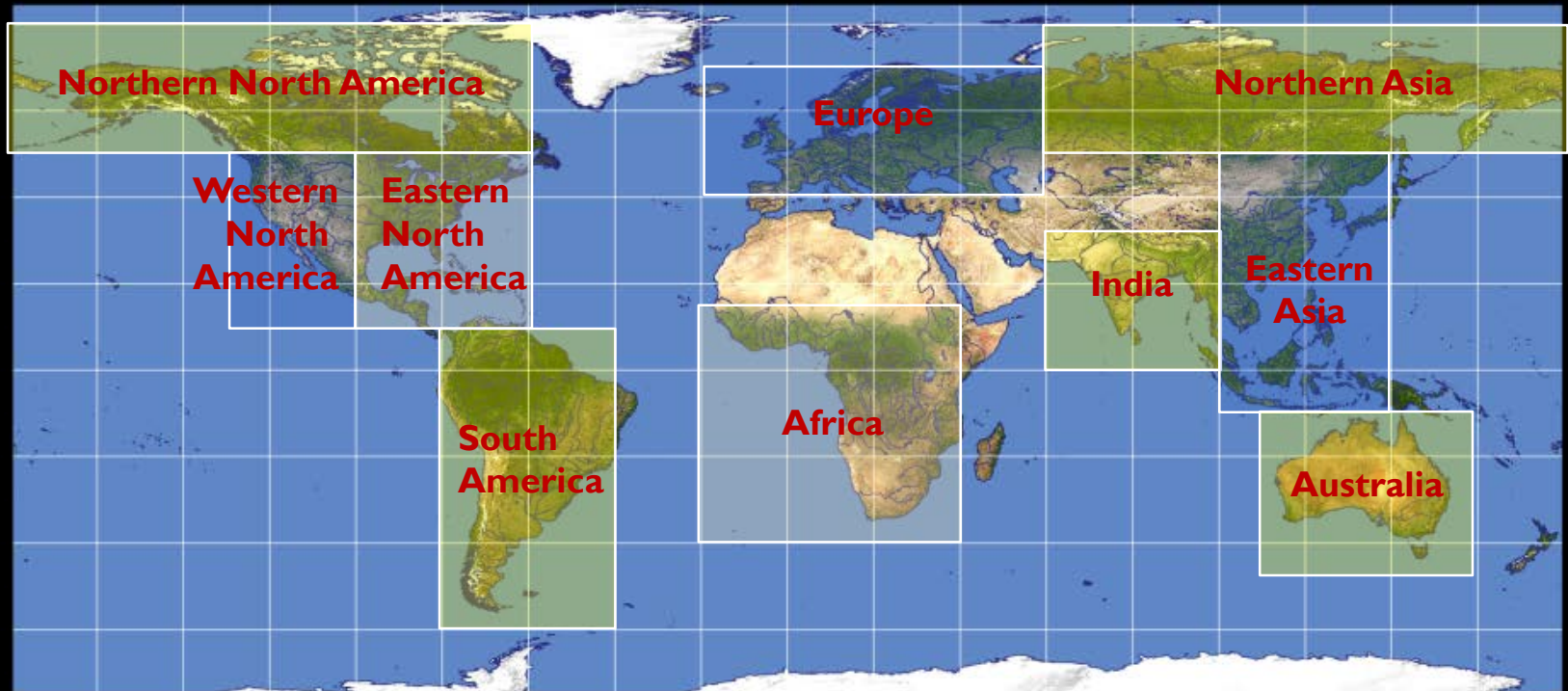
NOAA Center for Weather and Climate Prediction

Conference Center • 5830 University Research Court • College Park, MD 20740

Potential Updates of the Land Aerosol Models for the EPS AOD Algorithm

**Hongqing Liu
and NOAA STAR Aerosol Cal/Val Team**

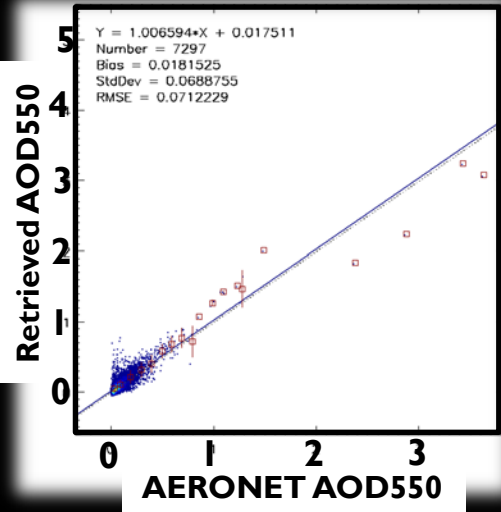
Evaluation Regions



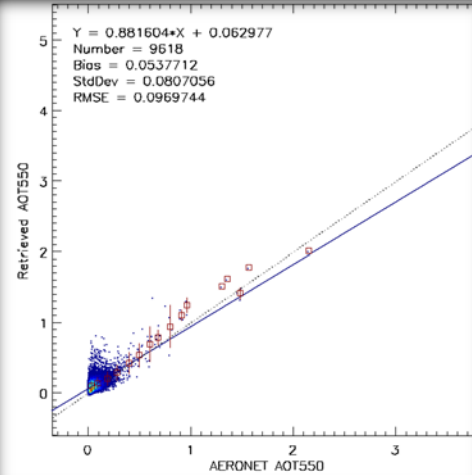
Domain	Longitude	Latitude
Northern North America	180° W - 60° W	50° N - 80° N
Northern Asia	60° E - 180° E	50° N - 80° N
Europe	20° W - 60° E	40° N - 70° N
Western North America	130° W - 100° W	10° N - 50° N
Eastern North America	100° W - 60° W	10° N - 50° N
South America	80° W - 40° W	60° S - 10° N
South Africa	20° W - 40° E	40° S - 15° N
India	60° E - 100° E	0° - 30° N
Eastern Asia	100° E - 140° E	10° S - 50° N
Australia	110° E - 160° E	50° S - 10° S

Regional Performance (I)

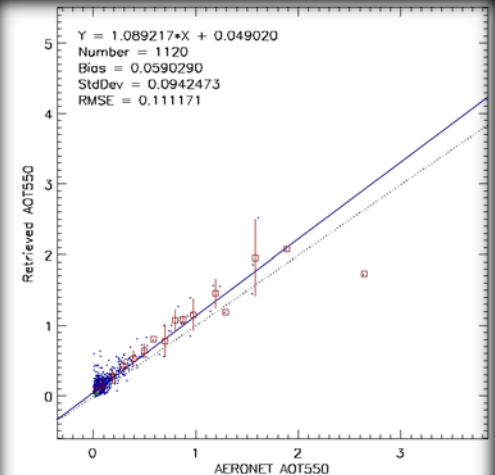
Eastern North America



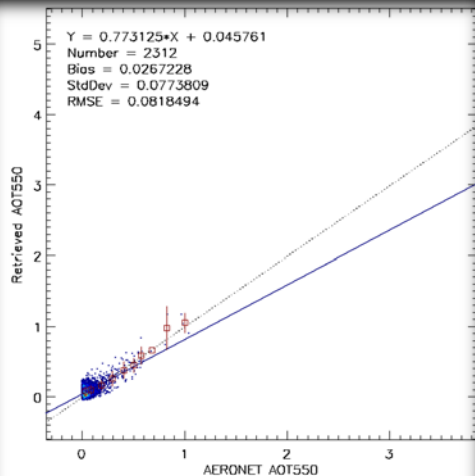
Western North America



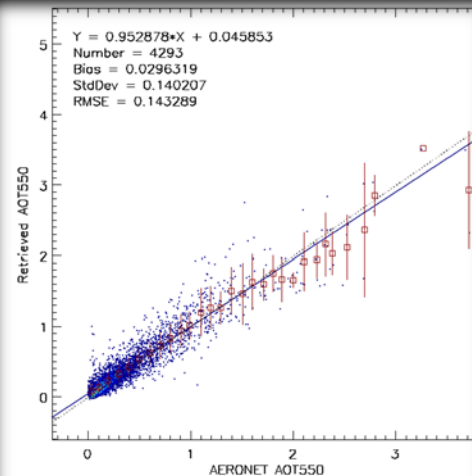
Northern North America



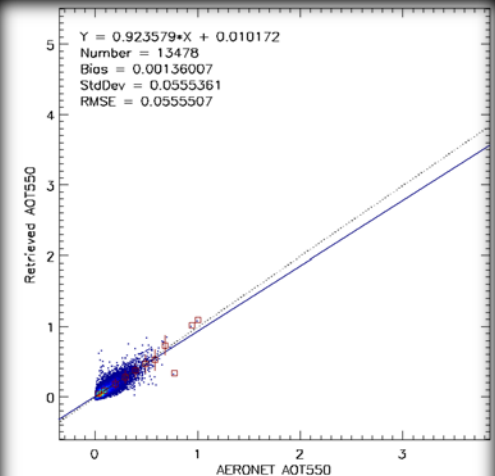
South America



Eastern Asia

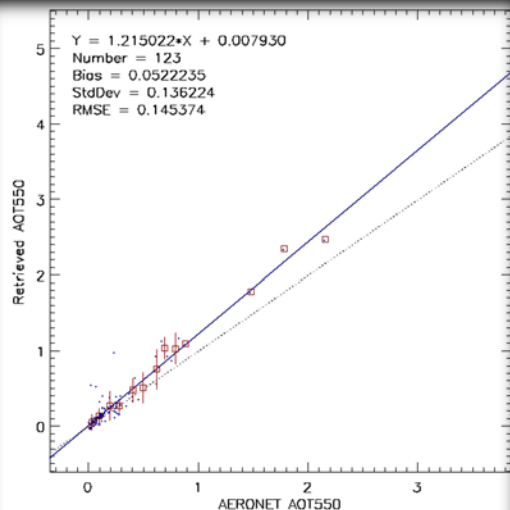


Europe

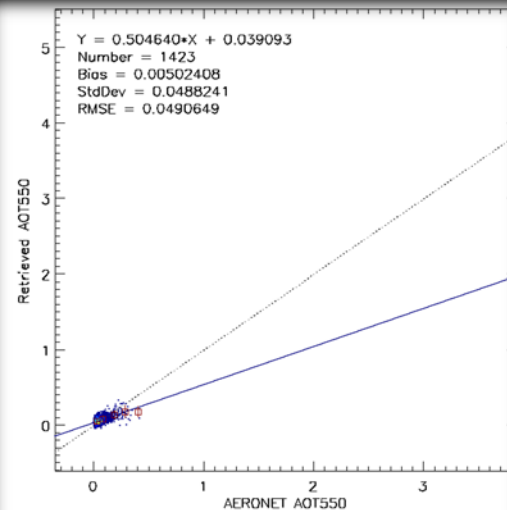


Regional Performance (2)

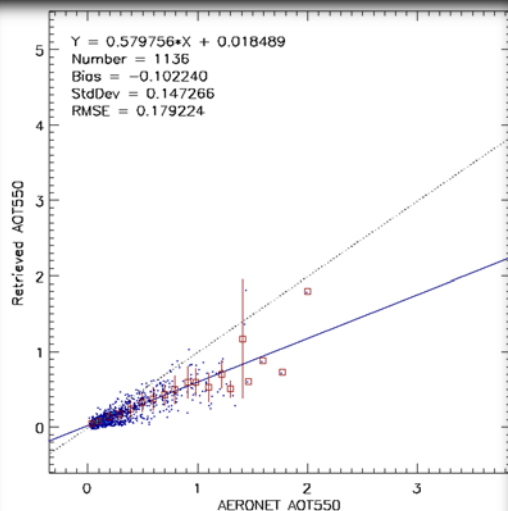
Northern Asia



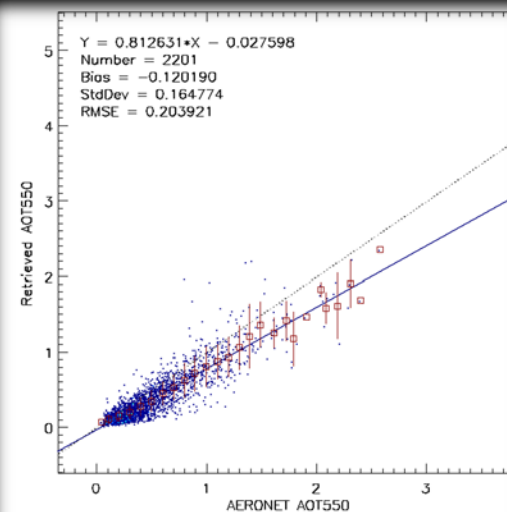
Australia



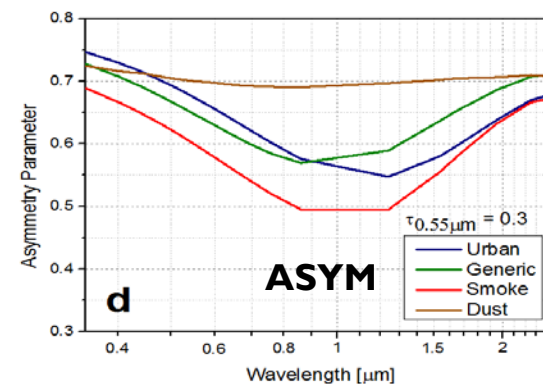
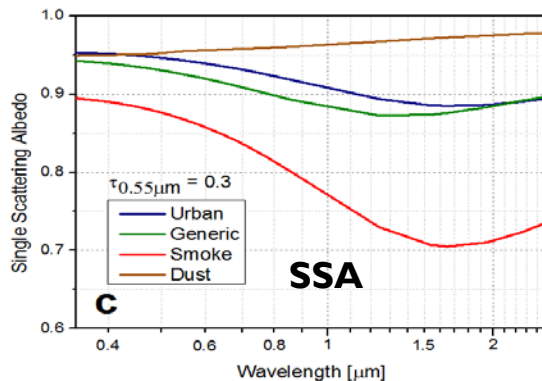
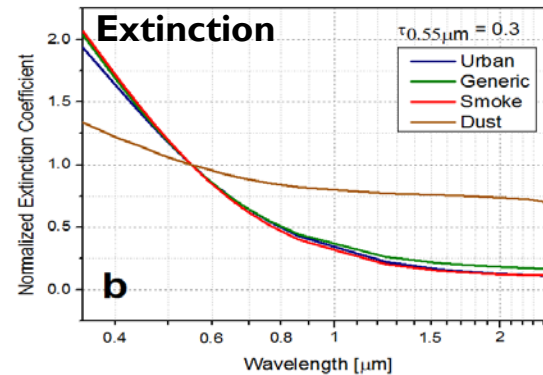
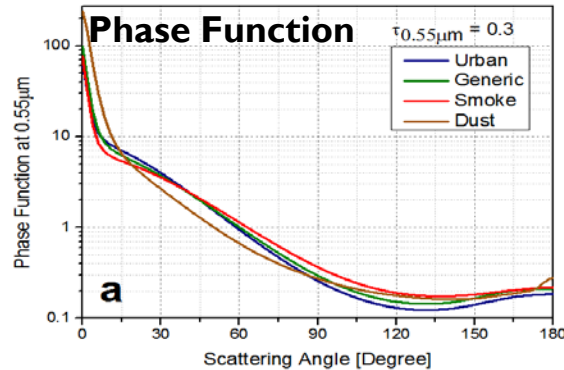
Africa



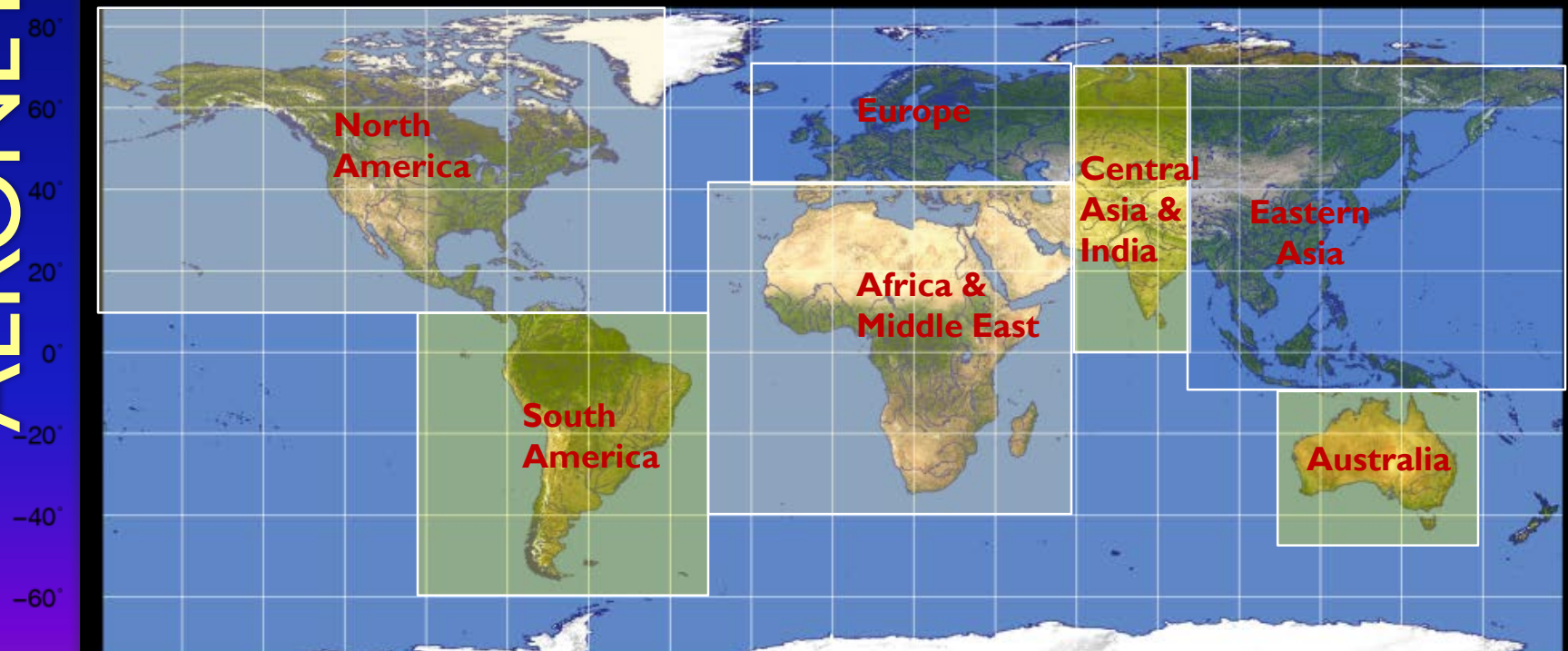
India



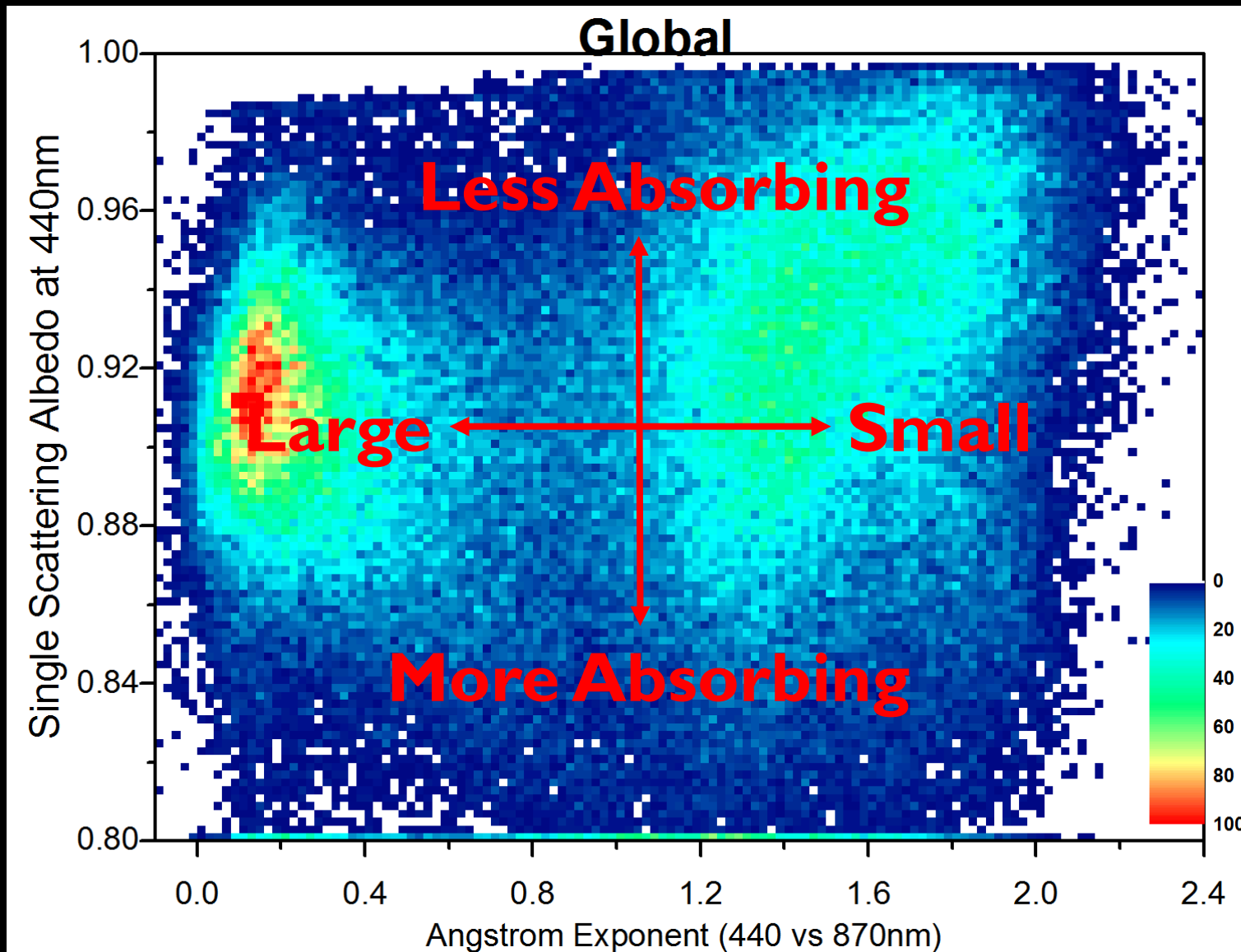
- Current land aerosol models (four types) might not be representative enough for global aerosol retrievals
 - Large errors over Africa and India



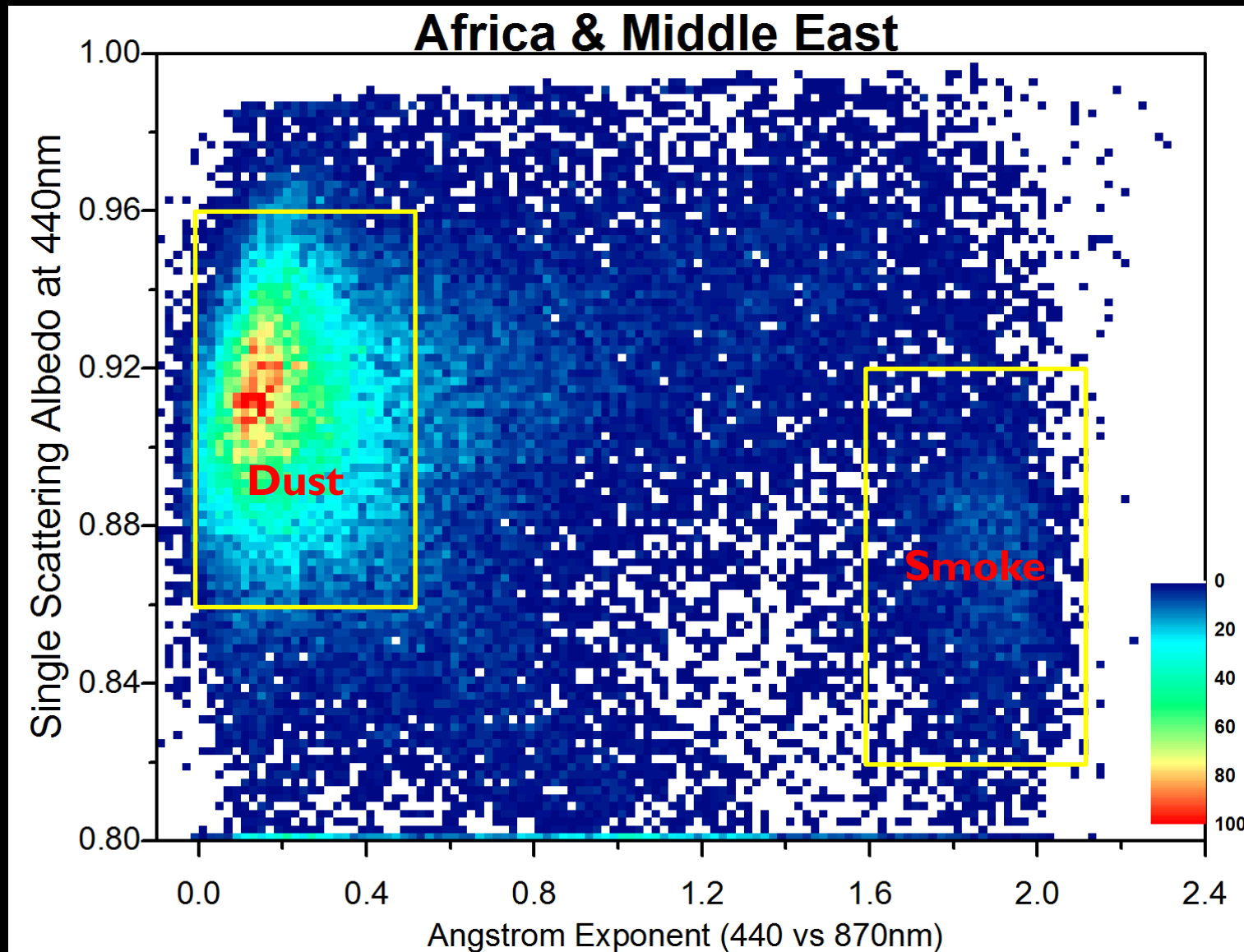
- AERONET Version 2 inversion products
 - Sun photometers measurements in almucantar and principle planes
 - Produce aerosol optical properties: single scatter albedo, size distribution, complex index of refraction, etc.



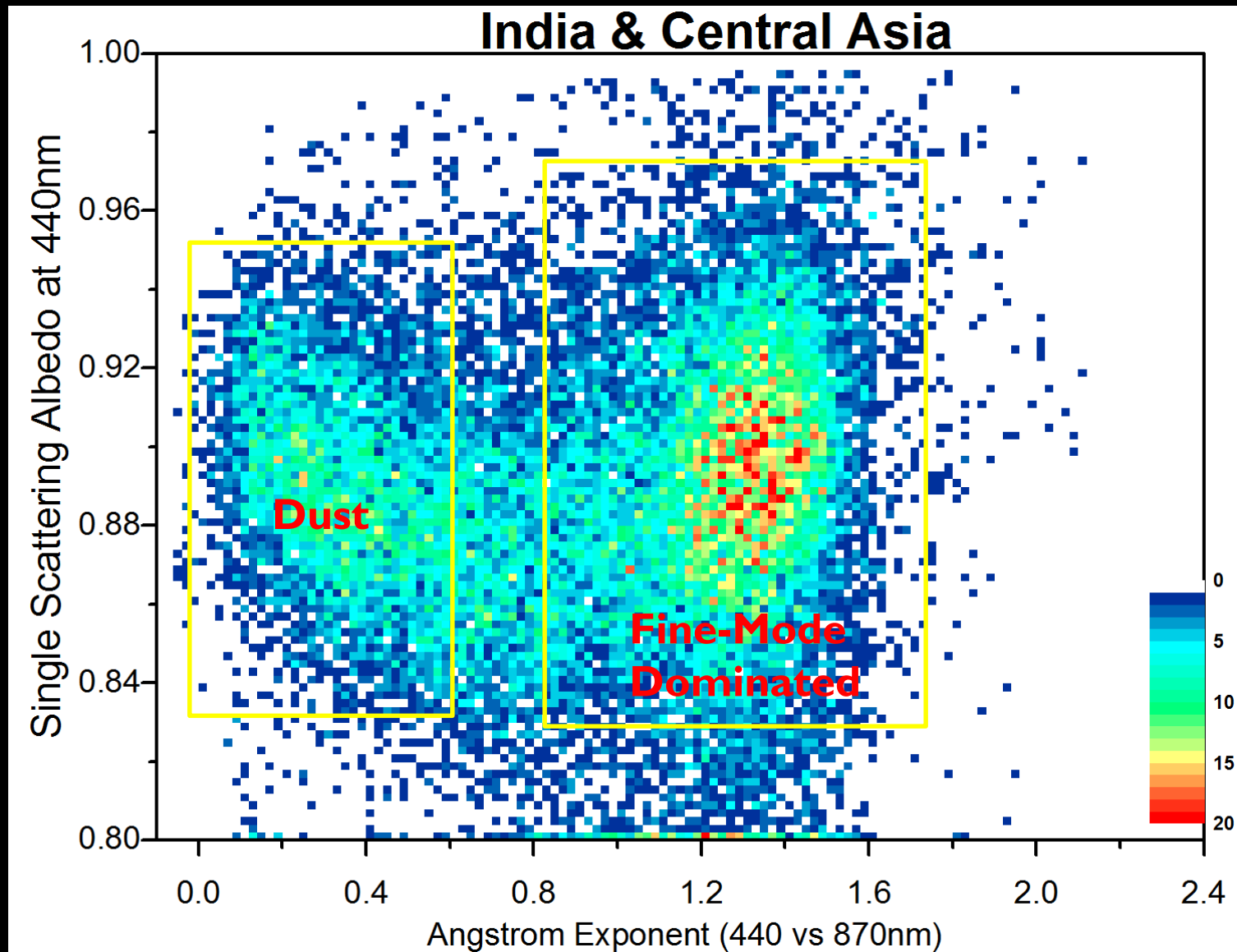
Global Aerosol Properties



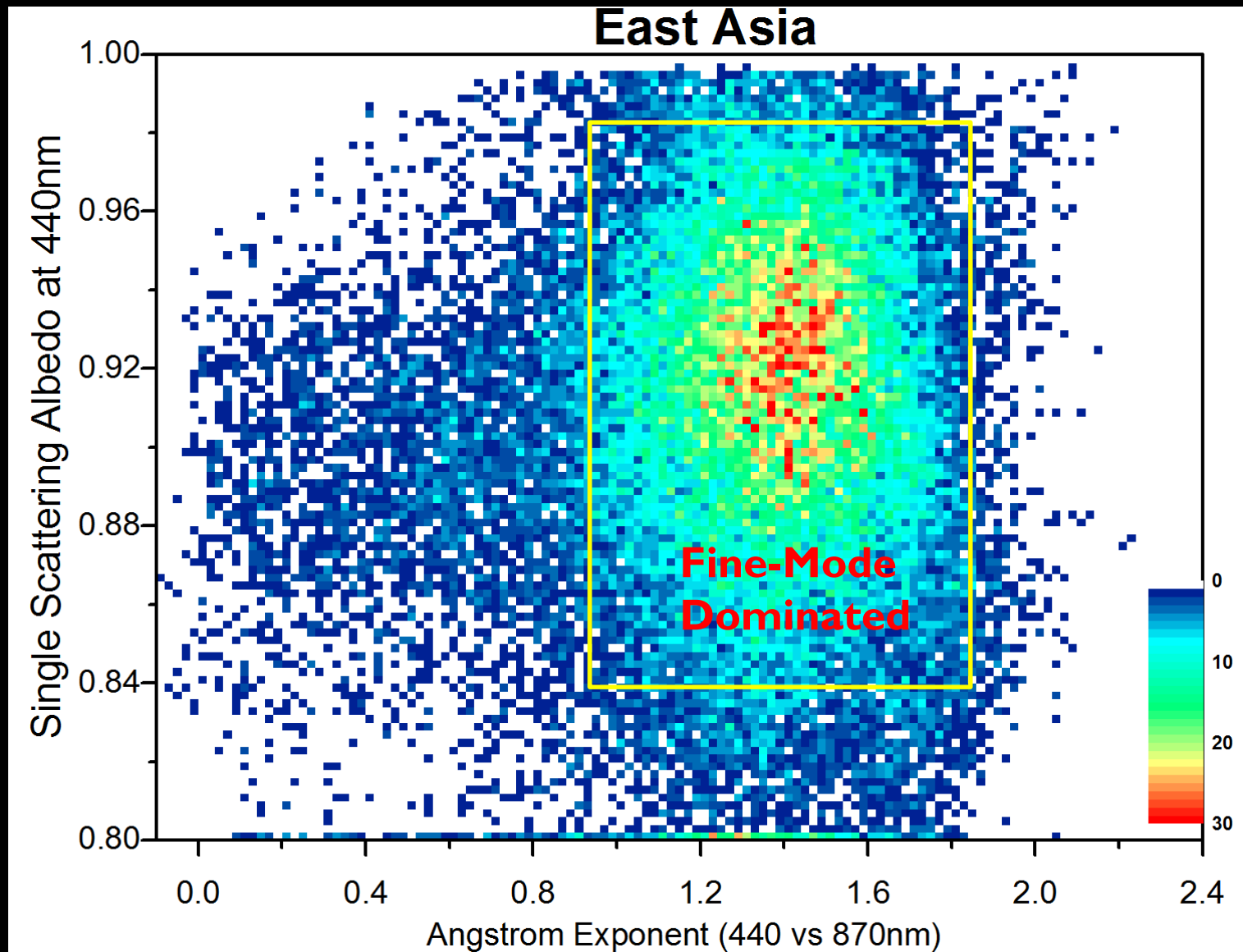
Regional Aerosol Properties (I)



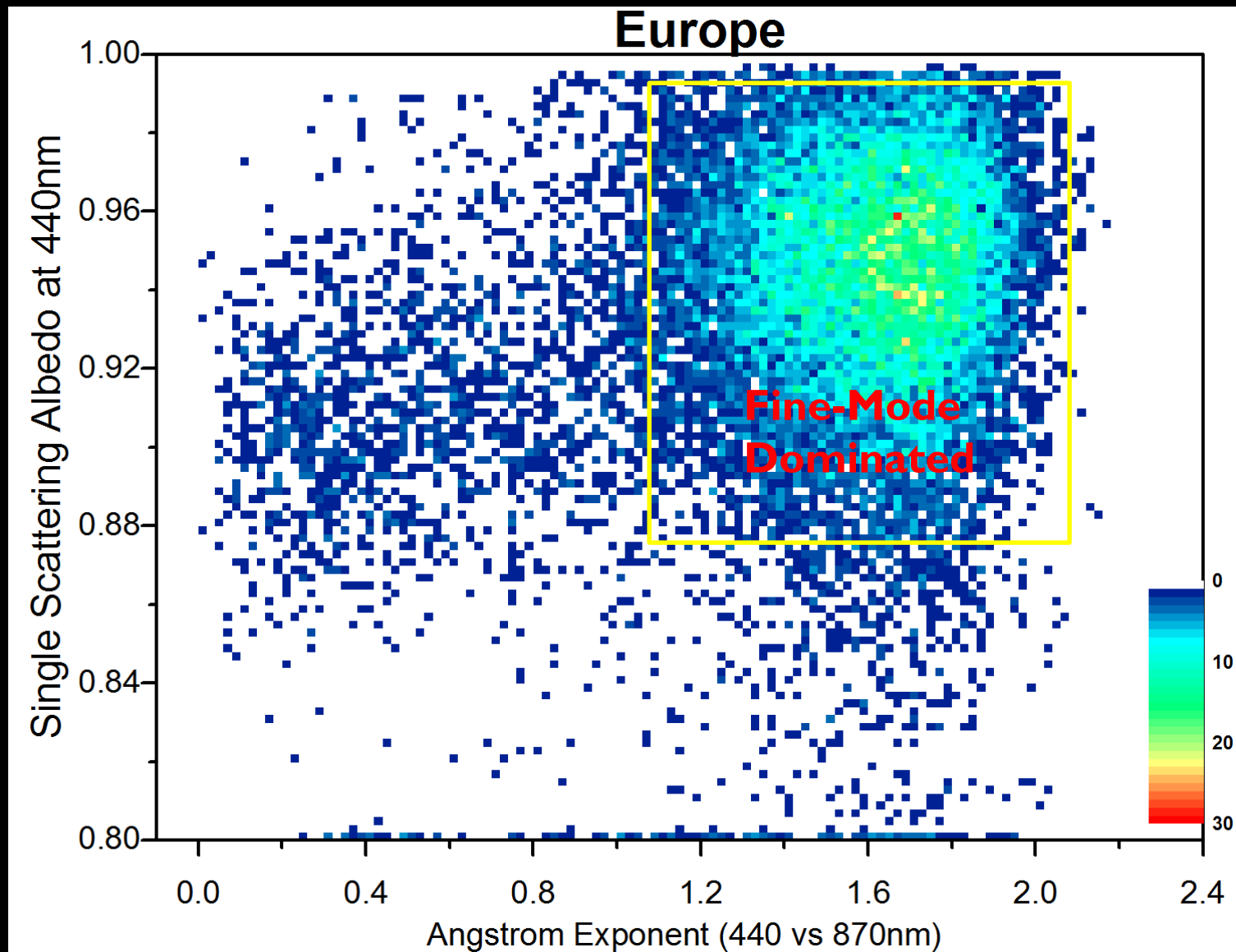
Regional Aerosol Properties (2)



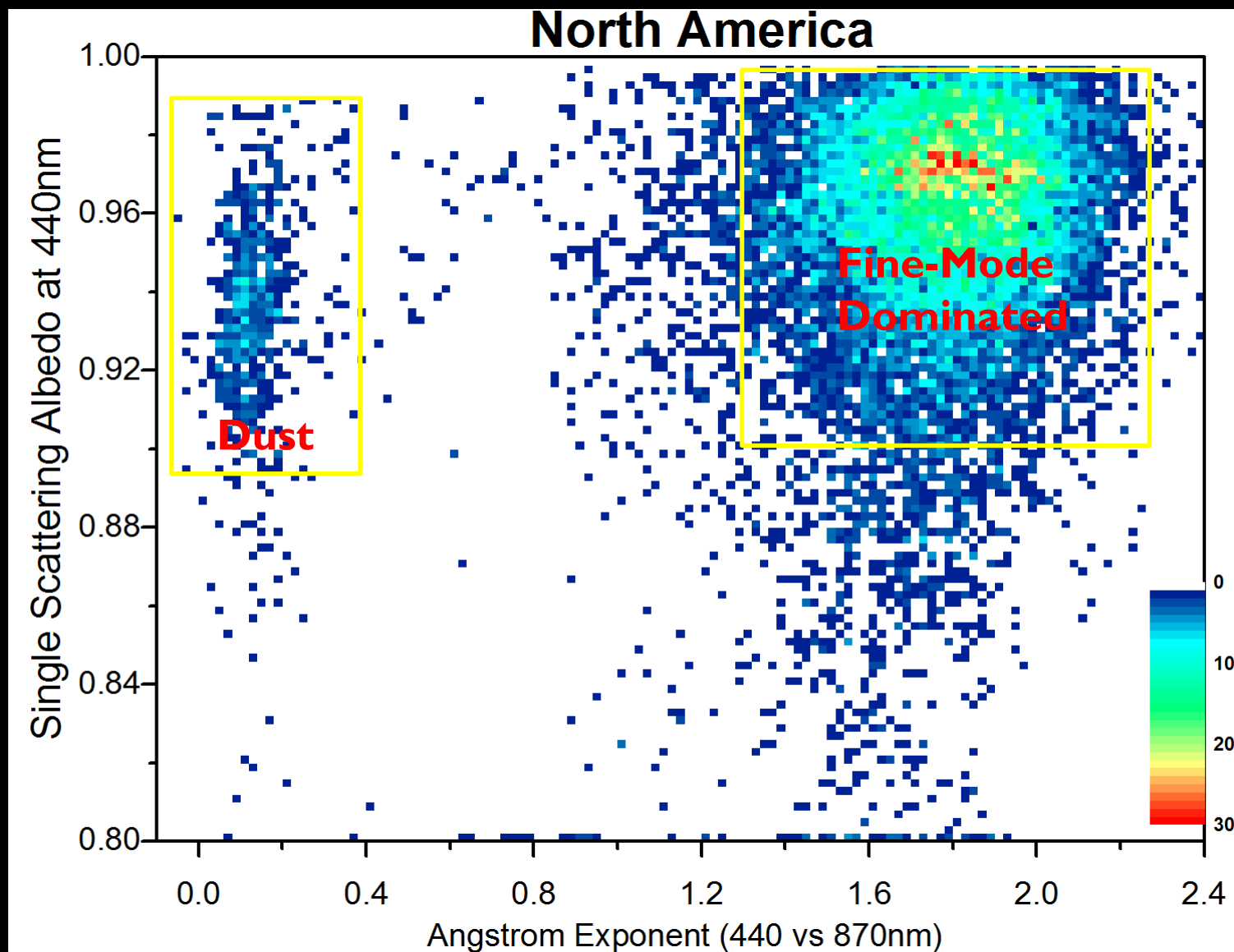
Regional Aerosol Properties (3)



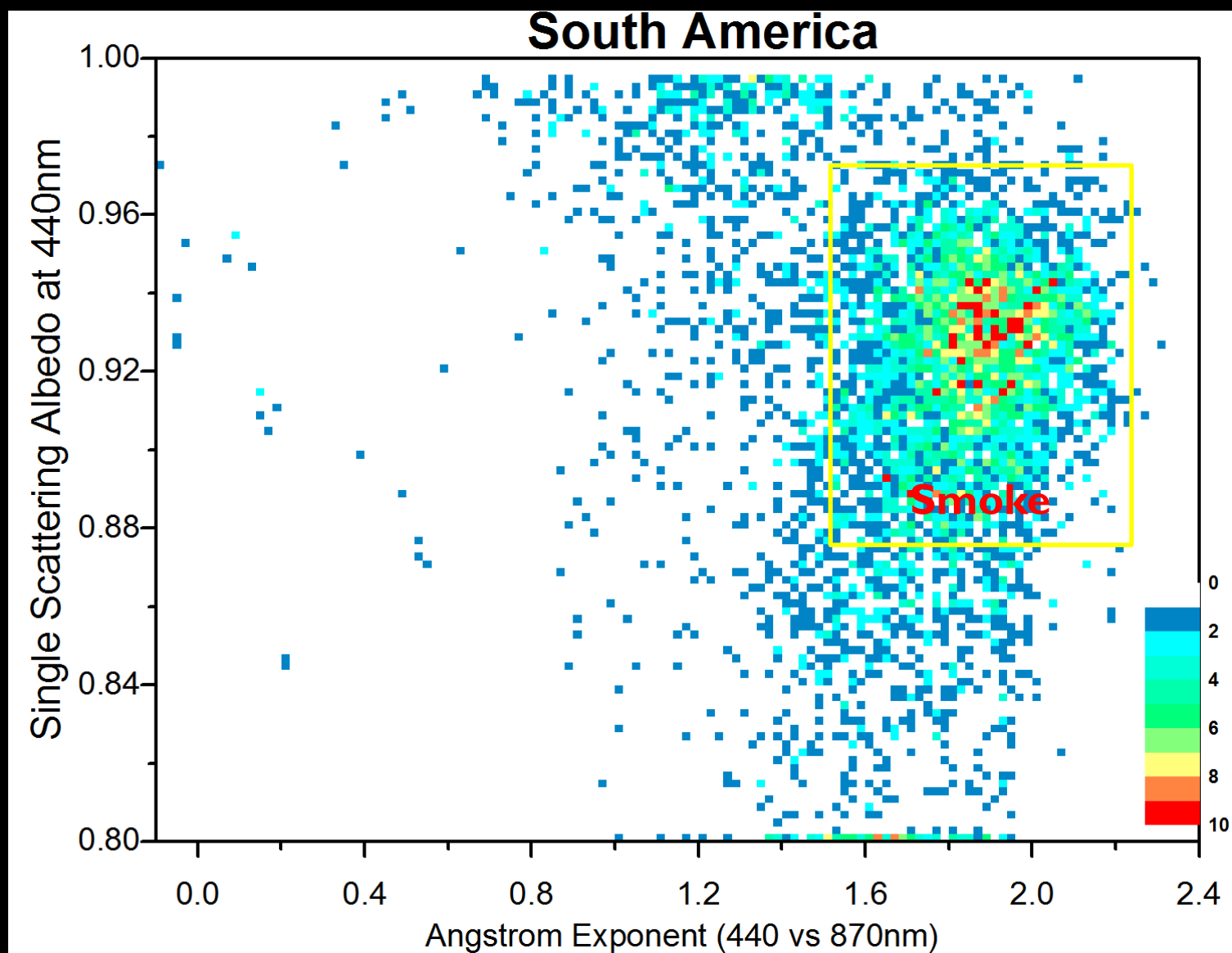
Regional Aerosol Properties (4)

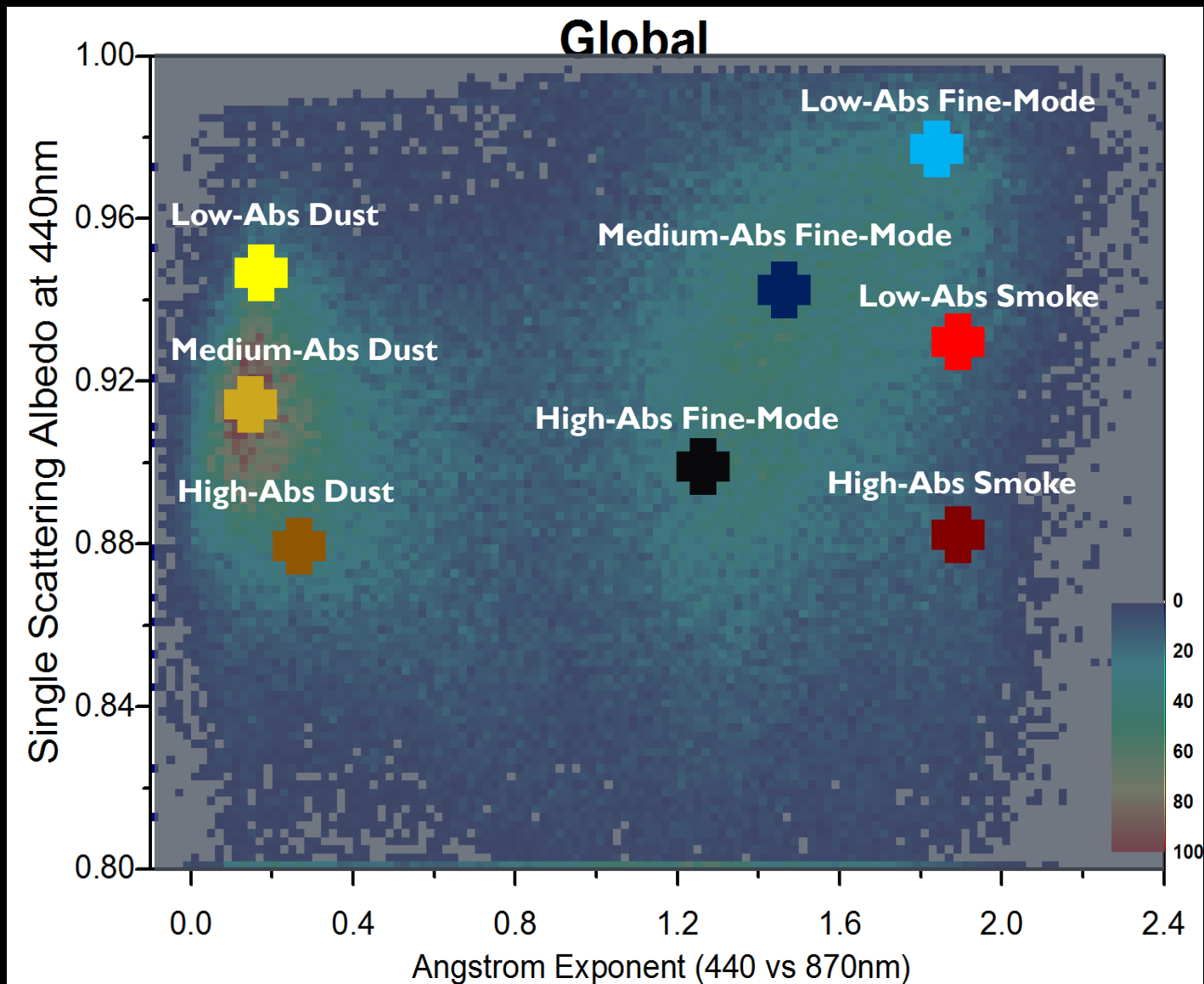


Regional Aerosol Properties (5)



Regional Aerosol Properties (6)

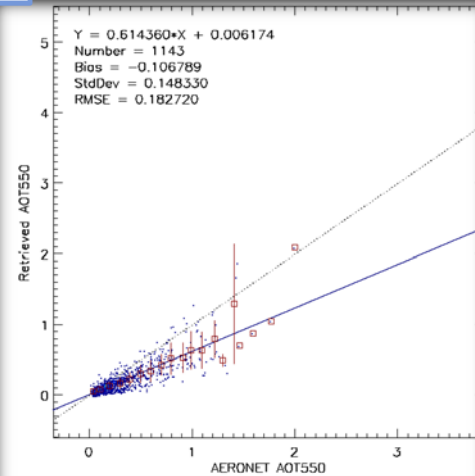




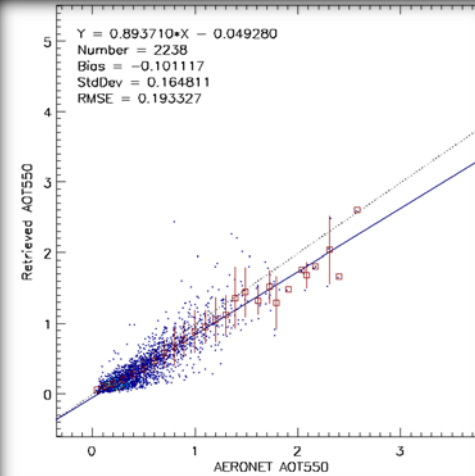
- Generate new lookup table with new land aerosol models and apply to the EPS AOD algorithm
 - Retrieval bias is reduced over Africa and India

BEFORE

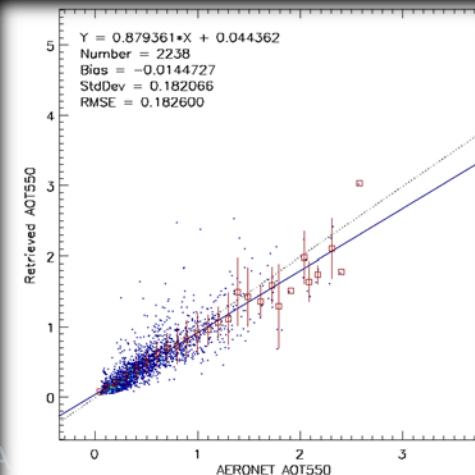
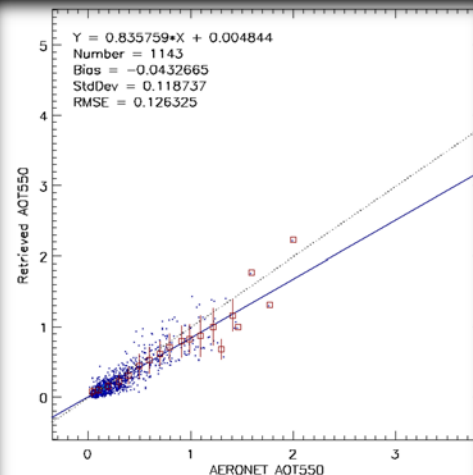
Africa



India



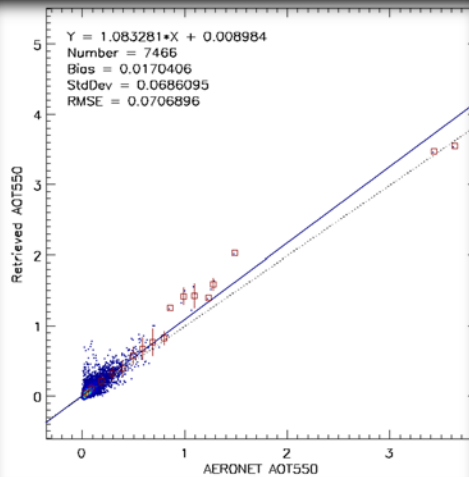
AFTER



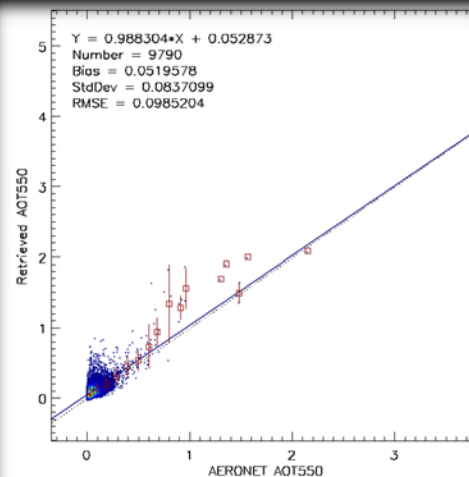
- But not so over other areas
 - Difficulty of picking right aerosol model at low AOD

BEFORE

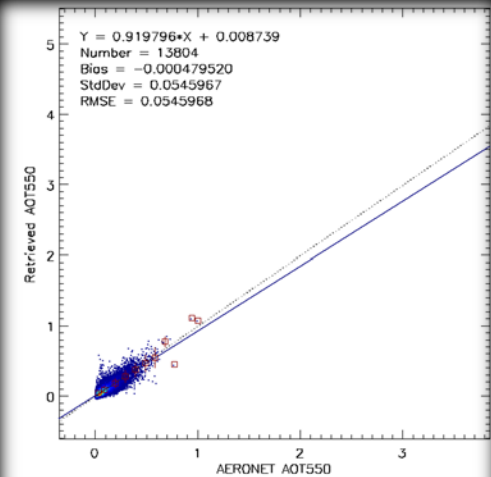
Eastern NA



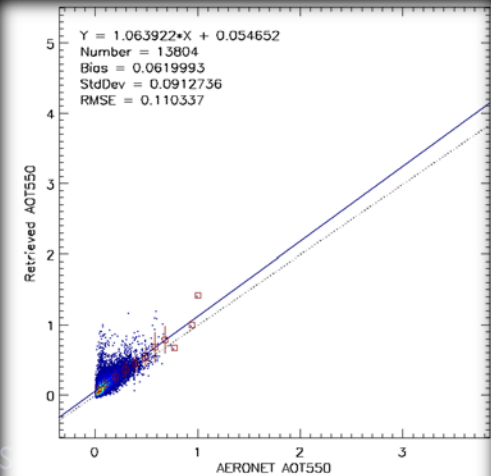
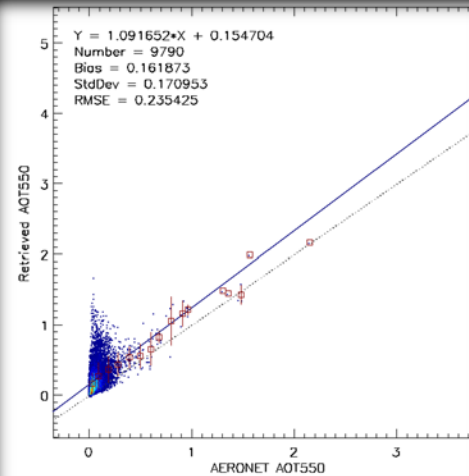
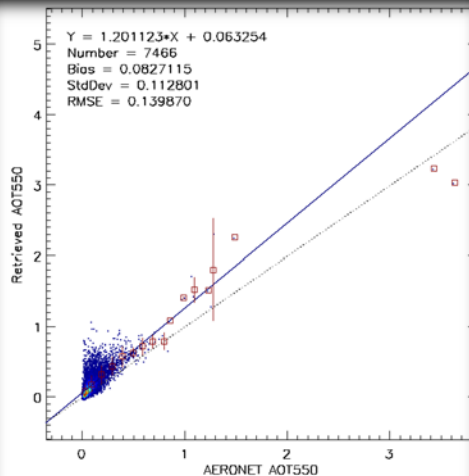
Western NA



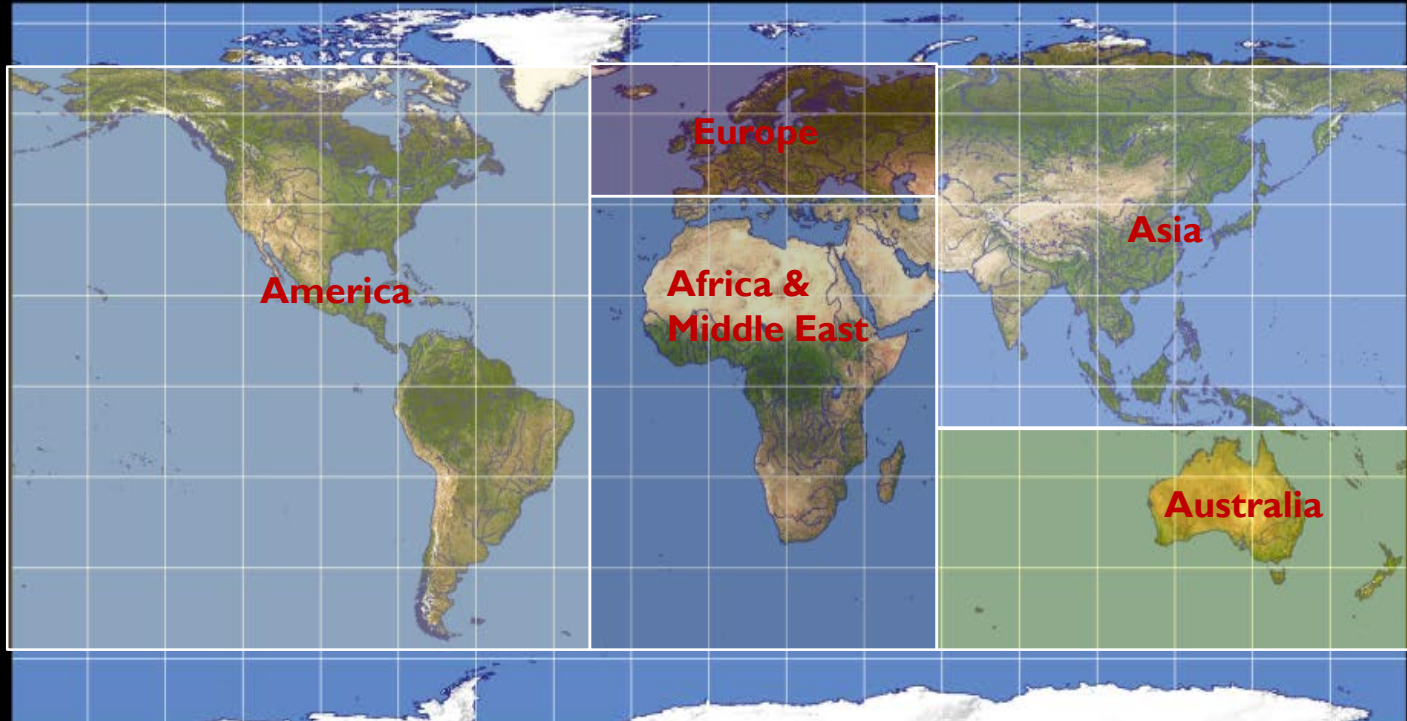
Europe



AFTER



- Candidate aerosol models are specified over land domains.

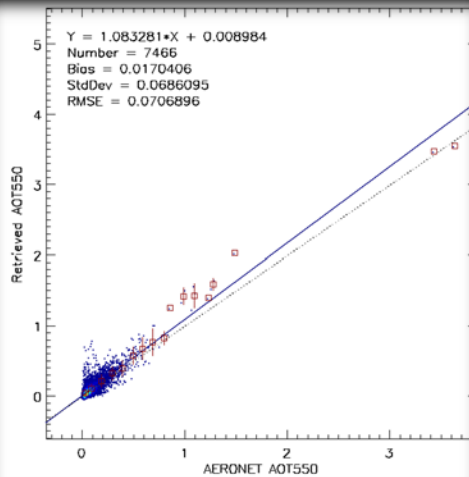


Domain	Longitude	Latitude	Aerosol Models
America	180° W - 30° W	60° S - 70° N	Fine (L,M), Dust (L), Smoke(L)
Europe	30° W - 60° E	40° N - 70° N	Fine (L,M), Dust (L), Smoke(L)
Africa & Middle	30° W - 60° E	60° S - 40° N	Fine(L), Dust(L,M,H), Smoke(L,H)
Asia	60° E - 180° E	10° S - 70° N	Fine(L,M,H), Dust(M,H), Smoke(L)
Australia	60° E - 180° E	60° S - 10° S	Fine(L), Dust(L), Smoke(L)
High Latitude	180° W - 180° E	70° N - 90° N 90° S - 60° S	Fine(L)

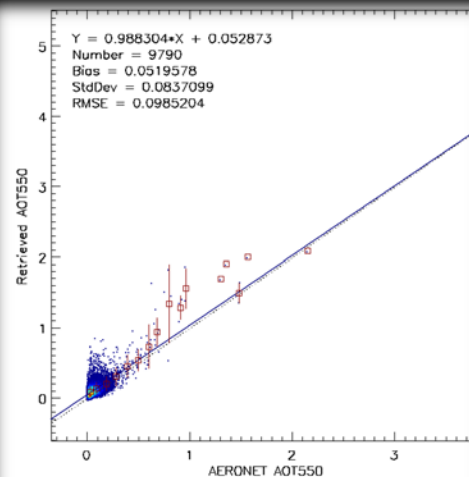
- With regional candidates of aerosol models, improvement is not significant at low AOD

BEFORE

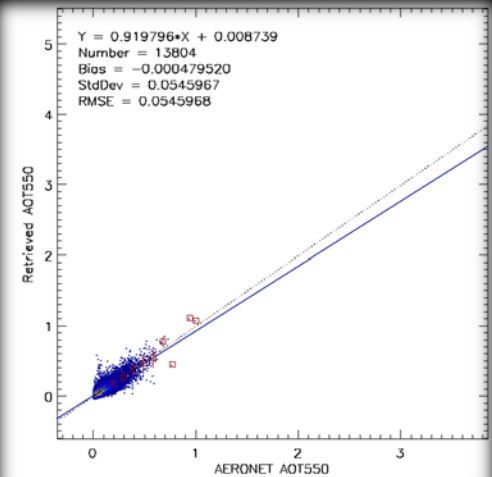
Eastern NA



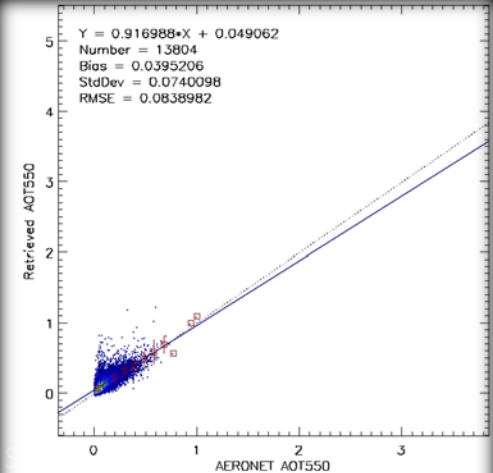
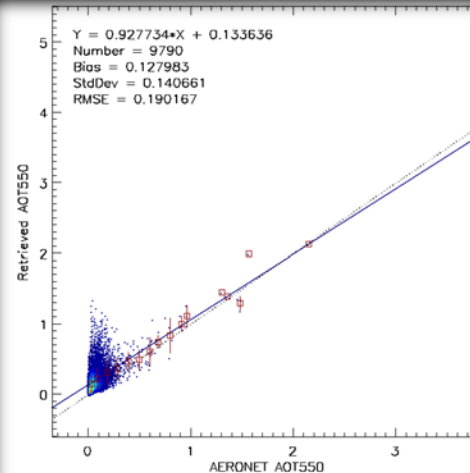
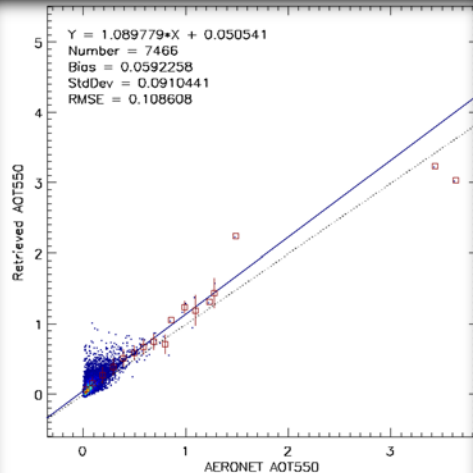
Western NA



Europe



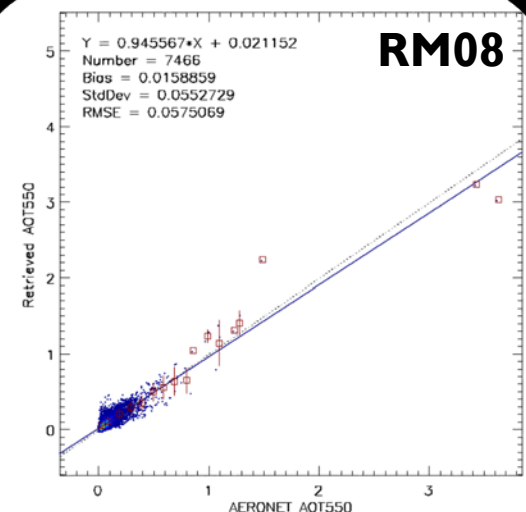
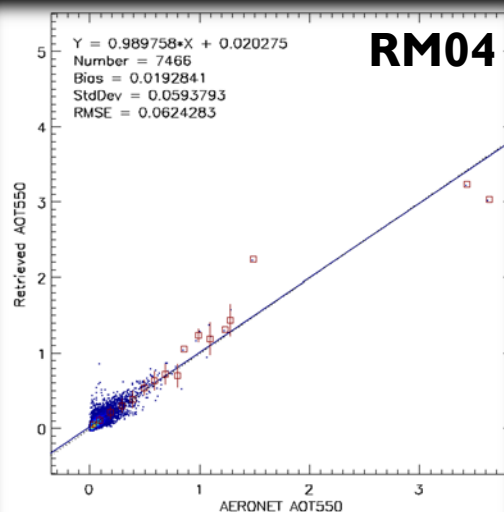
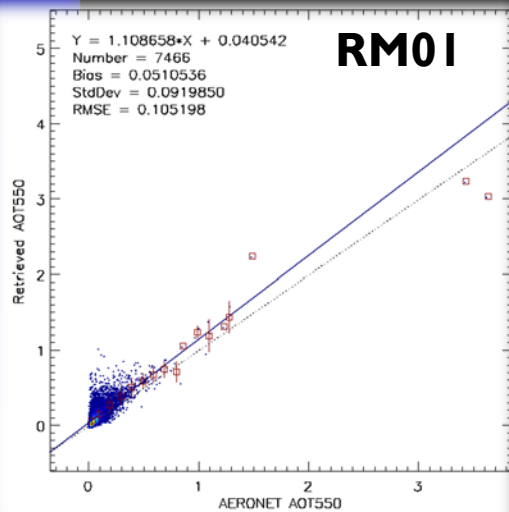
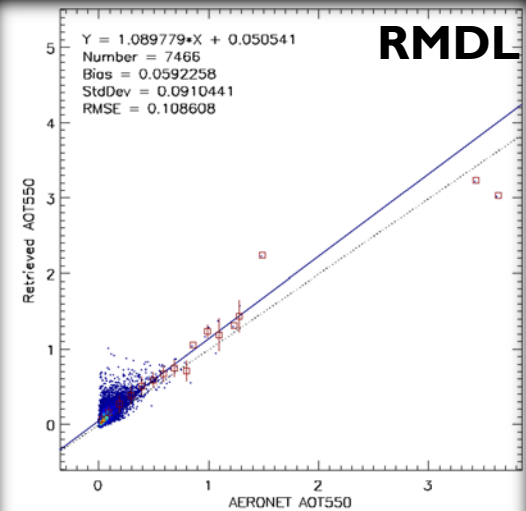
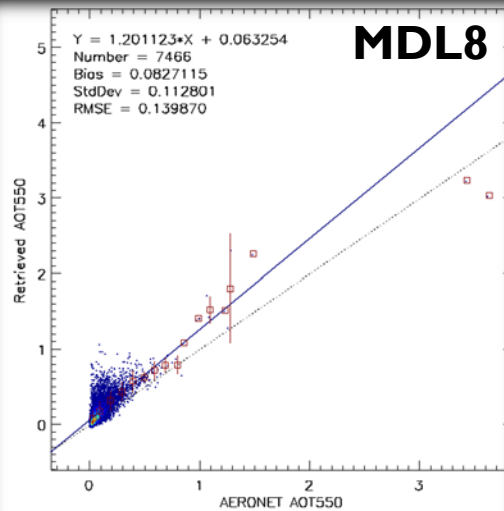
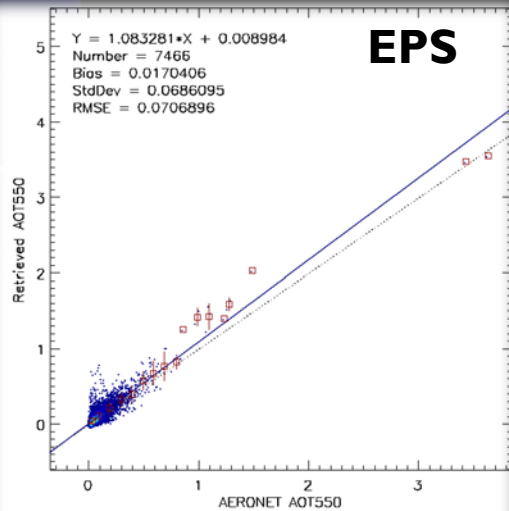
AFTER



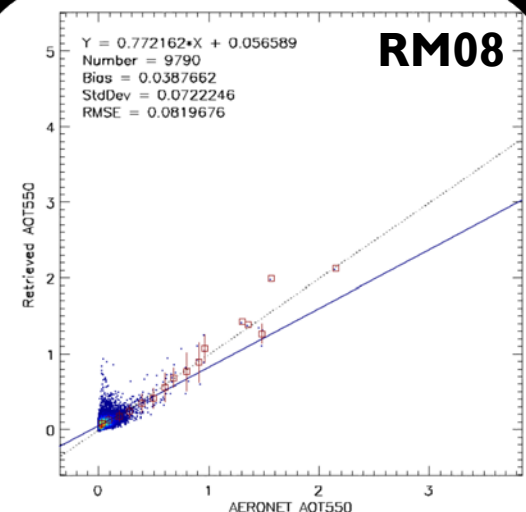
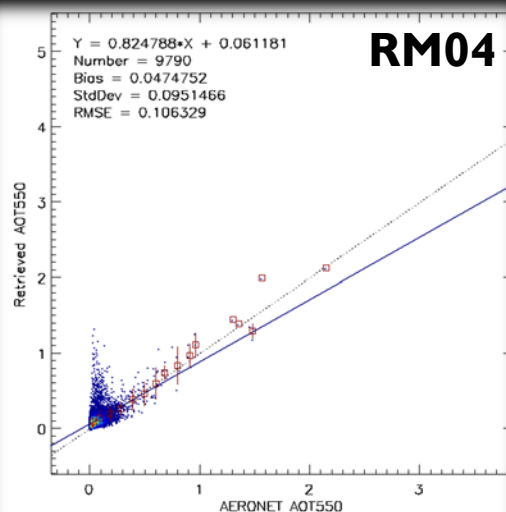
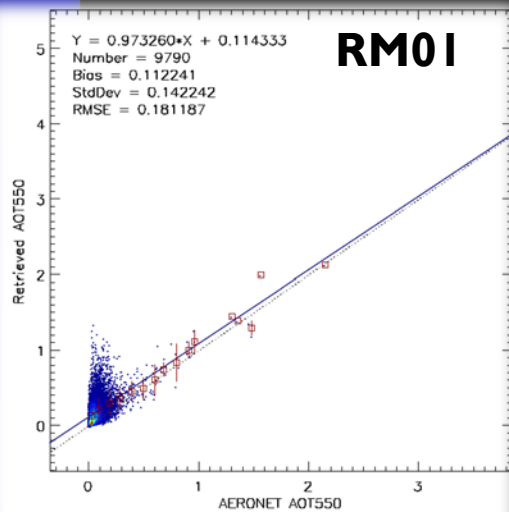
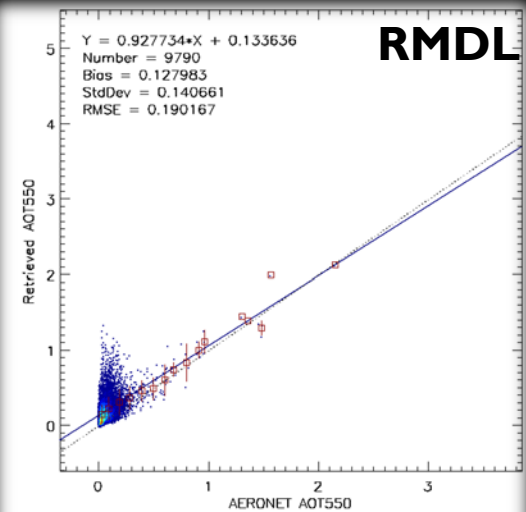
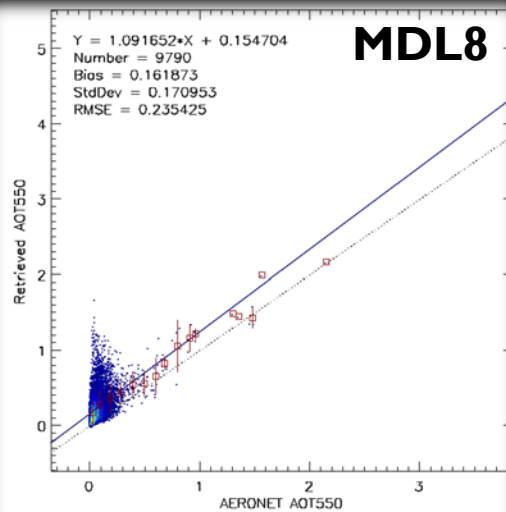
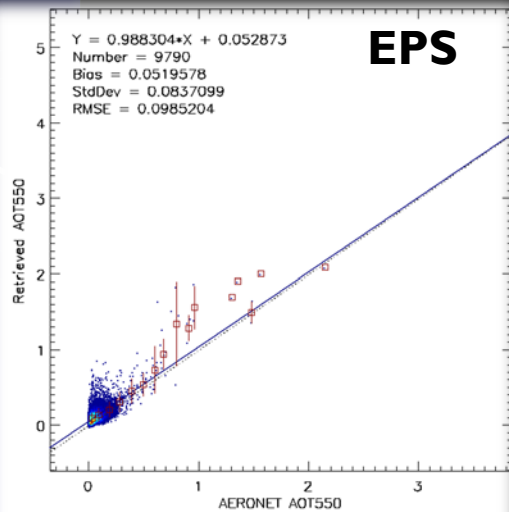
- Over-estimation at low AOD by using new aerosol models
 - **Causes:** picking absorbing or dust models incorrectly
 - **Potential solution:** using fine-mode dominated low-absorbing aerosol F(L) model if AOD is low
 - **Tests:** using F(L) model only if
 - Retrieved AOD < 0.1
 - Retrieved AOD < 0.4
 - Retrieved AOD < 0.8

Selecting aerosol models only if F(L) AOD is larger than the threshold

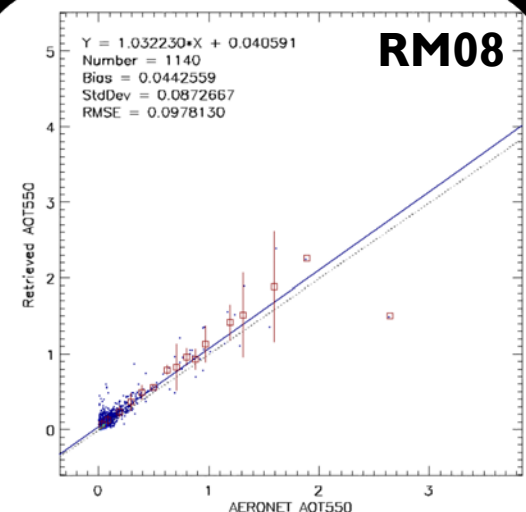
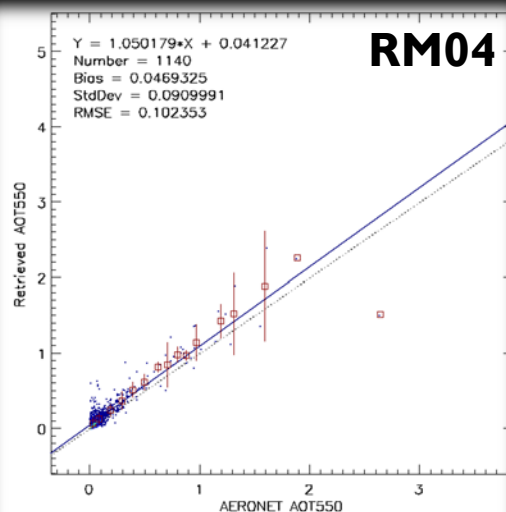
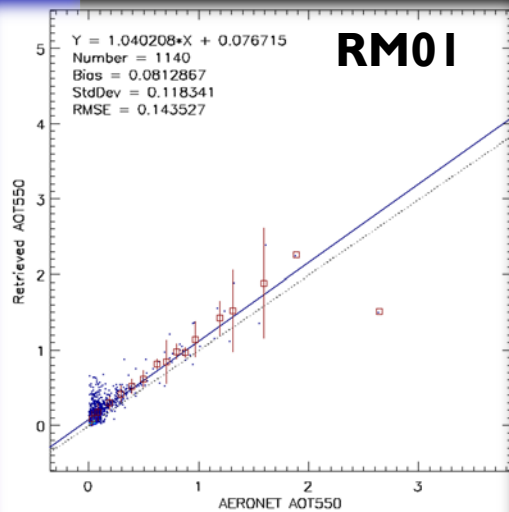
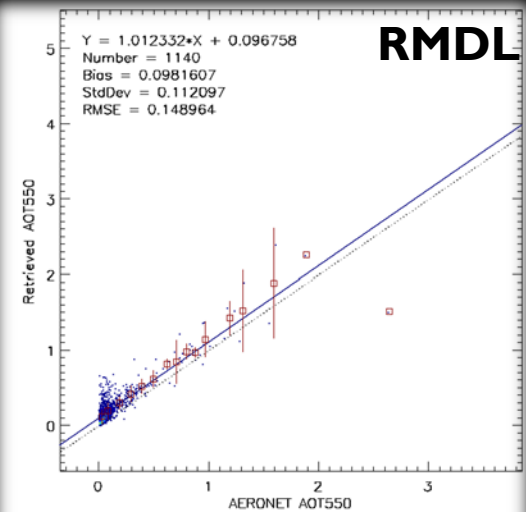
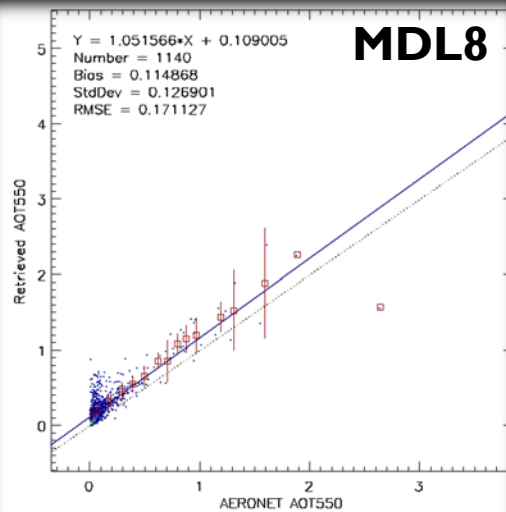
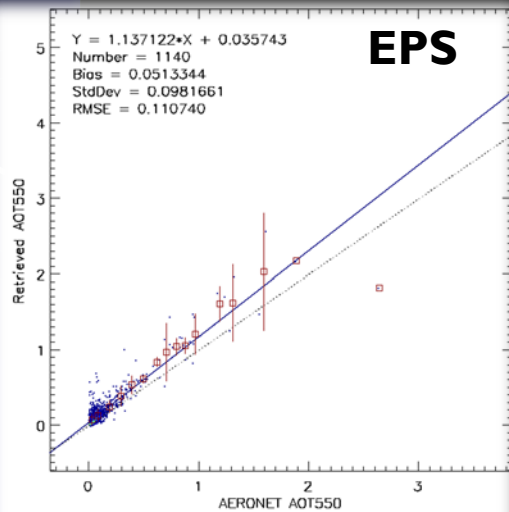
Eastern North America



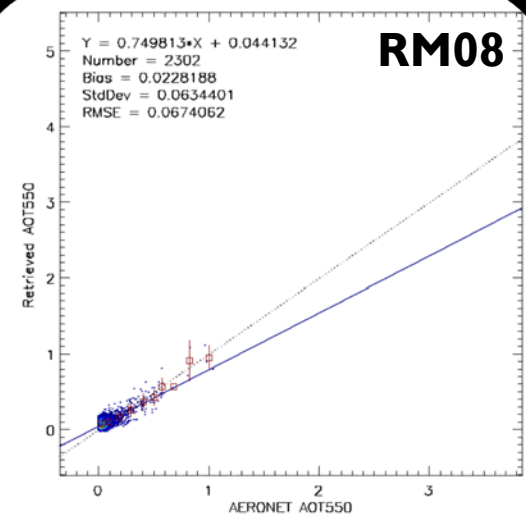
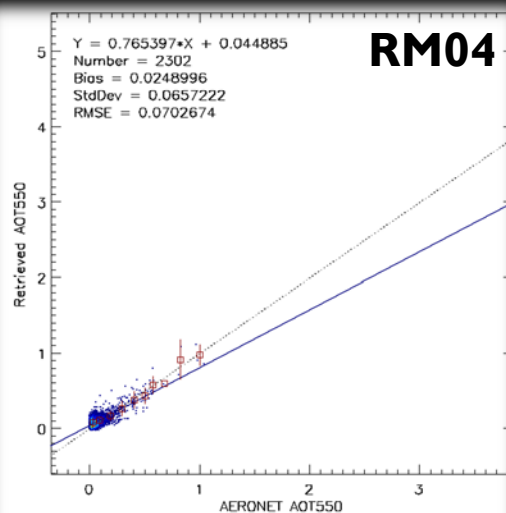
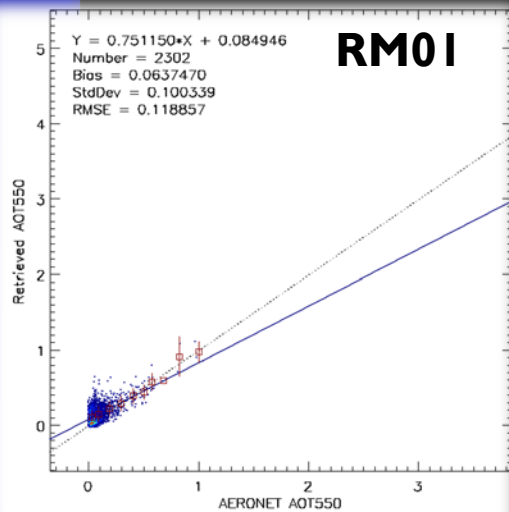
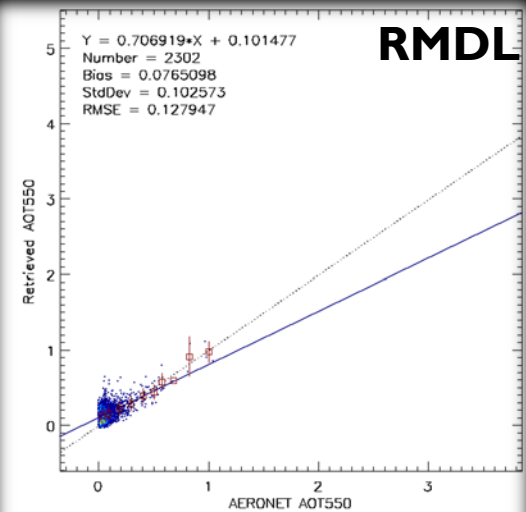
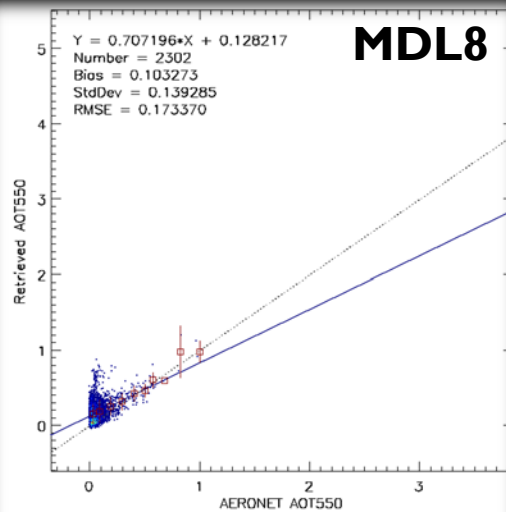
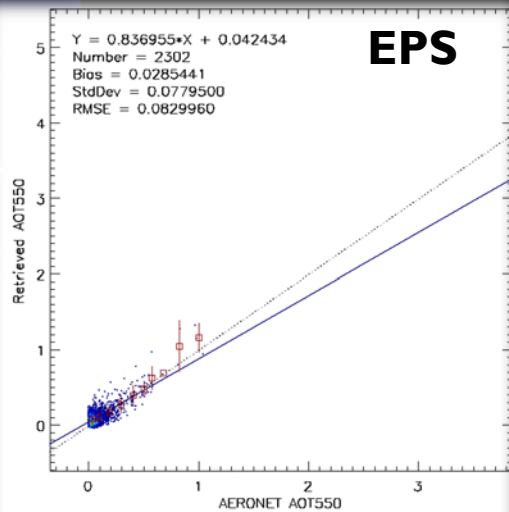
Western North America



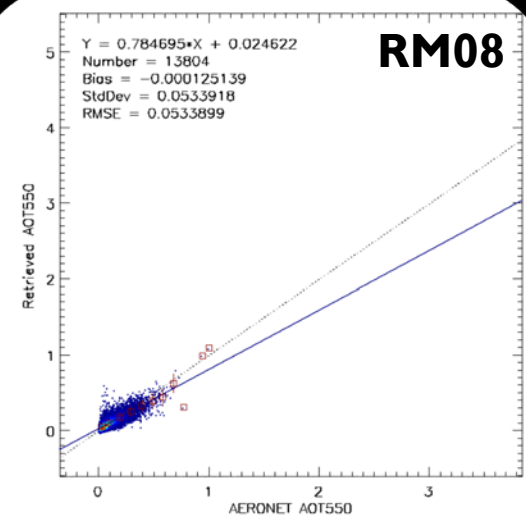
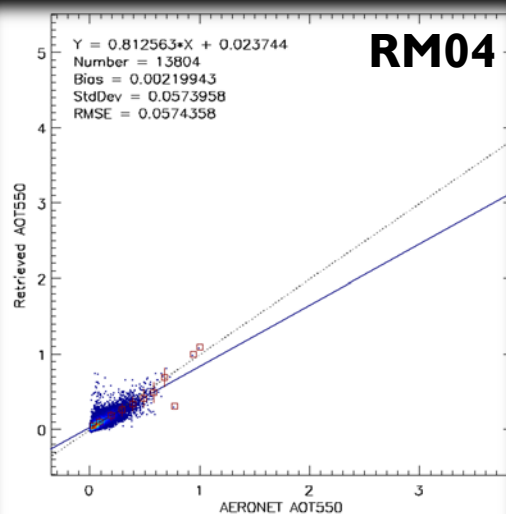
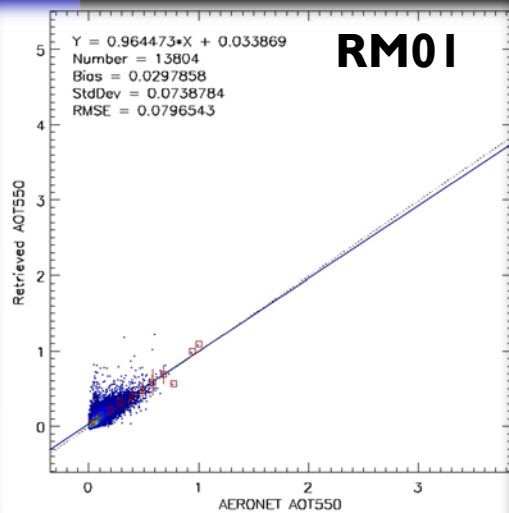
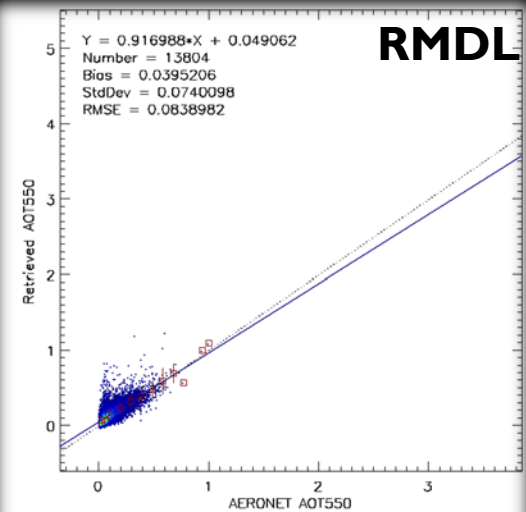
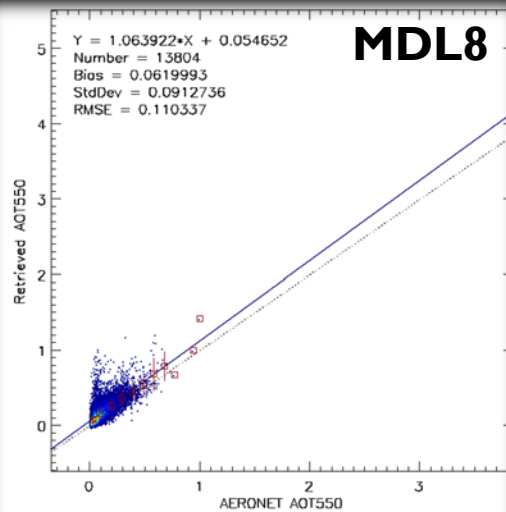
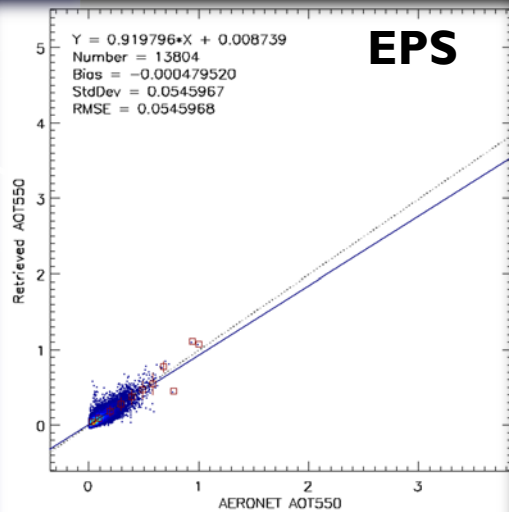
Northern North America



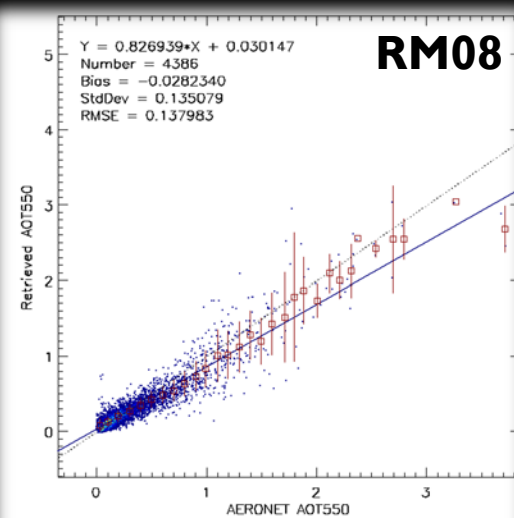
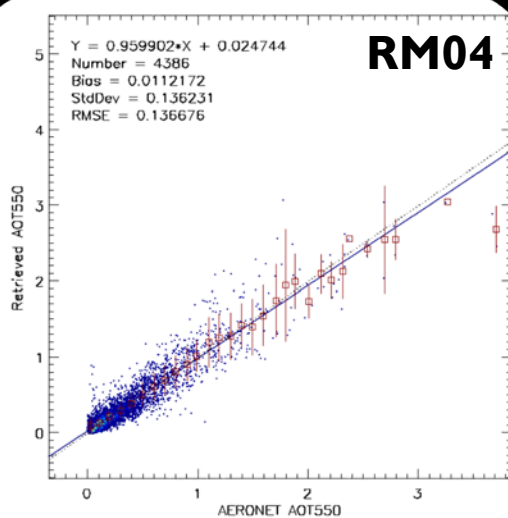
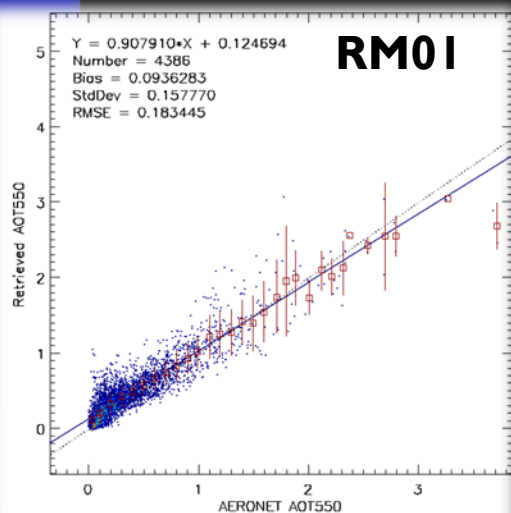
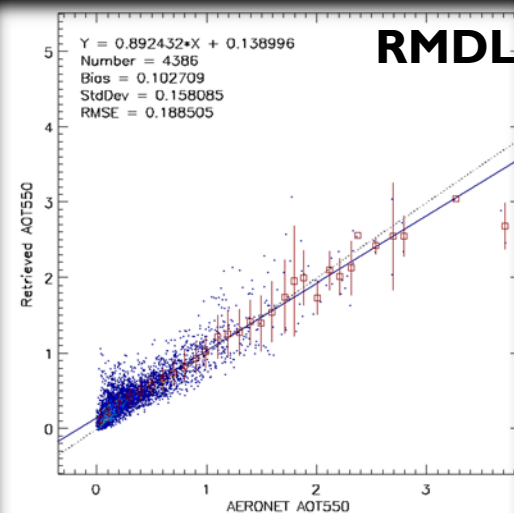
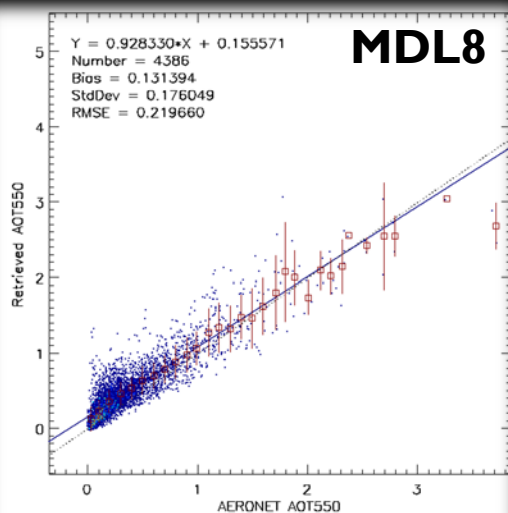
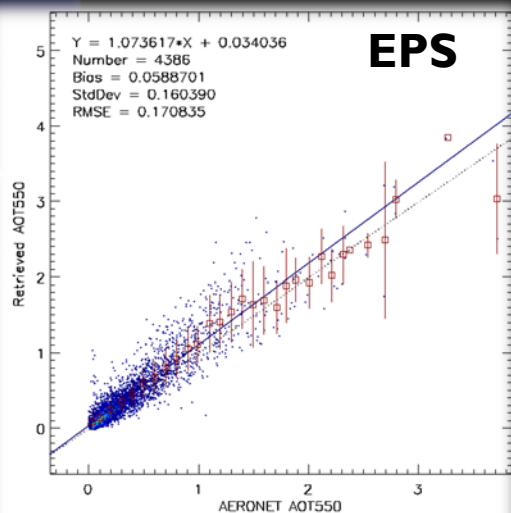
South America



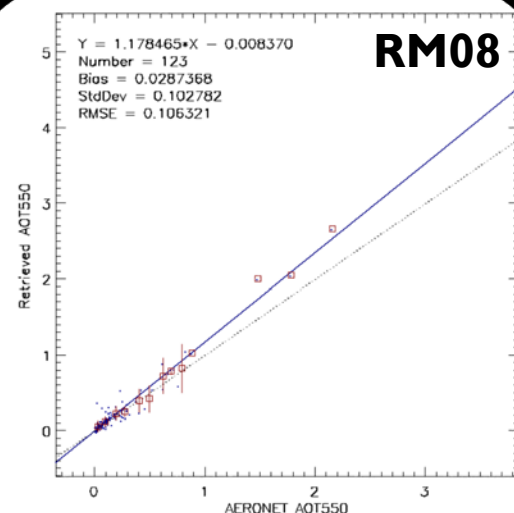
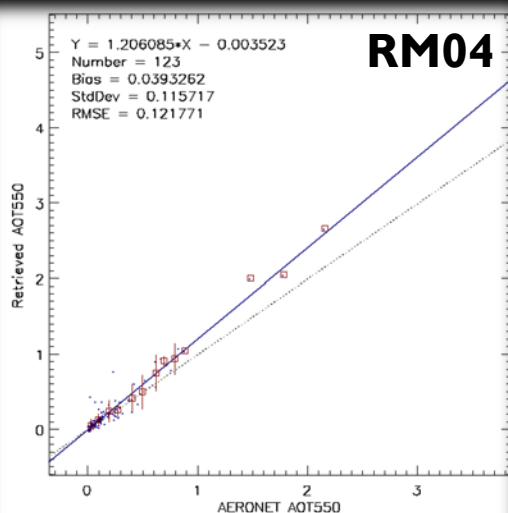
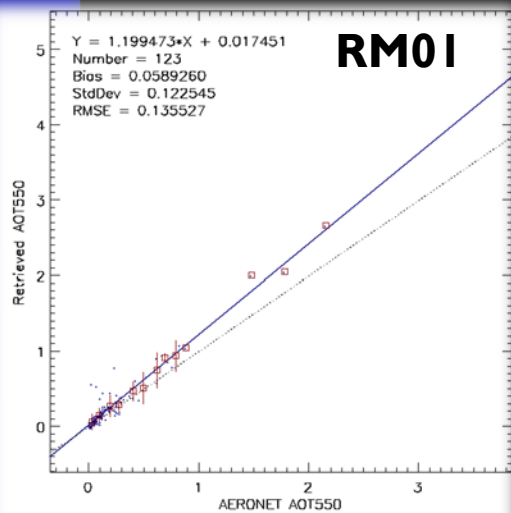
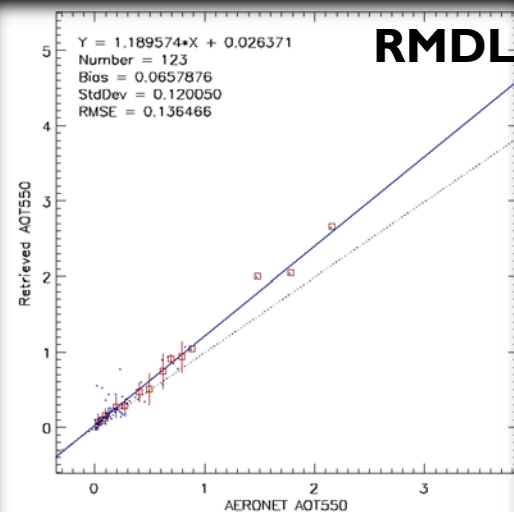
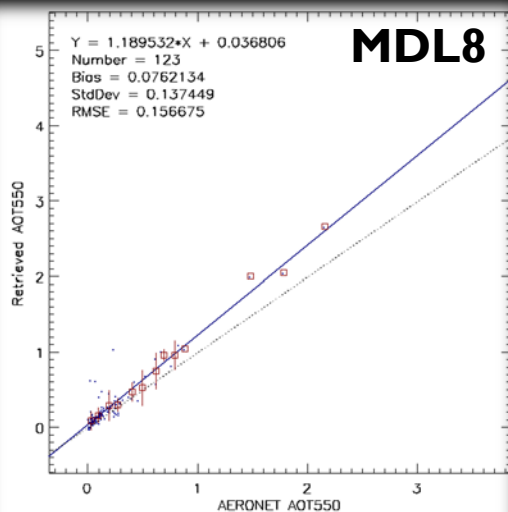
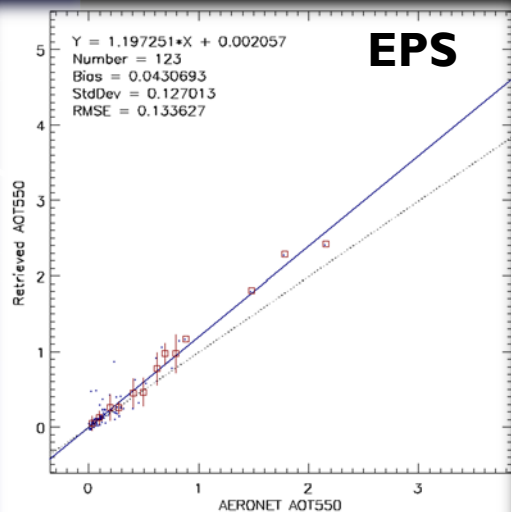
Europe



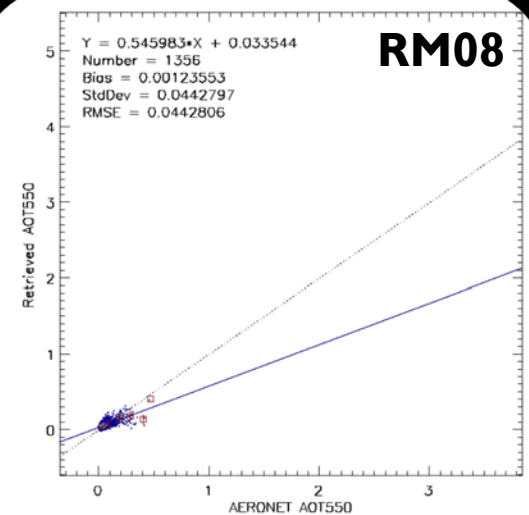
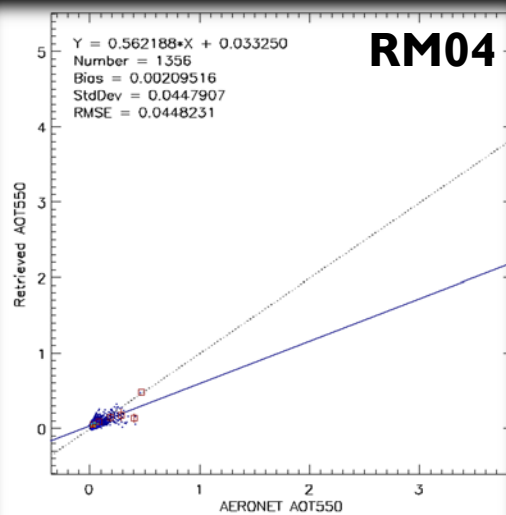
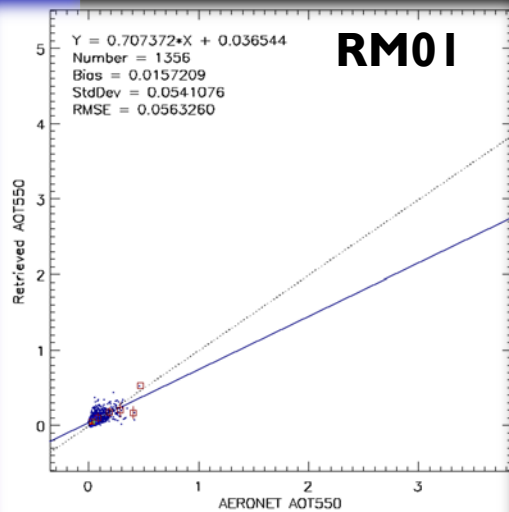
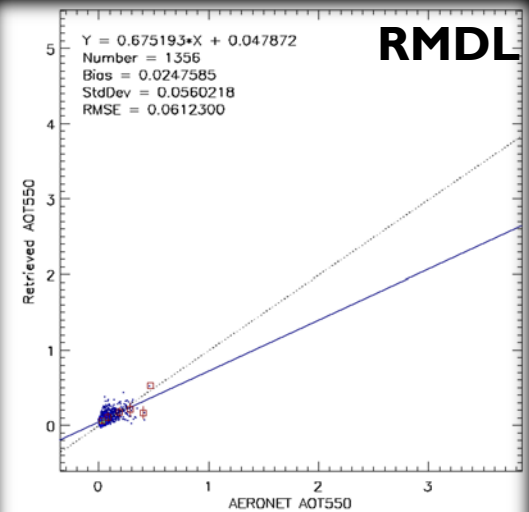
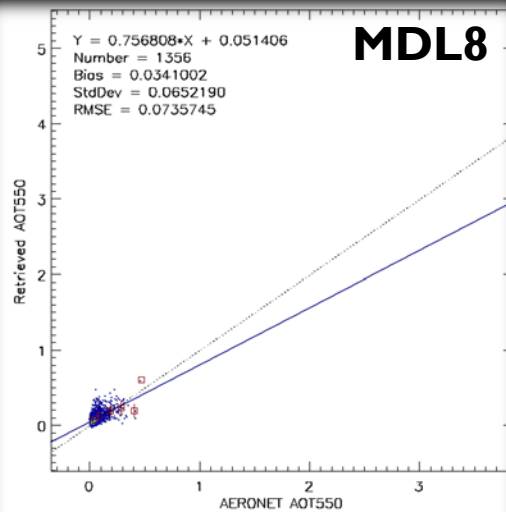
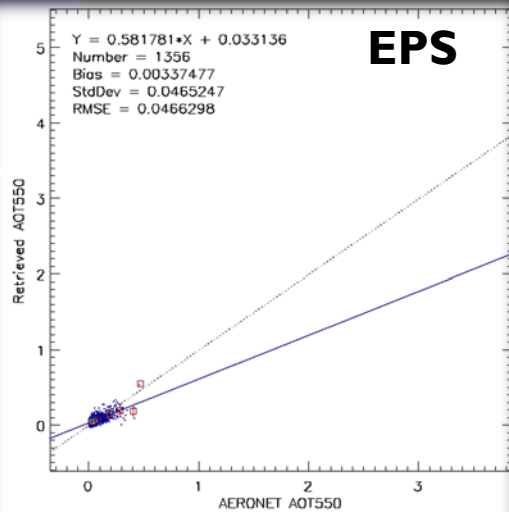
Eastern Asia



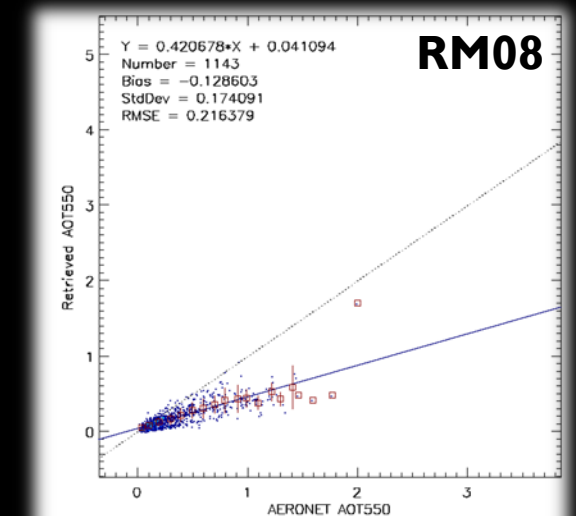
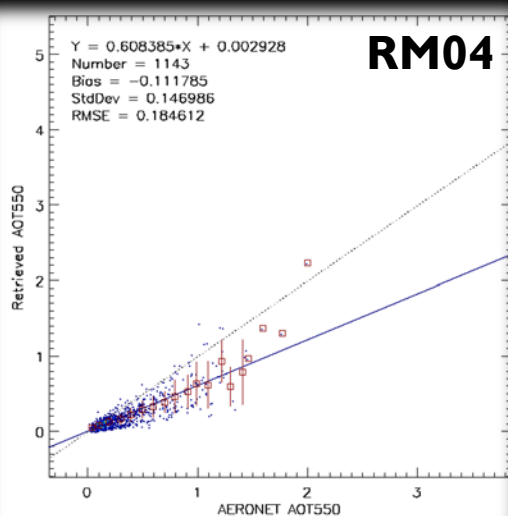
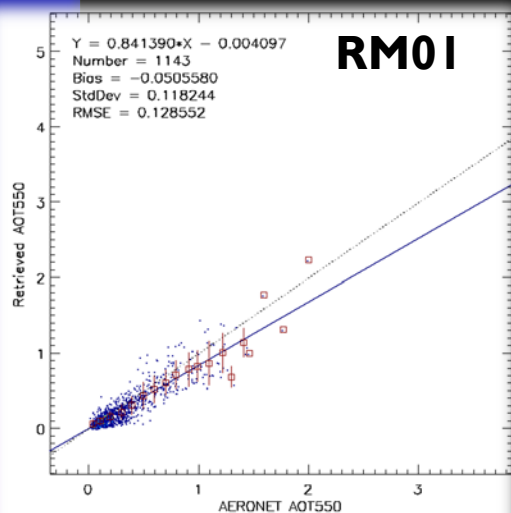
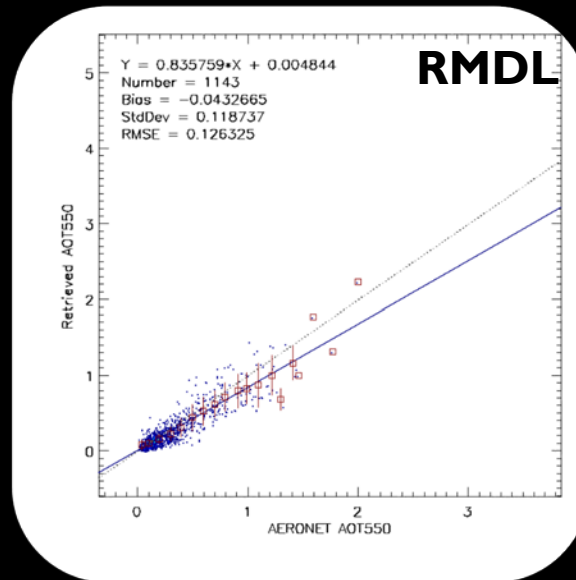
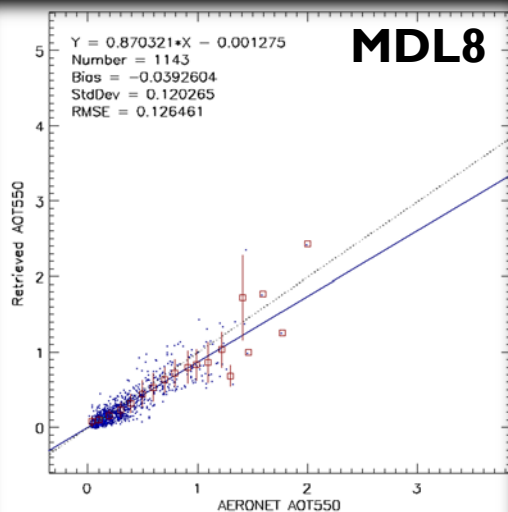
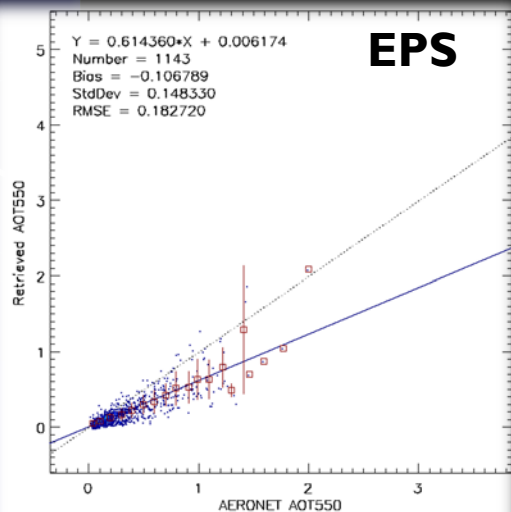
Northern Asia



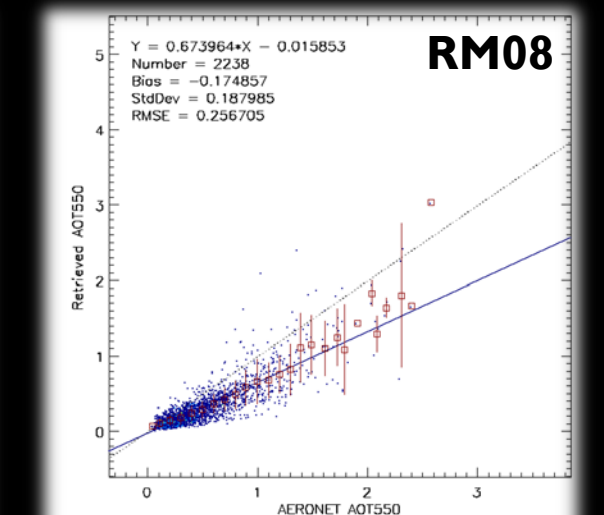
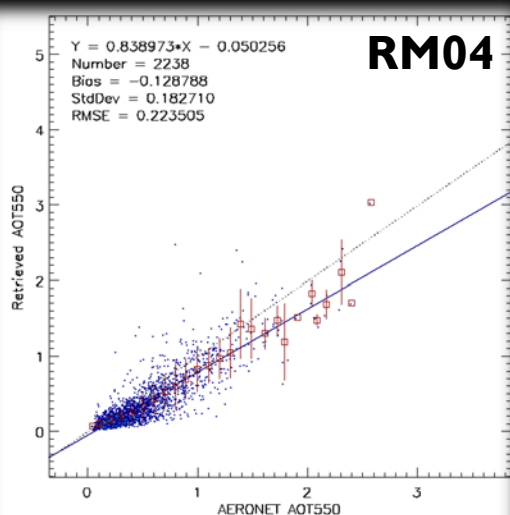
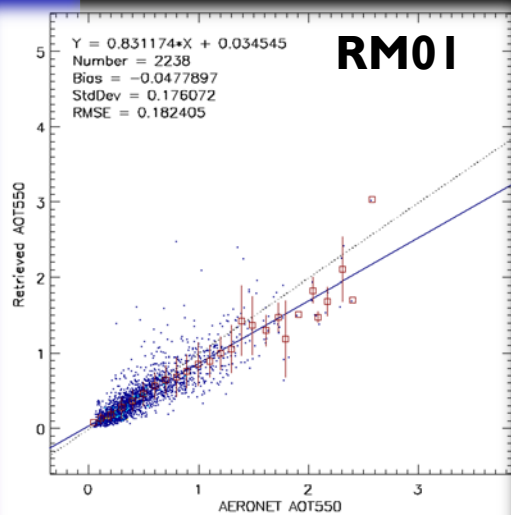
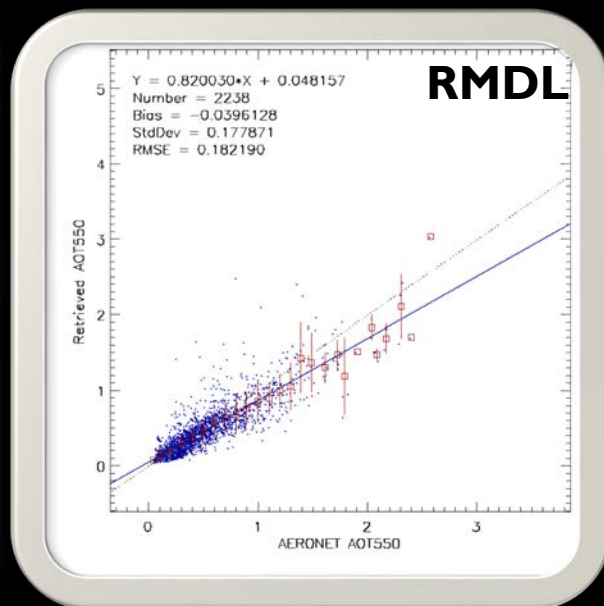
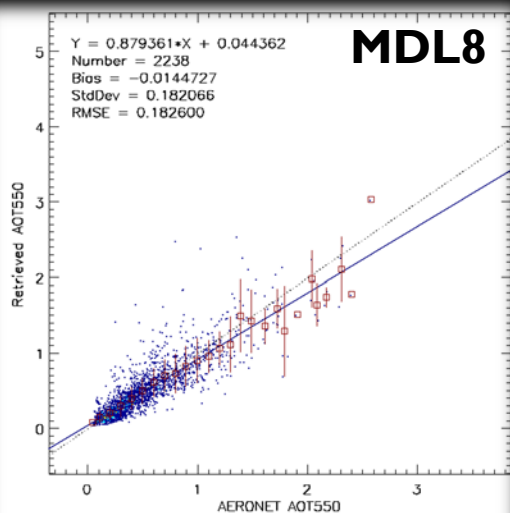
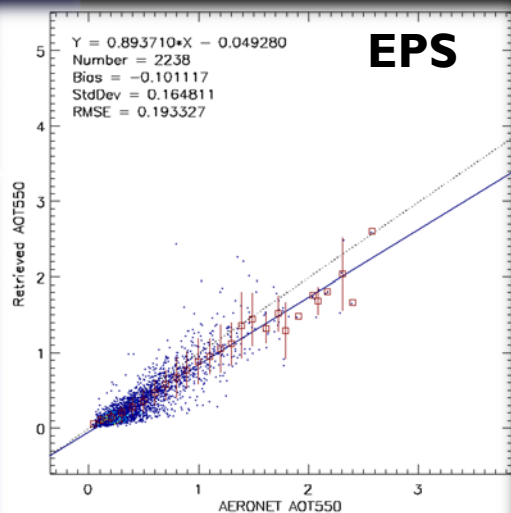
Australia



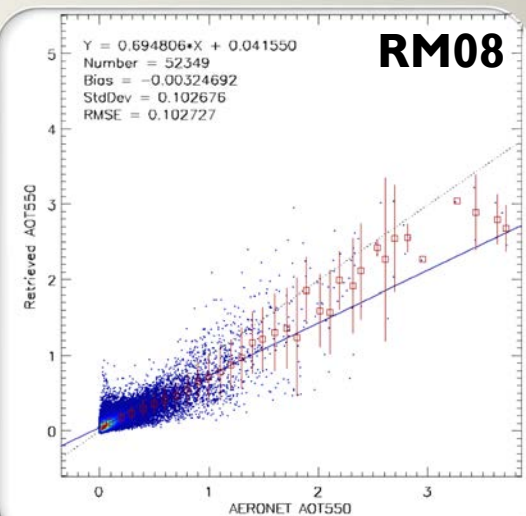
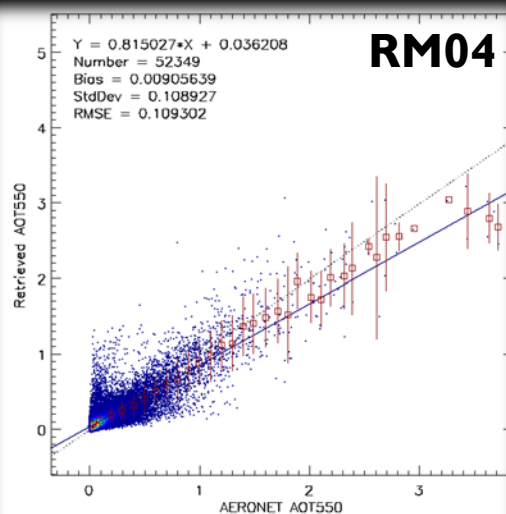
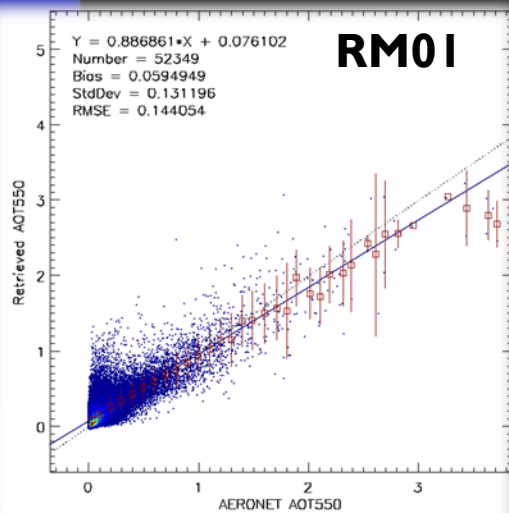
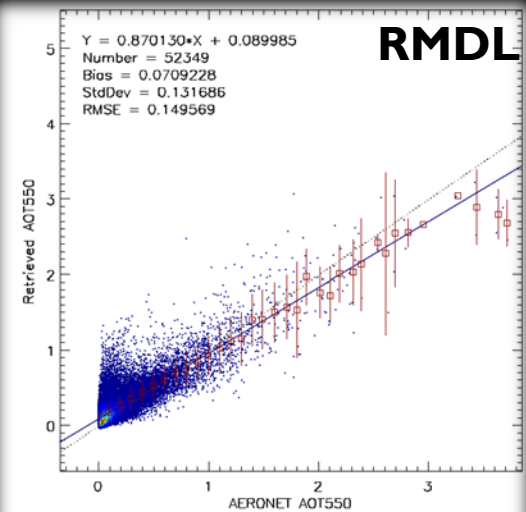
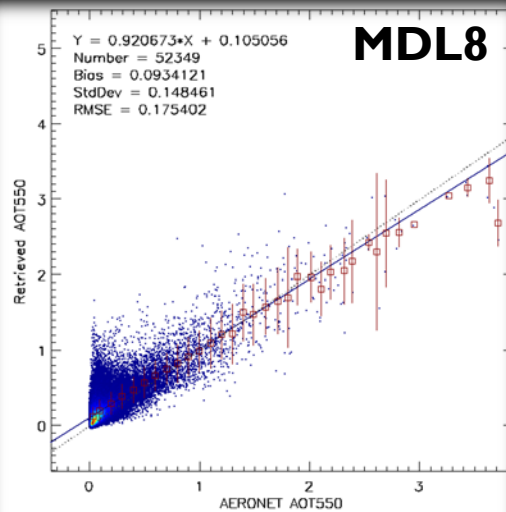
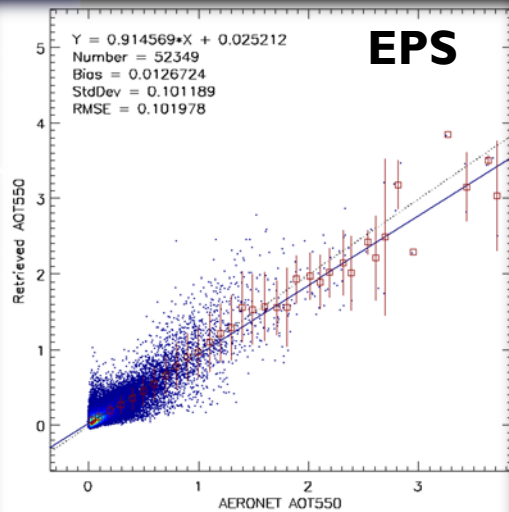
Africa



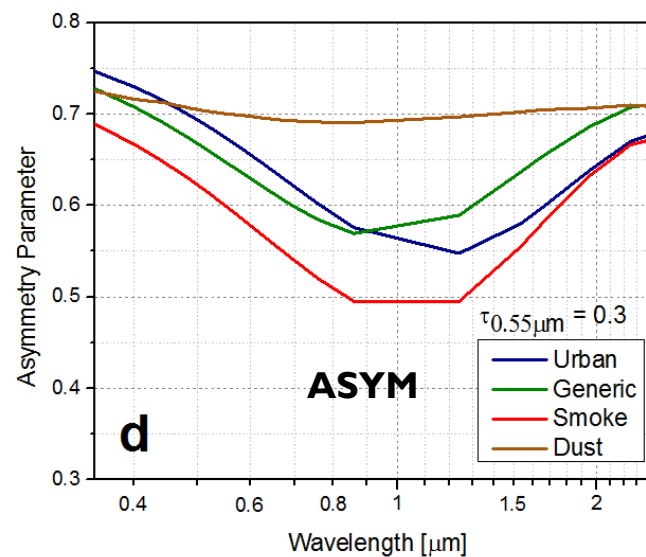
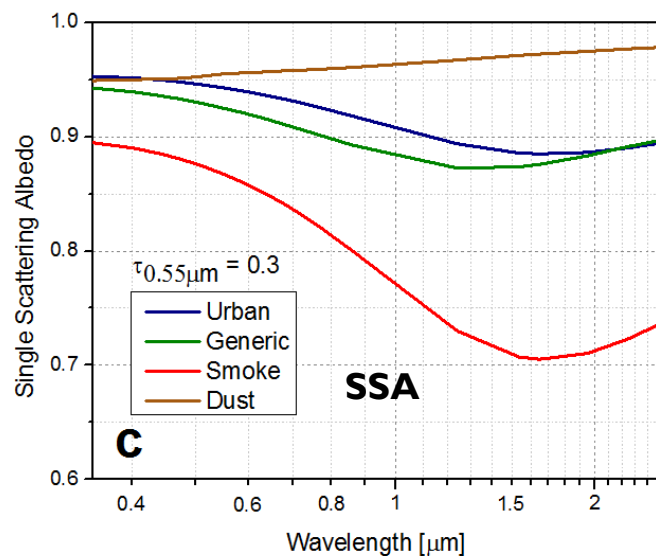
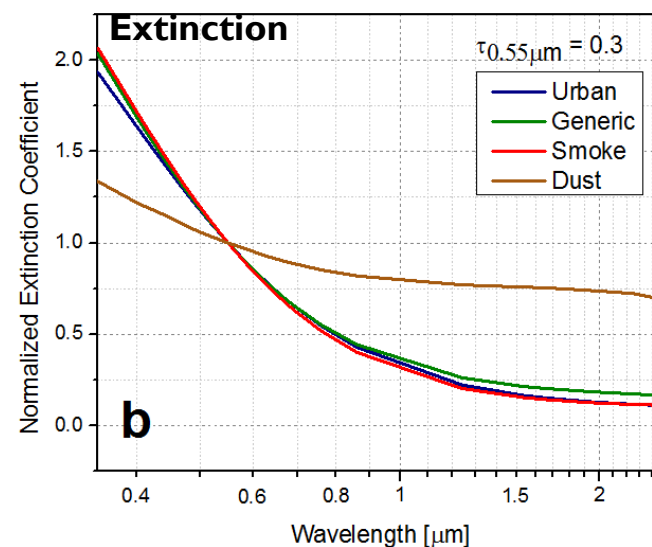
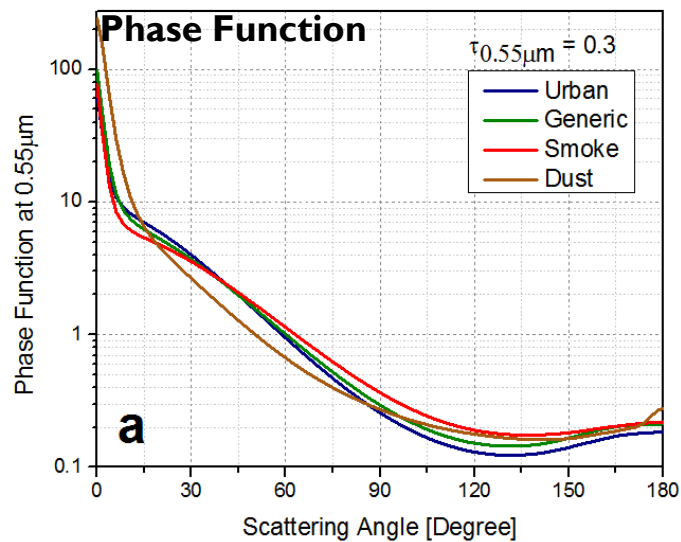
India

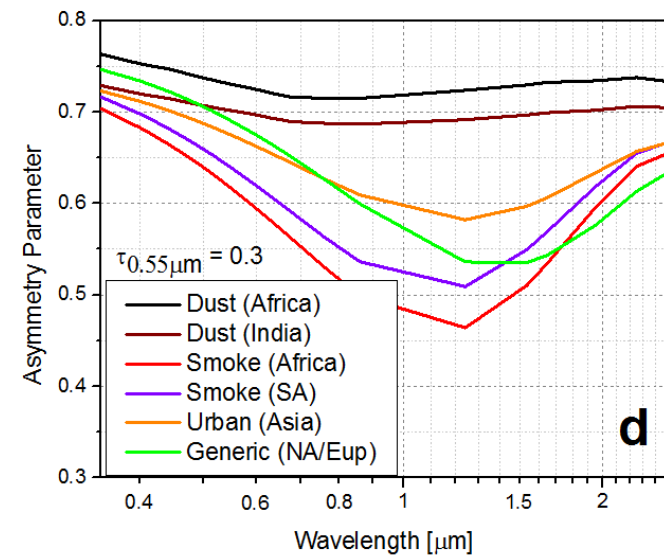
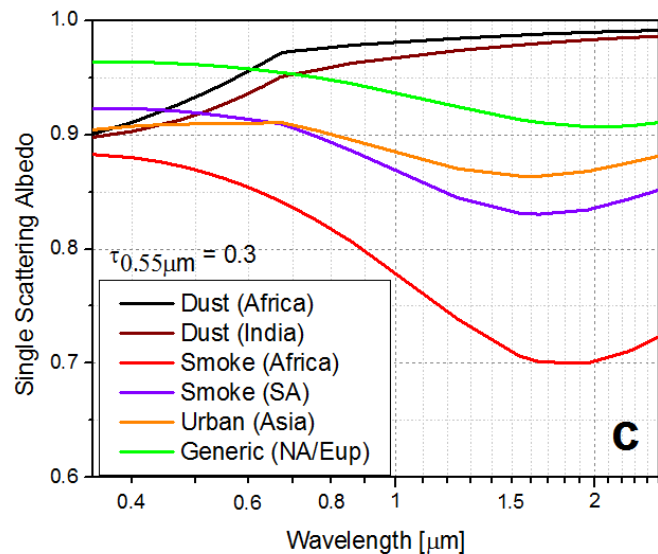
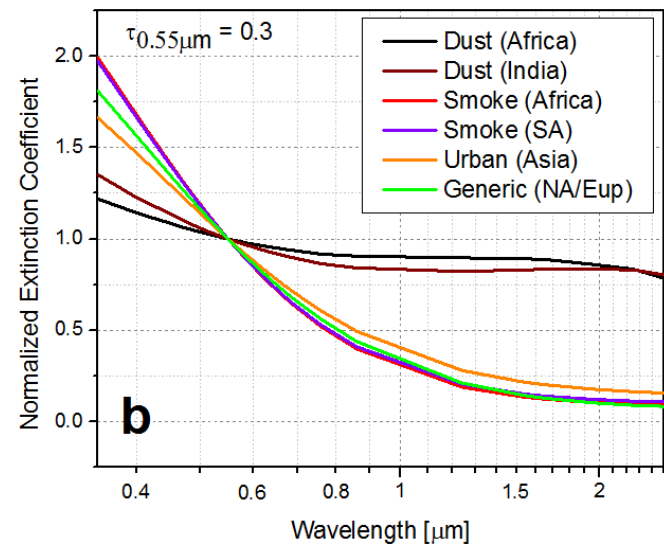
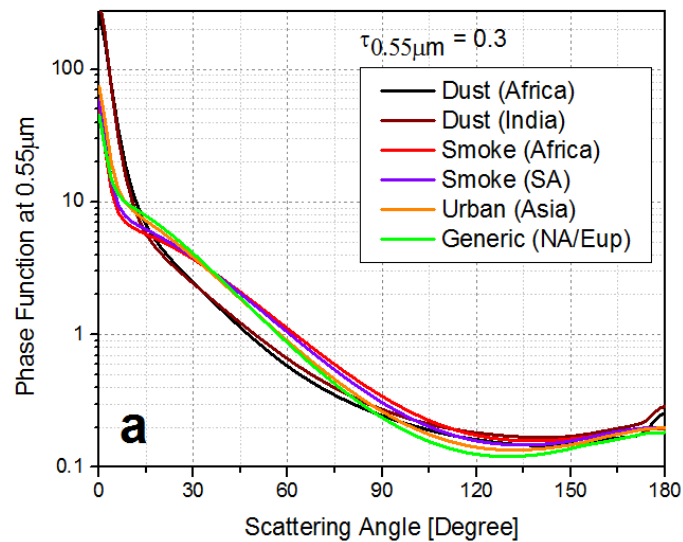


Global



- New land aerosol models are derived from AERONET inversions
 - Dust: low/medium/high absorbing
 - Smoke: low/high absorbing
 - Fine-mode Dominated: low/medium/high absorbing
- Potential updates on the EPS AOD algorithm is investigated
 - Dynamic selection among all/subset of aerosol models at all/high AOD cases
 - Algorithm has the difficulty to pick the right aerosol model at low AOD cases







Entangling Snow/Snowmelt Screening and Smog AOT Retrievals in the VIIRS Aerosol Algorithm

Jingfeng Huang

UMD/ESSIC/CICS @ NOAA/NESDIS/STAR

**Shobha Kondragunta, Istvan Laszlo, Hongqing Liu, Hai
Zhang, Pubu Ciren, Lorraine A. Remer**

- Part 1: Towards a Better Snow/Snowmelt Screening in the IDPS VIIRS Aerosol Algorithm
- Part 2: The missing China Smog AOT Retrievals in the IDPS VIIRS AOT Product
- Part 3: Balance Snow/Snowmelt Screening and China Smog Detection in the EPS Aerosol Algorithm
- Summary



The Two VIIRS Aerosol Algorithms



1. The Two S-NPP VIIRS AOT Algorithms
 - IDPS: Interface Data Processing Segment (Current Operational VIIRS Aerosol Algorithm)
 - EPS: Enterprise Processing System (Currently under testing and will replace IDPS in operation soon)
2. Improvements in EPS:
 1. Pixel screening procedures – *eliminate artifacts*
 2. New algorithm science – *provides enhanced spatial coverage*
3. EPS: Characterization of China Smog Events

IDPS vs. EPS: Main Differences

- Detection, observation and quantification of global aerosol outbreaks is one of many important applications of the global satellite aerosol products

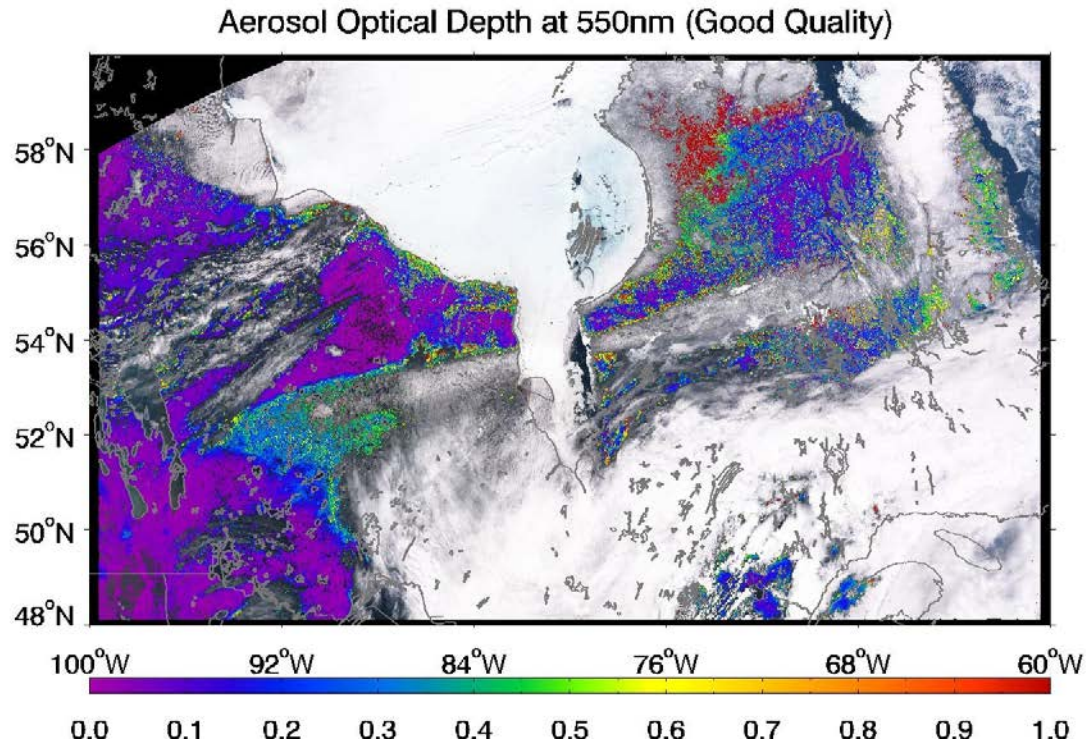
	IDPS Aerosol Algorithm (Current Operational)	EPS Aerosol Algorithm (Upcoming Operational)
AOT range	[0, 2.0]	[-0.05, 5.0]
Retrieval surfaces over land	Dark surface only	Both dark and bright surfaces
Cloud overscreening	Heavy aerosol mis-identified as clouds in some pixels	internal heavy aerosol callback test
Internal snow test over land	Smog mis-identified as snow in some pixels	Improved snow test
Internal Ephemeral Water Test	Aerosol mis-identified as ephemeral water in some pixels	Improved ephemeral water test

PART 1:

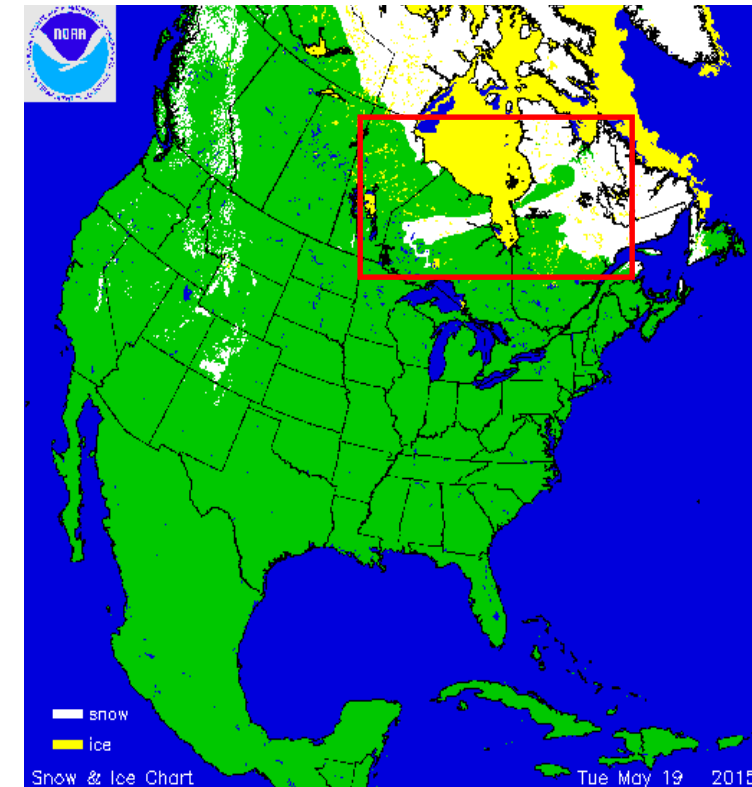
TOWARDS A BETTER SNOW/SNOWMELT SCREENING IN THE IDPS VIIRS AEROSOL ALGORITHM

Problem: Snow/Snowmelt Underscreening (regional)

May 19, 2015

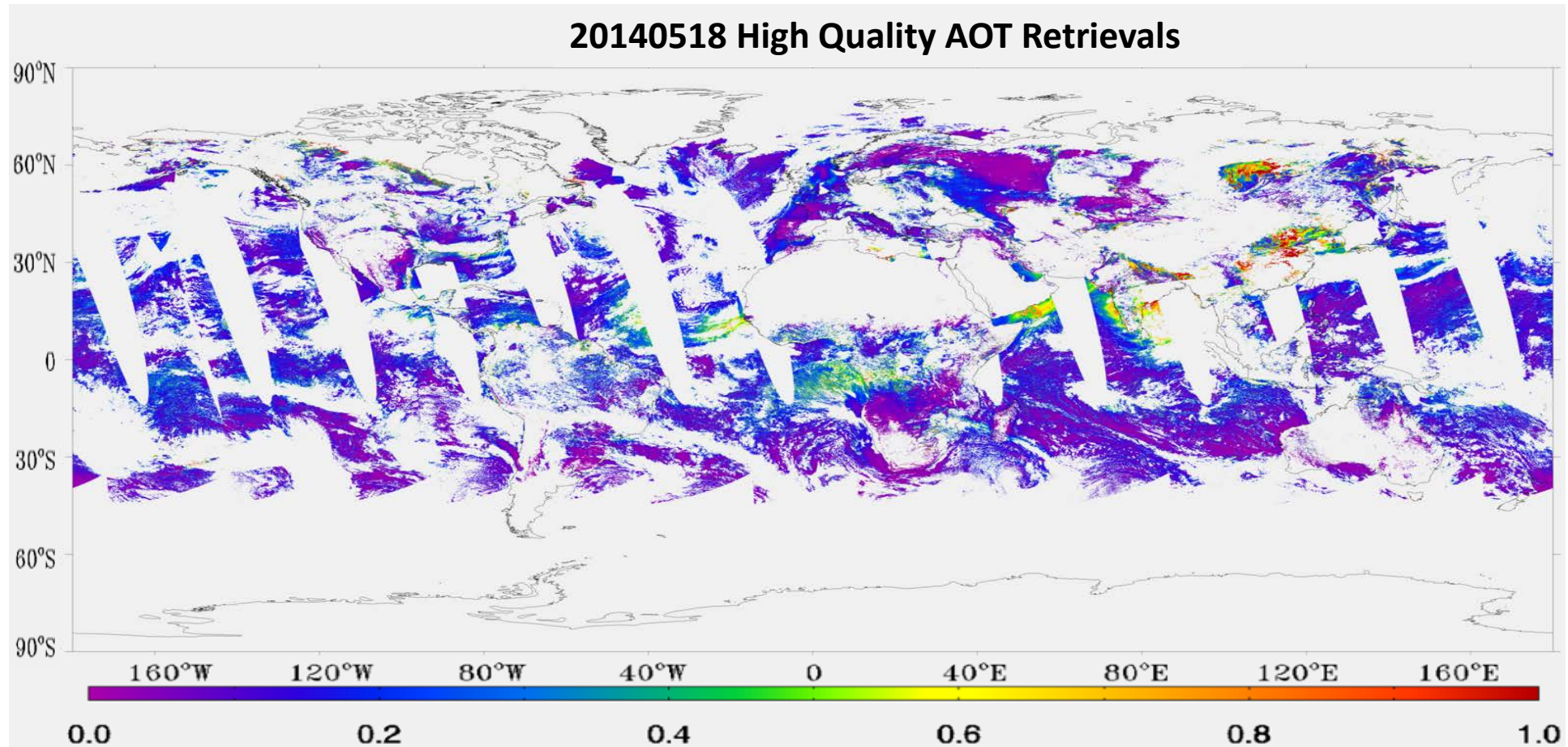


**IDPS VIIRS 'Good' quality AOT retrievals on
May 19, 2015**

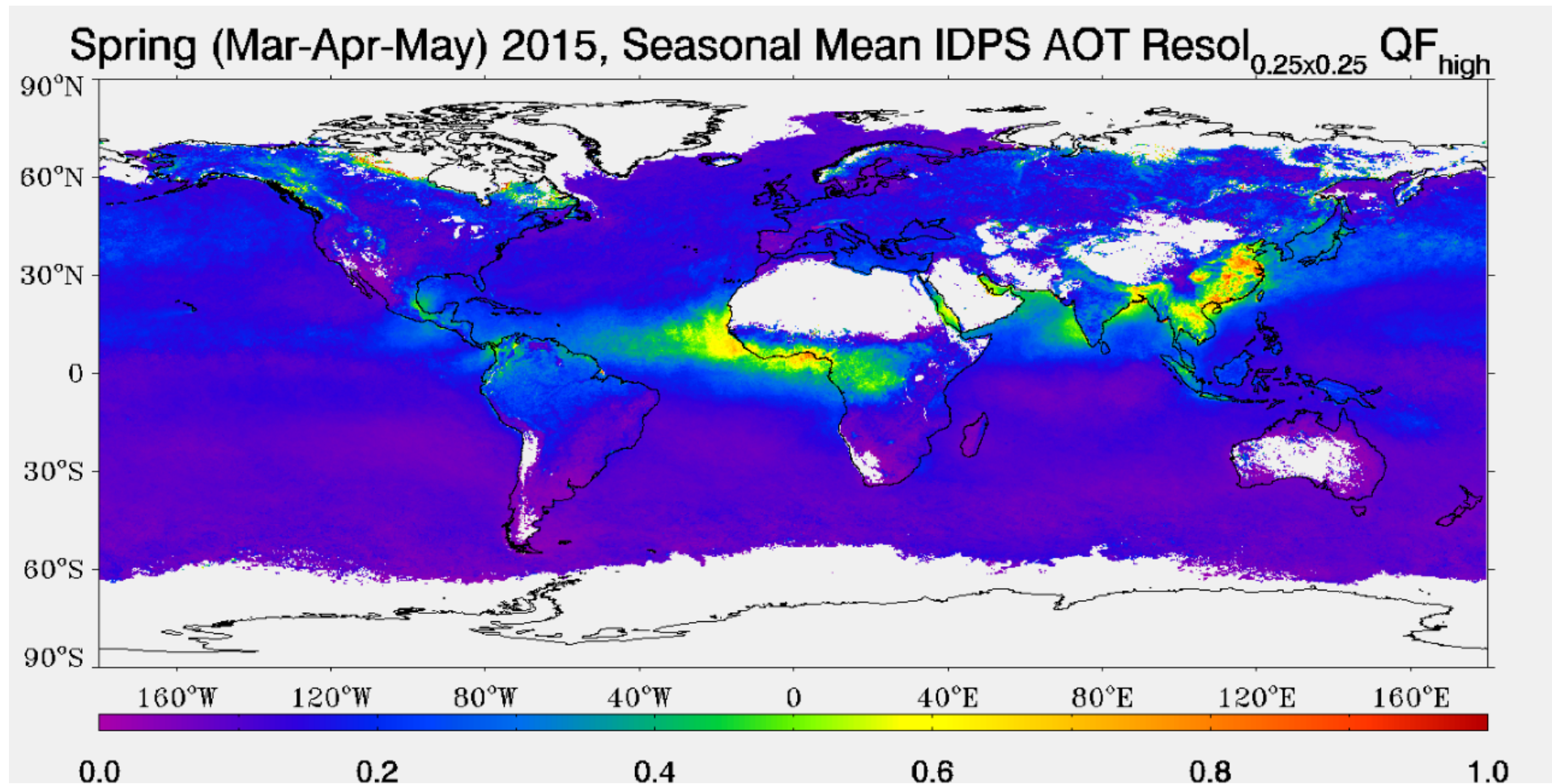


the snow cover map produced by NOAA National Centers for Environmental Information (NCEI)
(<https://www.ncdc.noaa.gov/snow-and-ice/snow-cover/us/20150519>).

Problem: Snow/Snowmelt Underscreening (Global, Daily)



Problem: Snow/Snowmelt Underscreening (Global, Seasonal)

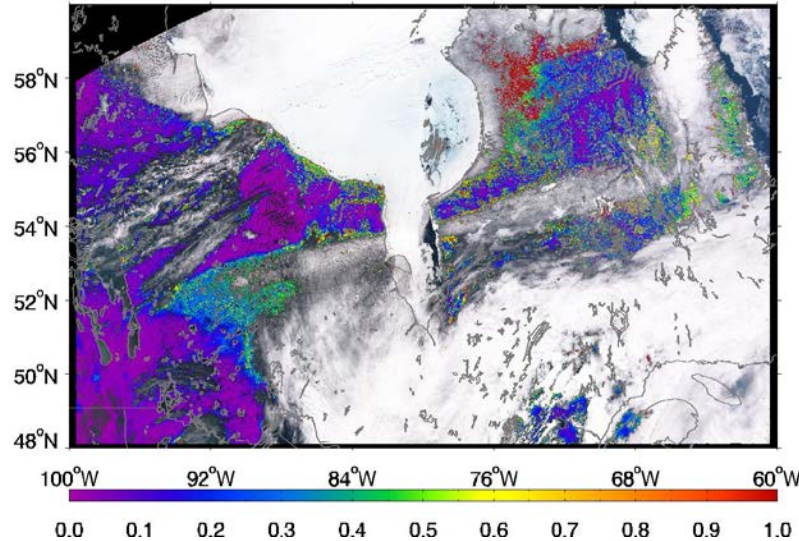


New NDSI and BT11 based Snow Test

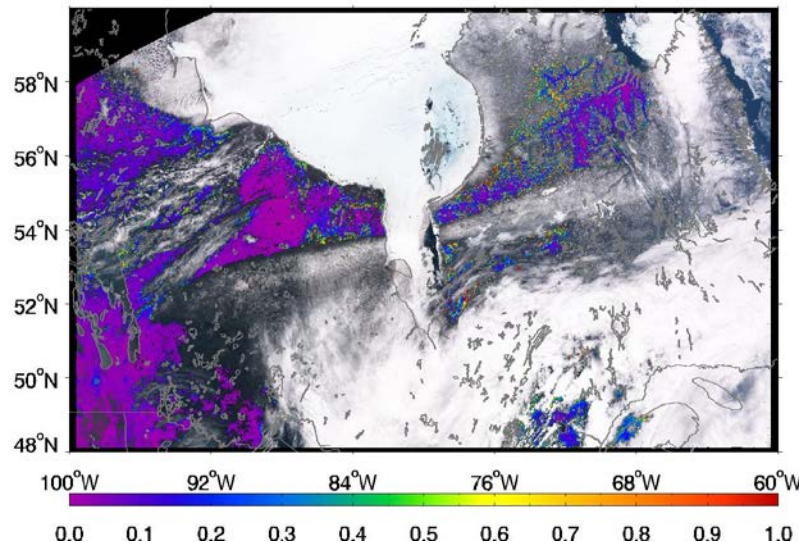
Tests	Old VRA Based Test	New NDSI Based Snow Test	Snow Adjacency Test	Spatial Filter
Criteria	<ol style="list-style-type: none"> 1. $VRA > 0.02$; 2. $rM8/rM7 < 0.9$; 3. Surface Temperature (ST) $< 278\text{ K}$ 	<ol style="list-style-type: none"> 1. $NDSI > C$; 2. $BT_{10.76\text{ }\mu\text{m}} < 285\text{ K}$ 	If any of 7x7 surrounding pixels is snow	If the standard deviation of 3x3 M1 is higher than 0.05
Quality	Not Produced	Not Produced	Degraded to Medium	Degraded to Medium
Notes	<ol style="list-style-type: none"> 1. $VRA = crM3 - 0.5 * crM5$; 2. ST derived from $BT_{10.76\text{ }\mu\text{m}}$ and $BT_{12.01\text{ }\mu\text{m}}$ 	<ol style="list-style-type: none"> 1. $NDSI = (rM7 - rM8) / (rM7 + rM8)$; 2. $C = 0.01$ for IDPS; 3. $C = 0.10$ for EPS 	Check high quality AOT retrievals at central pixel only	Check high quality AOT retrievals at central pixel only

Better Snow/Snowmelt Screening

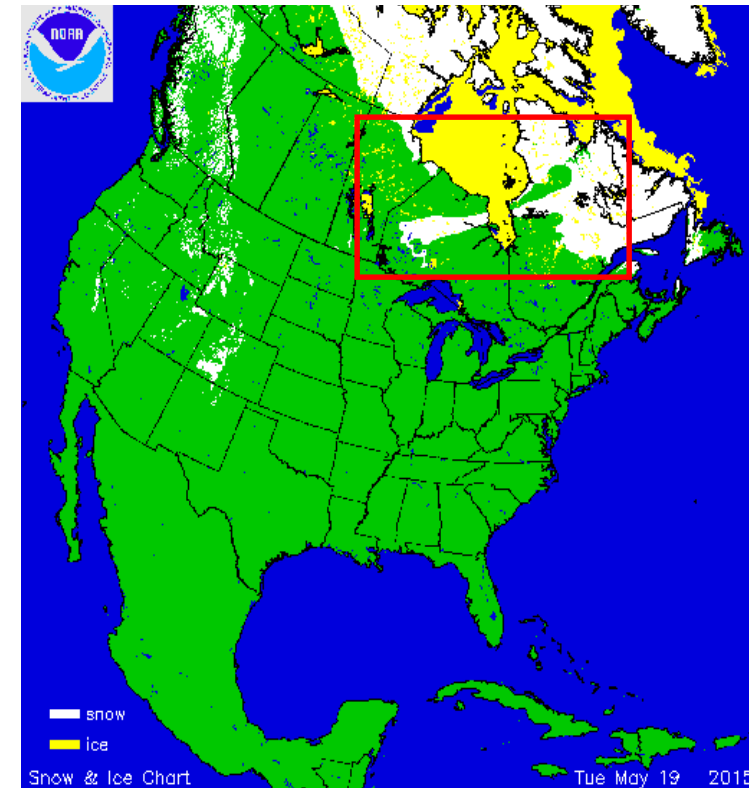
Aerosol Optical Depth at 550nm (Good Quality)



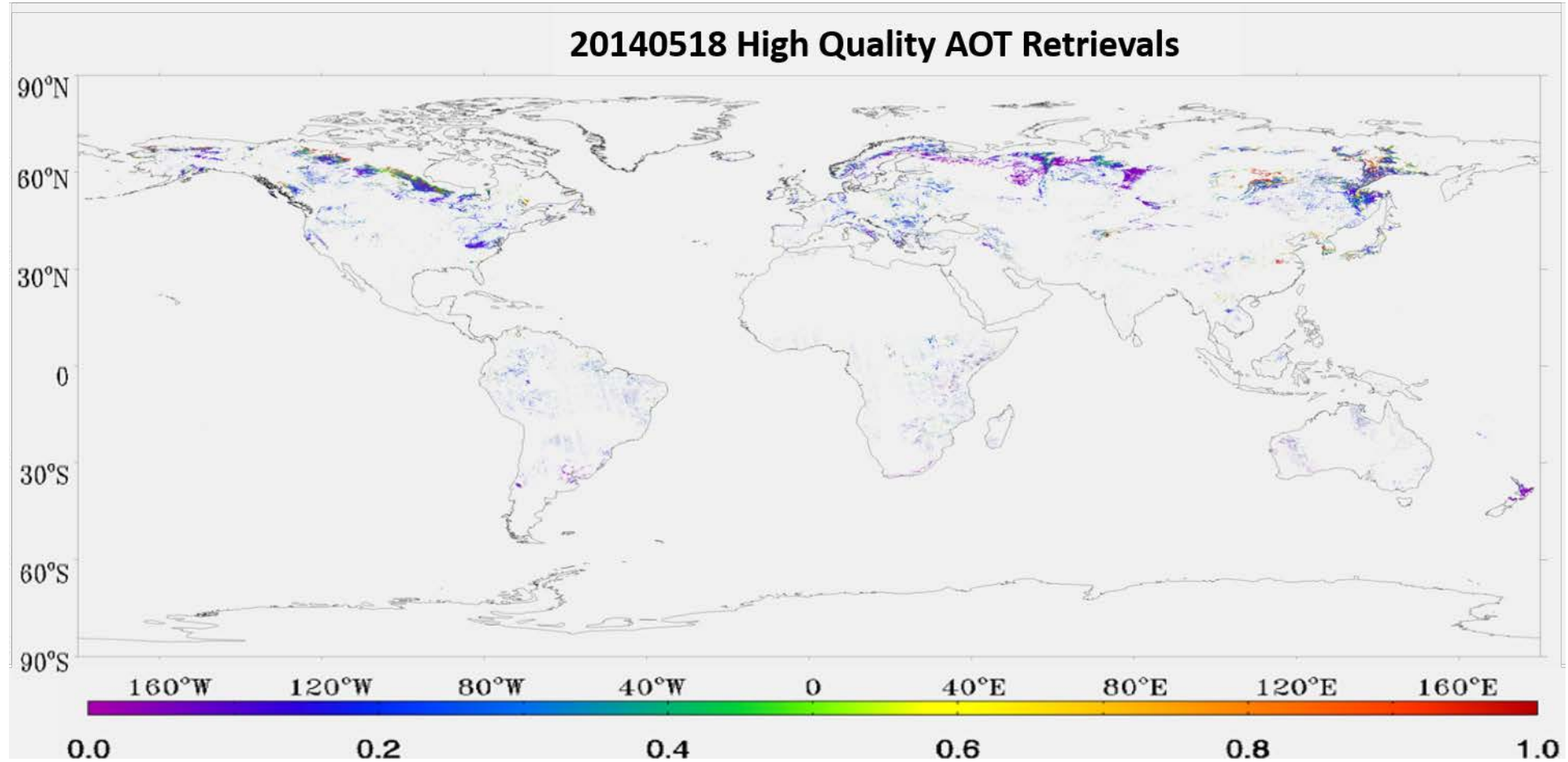
Aerosol Optical Depth at 550nm (Good Quality)



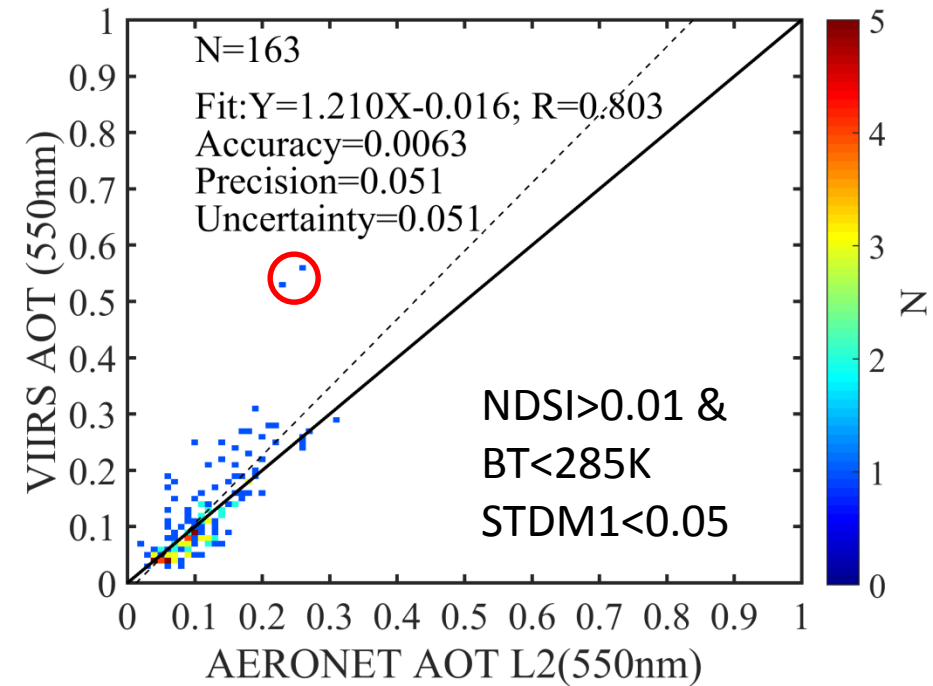
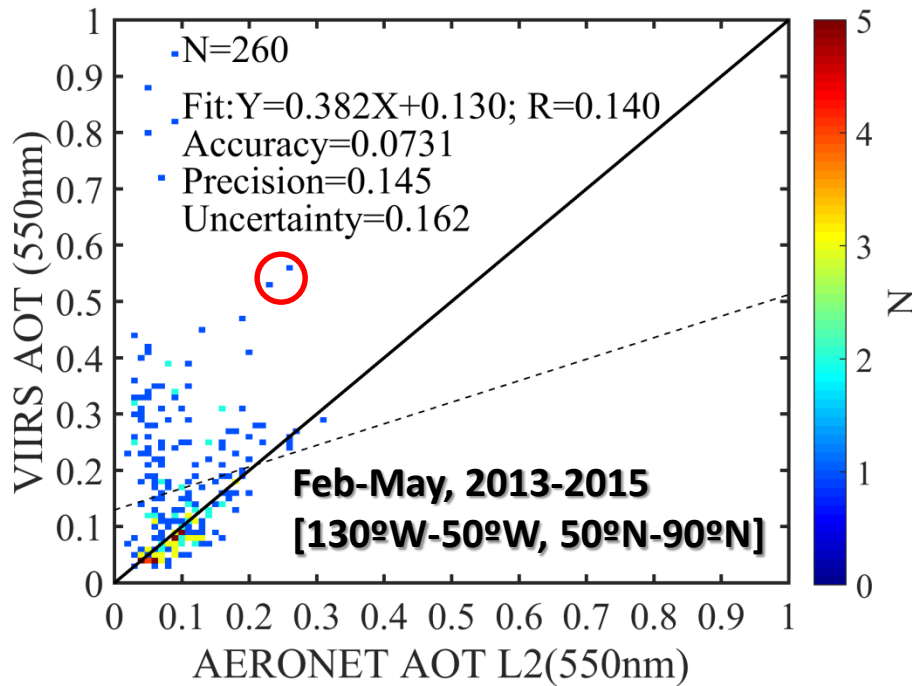
'Good' quality AOT retrievals on May 19, 2015



Better Snow Screening



Better Snow/Snowmelt Screening



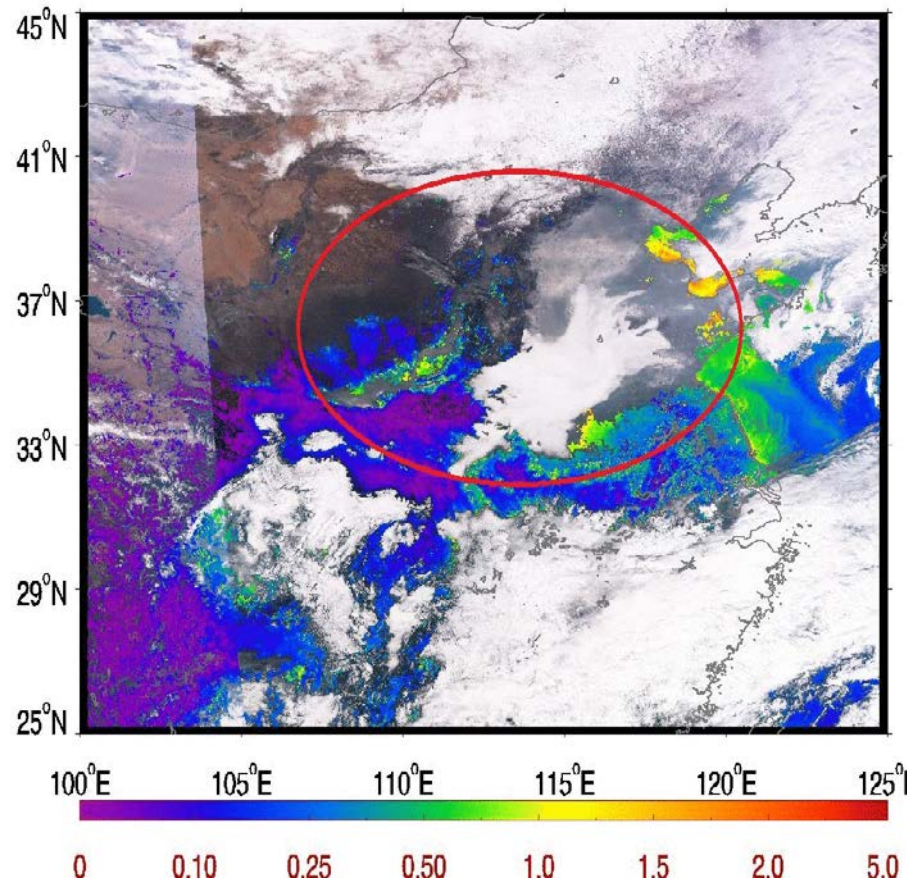
	N	Snow	SnowAdj	SpaFil	N'
Case1	260	43	94	0	163

PART 2:

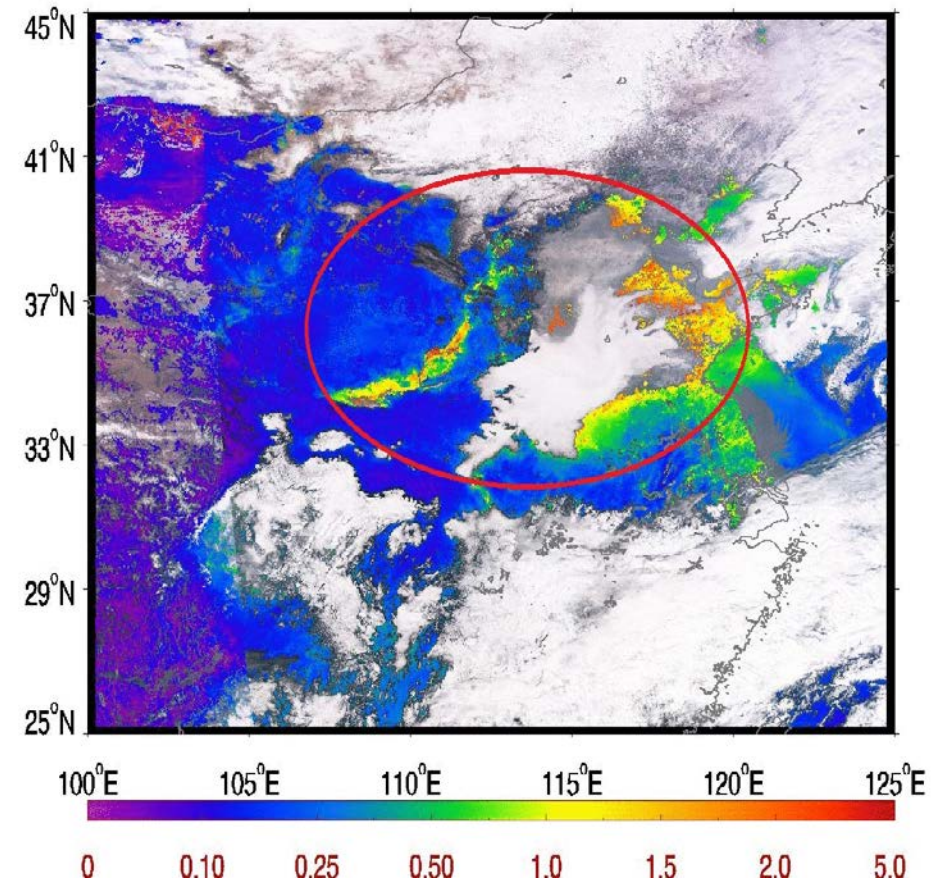
THE MISSING CHINA SMOG AOT RETRIEVALS IN THE IDPS VIIRS AOT PRODUCT

IDPS vs. EPS: Best Quality AOT Animation

IP Aerosol Optical Depth at 550nm (High Quality), 20151129



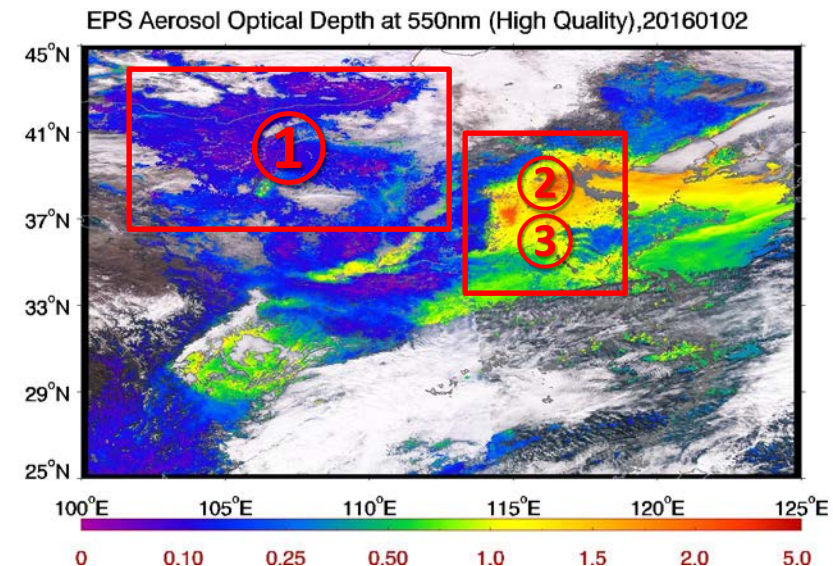
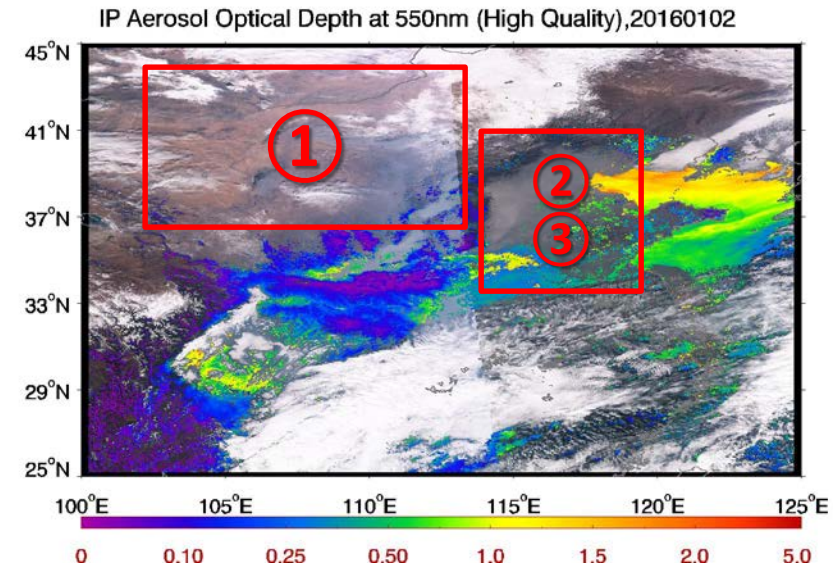
EPS Aerosol Optical Depth at 550nm (High Quality), 20151129



① IDPS only has dark surface retrieval over land; EPS has both dark and bright surface retrievals over land.

② IDPS had AOT retrieval up to 2.0; EPS had AOT retrieval higher than 2.0 and up to 5.0

③ Main Focus: IDPS missed heavy smog AOT retrievals; EPS regained these retrievals.



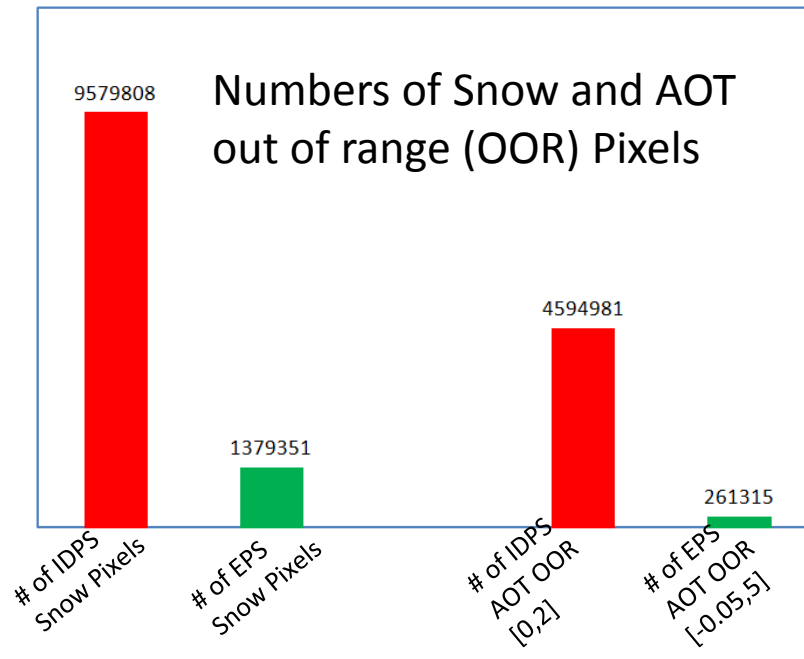
Why did IDPS miss the smog AOT retrievals?

Data Collection:

- ✓ 13 smog events ([25-45N, 100-125E], Winter 2015-2016)
- ✓ IDPS AOT with QF not produced or excluded
- ✓ EPS AOT (Best Quality) > 0.5
- ✓ 448881 Pixels In Total

Statistical Results:

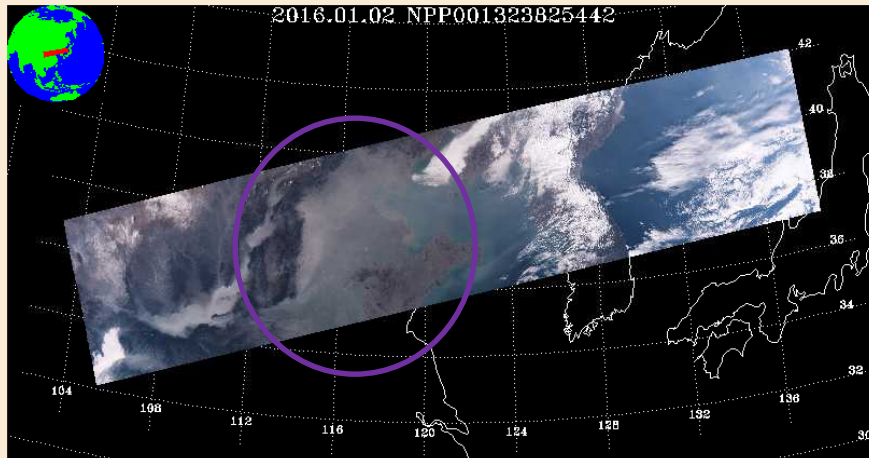
- ✓ **49.7% had smog mis-identified as snow**
- ✓ **43.7% had IDPS AOT retrievals out of range [0.0, 2.0]**



- Internal Snow Over Screening and AOT Out Of Range (OOR) were identified as the Top Two factors that prevented IDPS best quality AOT retrievals over smog pixels;
 - EPS /IDPS Snow Pixels: 14.4%
 - EPS/IDPS AOT OOR pixels: 5.7%
- (Note: EPS has larger AOT range than IDPS)

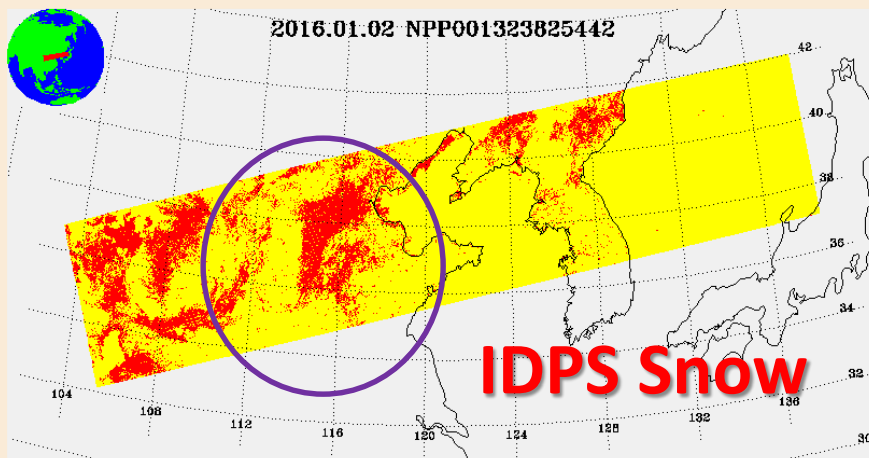
IDPS vs. EPS: Internal Snow Test

RGB Image [R=M5 (672 nm), G=M4 (555 nm), B=M3 (488 nm)]



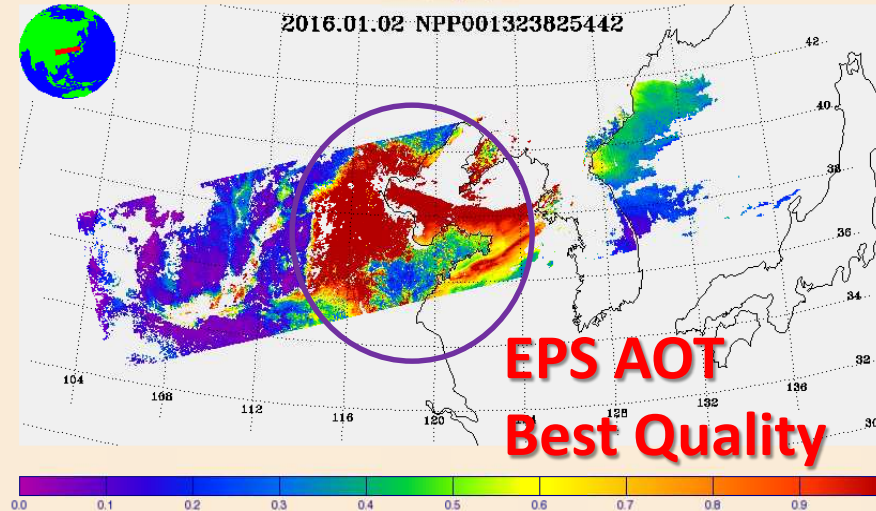
VAOT_npp_d20160102_t0455425_e0457066_b21662_c20160524141400638713_noaa_ops.h5

IP Snow/Ice

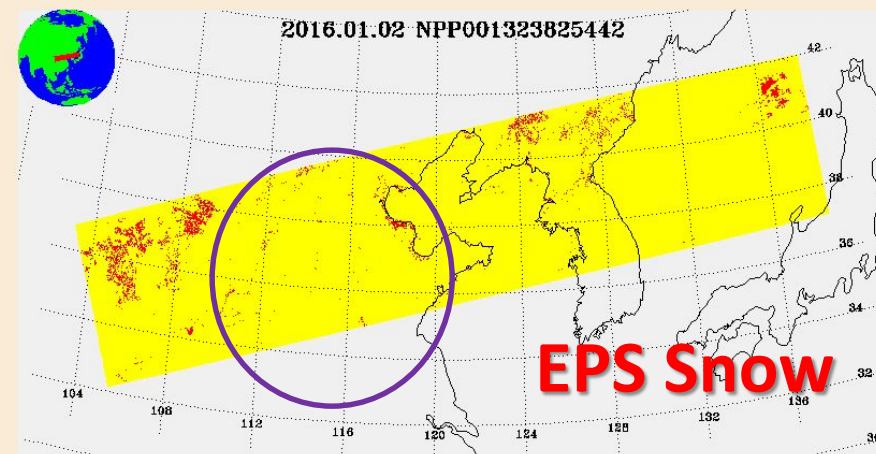


2016002_t0455425.h5

AOT at 550nm
Overall Quality Flag=High



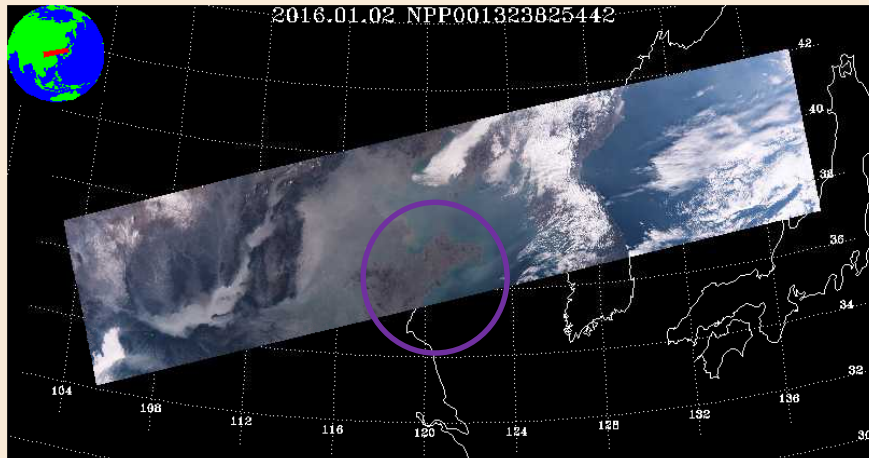
SnowIce (Internal Test)



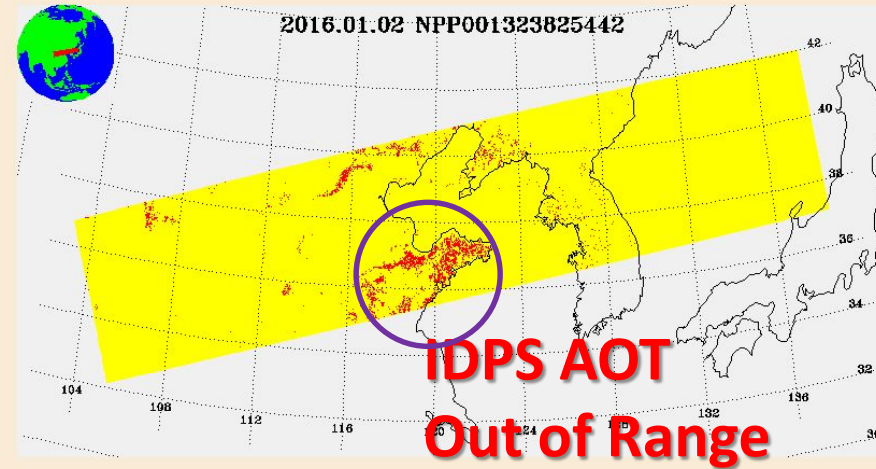
IDPS vs. EPS: AOT Out Of Range (OOR)

IVAOT_npp_d20160102_t0455425_e0457066_b21662_c20160524141400638713_noaa_ops.h5

RGB Image [R=M5 (672 nm), G=M4 (555 nm), B=M3 (488 nm)]

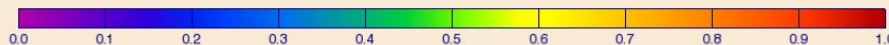
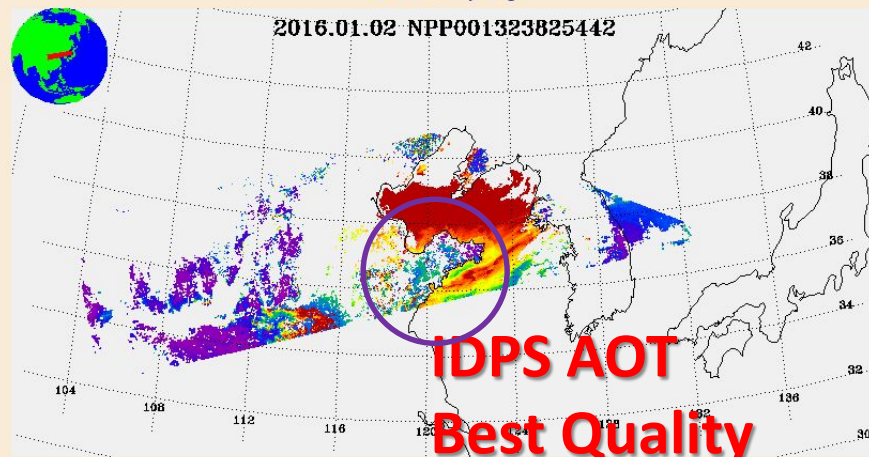


IP AOT Out of Spec Range

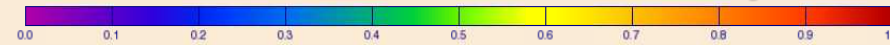
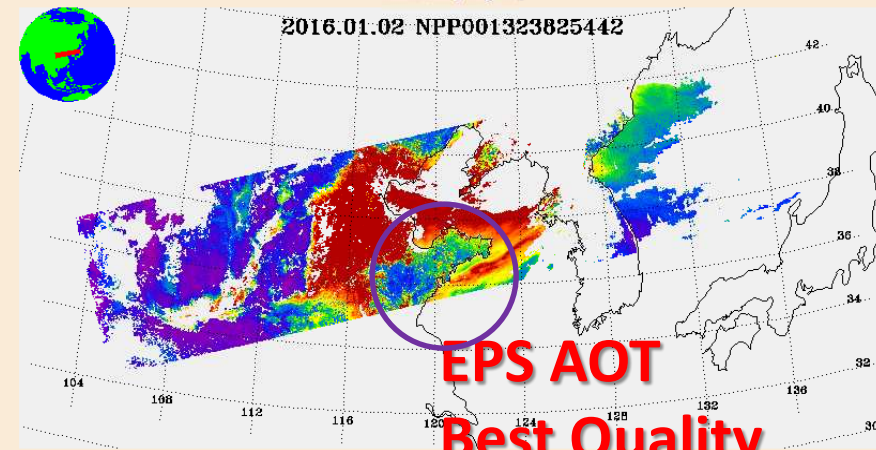


IVAOT_npp_d20160102_t0455425_e0457066_b21662_c20160524141400638713_noaa_ops.h5

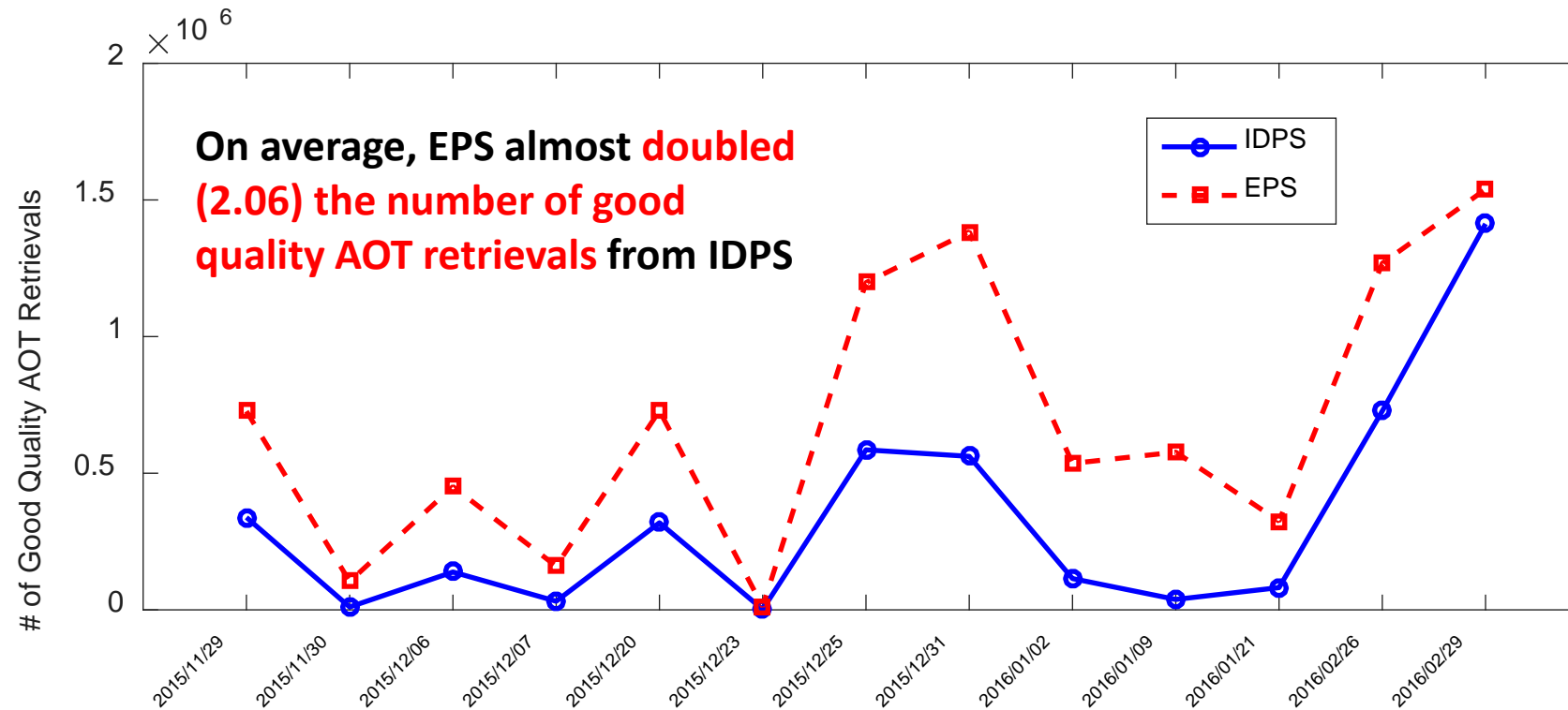
Aerosol Optical Thickness (IP) at 550nm
IP AOT Quality=High



AOT at 550nm
Overall Quality Flag=High

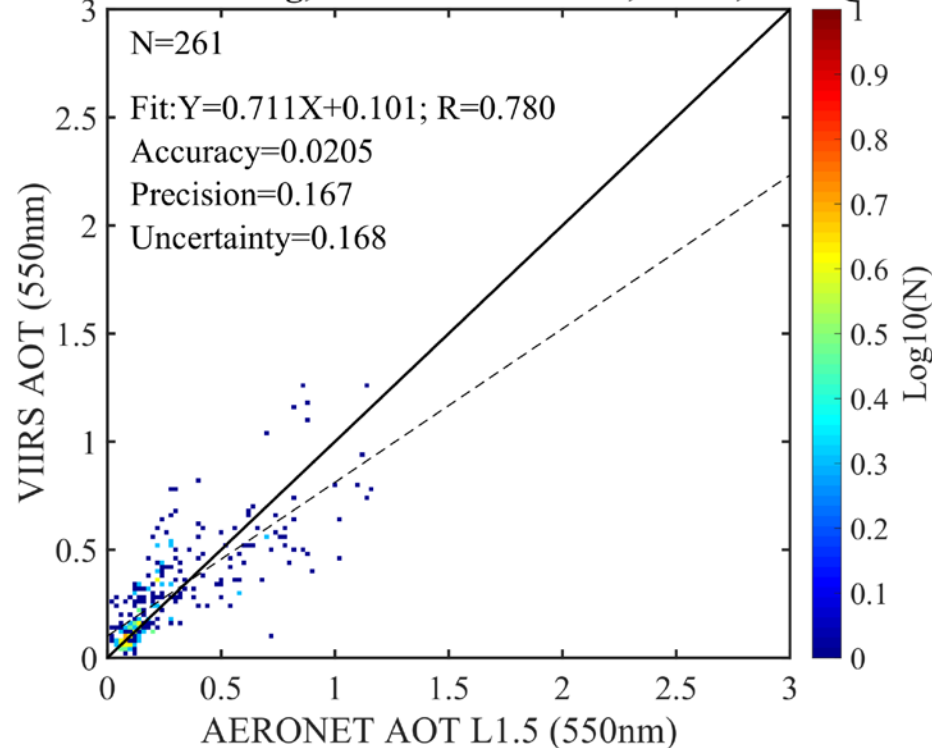


IDPS vs. EPS: Number of Good Quality AOT



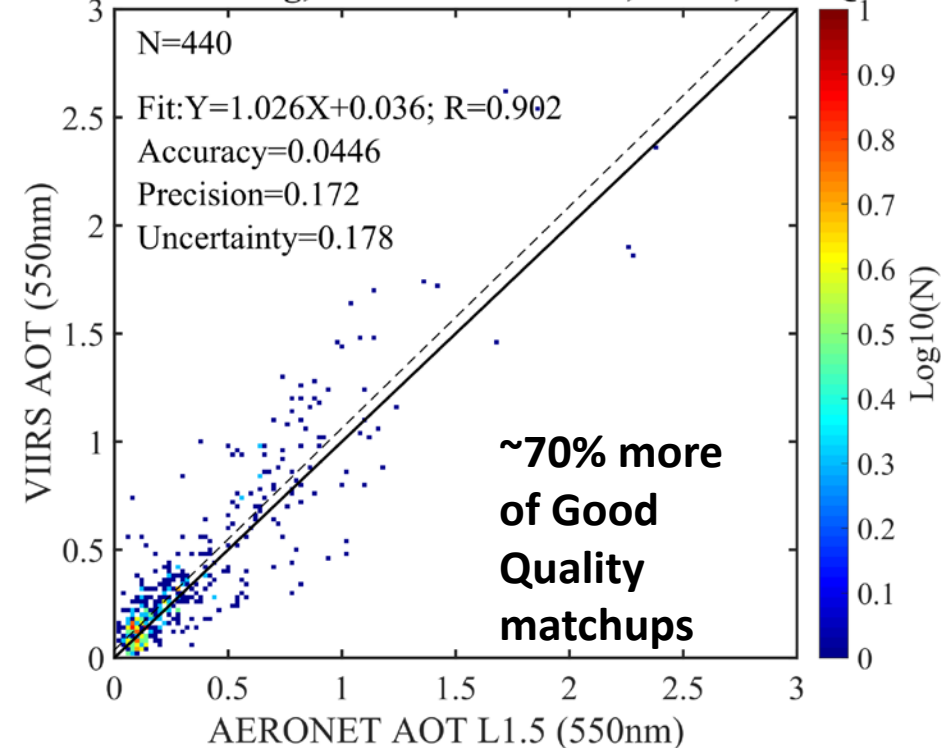
IDPS vs. EPS: Comparison to AERONET

IDPS: China Smog, 2015 Nov-2016 Feb, M2M, Best QA



IDPS vs. AERONET L1.5

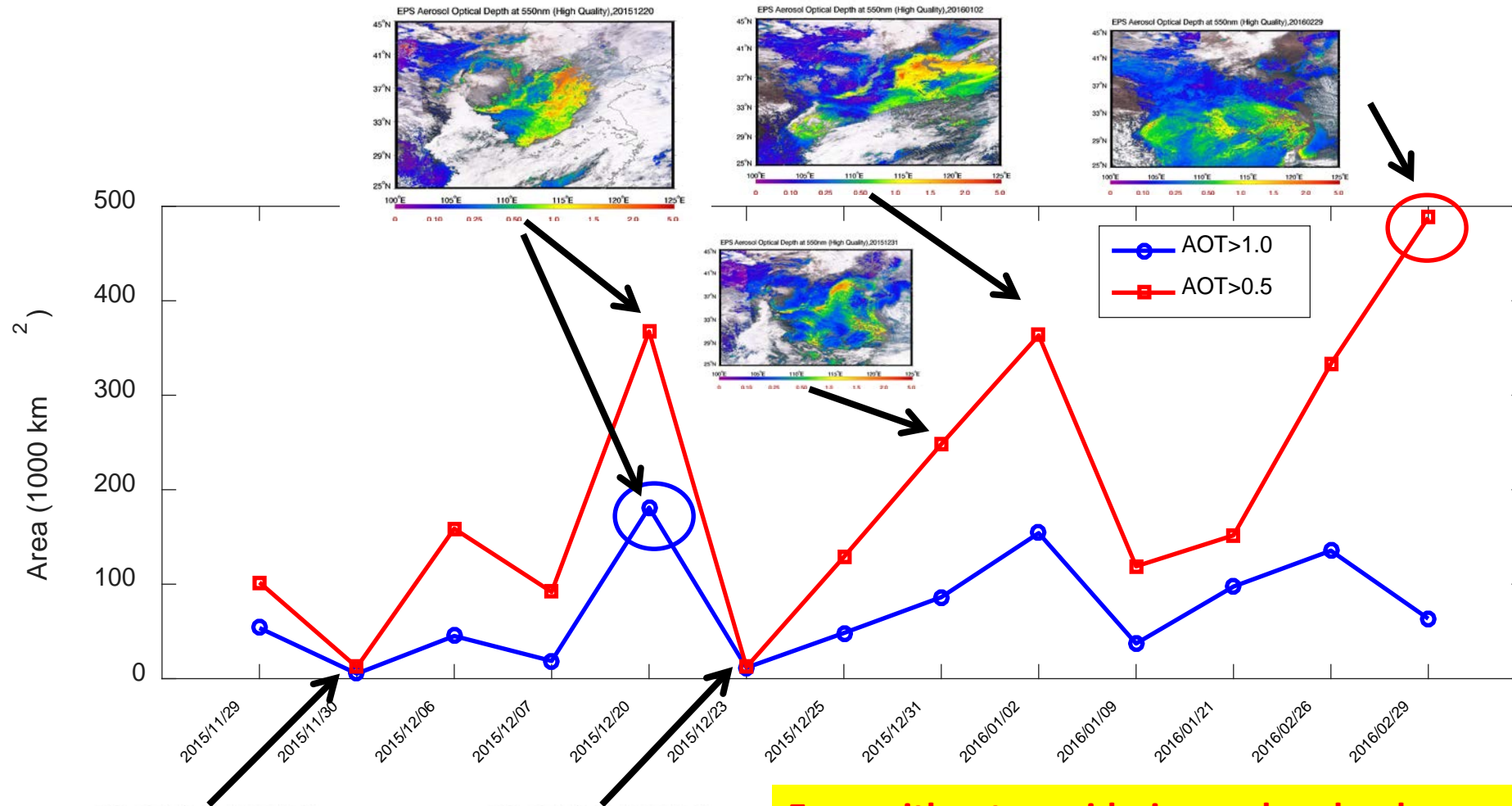
EPS: China Smog, 2015 Nov-2016 Feb, M2M, Best QA



EPS vs. AERONET L1.5

In the matchup with AERONET L1.5, EPS VIIRS Aerosol Algorithm increased best quality AOT matchups by ~70% more than IDPS

EPS evaluated Smog Spatial Coverage



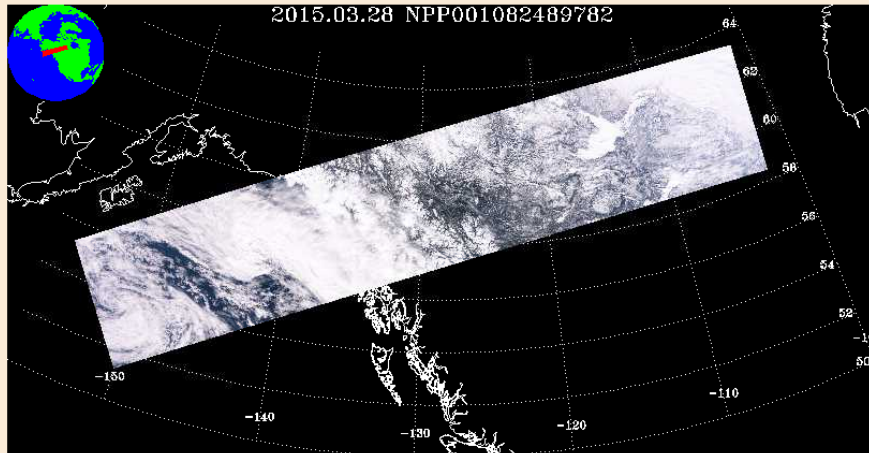
Even without considering under-cloud smog:

- AOT > 1.0: can be as large as 200,000 km²
- AOT > 0.5: can be as large as 500,000 km²

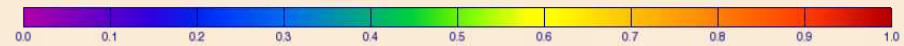
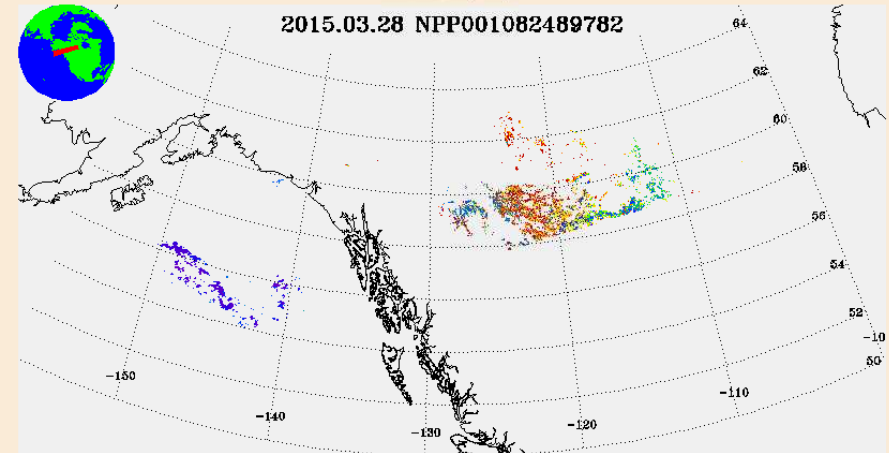
Fine Tuned Spatial Filter in EPS

IVAOT_npp_d20150328_t2109372_e2111014_b17699_c20150328230603123444_noaa_ops.h5

RGB Image [R=M5 (672 nm), G=M4 (555 nm), B=M3 (488 nm)]

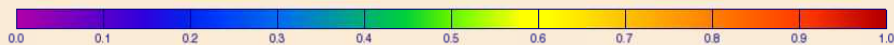
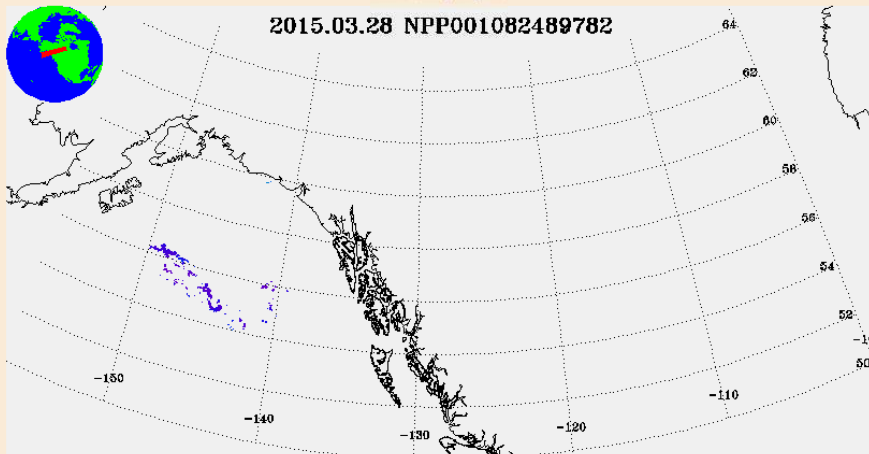


Aerosol Optical Thickness (IP) at 550nm
IP AOT Quality=High



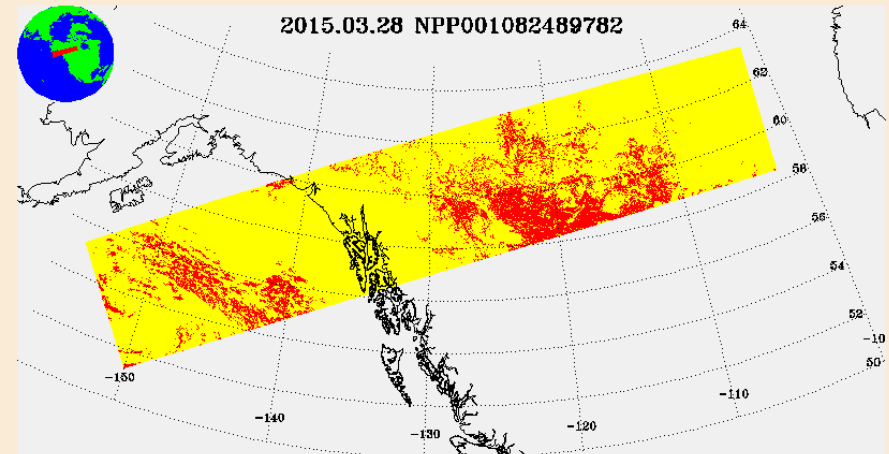
2015087_t2109372.h5

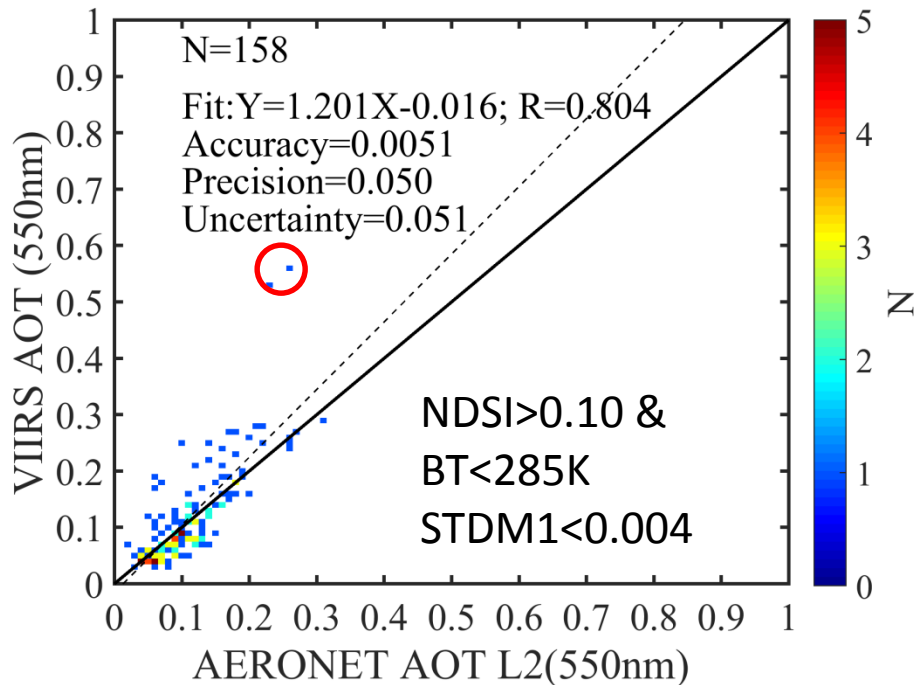
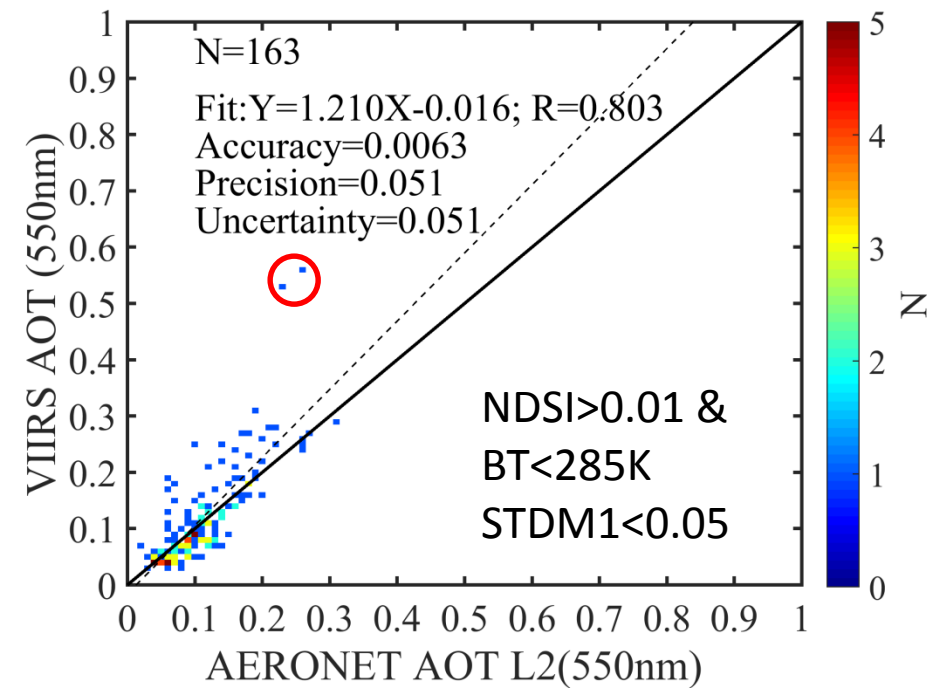
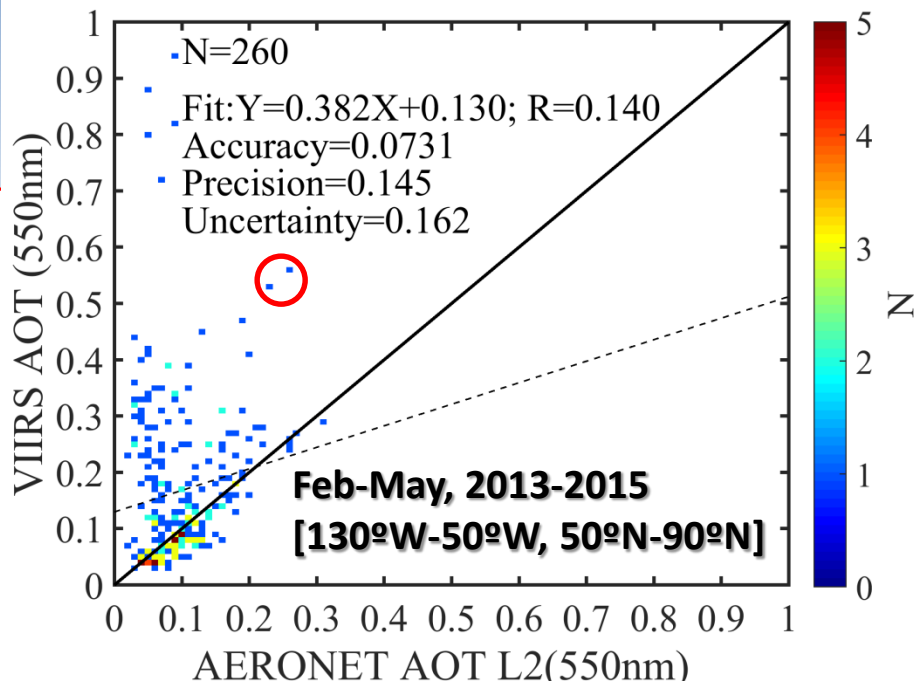
AOT at 550nm
Overall Quality Flag=High



2015087_t2109372.h5

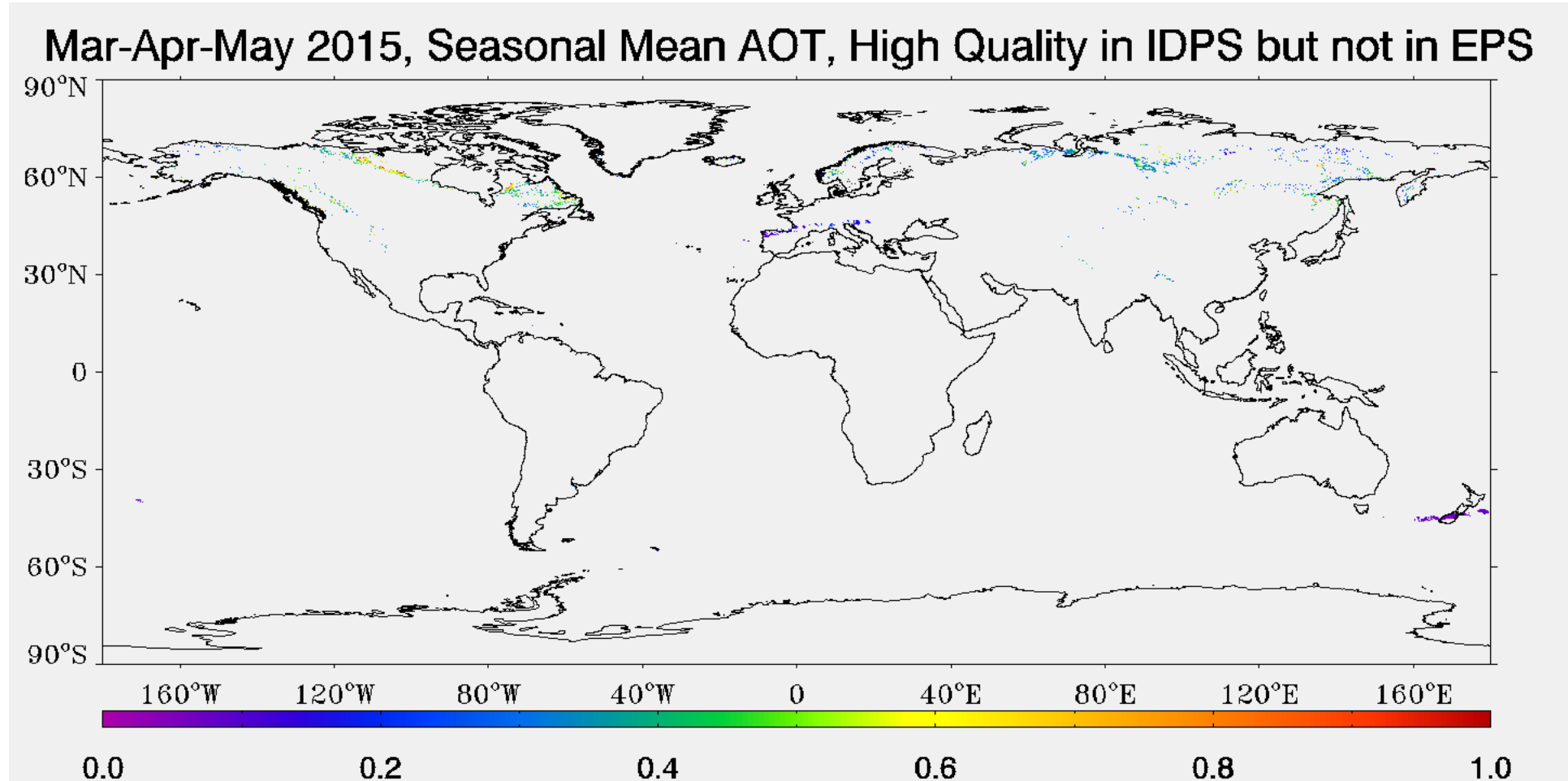
Inhomogeneity (Internal Test)





	Initial N	Snow	SnowAdj	SpaFil	New N
IDPS Thresholds	260	43	94	0	163
EPS Thresholds	260	30	94	81	158

IDPS vs. EPS: Boreal Spring AOT



- The NDSI and BT11 based snow test, combining with the complement snow adjacency test and spatial filter, improves the snow/snowmelt screening in the IDPS VIIRS aerosol products;
- However, AOT retrievals in heavy China Smog events were found missing in the IDPS aerosol product;
- The main reason for the missing smog AOT retrievals is snow over screening, followed by AOT out of range;
- The snow test and spatial filter were fine tuned to regain the missing China Smog AOT retrievals and to keep the same level of snow/snowmelt screening;
- With the new tests, EPS VIIRS Aerosol Algorithm has much more smog AOT retrievals than IDPS; and with more retrievals, EPS AOT also demonstrated better correlation with AERONET than IDPS; and yet, the high biases in the snow/snowmelt region remain screened.
- The EPS VIIRS aerosol algorithm will replace the IDPS algorithm and become operational in 2017



A New Dust Dataset from the IMPROVE Ground Network

Daniel Tong, Julian Wang, Hang Lei and Barry Baker
NOAA Air Resources Laboratory, College Park, MD

Thomas Gill
University of Texas at El Paso, TX

Binyu Wang
George Mason University, Fairfax, VA

(JPSS Science Meeting 2017, College Park, MD)



The “Dust Bowl” During the Great Depression (1930s)



- ◆ **Dust Bowl:** A period of severe dust storms during the 1930s;
- ◆ **Causes:** Extended droughts and poor land management;
 - ✓ **Homestead Acts:** settlement over the Plains for agriculture ;
 - ✓ **“Rain follows the plow”:** unusually wet climate;
 - ✓ **New agricultural machinery:** Deep plowing, eliminating native grass;
 - ✓ **Favorable dust storm conditions during 1930s drought;**





The “Dust Bowl”



Impacts:

- ✓ Stripped 75% of top soils over thousands of farms;
- ✓ Destroyed agriculture and ecosystem (~1950s);
- ✓ > 500,000 lost homes and communities;

"And then the dispossessed were drawn west--from Kansas, Oklahoma, Texas, New Mexico; from Nevada and Arkansas, families, tribes, dusted out, tractored out... They streamed over the mountains, hungry and restless--restless as ants, scurrying to find work ... anything, any burden to bear, for food. The kids are hungry. We got no place to live..."

-- John Steinbeck in the Grapes of Wrath



Hundreds of thousands fled the 1930s US Dust Bowl; more drought-spurred migrations are expected.



Another “Dust Bowl”?



- ◆ Central U.S. plains saw severe droughts about once or twice a century over the past 400 years (Woodhouse & Overpeck, 1998).
- ◆ This recurring trend may be enhanced global climate change (Schubert et al., 2004).
- ◆ Global warming → Precipitation shift from subtropics, greater evaporation, less snow/ice, and earlier spring → amplify the effects of natural climatic variations → intensified droughts and “dust-bowlification” (Romm, 2011).

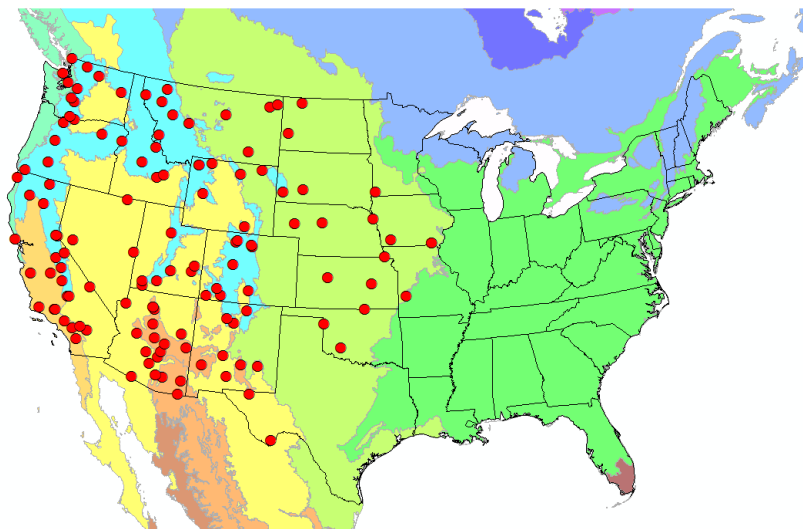
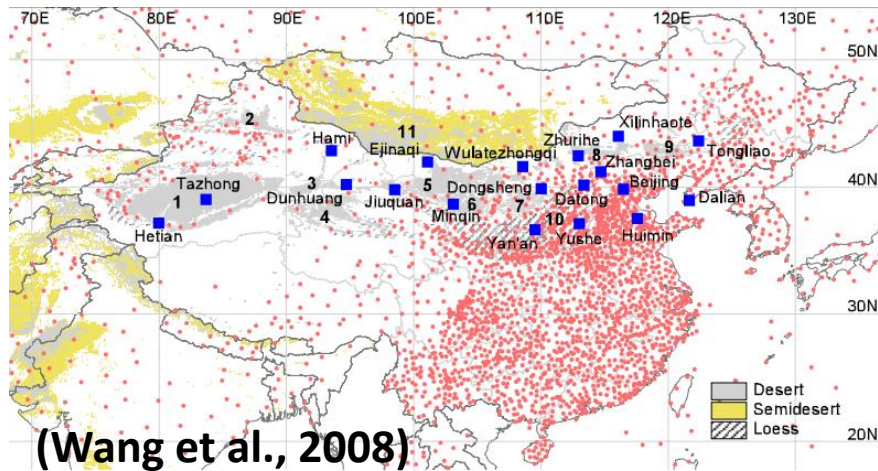
(Source: Romm, 2011)



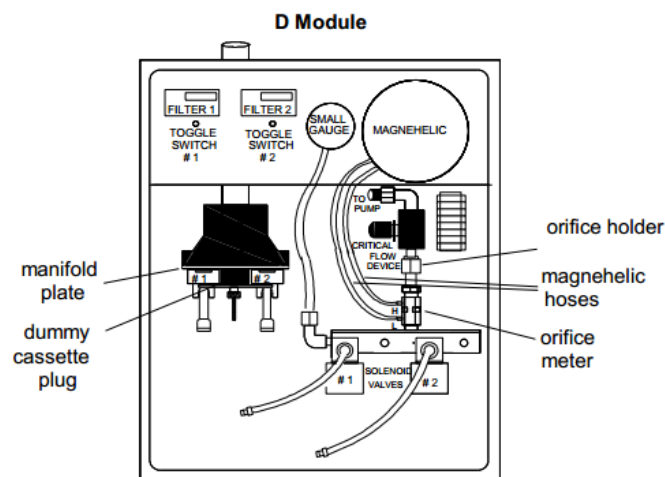
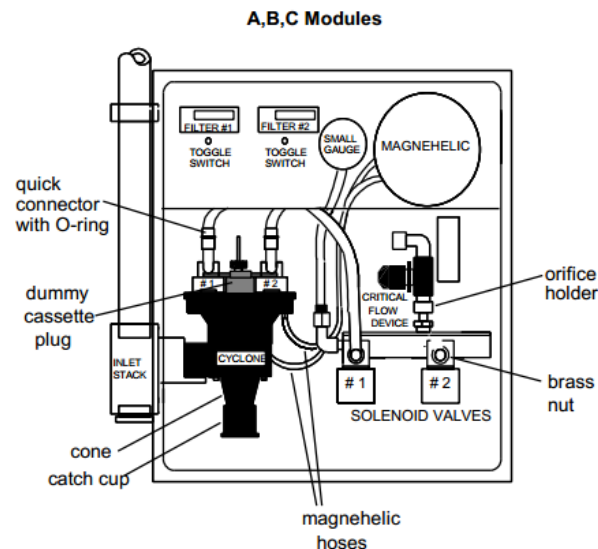
Then and now: sun-baked dry soils kick up clouds of dust in the 1930s (left) and in the modern United States (right).

How to Monitor Dust Storms

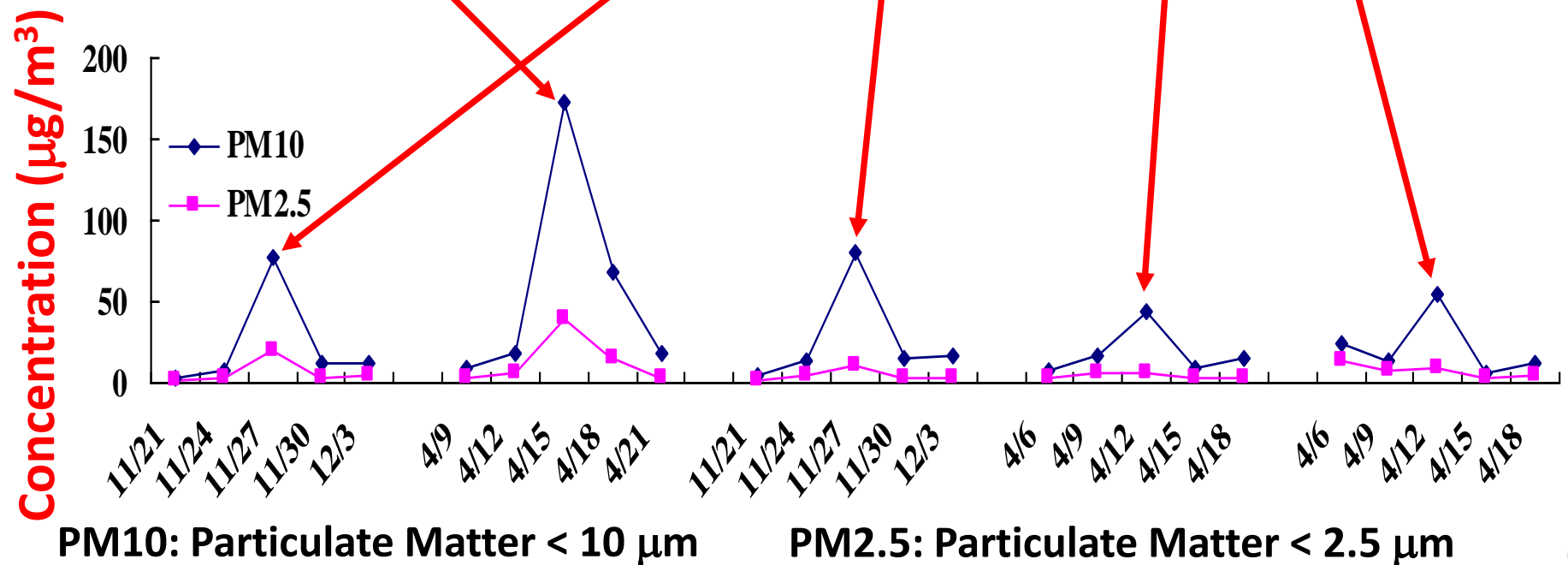
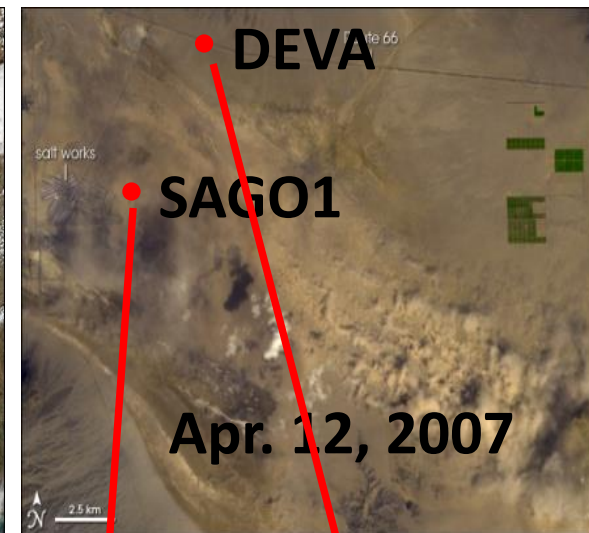
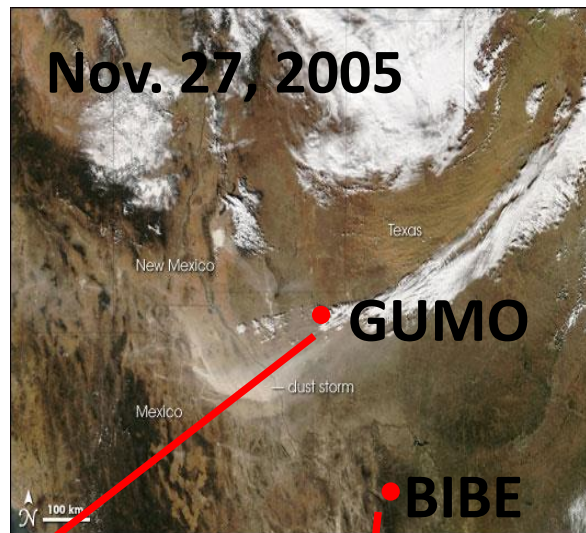
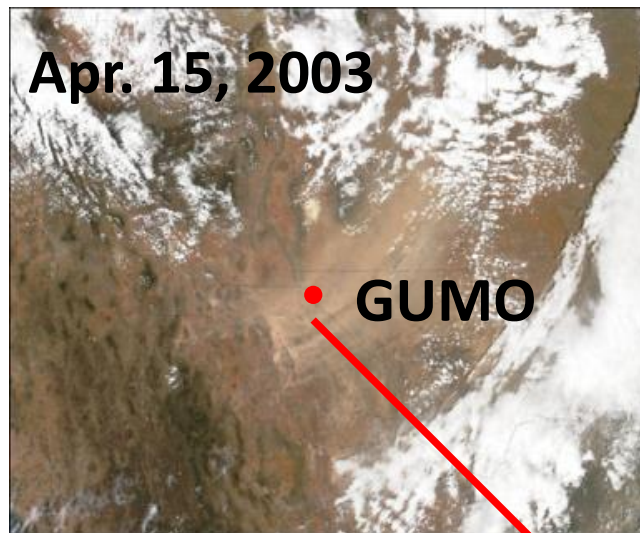
Chinese Sand and Dust Network

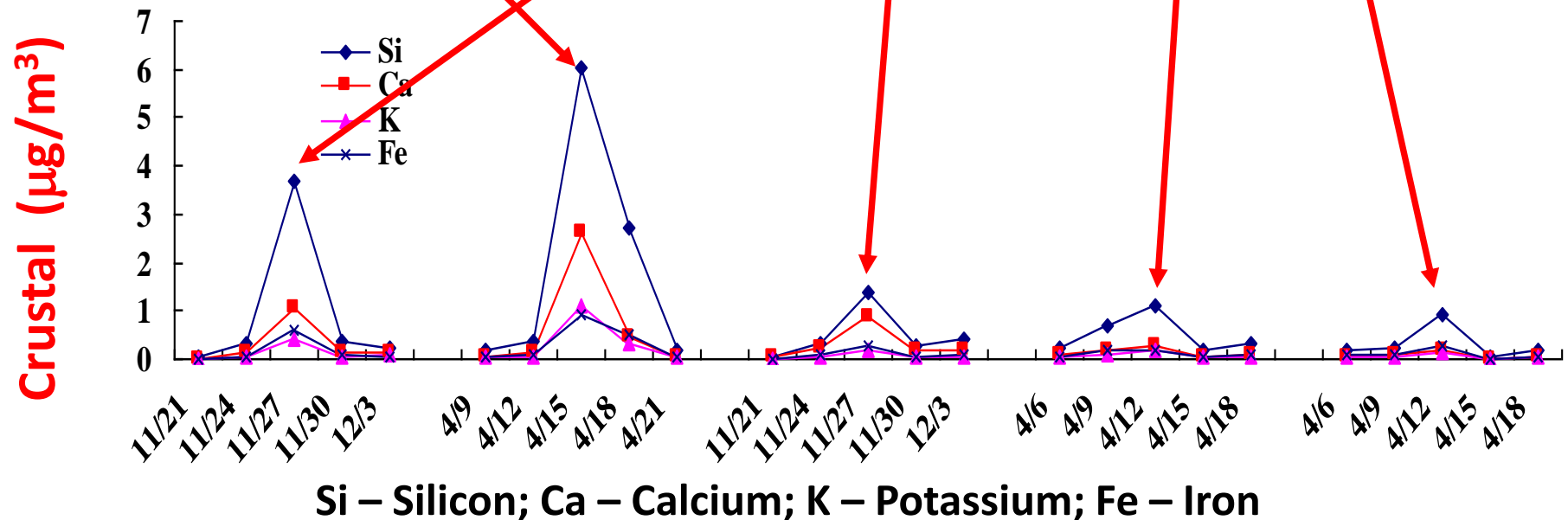
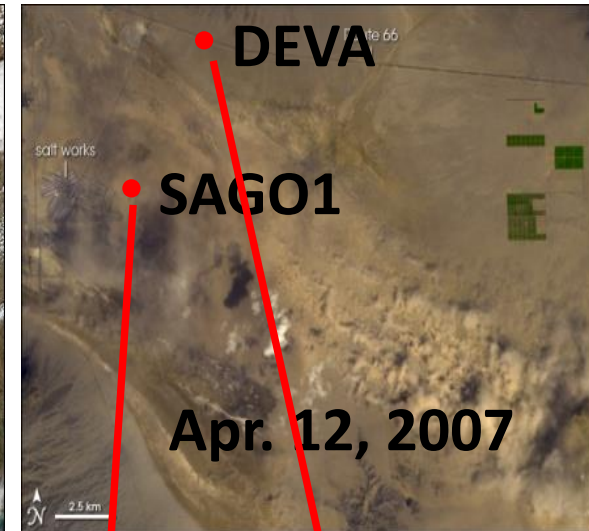
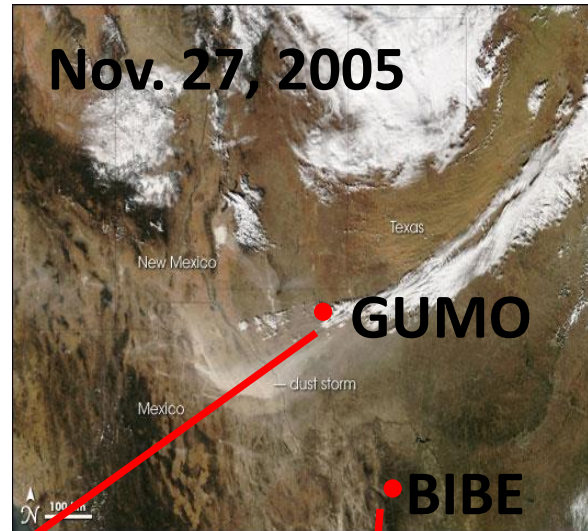
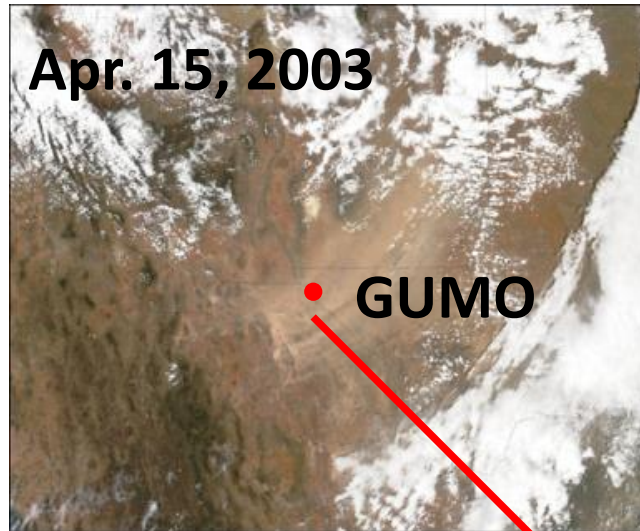


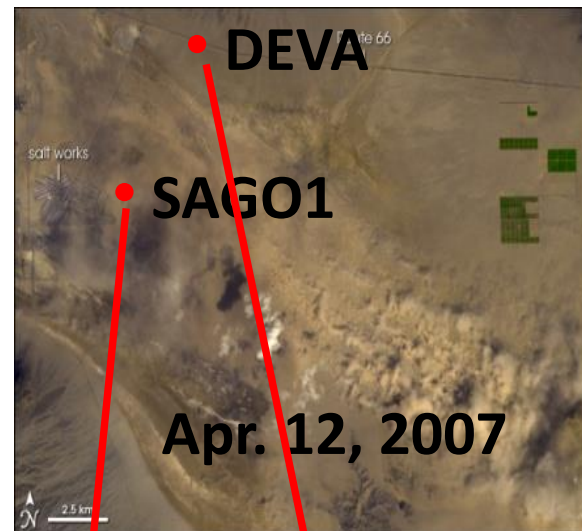
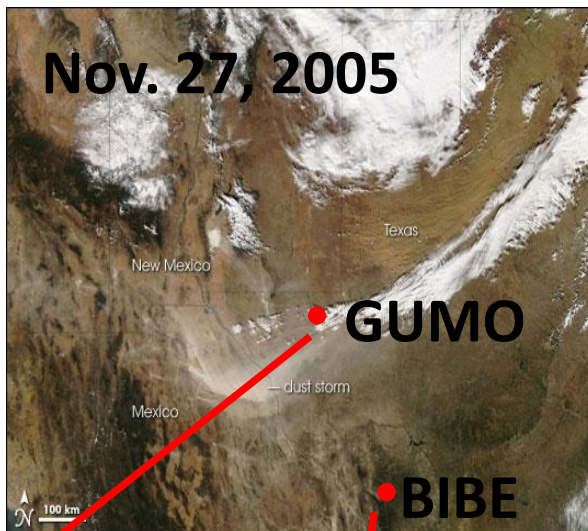
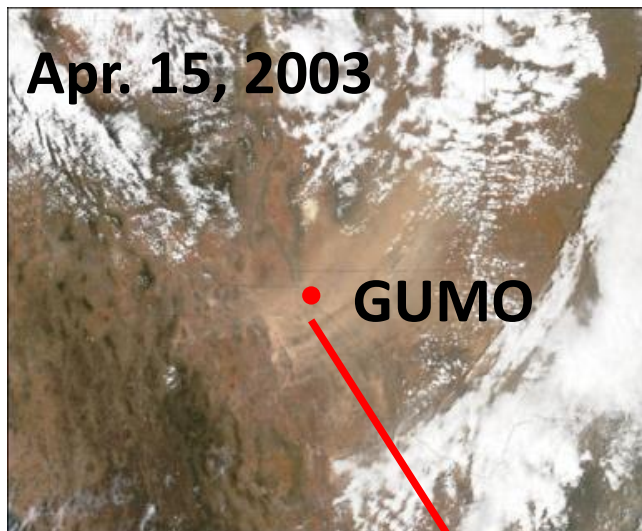
The US Aerosol Network IMPROVE



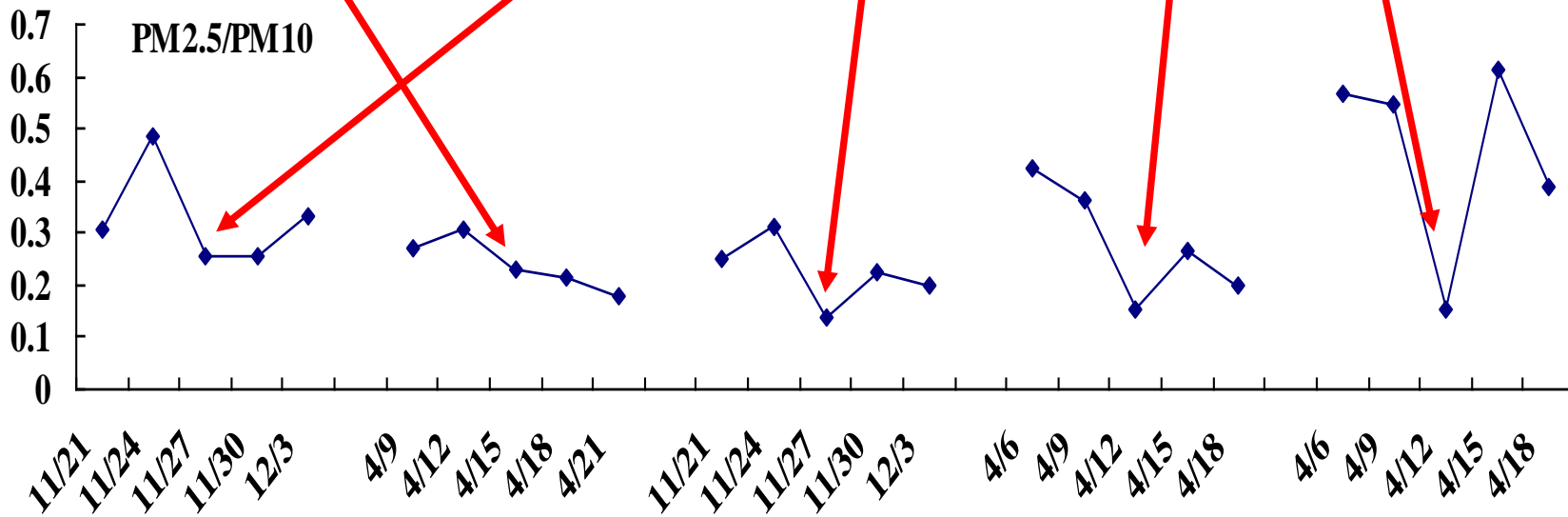
IMPROVE Samplers
Samples Analyzed at UC-Davis







PM25/PM10 Ratio





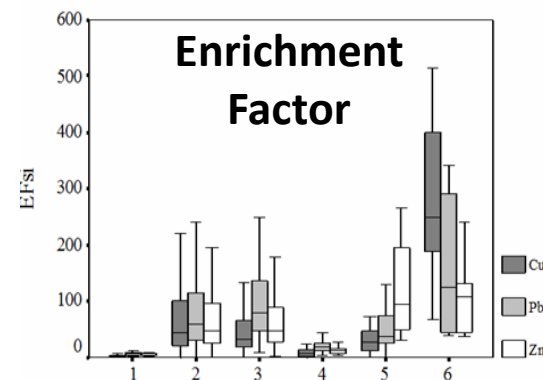
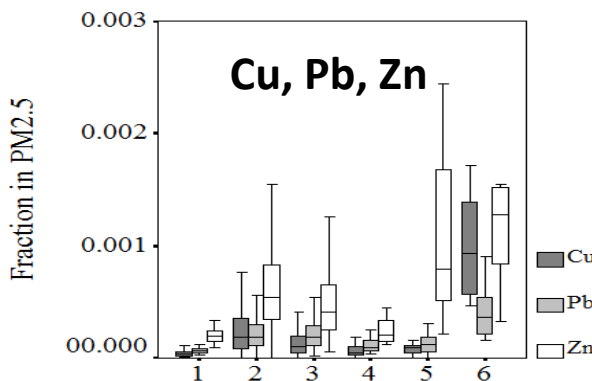
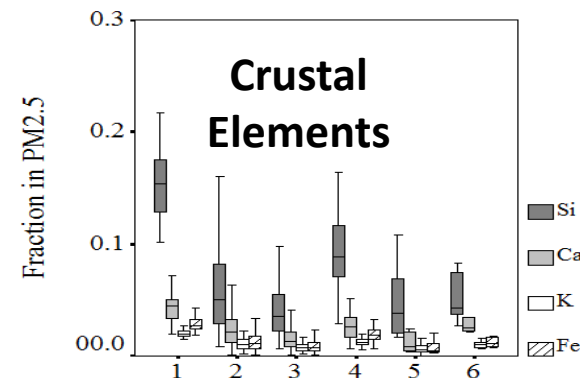
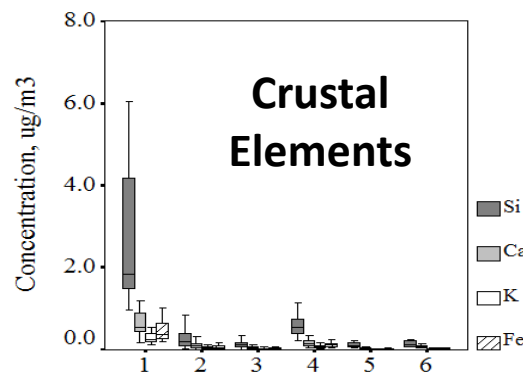
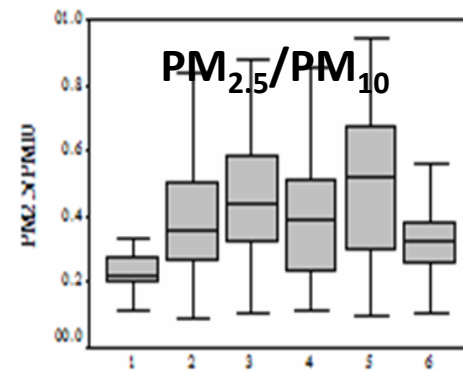
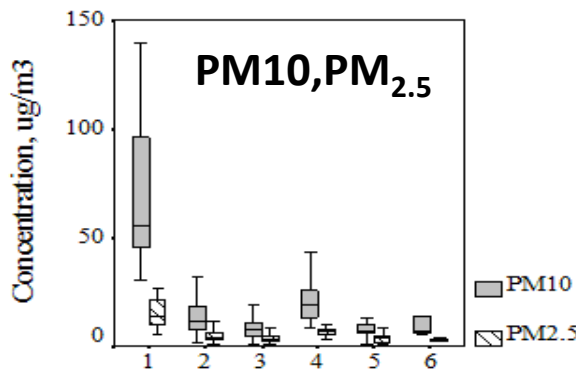
Dust Identification through Cluster Analysis



Five Dust Indicators:

- ❖ High PM_{10} , $PM_{2.5}$;
- ❖ Low $PM_{2.5}/PM_{10}$ ratio
- ❖ High Crustal Fraction
- ❖ Low anthropogenic Fraction;
- ❖ Low Enrichment Factor;

Cu – Copper
Pb – Lead
Zn – Zinc

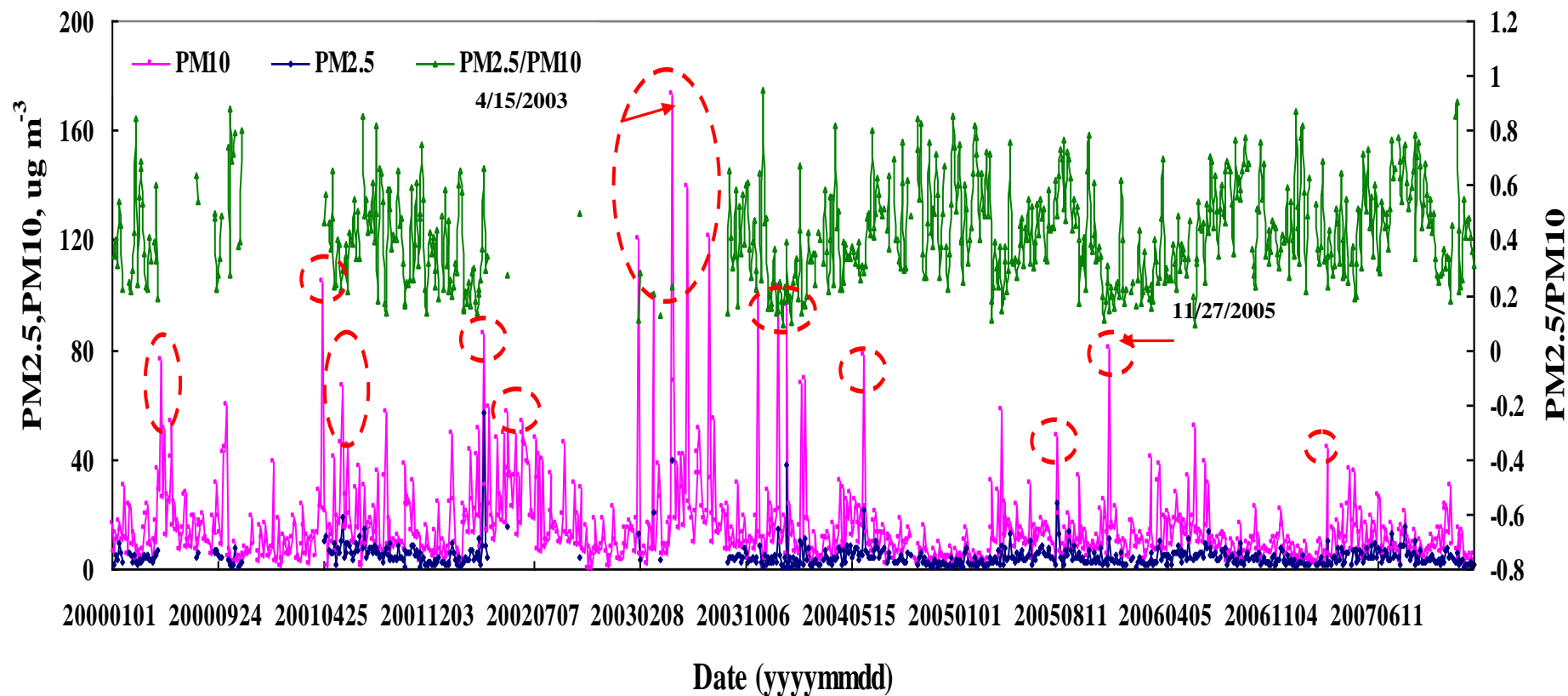




Detecting Dust Storms



Guadalupe Mountains National Park

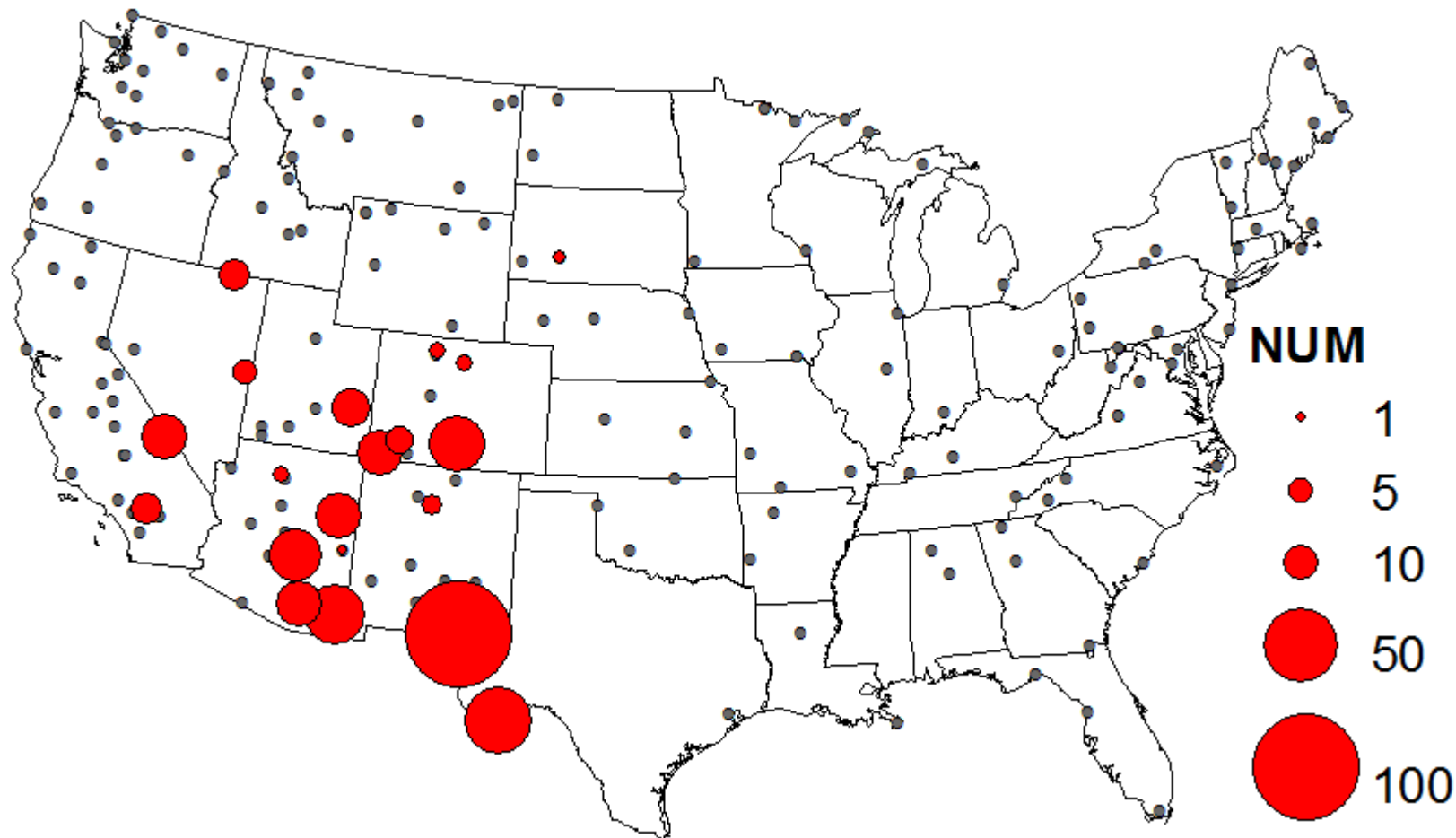


(Source: Mo Dan)

This algorithm, combined with cluster analysis, can pin-point dust.



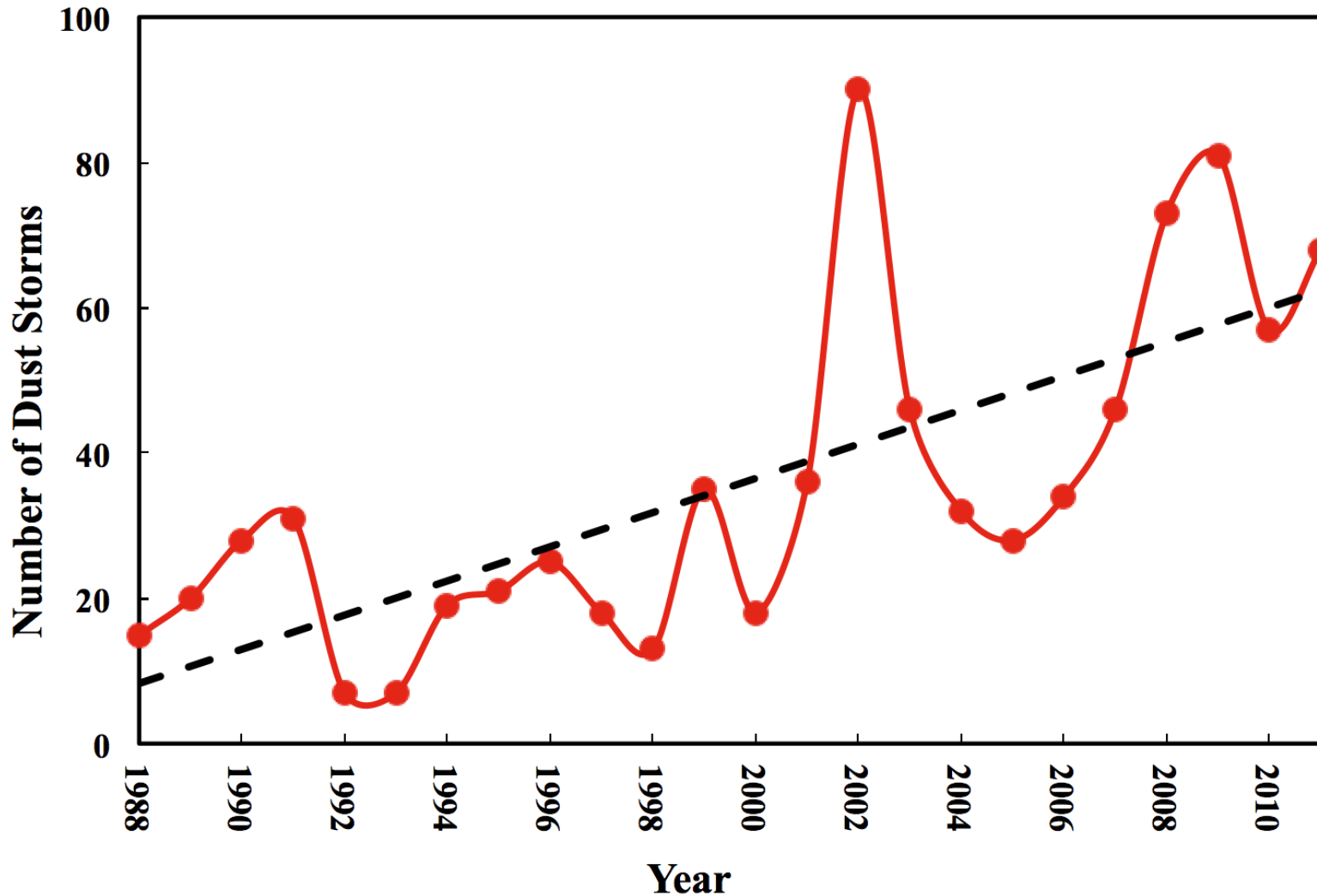
Locations of Dust Storms



Dust storms detected at 29 sites with continuous data records.



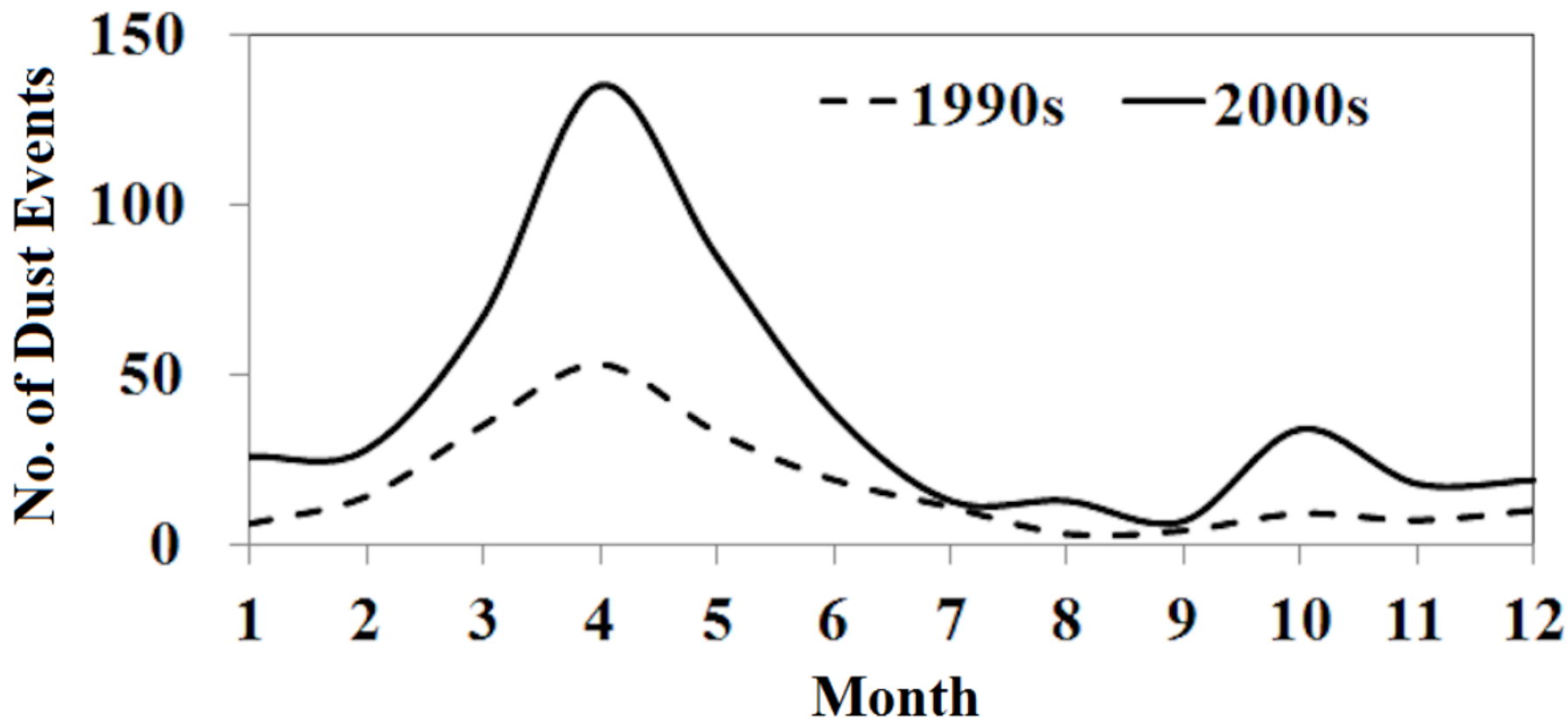
Long-term Dust Trend



20 Giant Storms in 1990s → 48 Storms in 2000s;



Seasonal Variation



Increase in Spring (mostly) and Fall;

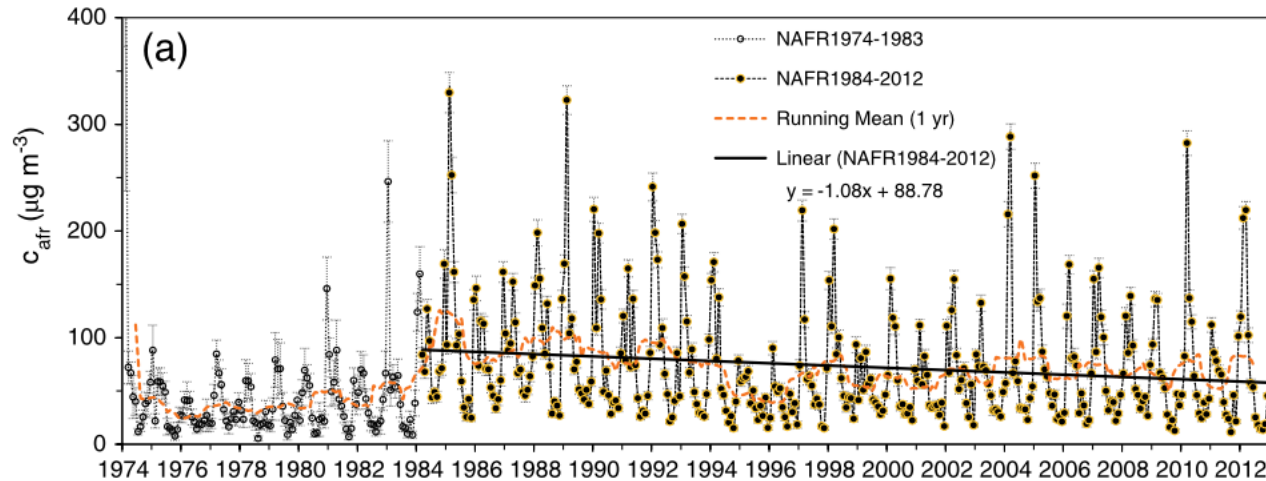
Almost no change in Summer/Wet Season;



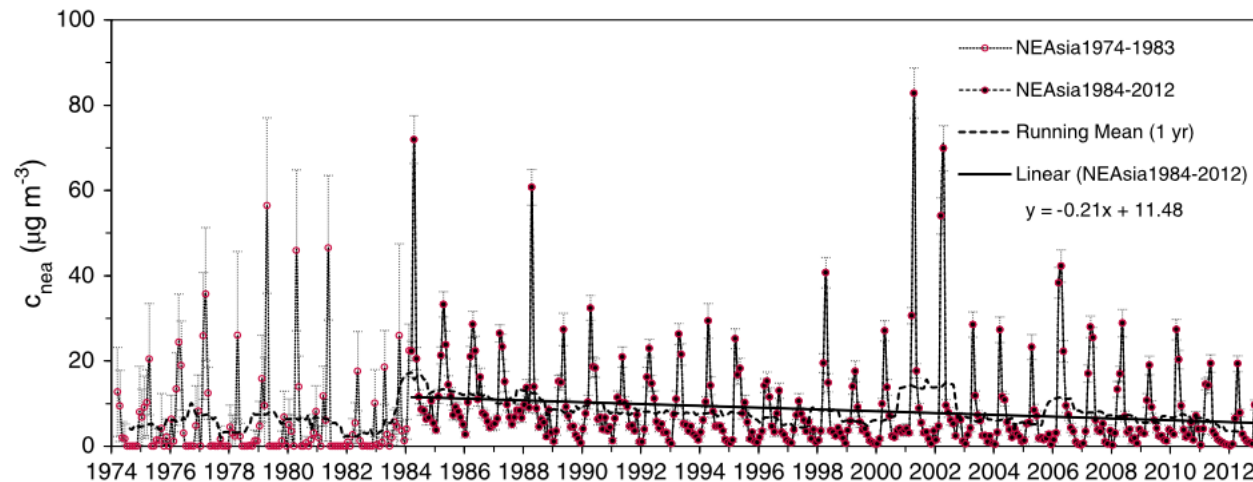
Decreasing Dust Trends in Asia and Africa



(Shao et al., 2013)



**Northern
Africa**

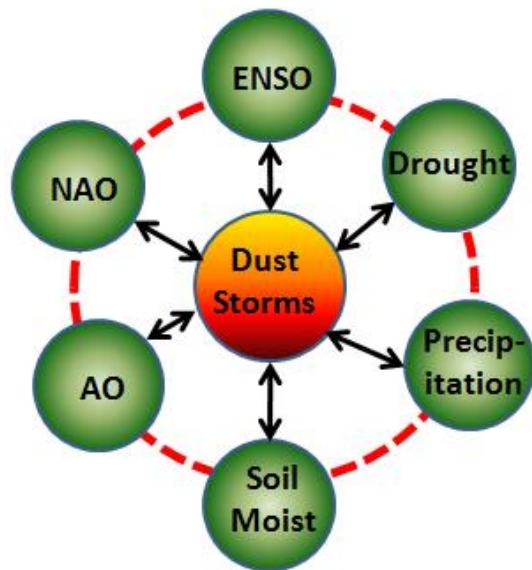


**Northern
Asia**

**Global dust concentration decreased
at 1.2%/yr from 1984 –2012**

What Drives the Dust Trend?

(Contributed by Hang Lei)



ENSO - El-Nino Southern Oscillation

PDO - Pacific Decadal Oscillation

NAO - North Atlantic Oscillation

PNA - Pacific/North American Oscillation

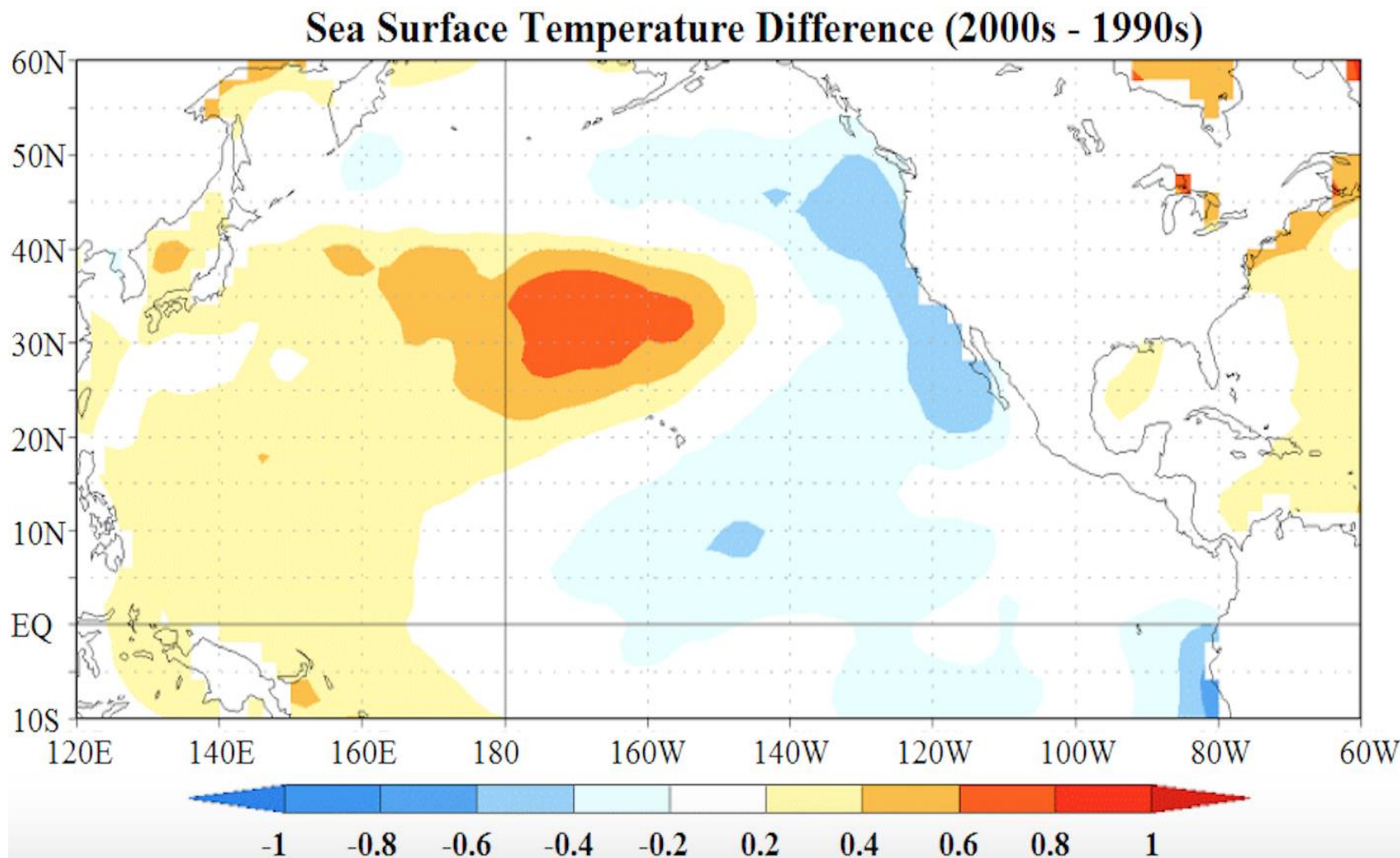
AO - Arctic Oscillation

	ENSO	PDO	NAO	PNA	AO
LL-dust	-0.44	-0.62	-0.41	-0.33	0.38
HL-dust	-0.32	-0.73	-0.40	-0.56	0.33

LL – Low Latitude North American deserts (Chihuahua, Mojave, and Sonoran);

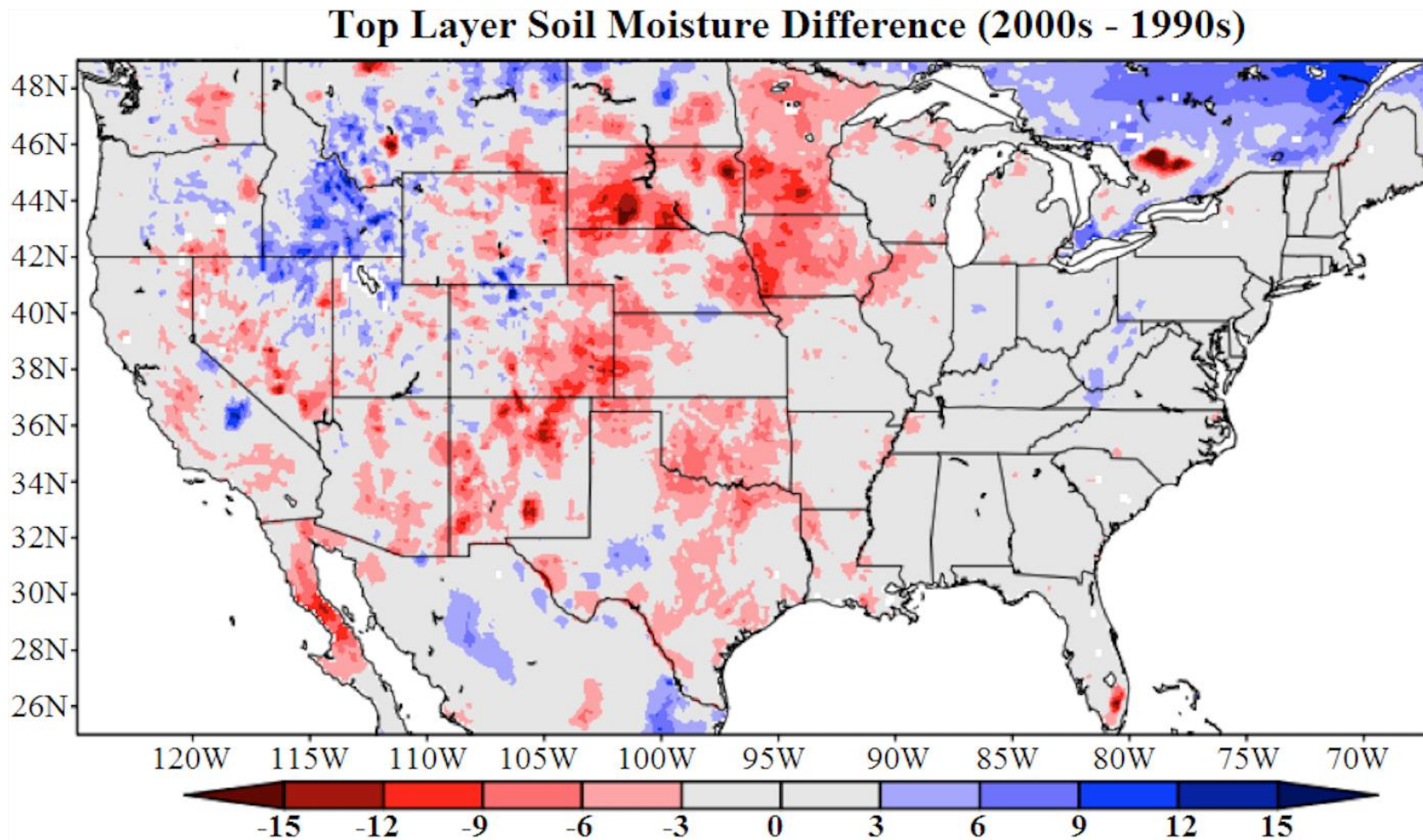
HL – High Latitude Deserts (Great Basin and Colorado Plateau)

Changes in Sea Surface Temperature



(Contributed by Julian Wang)

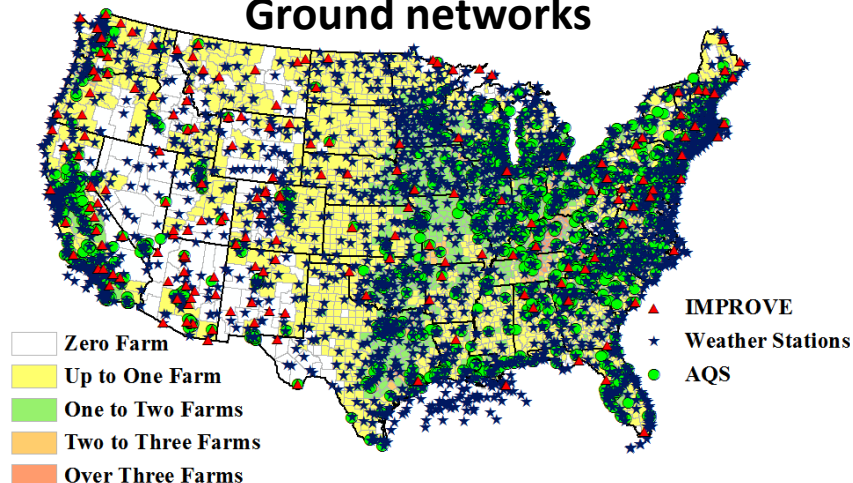
Changes in Soil Moisture



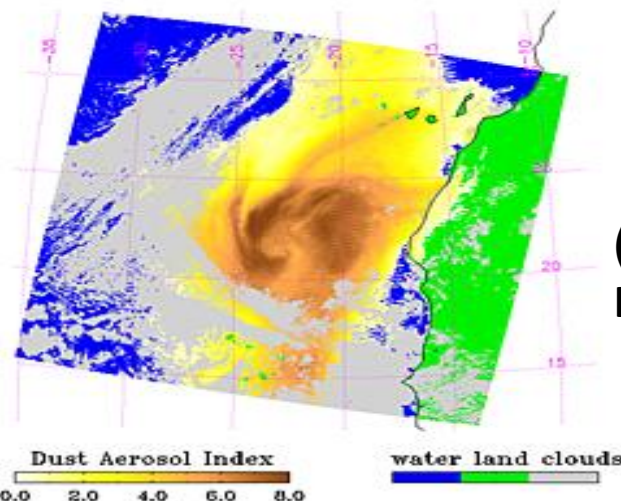
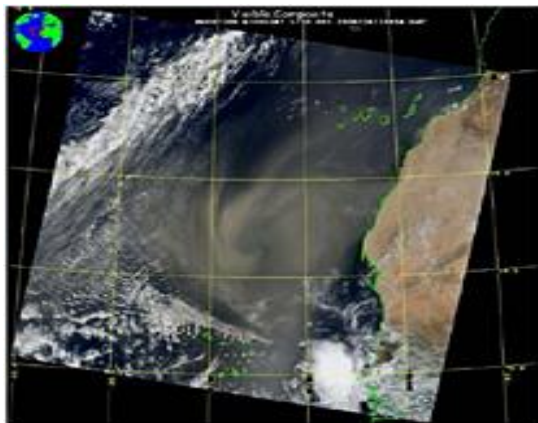
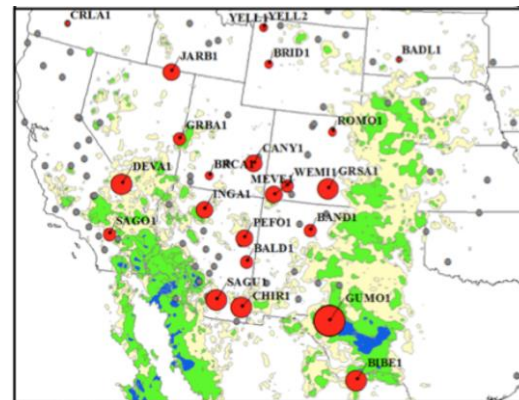
(Contributed by Julian Wang)

What's Next?

Ground networks



IMPROVE vs MODIS Dust Frequency (MODIS data - Ginoux et al., 2012)



(source: Ciren and Kondragunta, 2014)

- Build community consensus on the long-term trend;
- Use ground data for satellite product validation.



Summary



- ◆ **We developed a new dust identification method for IMPROVE dataset for VIIRS Dust validation**
- ◆ **The frequency of dust storms more than doubled from 1990s to 2000s in the Southwest United States.**
- ◆ **The dust trend is likely driven by large-scale variations of sea surface temperature in the Pacific Ocean.**

- **Further information:**

Tong et al., Atmospheric Chemistry & Physics, 2012;

Lei et al., Climate Dynamics, 2016;

Tong et al., Geophysical Research Letter, 2017;



Acknowledgment & Data Access

- **Funding Support:** NASA ROSES and NOAA USWRP;
 - **Data:** EPA, NOAA, NASA, CDC and Arizona DHS;
 - **Many colleagues** for inspiring discussion.
-
- **Data Access:** Email qtong@gmu.edu
 - **Project Website:** <http://ws.laits.gmu.edu/nca>